

Azura Amid · Sarina Sulaiman
Dzun Noraini Jimat
Nor Fadhillah Mohamed Azmin *Editors*

Multifaceted Protocol in Biotechnology

Multifaceted Protocol in Biotechnology

Azura Amid • Sarina Sulaiman
Dzun Noraini Jimat
Nor Fadhilah Mohamed Azmin
Editors

Multifaceted Protocol in Biotechnology

 Springer

Editors

Azura Amid
International Institute for Halal Research
and Training (INHART)
International Islamic University Malaysia
Kuala Lumpur, Malaysia

Sarina Sulaiman
Department of Biotechnology Engineering,
Kulliyah of Engineering
International Islamic University Malaysia
Kuala Lumpur, Malaysia

Dzun Noraini Jimat
Department of Biotechnology Engineering,
Kulliyah of Engineering
International Islamic University Malaysia
Kuala Lumpur, Malaysia

Nor Fadhillah Mohamed Azmin
Department of Biotechnology Engineering,
Kulliyah of Engineering
International Islamic University Malaysia
Kuala Lumpur, Malaysia

ISBN 978-981-13-2256-3 ISBN 978-981-13-2257-0 (eBook)
<https://doi.org/10.1007/978-981-13-2257-0>

Library of Congress Control Number: 2018963298

© Springer Nature Singapore Pte Ltd. 2018

This work is subject to copyright. All rights are reserved by the Publisher, whether the whole or part of the material is concerned, specifically the rights of translation, reprinting, reuse of illustrations, recitation, broadcasting, reproduction on microfilms or in any other physical way, and transmission or information storage and retrieval, electronic adaptation, computer software, or by similar or dissimilar methodology now known or hereafter developed.

The use of general descriptive names, registered names, trademarks, service marks, etc. in this publication does not imply, even in the absence of a specific statement, that such names are exempt from the relevant protective laws and regulations and therefore free for general use.

The publisher, the authors, and the editors are safe to assume that the advice and information in this book are believed to be true and accurate at the date of publication. Neither the publisher nor the authors or the editors give a warranty, express or implied, with respect to the material contained herein or for any errors or omissions that may have been made. The publisher remains neutral with regard to jurisdictional claims in published maps and institutional affiliations.

This Springer imprint is published by the registered company Springer Nature Singapore Pte Ltd.
The registered company address is: 152 Beach Road, #21-01/04 Gateway East, Singapore 189721, Singapore

Preface

Multifaceted Protocol in Biotechnology consists of methods and techniques commonly used in biotechnology studies. There are four sections covered in this book – bioprocess, whole cells and isolated biocatalyst, characterization of biochemical products, and cell isolation and culture. A brief introductory supported with each protocol/method designated for better understanding. The first part of this book consists of recent methodologies for discovering the whole cell and isolated biocatalysts as to improve their current properties which significantly contribute to the development of new industrial processes. It encompasses five chapters covering topics on the mutagenesis of cyanobacteria, site-directed mutagenesis on a plasmid, construction of metagenomics DNA libraries, and isolation of bacteria producing enzymes. It is expected that these chapters will bring about the current status of research and developments in biotechnology area with a critical perspective. The second part covers four chapters covering researches in modern biotechnology focusing in bioprocess areas such as biofuel, catalyst, microbial, and enzyme. It is expected that these chapters will bring about the current methods of research and developments in bioprocess areas. The third part of this book encompasses topics such as preparation and characterization of some biochemical products such as nitrocellulose, proteins, poly(lactic acid), and electrochemical transducer for the biosensor. It consists of five chapters covering reviews of the current state of the characterization of biochemical products that may be useful in identifying biochemical products with a different approach. Characterization of biochemical products is an important part of the early stage of process development of biochemical products. It is due to ensuring specification of the product especially its quality and consistency of the product is met before commercialized. It is expected that these chapters will benefit other researchers to apply in determining the characteristics of their biochemical products. The final part covers cell isolation and culture, encompassing a wide range of multifaceted areas including chemistry, biology, engineering, and statistics. This part comprises of five chapters covering the method for isolation of bacterial strain from contaminated soil, monitoring the growth of plant cell suspension culture, culturing and maintaining mammalian cell culture,

integrated data analysis model for screening cell line producer, and skim latex serum as an alternative nutrition for bacterial growth. Advances in cell isolation and cultures technology discussed in these chapters are not a means to an end in this research area but as a paved path for other researchers to explore.

Kuala Lumpur, Malaysia

Azura Amid

Contents

| | | |
|----------|---|-----------|
| 1 | Site-Directed Mutagenesis on Plasmid Using Polymerase Chain Reaction | 1 |
| | Abdul Aziz Ahmad, Hamzah Mohd Salleh, and Ibrahim Ali Noorbatcha | |
| 2 | Isolation of Halophilic Bacteria | 13 |
| | Nadiah Syuhada Abd. Samad and Azura Amid | |
| 3 | Construction of Metagenomic DNA Libraries and Enrichment Strategies | 23 |
| | Farah Fadwa Benbelgacem, Hamzah Mohd. Salleh, and Ibrahim Ali Noorbatcha | |
| 4 | Thermotolerant Bacteria Producing Fibrinolytic Enzyme | 43 |
| | Azura Amid and Nurul Aqilah Ab. Shukor | |
| 5 | Chemical Mutation Method for High CO₂-Requiring-Mutants of the Cyanobacterium <i>Synechococcus sp.</i> PCC 7002 | 53 |
| | Umami Syuhada Halmi Shari, Azlin Suhaida Azmi, and Azura Amid | |
| 6 | Identification of Fatty Acid Methyl Ester in Palm Oil Using Gas Chromatography-Mass Spectrometer | 63 |
| | Sarina Sulaiman | |
| 7 | Procedure to Develop Binodal Curve and Phase Diagram for Aqueous Two-Phase System | 75 |
| | Zatul Iffah Mohd Arshad and Azura Amid | |
| 8 | Technique to Produce Catalyst from Egg Shell and Coconut Waste for Biodiesel Production | 83 |
| | Sarina Sulaiman and Nur Syakirah Talha | |

| | | |
|-----------|--|------------|
| 9 | Carrier-Free Enzyme Immobilization by Cross-Linked Enzyme Aggregates (CLEA) Technology | 93 |
| | Faridah Yusof and Soofia Khanahmadi | |
| 10 | Isolation of Microfibrillated Cellulose (MFC) Via Fungal Cellulases Hydrolysis Combined with Ultrasonication | 109 |
| | Dzun Noraini Jimat and Aviceena | |
| 11 | Characterization of Electrochemical Transducers for Biosensor Applications | 119 |
| | Farrah Aida Arris, Abdel Mohsen Benoudjit, Fahmi Sanober, and Wan Wardatul Amani Wan Salim | |
| 12 | Polymerization Methods and Characterizations for Poly(Lactic Acid) (PLA) Based Polymers | 139 |
| | Fathilah Binti Ali and Norshafiq Ismail | |
| 13 | Polymers in Biosensors | 151 |
| | Jia Jia Long, Abdel Mohsen Benoudjit, Farrah Aida Arris, Fathilah Ali, and Wan Wardatul Amani Wan Salim | |
| 14 | Characterization of Conformational and Oligomeric States of Proteins | 167 |
| | Fazia Adyani Ahmad Fuad | |
| 15 | Skim Latex Serum as an Alternative Nutrition for Microbial Growth | 179 |
| | Vivi Mardina and Faridah Yusof | |
| 16 | Method for Isolation of Bacterial Strain from Contaminated Soil for Biodegradation of Polycyclic Aromatic Hydrocarbons (PHAs) | 197 |
| | Nooraidah Binti Mustaffa, Parveen Jamal, Kola Saheed Olorunnisola, and Abdul Haseeb Ansari | |
| 17 | Monitoring the Growth of Plant Cells in Suspension Culture | 203 |
| | Noor Illi Mohamad Puad and Tajul Afif Abdullah | |
| 18 | Culturing and Maintaining Mammalian Cell Culture | 215 |
| | Raha Ahmad Raus, Ghassan Ali Salih, and Mustaffa Nameer Shaban | |
| 19 | Integrated Data Analysis Model for Screening Cell Line Producer | 227 |
| | Nor Fadhillah Mohamed Azmin | |
| | Index | 235 |

Chapter 1

Site-Directed Mutagenesis on Plasmid Using Polymerase Chain Reaction



Abdul Aziz Ahmad, Hamzah Mohd Salleh, and Ibrahim Ali Noorbacha

Abstract Site-directed mutagenesis (SDM) is a very useful technique to study changes in protein function that may occur as a result of the DNA manipulation. A detail procedure to employ SDM on whole plasmid using polymerase chain reaction (PCR) with successful application of the method on a pET28a plasmid harboring an endoglucanase I gene from *Fusarium oxysporum* is described here.

Keywords Site directed mutagenesis · Endoglucanase · *Fusarium oxysporum*

1.1 Introduction

Mutagenesis is the process of making a genetic mutation which may occur spontaneously or be stimulated by mutagens. Researchers use a number of methods to create mutations, including transposon mutagenesis to generate random gene knockouts, and site-directed mutagenesis, which makes use of the polymerase chain reaction (PCR) to introduce specific mutations. Site-directed mutagenesis (SDM), is a very useful technique to study gene and protein functions relationship. For instance, one may mutate the specific location of a protein and observed the activity increases by many folds. SDM enables researchers to study other properties of proteins such as thermostability. For example, Akcapinar et al. (2015) had identified three thermostabilizer mutations (Q126F, K272F, Q274V) in endoglucanase I from *Trichoderma reesei*, through molecular dynamics simulations. These mutations were then introduced into the endoglucanase I gene, using site-directed

A. A. Ahmad · I. A. Noorbacha
BioProcess and Molecular Engineering Research Unit, Kulliyyah of Engineering,
International Islamic University Malaysia, Kuala Lumpur, Malaysia

H. M. Salleh (✉)
BioProcess and Molecular Engineering Research Unit, Kulliyyah of Engineering,
International Islamic University Malaysia, Kuala Lumpur, Malaysia

International Institute for Halal Research and Training, International Islamic University
Malaysia, Kuala Lumpur, Malaysia
e-mail: hamzah@iium.edu.my

mutagenesis, and the thermostability of the enzymes was found to increase. The experimental method for introducing mutations in endoglucanase from *Fusarium oxysporum* (EGuia) will be described in this chapter. The experimental method to analyze enzymes by enzyme assays have been presented elsewhere (Salleh 2011), and hence it will not be repeated here.

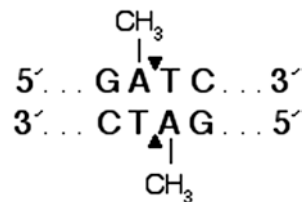
1.2 Site-Directed Mutagenesis on Plasmid

The initial methods for SDM required single-stranded DNA (ssDNA), as the template (Kunkel 1985; Sugimoto et al. 1989; Taylor et al. 1985; Vandeyar et al. 1988). These methods need subcloning and are labor intensive, in addition to the necessity of specialized vectors and the presence of unique restriction sites. The method proposed by Papworth et al. (1996), allows site-specific mutation in virtually any double-stranded plasmid, thus eliminating the need for subcloning into M13-based bacteriophage vectors and for single-stranded DNA rescue. Plasmid DNA isolated from almost all of the commonly used *E.coli* strains (*dam*⁺) is methylated and is a suitable template for mutagenesis, whereas the plasmid DNA isolated from the exceptional (*dam*⁻) *E.coli* strains are not suitable.

1.2.1 Principle

The fundamental process makes use of a supercoiled double-stranded deoxyribonucleic acid (dsDNA) vector with the site of interest to be mutated and two synthetic oligonucleotide primers having the needed mutation. The oligonucleotide primers, each complementary to each other, are extended in the temperature cycling by high-fidelity DNA polymerase. The high-fidelity DNA polymerase replicates both plasmid strands with high fidelity and without displacing the mutant oligonucleotide primers. Integration of the oligonucleotide primers produces a mutated plasmid containing staggered nicks. Subsequent to temperature cycling, the PCR product is digested with *DpnI*. The *DpnI* endonuclease target sequence is specific for methylated and hemi-methylated DNA (Fig. 1.1) and is employed to digest the parental DNA template.

Fig. 1.1 *DpnI* endonuclease recognition site



1.2.2 Objective of Experiment

The objective of this procedure is to introduce the desired mutation at a specific predetermined location into a plasmid (a vector with gene insert of interest) using PCR approach which will afford site-directed mutation(s) (Fig. 1.2).

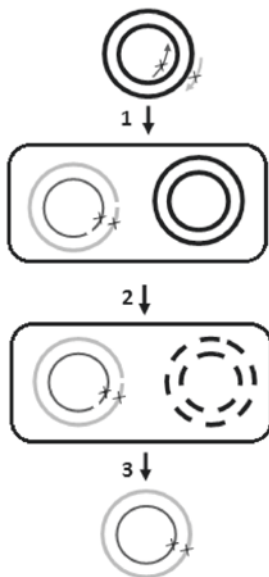
1.3 Materials and Skills Required

Required Basic Skills

1. DNA Primer design
2. Basic lab equipment operation

Materials

1. PCR reagents
2. Thin-walled 200 μ l PCR tubes
3. Petri dishes
4. Inoculating loop
5. 15 ml falcon tube
6. *DpnI* restriction enzyme
7. Competent cells
8. Mini-prep plasmid extraction kit (Qiagen)



1. Mutant Strand Synthesis

Perform PCR to:

- Denature DNA template
- Anneal DNA mutagenic primer containing desired mutation
- Extend DNA primers with high-fidelity DNA polymerase
- Some parental DNA may remain as such

2. *DpnI* Digestion

- Digest parental methylated and hemimethylated DNA.
- Mutant strand will not be digested by *DpnI* restriction enzyme.

3. Transformation

Transform the mutated molecule into competent cells for nick repair.

Fig. 1.2 Flow of the overall mutagenesis procedure. The dark thick circles refer to parental methylated DNA. The broken thick circles refer to parental methylated DNA degraded by *DpnI*. The dark thin and grey circles refer to the forward and reverse strand of the mutant DNA respectively. The “x” mark refers to the mutation site (Image derived from Agilent Technologies QuikChange Mutagenesis workflow)

Equipment

1. PCR thermocycler
2. Incubator shaker
3. Microcentrifuge
4. Centrifuge

1.4 Methodology

1.4.1 Template Preparation

The double-stranded plasmid DNA template is obtained by extraction from an *E. coli* (dam⁺) strain with miniprep plasmid extraction kit (Qiagen GmbH, Germany).

1.4.2 Mutagenic Primer Design

The mutagenic DNA primer to be used in this method should be designed individually according to the desired mutation. Consider the following when designing the mutagenic DNA primers:

1. The forward and reverse mutagenic primers must contain the desired mutation and anneal to the same sequence on opposite strands of the plasmid template.
2. The desired mutation should be in the middle of the primer with ~10–15 bases of correct sequence on both sides.
3. The primers optimally should have a minimum GC content of 40% and should terminate in one or more C or G bases.

1.4.3 Polymerase Chain Reaction (PCR)

Prepare two sets of 50 μ l reaction mixtures containing forward and reverse primers in 200 μ l PCR tubes as follows (Table 1.1 and Fig. 1.3):

Part A: Initial denaturing of the [double helix](#) DNA template at 94 °C–95 °C.

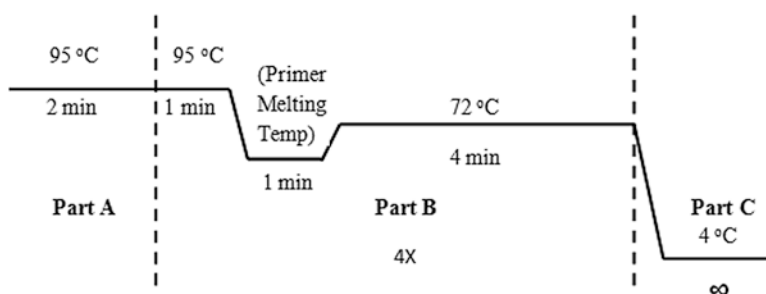
Part B: Starts by denaturation at 94 °C–95 °C followed by cooling the sample to moderate temperature, approximately 54 °C, which facilitates the annealing of the mutagenic DNA primers to the single-stranded DNA templates. In the third step of the cycle, the sample is reheated to 72 °C, the ideal temperature for thermostable DNA polymerase, for elongation process. Part B is repeated four times in the first cycle.

Part C: This is simply for storage at 4 °C, no reaction occurs in this part.

Table 1.1 Reaction mixtures containing forward and reverse primers

| Reagent | Forward (μ l) | Reverse (μ l) |
|-----------------------------|--------------------|--------------------|
| 1. 10X reaction buffer | 5.0 | 5.0 |
| 2. Plasmid | 1.0 | 1.0 |
| 3. Forward mutagenic primer | 2.5 | – |
| 4. Reverse mutagenic primer | – | 2.5 |
| 5. DMSO | 1.5 | 1.5 |
| 6. dNTP mix | 1.0 | 1.0 |
| 7. Distilled water | 38.5 | 38.5 |
| 8. High-fidelity polymerase | 0.5 | 0.5 |

Note: Always keep the reagents on ice while preparing the reaction mixture

**Fig. 1.3** Cycling parameters for 1st cycle

In the second cycle, mix 25 μ l of forward and 25 μ l of reverse reaction mixtures from the first cycle in a new 200 μ l PCR tube and repeat the whole process (Part A, B and C) with the same parameters, except the Part B is repeated 12–18 times according to the type of mutation desired as follows (Tables 1.2 and 1.3):

1.4.4 *DpnI* Digestion

Add 1 μ l of the *DpnI* restriction enzyme (10 U/ μ l) to each PCR product. Gently mix each reaction mixture by pipetting the solution up and down several times. Spin down the reaction mixtures using a microcentrifuge for 1 min and incubate each reaction at 37 °C for 1 h to digest the parental supercoiled double-stranded DNA.

1.4.5 Transformation: Nick Repair

To repair the nick caused by the non-strand replacing high-fidelity DNA polymerase during PCR, the plasmid needs to be transformed into competent cells.

Table 1.2 Type of mutation and number of times Part B repeated

| Type of mutation desired | No. of repeats |
|---|----------------|
| Point mutations | 12 |
| Single amino acid changes | 16 |
| Multiple amino acid deletions or insertions | 18 |

Table 1.3 Designed mutagenic primer

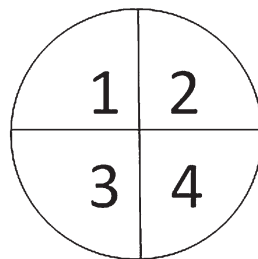
| Primer name (length) | Sequence (5' ----- 3') |
|----------------------|---|
| T224Ef (27nt) | CTC TAC GGC TGC G AA GGC GAT GAG TGC |
| T224Er (27nt) | GCA CTC ATC GCC T TC GCA GCC GTA GAG |

1. Gently thaw chemically competent cells (e.g., DH5 α) on ice for 20–30 min.
2. Mix 10 μ l of the *DpnI* digested mixture with 10 μ l TE buffer and add the mixture to competent cells. Swirl the transformation reaction mixture very gently and incubate on ice for another 20–30 min.
3. Heat shock the transformation reactions for 45 s at 42 °C and then place the reactions back to ice immediately and allow the cells to recover on ice for 10 min and add 1 ml of Luria Bertani (LB) liquid media.
4. Place the tube in an incubator shaker at 37 °C for 90 min.
5. Plate on 1-2 LB agar plates containing appropriate selection antibiotics.
6. Grow plates overnight at 37 °C.
7. Randomly choose 4–10 single colonies from the plate(s) and streak on a plate divided into four sectors as shown in Fig. 1.4.
8. Incubate overnight and randomly select few sectors and isolate the plasmid using mini-prep plasmid extraction kit. To isolate the plasmid, it is possible to scratch the fully grown sectors or prepare a culture broth with appropriate antibiotics inoculated with the randomly selected sectors. Optional: Check the presence of the plasmid on 1% agarose gel.

1.4.6 Confirmation by DNA Sequencing

To confirm the success of the mutagenesis, the plasmid harboring the mutated gene needs to be sequenced. This step can be outsourced by sending the plasmid harboring the mutated gene along with the appropriate sequencing primers to DNA sequencing service providers.

Fig. 1.4 One Petri dish divided into four sectors



1.5 Case Study: Mutating EGuia

EGuia is an endoglucanase I from *Fusarium oxysporum* and it is termed as wild-type in this current procedure. We have successfully mutated EGuia amino acid at position 224 from Threonine to Glutamic acid (T224E) following the method described above.

1.5.1 Results and Discussion

T224Ef and T224Er are the forward (sense) and reverse (antisense) DNA mutagenic primers respectively, designed for introducing Threonine to Glutamic acid mutation at position 224 (single amino acid change) in wild-type EGuia endoglucanase I. Codon changed is bold and underlined.

1.5.1.1 DNA Sequencing Result

The following is the nucleotide sequence comparison between the wild-type (WT) EGuia and the T224E mutant. (DNA sequencing service provided by AIT Biotech (Singapore) via NextGene Sdn. Bhd.)

1.5.1.2 Discussion

Figures 1.5 and 1.6 are the aligned nucleotide and amino acid sequence for wild-type EGuia and the expected T224E mutant. An asterisk (*) denotes that conservation of nucleotide and amino acid. At nucleotide position 673 and 674 and the amino acid at position 224, the absence of an asterisk indicates the nucleotides in both the sequence are not identical. The DNA sequencing result above indicates the intended point mutation of changing threonine (T) to glutamic acid (E) was successfully introduced at position 224 of EGuia. A set of five positive samples were sent for DNA sequencing; three of the samples contained the mutation at the intended position. There was no mutation in the 4th sample and the final sample, additional

```

WT      1  ATGCAGACCCCGACAAGGCCAAGGAGCAACCCCAAGCTCGAGACCTACCCTGCACC
T224E   1  ATGCAGACCCCGACAAGGCCAAGGAGCAACCCCAAGCTCGAGACCTACCCTGCACC
*****

WT      61  AAGGCCTCCGGCTGCAAGAAGCAGACCAACTACATCGTCGCCGACGCAGGTATTACCGGC
T224E   61  AAGGCCTCCGGCTGCAAGAAGCAGACCAACTACATCGTCGCCGACGCAGGTATTACCGGC
*****

WT      121  ATCCACCAAAAGAACGGCGCCGGCTCGGGTACTGGGACAAAAGCCCAACGCCACAGCC
T224E   121  ATCCACCAAAAGAACGGCGCCGGCTCGGGTACTGGGACAAAAGCCCAACGCCACAGCC
*****

WT      181  TGTCCCGATGAGGCTTCTCGCCGAAGAACTGTATCCTCAGTGGTATGGACTCAAACGCT
T224E   181  TGTCCCGATGAGGCTTCTCGCCGAAGAACTGTATCCTCAGTGGTATGGACTCAAACGCT
*****

WT      241  TACAAGAACGCTGGTATCACTACTTCTGGCAACAAGCTTCGTCTCAGCAGCTTATCAAC
T224E   241  TACAAGAACGCTGGTATCACTACTTCTGGCAACAAGCTTCGTCTCAGCAGCTTATCAAC
*****

WT      301  AACCAGCTTGTTCCTCCTCGAGTTTATCTGCTTGAGGAGAACAAAGAAGTATGAGATG
T224E   301  AACCAGCTTGTTCCTCCTCGAGTTTATCTGCTTGAGGAGAACAAAGAAGTATGAGATG
*****

WT      361  CTTCACTCACTGGCACTGAGTTCTCTTTTGATGTTGAGATGGAGAAGCTTCCTTGTGGT
T224E   361  CTTCACTCACTGGCACTGAGTTCTCTTTTGATGTTGAGATGGAGAAGCTTCCTTGTGGT
*****

WT      421  ATGAATGGTCTCTGTACCTTTCTGAGATGCCCAAGGATGGCGGTAAAGCAGCAGCCGA
T224E   421  ATGAATGGTCTCTGTACCTTTCTGAGATGCCCAAGGATGGCGGTAAAGCAGCAGCCGA
*****

WT      481  AACAGCAAGGCTGGCGCTACTATGGTGTGGATACTGTGATGCCCAAGTGTACGTCACT
T224E   481  AACAGCAAGGCTGGCGCTACTATGGTGTGGATACTGTGATGCCCAAGTGTACGTCACT
*****

WT      541  CCTTTCATTAACGGAGTTGGAACATCAAGGGACAGGGTGTCTGCTGTAACGAGCTCGAC
T224E   541  CCTTTCATTAACGGAGTTGGAACATCAAGGGACAGGGTGTCTGCTGTAACGAGCTCGAC
*****

WT      601  ATCTGGGAGGCCAACTCCCGGCAACTCACATTGCTCCTCACCCCTGCAACAAGCCCGGC
T224E   601  ATCTGGGAGGCCAACTCCCGGCAACTCACATTGCTCCTCACCCCTGCAACAAGCCCGGC
*****

WT      661  CTCACGGCTGCAAGGCGATGAGTGGCGAGCTCCGGTATCTGCGCAAGGCTGGTGC
T224E   661  CTCACGGCTGCAAGGCGATGAGTGGCGAGCTCCGGTATCTGCGCAAGGCTGGTGC
*****

WT      721  GGCTGGAACCAACAACCGCATCAACGTGACCGACTTCTACGGCCCGGCAAGCAGTACAAG
T224E   721  GGCTGGAACCAACAACCGCATCAACGTGACCGACTTCTACGGCCCGGCAAGCAGTACAAG
*****

WT      781  GTCGACAGTACCCGCAAGTTCACCGTGACATCCAGTTCGTGCGCAACAGCAGGGCGAC
T224E   781  GTCGACAGTACCCGCAAGTTCACCGTGACATCCAGTTCGTGCGCAACAGCAGGGCGAC
*****

WT      841  CTCATCGAGCTGCACCGCCACTACATCCAGSACAACAGGTCATCCAGTCAAGTCTCGTC
T224E   841  CTCATCGAGCTGCACCGCCACTACATCCAGSACAACAGGTCATCCAGTCAAGTCTCGTC
*****

WT      901  AACATCTCCGGCCCTCCCAAGATCAATTTTCATCAACGACAAGTACTGCGCTGCCACTGGA
T224E   901  AACATCTCCGGCCCTCCCAAGATCAATTTTCATCAACGACAAGTACTGCGCTGCCACTGGA
*****

WT      961  GCTAACGAGTACATGCGCCTCGGCGTACTAAGCAAATGGGCGATGCCATGTCCCGCGGA
T224E   961  GCTAACGAGTACATGCGCCTCGGCGTACTAAGCAAATGGGCGATGCCATGTCCCGCGGA
*****

WT      1021  ATGTTTCTCGCCATGAGCGTCTGTTGGAGCGAGGGTGATTTTCATGGCCTGTTGGATCAG
T224E   1021  ATGTTTCTCGCCATGAGCGTCTGTTGGAGCGAGGGTGATTTTCATGGCCTGTTGGATCAG
*****

WT      1081  GGCCTTGCTGGACCTGTGACGCCACTGAGGCGATCCCAAGAACATCGTCAAGTGCAG
T224E   1081  GGCCTTGCTGGACCTGTGACGCCACTGAGGCGATCCCAAGAACATCGTCAAGTGCAG
*****

WT      1141  CCCAACCCCTGAAGTGACATTCAGCAACATCCGAATGGAGAGATGGATCTACTTCGTGC
T224E   1141  CCCAACCCCTGAAGTGACATTCAGCAACATCCGAATGGAGAGATGGATCTACTTCGTGC
*****

WT      1201  GTC AAGGCTCCTGCGTATCCTGGTCTCACCGCTTGT AAGGGCTGAGC
T224E   1201  GTC AAGGCTCCTGCGTATCCTGGTCTCACCGCTTGT AAGGGCTGAGC
*****

```

Fig. 1.5 Nucleotide comparison between wild type (WT) EGuia and T224E mutant


```

WT      1  MQTPDKAKEQHPKLETYRCTKASGCKKQTNYIVADAGIHGIHQKNGAGCGDWGQKPNATA
T224E  1  MQTPDKAKEQHPKLETYRCTKASGCKKQTNYIVADAGIHGIHQKNGAGCGDWGQKPNATA
*****

WT      61  CPDEASCAKNCILSGMDSNAYKNAGITTSGNKLRLLQQLINNLVSPRVYLLEENKKKYEM
T224E  61  CPDEASCAKNCILSGMDSNAYKNAGITTSGNKLRLLQQLINNLVSPRVYLLEENKKKYEM
*****

WT      121  LHLTGTEFSFDVEMEKLPCGMNGALYLSEMPQDGGKSTSRNSKAGAYYGAGYCDACQCVT
T224E  121  LHLTGTEFSFDVEMEKLPCGMNGALYLSEMPQDGGKSTSRNSKAGAYYGAGYCDACQCVT
*****

WT      181  PFIGVGNIKGQGVCCNELDIWEANSRATHIAPHPCNKPGLYGCTGDECGSSGICDKAGC
T224E  181  PFIGVGNIKGQGVCCNELDIWEANSRATHIAPHPCNKPGLYGCEGDECGSSGICDKAGC
*****

WT      241  GWNHNRINVTFYGRGKQYKVDSTRKFTVTSQFVANKQGDLLIELHRHYIQDNKVIESAVV
T224E  241  GWNHNRINVTFYGRGKQYKVDSTRKFTVTSQFVANKQGDLLIELHRHYIQDNKVIESAVV
*****

WT      301  NISGPPKINFINDKYCAATGANEYMLGGTKQMGDAMSRGMVLAMSVVWSEGDFMAWLDQ
T224E  301  NISGPPKINFINDKYCAATGANEYMLGGTKQMGDAMSRGMVLAMSVVWSEGDFMAWLDQ
*****

WT      361  GVAGPCDATEGDPKNIVKVQPNPEVTFNSNIRIGEIGSTSSVKA PAYPGPHRL
T224E  361  GVAGPCDATEGDPKNIVKVQPNPEVTFNSNIRIGEIGSTSSVKA PAYPGPHRL
*****
    
```

Fig. 1.6 Translated amino acid sequence comparison between wild type (WT) EGuia and T224E mutant

nucleotide was present at the intended mutation region. The 4th sample might be the parental strand which escaped the *DpnI* digestion, and since it has the antibiotic resistance gene (kanamycin), it survives on the plate. In the final sample, the reason this happened is that the primers are complementary each other. In the PCR amplification, the primers dimerized into double-strand small DNA fragments while the PCR products are blunt end fragment (produced by proofreading thermal DNA polymerase). When transformed the PCR product into a cell, the cell DNA repair system did a blunt-end ligation of the PCR fragment with primer dimer rather than do a nick repair.

1.6 Conclusion

An *in-vitro* mutagenesis technique presented. The technique was successful in introducing site-specific mutation as described in the case study. A point mutation from threonine to glutamic acid at position 224 (T224E) was introduced to the endoglucanase I gene from *Fusarium oxysporum*.

Acknowledgement The authors would like to acknowledge the Ministry of Higher Education, (MoHE) Malaysia for awarding fund via Fundamental Research Grant Scheme: Grant No: FRGS-13-070-0311 and Professor S.G. Withers (UBC, Vancouver) for providing the original wild-type plasmid construct.

List of Abbreviations

| | |
|-------------|--|
| SDM | Site-directed mutagenesis |
| PCR | Polymerase chain reaction |
| M13 | Is a filamentous bacteriophage composed of circular single-stranded DNA |
| DNA | Deoxyribonucleic acid |
| ssDNA | single-stranded DNA |
| <i>dam</i> | gene encoding Dam. Dam stands for DNA adenine methyltransferase, an enzyme of ~32 kDa that does not belong to a restriction/modification system. The target recognition sequence for <i>E. coli</i> Dam is GATC and the methylation occurs at the N6 position of the adenine in this sequence (GmATC). <i>dam</i> ⁺ has the ability for methylation and <i>dam</i> ⁻ does not have this ability. |
| <i>DpnI</i> | <i>DpnI</i> is a restriction enzyme from <i>Diplococcus pneumoniae</i> . This enzyme recognizes the double-stranded DNA <u>methylated</u> sequence GATC. It works well in the presence of Zn ²⁺ ions. <i>DpnII</i> recognizes the double-stranded DNA <u>unmethylated</u> sequence GATC and cleave before G-1. |

List of Nucleobases

| Nucleobase | Abbreviated names |
|------------|-------------------|
| Adenine | A |
| Thymine | T |
| Guanine | G |
| Cytosine | C |

List of Naturally Occurring Amino Acids

| Amino acid | Abbreviated names | |
|---------------|-------------------|---|
| Glycine | Gly | G |
| Alanine | Ala | A |
| Valine | Val | V |
| Leucine | Leu | L |
| Isoleucine | Ile | I |
| Proline | Pro | P |
| Cysteine | Cys | C |
| Methionine | Met | M |
| Serine | Ser | S |
| Threonine | Thr | T |
| Asparagine | Asn | N |
| Glutamine | Gln | Q |
| Aspartic Acid | Asp | D |
| Glutamic Acid | Glu | E |
| Histidine | His | H |
| Lysine | Lys | K |
| Arginine | Arg | R |
| Phenylalanine | Phe | F |
| Tyrosine | Tyr | Y |
| Tryptophan | Trp | W |

References

- Akcapinar GB, Alessandro VA, Pier LM, Casadio R, Ugur OS (2015) Modulating the thermostability of endoglucanase I from *Trichoderma reesei* using computational approaches. *Protein Eng Des Sel* 28(5):127–135
- Kunkel TA (1985) Rapid and efficient site-specific mutagenesis without phenotypic selection. *Proc Natl Acad Sci USA* 82(2):488–492
- Papworth C, Bauer JC, Braman J, Wright DA (1996) Site-directed mutagenesis in one day with >80% efficiency. *Strateg Mol Biol* 9:3–4
- Salleh HM (2011) In: Noorbacha IA, Karim MIA, Salleh HM (eds) *Experimental methods in modern biotechnology*, vol 1. IIUM Press, Kuala Lumpur
- Sugimoto M, Esaki N, Tanaka H, Soda K (1989) A simple and efficient method for the oligonucleotide-directed mutagenesis using plasmid DNA template and phosphorothioate-modified nucleotide. *Anal Biochem* 179(2):309–311
- Taylor JW, Ott J, Eckstein F (1985) The rapid generation of oligonucleotide-directed mutations at high frequency using phosphorothioate-modified DNA. *Nucleic Acids Res* 13(24):8765–8785
- Vandeyar MA, Weiner MP, Hutton CJ, Batt CA (1988) A simple and rapid method for the selection of oligodeoxynucleotide-directed mutants. *Gene* 65(1):129–133

Chapter 2

Isolation of Halophilic Bacteria



Nadiyah Syuhada Abd. Samad and Azura Amid

Abstract Protease the hydrolytic enzyme has very broad applications in industries. Identifying new protease source from food by isolating the protease producing microbe is consider a safe approach compare to isolating it from other sources which may be dangerous for human consumption. Therefore, this chapter discusses the method of isolating the microbial strain that can produce safe protease enzyme from fermented food.

Keywords Halophilic · Protease · Salt-tolerant · Milk-salt agar · Halotolerant

2.1 Introduction

Proteases are hydrolytic enzymes that break peptide bonds between amino acid residues and are widely used in various industries, such as those involving food, detergents, pharmaceuticals, leather, waste management and diagnostic reagents (Kumar and Takagi 1999). Halophiles are microorganisms that can grow in highly saline conditions. Previous researches have shown that halophilic microorganisms can be isolated from saline water, saline oil, salty food, salt lakes and seawater (Setati 2010; Karan et al. 2012). Halophilic microorganisms are expected to produce salt-tolerant enzymes owing to their ability to perform catalysis under high salinity. These microbes can be classified into three groups based on their salt requirement (Ventosa et al. 1998):

1. Slight halophiles which grow optimally at 0.20–0.85 M (1–5% sodium chloride; NaCl).
2. Moderate halophiles which show rapid growth at 0.85–3.40 M (5–20% NaCl).
3. Extreme halophiles which grow optimally at 3.4–5.1 M (20–30% NaCl).

N. S. A. Samad · A. Amid (✉)

Department of Biotechnology Engineering, Faculty of Engineering, International Islamic University Malaysia, Kuala Lumpur, Malaysia

e-mail: azuraamid@iium.edu.my

2.2 Principles

The purpose of isolating bacteria from the sample is to obtain pure cultures of bacteria. Culture methods can be divided into two: culture on solid media or liquid media. Some solid culture media are nonselective (e.g., nutrient agar) and allow a wide variety of bacteria to grow on it. Meanwhile, some types of agar are more selective (e.g., MacConkey agar). MacConkey agar with added bile salts is specifically used to isolate bacteria like *Escherichia coli* and *Enterococcus faecalis*, both of which are found in large intestines of humans and are known as ‘bile-tolerant’ bacteria.

Another way to culture bacteria is by using liquid media (broth). Bacterial growth can be easily observed as the clear liquid medium turns cloudy or turbid within 24–48 h. Broth culture is significantly more sensitive compared to the direct culture on agar. However, mixed growth can occur, and this makes it difficult to determine the type of bacteria present. Thus, broth media must be subcultured in solid agar to obtain pure cultures.

In this case, the spread plate technique can be used to isolate individual colonies. The advantage of this technique is that it distributes bacteria evenly on a petri dish. Moreover, it is also a quantitative technique which allows the determination of the number of bacteria in a sample.

Milk salt agar is composed of standard nutrient agar with the addition of NaCl and skim milk powder. This agar is used to screen and identify colonies that show proteolytic activity and can tolerate high concentrations of NaCl. Proteases (extracellular enzymes) produced by these microorganisms are secreted into the surrounding media, where they break down the casein in the said agar to give small peptides and individual amino acids which will then be taken up by the microorganisms to produce energy or undergo anabolism. This hydrolysis reaction gives rise to clear zones around the colonies. The presence of NaCl in skim milk agar inhibits the growth of non-halophiles and selects for bacteria that can grow in high salt content. Halophiles may produce halotolerant proteases which can withstand extreme condition, i.e., high NaCl concentrations (Karan et al. 2012).

2.2.1 Objective of Experiment

This experiment aims to isolate from fermented food halophilic bacteria which produce halotolerant proteases.

2.3 Materials and Methods

2.3.1 Materials (Tables 2.1, 2.2 and 2.3)

Table 2.1 Consumable items used

| No | Equipment | Aims of usage |
|----|--|---|
| 1 | Pipettes (200 μ L, 1 mL, 5 mL) | To add solutions into cuvettes |
| 2 | Felcon Tube (50 mL) | To culture microorganisms |
| 3 | Microcentrifuge tube (2 mL) | To perform enzyme assay and determine total protein |
| 4 | Sterilized hockey-stick and loop wires | To spread and streak culture onto plate |
| 5 | Plate/Petri Dish | To contain culture medium (agar) |

Table 2.2 Equipment used

| No | Equipment | Usage |
|----|--|---|
| 1 | Weighing balance | To weigh chemicals and reagents |
| 2 | Shaking incubator Brand: Stuart SI500 (Bibby Scientific) | To grow and culture microorganisms |
| 3 | Microplate Spectrophotometer Brand: Multiskan | To measure absorbance during determination of enzyme activity and total protein |
| 4 | GO (Fisher Scientific) pH meter Brand: Accumet Basic AB15 Plus Fisher Scientific | To measure pH |

Table 2.3 Chemicals and reagents used

| No | Chemicals | Manufacturer |
|----|---|--------------------|
| 1 | Bacteria lysate | NA |
| 2 | Nutrient Broth | Sigma-Aldrich, USA |
| 3 | Nutrient Agar | Sigma-Aldrich, USA |
| 4 | Skim milk agar | Sigma-Aldrich, USA |
| 5 | Casein | Sigma-Aldrich, USA |
| 6 | Trichloroacetic Acid | Sigma-Aldrich, USA |
| 7 | Sodium Carbonate | Sigma-Aldrich, USA |
| 8 | Folin & Ciocalteu's Phenol | Sigma-Aldrich, USA |
| 9 | Reagent Quick Start Bradford 1x Dye Reagent | Bio-rad, USA |

2.3.2 Isolation of Strains for Proteolytic Activities

1. From 1 L of nutrient broth, 25 g of it is taken out, the weight of which is measured using an electronic balance. The pH of the culture medium is adjusted to 7 using HCl or NaOH with the help of a pH meter. Then, distilled water is added until the volume reaches 1 L.
2. 0.1 ml of the sample is diluted with 1 ml of sterilized distilled water and incubated in 4.9 ml of nutrient broth (pH 7) at 37 °C for 24 h in a shaker incubator at 250 rpm.
3. To prepare 1 L of 5% NaCl nutrient agar, 28 g of nutrient agar powder and 50 g of NaCl are weighed using an electronic balance. The pH of the agar is adjusted to 7 using HCl or NaOH with the help of a pH meter. Then, distilled water is added until the volume reaches 1 L.
4. Samples in the nutrient broth are serially diluted, and 0.1 ml of suspension is spread uniformly on the 5–10% NaCl nutrient agar plates using a sterile hockey stick wire. The plates are then incubated at 37 °C for 24 h to isolate the colonies.
5. Colonies are selected and grouped based on their differences in morphology, size, and color.

2.3.3 Screening of Strains for Extracellular Protease Activity

1. The colonies are further screened on skim milk agar, which contained concentrations of NaCl ranging from 5 to 10% (w/v), to identify the presence of proteolytic activity in the isolates.
2. To prepare 1 L of 1.5% (w/v) skim milk agar containing 5% (w/v) NaCl, skim milk solution is prepared separately from the nutrient agar and NaCl solution. 28 g of nutrient agar is mixed with 50 g of NaCl. The pH is adjusted to 7, and distilled water is added until the volume of the agar reaches 800 ml. After that, 15 g of skim milk is weighed and distilled water added until the volume reaches 200 ml. The skim milk solution is autoclaved at 121 °C for 5 min. Both solutions (skim milk agar and NaCl nutrient agar) are then mixed to give a combined volume of 1 L.
3. Individual colonies on the 5% NaCl nutrient agar are streaked onto the skim milk agar using a sterile loop. Colonies which hydrolyze the skimmed milk will give rise to clear zones around them and will be considered as positive for protease production.

2.3.4 Gram Staining

1. A few drops of distilled water are placed on the surface of a glass slide, and bacterial colonies are smeared on it.
2. The water is dried and the specimen heat-fixed by moving the slide in and out of a flame for 2–3 times. Heat-fixing is needed to make sure the culture does not move about during visualization later.

3. A few drops of crystal violet are added to the fixed culture and left for 1 min. After that, it is washed off by using distilled water.
4. A drop of iodine is applied to the culture for 1 min and drained with distilled water after that.
5. A few drops of 95% ethanol are added for 10 s and washed off with distilled water later.
6. A few drops of safranin (a counterstain) are added for 45 s and then washed off with distilled water.
7. A few drops of oil are added to the slide to increase its resolution when viewed under a light microscope.

2.3.5 Preparation of Crude Enzyme

1. Selected colonies which show proteolytic activity are cultured in 5 ml of nutrient broth containing NaCl at 37 °C for 24 h in a shaking incubator at 250 rpm.
2. The cultures are centrifuged at 10,000 × g for 45 min at 4 °C. Extracellular enzymes which are produced from the microorganisms are in the solution mixture, so the supernatant fluid is collected when the pellet is removed.
3. The supernatant fluid is filtered using a 0.45 µm sterile syringe filter to remove the contaminants.

2.3.6 Protease Assay

1. A quantitative assessment of the volume (U/ml) of protease produced is determined using casein at 37 °C as a substrate. This procedure follows Sigma's non-specific protease activity assay (Sigma-Aldrich, Germany). 0.1 ml of the enzyme is added to 1 ml of casein (0.65% w/v in 50 mM potassium phosphate buffer, pH 7.5) and the mixture is incubated for 10 min.
2. 1 ml of trichloroacetic acid (110 mM) is added to terminate the reaction, and the mixture is incubated for 30 min.
3. The supernatant fluid is collected by centrifuging the mixture at 5000 rpm for 15 mins.
4. 0.5 ml of the supernatant fluid is mixed with 1.25 ml of sodium carbonate solution and 0.25 ml Folin & Ciocalteu's phenol reagent.
5. The reagents are mixed by gently inverting the tube several times. It is then centrifuged for 5 min at 14,000 rpm.
6. The supernatant fluid is collected by using a Millipore membrane filter and syringe. Absorbance is measured at 660 nm.
7. 1 unit of protease is defined as the amount of the enzyme required to liberate 1 µmol of tyrosine per minute under the predefined assay conditions.
8. The standard curve of tyrosine is constructed to calculate the amount (in µmol) of tyrosine equivalents released by using a standard curve linear equation.

9. Enzyme activity is calculated using the equation:

$$\text{Enzyme activity } U / ml = \frac{(\mu\text{mole tyrosine equivalent released}) \times (\text{total volume})}{(\text{Enzyme solution}) \times (\text{Colometric volume}) \times (\text{time})}$$

10. The specific activity of the enzyme is calculated using the equation:

$$\text{Specific activity } \frac{U}{\mu\text{g}} = \frac{\text{Enzyme activity } (U / ml)}{\text{Total protein } (\mu\text{g} / ml)}$$

2.3.7 Protein Determination

1. The protein concentration in the supernatant is determined by Bradford method using bovine serum albumin (BSA) as the standard (Bradford 1976). This procedure is in accordance with the manual instruction of Quick Start Bradford protein assay.
2. About 1 ml of 1x dye reagent (Quick Start Bradford) is added to microcentrifuge tube (or cuvette) and mixed with 0.2 ml of sample. Then, the tube is vortexed (or inverted).
3. The tube is incubated for 5 min – 1 h at room temperature. The absorbance of protein content is read at 595 nm.

2.4 Results and Discussion

2.4.1 Results (Figs. 2.1 and 2.2)



| Sample | Picture | Colony morphology | Bacterial shape | Gram staining |
|--------|---|------------------------|----------------------------|---------------|
| B1 |  | Irregular Off-white | Rods and groups in chains. | +ve (purple) |
| T1 |  | Circular Cream | Rods | +ve (purple) |

Fig. 2.1 Colony and bacterial morphology

Fig. 2.2 Clear zone around the colonies on skim milk agar plate showing protease production by the microorganisms

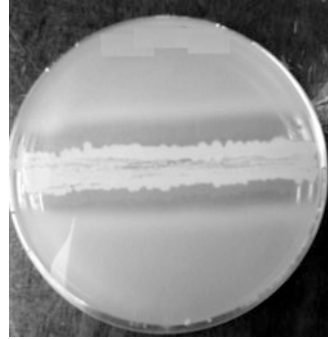


Table 2.4 Raw data for enzymatic activity of samples

| Test sample | Replicate readings | | Average | |
|-------------|--------------------|--------|---------|---------------------|
| B7 | 0.636 | 0.6354 | 0.6359 | 0.6358 ± 0.0003 |
| Blank | 0.030 | 0.0298 | 0.0297 | 0.0299 ± 0.0002 |

2.4.2 Discussion

Based on the observations for nutrient agar, the isolates were divided into two groups (Fig. 2.1) according to the morphology of the colonies. One group of colonies was irregular in shape, off-white and sticky while the other circular and cream-colored. After that, 40 colonies were streaked on milk salt agar to detect their proteolytic activities. Only 20 isolates produced proteases, as shown in Fig. 2.2. Clear zones indicated the hydrolysis of casein by proteases produced by the microorganisms. All of the 20 isolates were able to grow and tolerate NaCl concentrations of up to 10%. However, only 6 of them were selected for further analysis (i.e., enzyme assay).

The calculation of enzyme assay is shown below, using the raw data in Table 2.4:

$$\Delta A_{660} = \text{Average } \Delta A_{660nm}(\text{Sample}) - \text{Average } \Delta A_{660nm}(\text{Blank})$$

$$\begin{aligned} \text{Net absorbance} &= 0.6358 - 0.0299 \\ &= 0.6059 \end{aligned}$$

From net absorbance, the number of tyrosine equivalents (μmol) released is calculated from the linear equation of the standard curve of tyrosine (Fig. 2.3):

$$\begin{aligned} Y &= 4.181x \\ X &= 0.6059 / 4.181 \\ &= 0.1449 \mu\text{mol} \end{aligned}$$

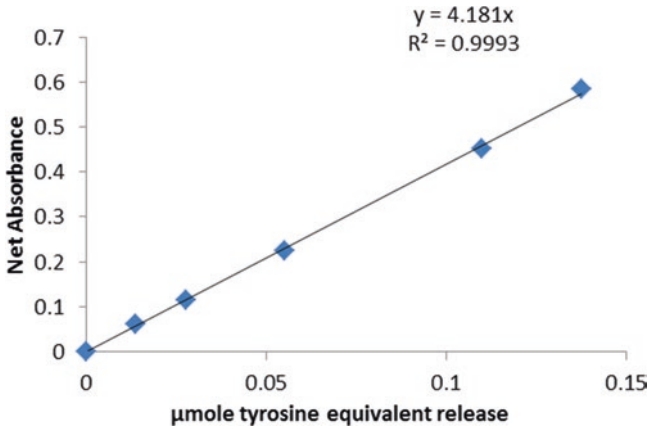


Fig. 2.3 Standard curve of tyrosine

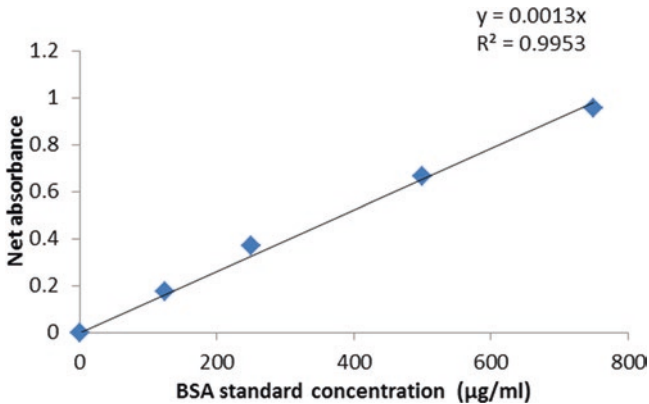


Fig. 2.4 Standard curve of bovine serum albumin (BSA)

Thus, a number of tyrosine equivalents released was $0.1449 \mu\text{mol}$ (Fig. 2.4). Then, the enzyme activity is calculated according to equation (2) below:

$$\text{Enzyme activity (U / ml)} = \frac{(0.1449 \mu\text{mol}) (2.2 \text{ ml total volume})}{(0.2 \text{ ml enzyme solution}) (0.5 \text{ ml colrimetric volume}) (10 \text{ min})}$$

$$= 0.3188 \text{ U / ml}$$

The protein content was also calculated from the linear equation of the standard curve of BSA (Fig. 2.3).

$$\Delta A_{595} = \text{Average } \Delta A_{595} \text{ nm (Sample)} - \text{Average } \Delta A_{595} \text{ nm (Blank)}$$

$$= 0.6389 - 0.5$$

$$= 0.1127$$

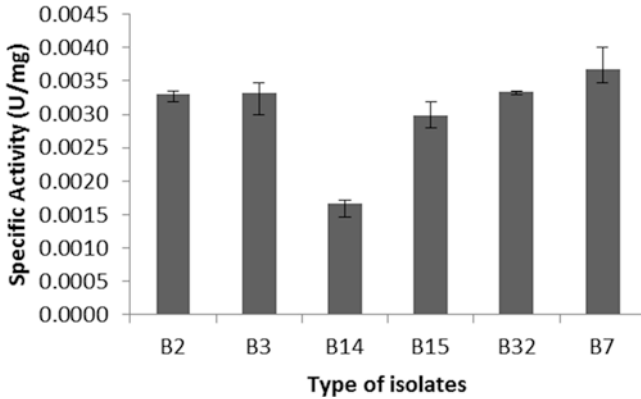


Fig. 2.5 Specific activity (U/mg) of different isolates. The bars indicate the standard deviation of the three replicates analyzed

Then,

$$y = 0.0013x$$

$$x = 0.1127 / 0.0013$$

$$x = 86.69 \mu\text{g} / \text{ml}$$

Thus, the specific activity (eq. 4) of protease can be calculated by:

$$\begin{aligned} \text{Specific activity (U / mg)} &= 0.3188 \text{ (U / ml)} / 86.69 \text{ (}\mu\text{g / ml)} \\ &= 0.00367 \text{ U / }\mu\text{g} \end{aligned}$$

Figure 2.5 shows the specific activity of different isolates. Evidently, isolate B7 has the highest specific activity compared to the others. Thus, it is selected for enzyme assay as the halophilic bacteria are highly likely to be able to produce halo-tolerant protease.

2.5 Conclusion

This study shows that it is possible to isolate bacterial strains that are capable of producing proteases by using skim milk agar. Moreover, such strains are also able to grow and tolerate NaCl concentrations of up to 10% NaCl which few microorganisms can survive and hence, the risk of microbial contamination can be reduced (Table 2.5).

Table 2.5 Raw data for protein content of samples

| Test sample | Replicate readings | | | Average |
|-------------|--------------------|--------|--------|-----------------|
| B7 | 0.6387 | 0.6388 | 0.6391 | 0.6389 ± 0.0002 |
| Blank | 0.5262 | 0.526 | 0.5263 | 0.5262 ± 0.0002 |

References

- Bradford MM (1976) A rapid and sensitive method for the quantitation of microgram quantities of protein utilizing the principle of protein-dye binding. *Anal Biochem* 72(1-2):248–254
- Karan R, Kumar S, Sinha R, Khare SK (2012) Halophilic microorganisms as sources of novel enzymes. In: Satyanarayana T (ed) *Microorganisms in sustainable agriculture and biotechnology*. Springer, Dordrecht/Heidelberg/London/New York
- Kumar CG, Takagi H (1999) Microbial alkaline proteases: from a bioindustrial viewpoint. *Biotechnol Adv* 17:561–594
- Setati ME (2010) Diversity and industrial potential of hydrolase- producing halophilic/halotolerant eubacteria. *Afr J Biotechnol* 9:1555–1560
- Ventosa A, Marquez MC, Garabito MJ, Arahal DR (1998) Moderately halophilic gram-positive bacteria diversity in hypersaline environment. *Extremophiles* 2:297–304

Chapter 3

Construction of Metagenomic DNA Libraries and Enrichment Strategies



**Farah Fadwa Benbelgacem, Hamzah Mohd. Salleh,
and Ibrahim Ali Noorbatcha**

Abstract Microorganisms are the main source of biocatalysts and with metagenomics approach it is now possible to overcome the major obstacle of microbiology which lies on the inability of the vast majority of microbes to grow under laboratory conditions. This chapter introduces and guides readers to a molecular biology approach that is useful for bioprospecting of novel, efficient and specific enzymes without escaping any unculturable or difficult to culture microorganisms. The first and necessary step of functional metagenomics is the metagenomic DNA library construction. It consists of metagenome extraction from the desired habitat, shearing of the DNA into sequences of desired size, end-repairing and cloning of these DNA sequences into a large-insert and high-copy number vector such as pCC1FOS with EPI300T^R *E. coli* as surrogate host, to the final step of storing the clones in glycerol stock for long term storage. Enrichment pre-DNA extraction step may be adopted to increase the likelihood that metagenomic DNA libraries hold the genes for the desired enzymatic activities.

Keywords Metagenomic library · Enrichment strategies · Function-based metagenomic · End-repair · High-throughput screening

F. F. Benbelgacem · I. A. Noorbatcha
Bioprocess and Molecular Engineering Research Unit, Kulliyah of Engineering,
International Islamic University Malaysia, Kuala Lumpur, Malaysia

H. M. Salleh (✉)
Bioprocess and Molecular Engineering Research Unit, Kulliyah of Engineering,
International Islamic University Malaysia, Kuala Lumpur, Malaysia

International Institute for Halal Research and Training, International Islamic University
Malaysia, Kuala Lumpur, Malaysia
e-mail: hamzah@iium.edu.my

Abbreviations and Chemical Formula

| | |
|--------------------------------------|----------------------------------|
| ATP | adenosine triphosphate |
| BACs: | bacterial artificial chromosomes |
| CMC | carboxyl methyl cellulose |
| DNA | deoxyribonucleic acid |
| dNTP | deoxyribonucleoside triphosphate |
| EDTA | ethylenediaminetetraacetic acid |
| EtBr | ethidium bromide |
| KCl | potassium chloride |
| K ₂ HPO ₄ | potassium hydrogen phosphate |
| LMP agarose | low melting point agarose |
| MgCl ₂ .6H ₂ O | magnesium chloride hexahydrate |
| MgSO ₄ .7H ₂ O | magnesium sulfate heptahydrate |
| NaCl | sodium chloride |
| Na ₂ CO ₃ | sodium carbonate |
| OD | optical density |
| PCR | polymerase chain reaction |
| POME | palm oil mill effluent |
| RNase | ribonuclease |
| TAE | tris-acetate-EDTA |
| TE | tris-EDTA |
| UV | ultraviolet |

3.1 Introduction

Up to 99% of existing microbial resources may be missed by using classic genomic study of microorganisms and traditional screening techniques. On the other hand metagenomics, culture-independent approach, which involves genomic analysis of DNA extracted from its natural environment is a more inclusive strategy to access microbial genetic reservoirs compared to traditional culture-dependent approaches to recover the whole microbial genetic information (Handelsman et al. 1998). Bioprospecting metagenomes is an attractive way of discovering potential new bioproducts such as enzymes. Depending on the screening strategy, metagenomic is divided into sequence- and functional-metagenomic approach by initially constructing metagenomic libraries of all microorganisms present from a habitat.

To increase the likelihood that metagenomic DNA libraries hold the genes for the desired enzymatic activities, an important optional pre-DNA extraction can be implemented; it is a selective method used to enhance the screening of microorganisms with special enzymatic activity favorably. The construction of metagenomic libraries from palm oil mill effluent for novel cellulose-degrading enzymes

is discussed here as an example of this approach. The chapter should help readers on how to:

1. Enhance enzymes bioprospecting with enrichment strategies.
2. Extract metagenomic DNA from a habitat and enrichment medium.
3. Construct metagenomic library for enzyme screening.

3.2 Metagenomic Approach

Environmental genomics, ecogenomics, community genomics or metagenomics, is the culture-independent novel strategy which revolutionized microbiology by paving the way for cultivation-independent assessment and exploitation of microbial communities present in complex ecosystems (Carola and Rolf 2011). A simple definition of metagenomics is a genomic analysis of microorganisms DNA isolated from their natural environment without going through the traditional, culture-dependent approaches. Depending on the screening type, two metagenomic approaches can be distinguished:

1. Function-based metagenomics (also known as functional metagenomics) involves library screening for functional activities resulting from the expression of genes within the bacterial metagenomic DNA. One major advantage of this approach is that this strategy has the potential to identify entirely new classes of genes encoding either known or indeed novel functions without requiring sequence-based information (Kennedy et al. 2011).
2. The sequence-driven analysis which involves the design and use of PCR primers or hybridization probes for the genes being targeted, which for enzymes is usually based on conserved regions of already well-characterized protein families.

The vector used in functional metagenomic approach should have the high efficiency of transformation and the capacity of self-maintenance in the cell host, and it has to be able to insert large DNA sequence to accommodate the gene or the cluster of genes needed. The vector necessitates a promoter and an appropriately located ribosome binding site (rbs) compatible with the host expression machinery. Proper transcription factors, inducers, precursors, chaperones, cofactors, post-translationally acting factors, and secretion mechanisms need to be provided by the host cell.

3.3 Library Construction Parameters

In the construction of metagenomic DNA library, high quantity of metagenomic DNA extract is required to cover the majority of microorganisms' genomes. Some metagenomic DNA Extraction Kits provide pre-extraction step to prepare the metagenomic DNA (Sabree et al. 2009).

3.3.1 Target Insert Size

The type of the gene target determines the size of the insert DNA sequence. If the enzyme is encoded by single gene, a small-insert library (~10 kb) can completely cover the gene, and if it is encoded by cluster of genes, a large-insert library can cover it, but in functional metagenomic approach it is preferable to work with the large one in order to avoid loss of genetic information (Sabree et al. 2009).

3.3.2 Cloning Vector

The choice of the cloning vector depends on the insert size and number of clones. For the construction of small-insert metagenomic library, plasmids (e.g., pUC derivatives, pBluescript SK(+), pTOPO-XL, and Pcf430) are used as vectors and for large-insert metagenomic library a fosmid vector (30–40 kb insert) or bacterial artificial chromosomes (BACs) (up to 200 kb insert) are used (Sabree et al. 2009).

3.3.3 Clones Number

Metagenomic libraries constructed with plasmid vectors require 3–20 times more clones comparing to fosmid libraries due to the small size of the insert. The fosmid vector pCC1FOS is characterized by the capability to control the copy number of clones by the addition of arabinose to increase the yield of DNA. This advantage makes the fasmids one of the important vectors in functional metagenomic approach (Sabree et al. 2009).

3.4 Enrichment Strategies

Enrichment of samples strategy is used to obtain microorganisms with special growth characteristics. It uses the principle of “natural selection”, wherein a mixed microbial population is inoculated in a medium of defined chemical composition and allowed to grow under controlled conditions (temperature, air supply, light, pH, etc.) in order to favor growth of certain types of microorganisms with specific characteristics (Praveen and Yasuhisa 2012). Enrichment of samples before metagenomic DNA extraction is an additional pre-screening method to facilitate and enhance enzyme screening with the addition of the substrate to be hydrolyzed by the enzyme in a medium almost similar to the habitat source. It is an important but non-compulsory step in metagenomics (Fig. 3.1). The DNA is extracted from the population within the sample that has been subjected to some pre-enrichment treatment.

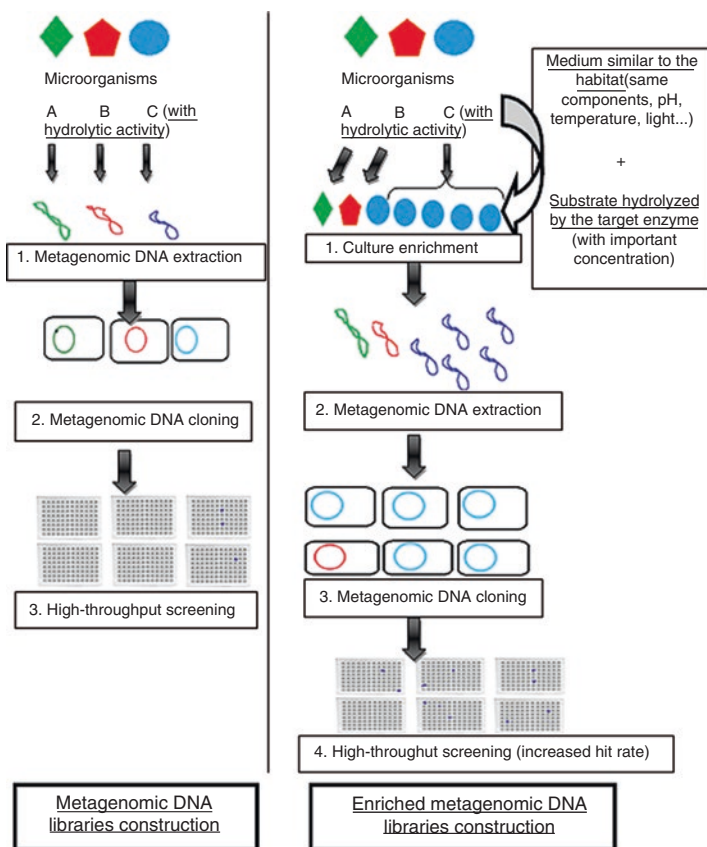


Fig. 3.1 Metagenomic DNA libraries construction using metagenomic DNA and enriched metagenomic DNA

In a metagenomic screening process (e.g., expression screening of metagenomic libraries), the target gene(s) represent a small proportion of the total nucleic acid fraction. Pre-enrichment of the sample thus provides an attractive means of enhancing the screening hit rate. The discovery of target genes can be significantly improved by applying one of the several enrichment options (Cowan et al. 2005) described in this chapter.

3.5 Materials

The most important apparatus, instruments, and chemicals needed for the construction of metagenomic DNA library with enrichment strategy are summarized in Table 3.1.

Table 3.1 General apparatus, instruments, chemicals and biochemicals needed in metagenomic DNA libraries construction with enrichment strategy

| | Apparatus/instrument | | Chemicals/biochemicals | | | |
|--|--|---------------------------|--|---|------------------|---|
| 1-Enrichment | Adjustable micropipette (100 µl – 1000 µl) | | CMC | | | |
| | Beakers | | MgCl ₂ .6H ₂ O | | | |
| | Conical flask | | CH ₃ CO ₂ H | | | |
| | Measuring cylinders | | K ₂ HPO ₄ | | | |
| | Incubator/shaker | | KCl | | | |
| | pH meter | | NH ₄ NO ₃ Yeast extract | | | |
| 2-Metagenomic DNA extraction | Microcentrifuge | | Washing buffer | | | |
| | Water bath | | Lysozyme (10% w/v) | | | |
| | Fridge/chiller (4 °C to 10 °C) | | | | | |
| | Freezer (–20 °C, –80 °C) | | RNase (1% w/v) | | | |
| | Filter vacuum | | Proteinase K (1% w/v) | | | |
| | 0.45 µm filter membrane | | MPC Isopropanol TE buffer, pH 8.0 | | | |
| 3-Metagenomic DNA Library Construction | (a) Size and concentration analysis | 20 cm agarose gel | TAE buffer Agarose | | | |
| | | Electrophoresis apparatus | Ethidium bromide | | | |
| | | UV transilluminator | | | | |
| | (b) End repair of insert DNA | Thermocycler | | End repair enzymes/buffer dNTPs ATP Loading dye | | |
| | | | *EPI300T1 ^R , plating strain | Petri dish | LB agar | |
| | | | (c) Size selection of End repair DNA | UV transilluminator | | LMP agarose gel TAE buffer 6× loading dye Ethidium bromide |
| | | | | | (d) DNA recovery | Electrophoresis apparatus with accessories |
| | Sterilized scissor | TE buffer | | | | |
| | (e) Ligation reaction | Thermocycler | | ATP (10 mM) Fast Link DNA ligase/buffer | | |
| | (f) Packaging fosmid clones and titer test | Flasks (50 ml & 250 ml) | | LB broth medium supplied (Maltose + MgSO ₄) | | |
| | | | Spectrophotometer | Max Plax Lambda packaging extract Overnight culture of EPI300T1 ^R Overnight culture of LE392MP Chloramphenicol LB agar plates. | | |

(continued)

Table 3.1 (continued)

| | Apparatus/instrument | Chemicals/biochemicals |
|---------------|---|-------------------------|
| For all steps | Micropipettes and tips (favorable for DNA work) | Distilled/sterile water |
| | Sterile conical tubes (15 ml and 50 ml) | Ice |
| | Microcentrifuge tubes (200 μ l, 500 μ l and 1.5 ml) | Ethanol (70% and 100%) |
| | Incubator shaker | |
| | Beakers/flasks | |
| | Waterbath | |
| | pH meter | |
| | Fridge (4 °C–10 °C) & Freezer (–20 °C, –80 °C) | |
| | Laminar flow hood | |

3.6 Methods of Construction of Metagenomic DNA Libraries

As an example, the construction of metagenomic DNA libraries from the palm oil mill effluent (POME) sample will be the case study (Fig. 3.2).

3.7 Sample Enrichment

Procedure

1. Get samples in sterile containers and preferably in the same day of the experiment.
2. Prepare 1 liter of culture medium with similar compositions to the original habitat, as follows: CMC (10 g), yeast extract (1 g), $MgCl_2 \cdot 6H_2O$ (0.6 g), NH_4NO_3 (0.75 g), KCl (2 g), K_2HPO_4 (1 g), CH_3COOH to adjust pH 4.2 (Rees et al. 2003).
3. Add 1 ml of “POME sample” to 200 ml of medium.
4. Incubate 7–15 days in similar conditions with regard to temperature, pH, and light.

3.8 Metagenomic DNA Extraction

Based on the same principle of genomic DNA extraction, metagenomic DNA can be directly extracted by cell lysis within sample matrix “for high yield and low metagenomic DNA size” (Voget et al. 2003) or indirectly when extraction of cells from the environmental material prior to the lytic release of DNA “for low yield and high metagenomic DNA size” (Kauffmann et al. 2004). Metagenomic DNA extraction is also classified into chemical method for lysis using enzymatic lysozyme or hot detergent (e.g., SDS), mechanical methods by disrupting the rigid cell structure

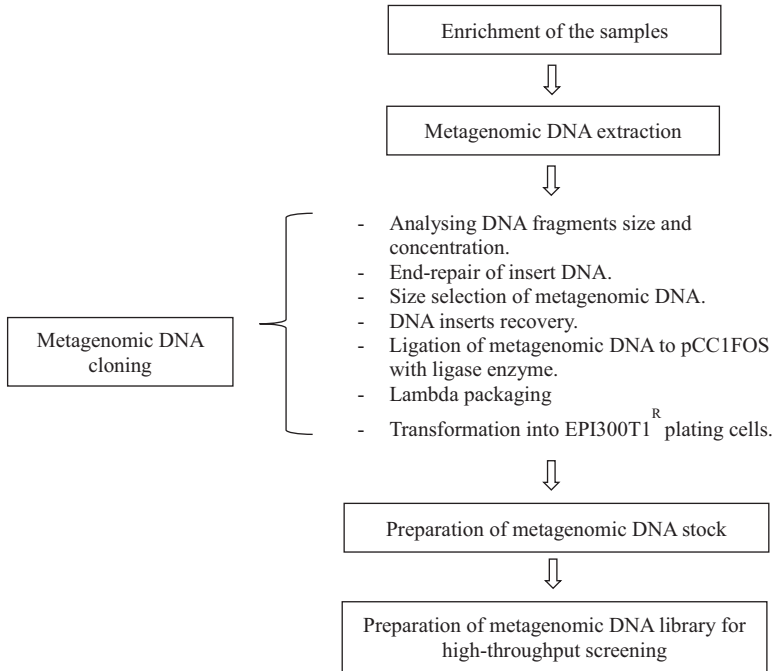


Fig. 3.2 Methodology for the construction of metagenomic DNA libraries with enrichment strategies

like bead beating, freeze-thawing and sonication methods and metagenomic DNA extraction can be carried out by combination of different methods for best quality and yield (Fig. 3.3).

Metagenomic DNA extraction can be performed using a special Kit (Meta-G-enomic DNA isolation Kit) designed to isolate randomly sheared DNA of ≈ 40 kb. The Kit is compatible with the library construction protocol and very useful in term of rapidity and efficiency. In the absence of this Kit, one can choose a direct chemical method for DNA extraction.

Procedure (adopted from Meta-G-enomic DNA isolation Kit; Epicentre as shown in Fig. 3.4)

1. Filter the sample using ultrafiltration apparatus and 0.45 μm filter membrane.
2. Remove the membrane and place it in a 50 ml tube, then add 1 ml of filter wash buffer containing 0.2% Tween 20 to the filter pieces to wash off microbes trapped on the membrane.
3. Vortex the tube at low-speed setting and then increases the setting to the highest speed for 2 min with intermittent breaks.

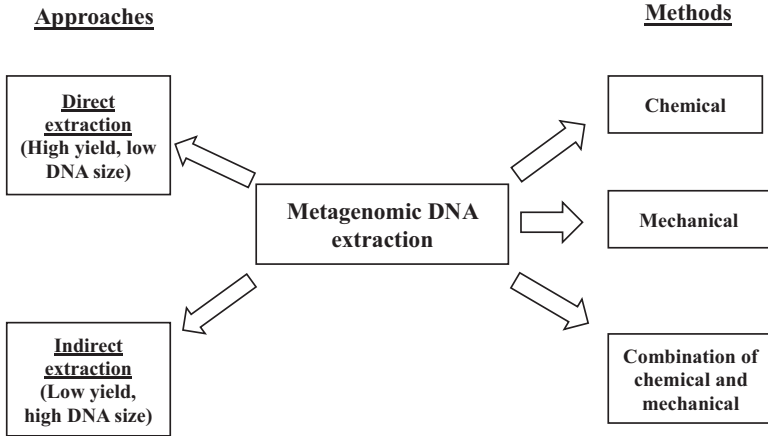


Fig. 3.3 Approaches and methods of metagenomic DNA extraction

- | | | |
|------------------------|---|--------------------------------------|
| 1) Washing buffer | ➡ | Microorganisms isolation |
| 2) Lysis solution | ➡ | Cell lysis |
| 3) RNaseA | ➡ | RNA degradation |
| 4) Proteinase K | ➡ | Cell proteins degradation |
| 5) MPC reagent | ➡ | DNA precipitation |
| 6) Ethanol/Isopropanol | ➡ | DNA purification |
| 7) TE buffer | ➡ | Solubilization of DNA and protection |

Fig. 3.4 Principle steps of metagenomic DNA extraction and their roles

4. Transfer the cell suspension to a clean microcentrifuge tube and centrifuged at 14,000×g for 2 min. Retain the cell pellet and discard the supernatant.
5. Resuspend the cell pellet in 300 µl of TE buffer and then add 2 µl of lysozyme solution and 1 µl of RNase A to the cell suspension.
6. Mix well by vortexing and then incubated at 37 °C for 30 min.
7. Add 1 µl of proteinase K and mix by vortexing.
8. Briefly, pulse-centrifuge the tube to ensure that all of the solutions is at the tube's bottom.
9. Incubate at 65 °C for 15 min.

10. Cool to room temperature, and then place on ice for 3–5 min.
11. Add 350 μl of MPC protein precipitation reagent to the tube and mix by vortexing vigorously for 10 s.
12. Pellet the debris by centrifugation for 10 min at 20,000 $\times g$ or maximum speed, in a microcentrifuge at 4 °C.
13. Transfer the supernatant to a clean microcentrifuge tube and discard the pellet.
14. Add 570 μl of isopropanol to the supernatant. Mix by inverting the tube several times.
15. Pellet the DNA by centrifugation for 10 min at 20,000 $\times g$ or maximum speed, in a microcentrifuge at 4 °C.
16. Use a pipet tip to remove the isopropanol without dislodging the DNA pellet. Briefly, pulse-centrifuge the sample and remove any residual liquid with a pipet tip, without disturbing the pellet.
17. Add 500 μl of 70% ethanol to the pellet without disturbing the pellet. Then centrifuge for 5 min at 20,000 $\times g$ or maximum speed, in a microcentrifuge at 4 °C. Use a pipet tip to remove the ethanol without dislodging the DNA pellet. Briefly, pulse-centrifuge the sample and remove any residual liquid with a pipet tip, without disturbing the pellet.
18. Air-dry the pellet for approximately 10 min at room temperature. (Note: Do not over-dry the DNA pellet.)
19. Resuspend the DNA pellet in 50 μl of TE buffer.

3.9 Molecular Cloning of Metagenomic DNA

Molecular cloning is an “*in vivo*” amplification method which permits the study of genetic information and protein expression as well. DNA library is a community of clones resulting from a cloning process which consist on a ligation after end-repairing of a DNA fragment (i.e. the DNA target of the study) to a vector to form a DNA recombinant using a ligase enzyme followed by its transformation into a cell host (generally a bacteria) by electroporation or phage infection. The vector can be natural like bacterial plasmids or phagic chromosome, or artificial vector with the advantage concerning the size of the DNA insert and the transformation stability. The auto-induction of bacterial multiplication results in the multiplication of the recombinant DNA to larger number of copy, and during the cell host metabolic activities, the appropriate proteins will be expressed. In this step, high molecular weight metagenomic DNA (≈ 40 kb) will be cloned into a pCC1FOS fosmid of the CopyControl Fosmid Library Production Kit (Epicentre) following the manufacturer’s protocol (Fig. 3.5).

The randomly-sheared metagenomic DNA is repaired to 5’-phosphorylated blunt ends. The DNA of 40 kb size is purified from low melting point (LMP) agarose gel electrophoresis and ligated to pCC1FOS fosmid, the advantage of this vector is the possibility of cloning into a stable low-copy-number vector, which during screening

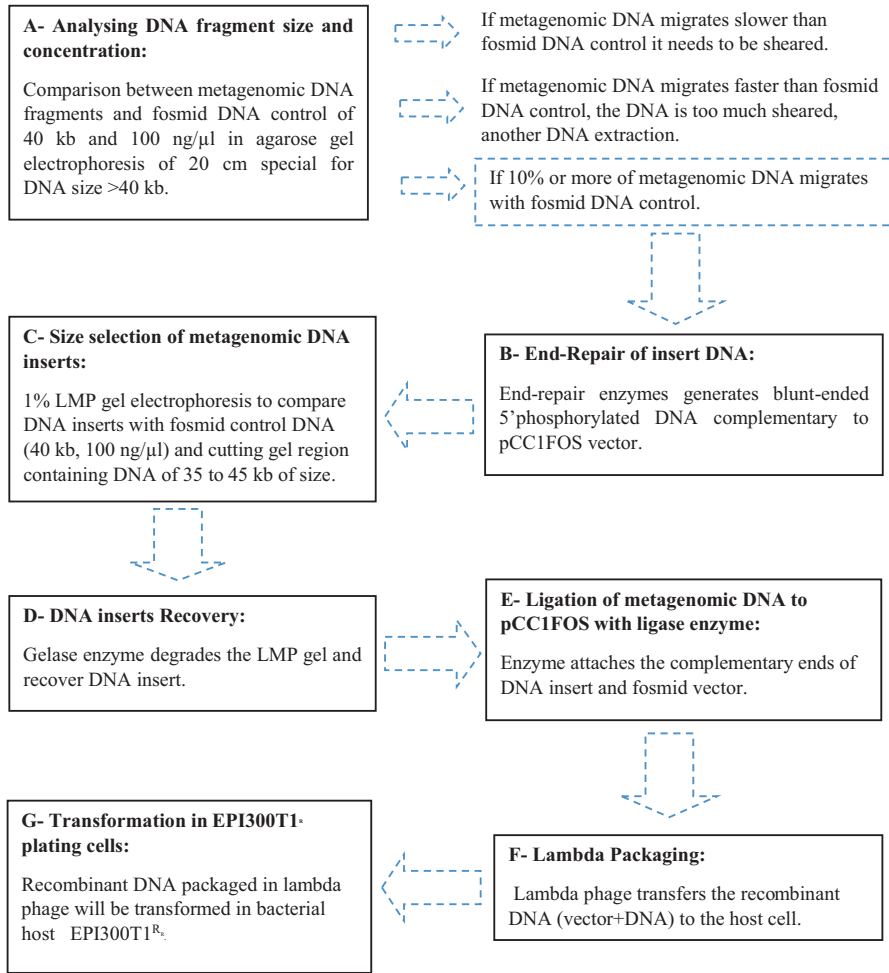


Fig. 3.5 Metagenomic DNA cloning to pCC1FOS and transformed into EPI300T1^R host cell

will induce to a high copy number. Since pCC1FOS fosmid vector accepts rather large DNA fragments, the library could be screened not only for small genes but also for whole operons. The pCC1FOS fosmid construct is packaged in lambda phages and plated on EPI300T1^R plating cells for the clones growing.

In case of construction of metagenomic DNA library using metagenomic DNA extracted by the classic method (i.e., without Meta-G-enomic DNA Isolation Kit), there is a need to shear the environmental DNA randomly by passing it several times through a small bore pipette tip and test the DNA size and the concentration by the procedure described below.

3.9.1 Analyzing DNA Fragment Size and Concentration

Procedure

1. In case of absence of PFGE apparatus prepare 20 cm of 1% agarose gel with TAE buffer.
2. Use only 2 μl of DNA because of the small amount of the DNA.
3. Use 1 μl of fosmid DNA (100 ng/ μl , 40 kb) to compare the metagenomic DNA size.
4. Run electrophoresis overnight (30–35 V only).
5. Stain the gel by submerging in 0.5 $\mu\text{g}/\text{ml}$ ethidium bromide solution for 30 min.
6. Wash the gel with distilled water for few minutes to remove the extra ethidium bromide.
7. Visualize the gel with UV transilluminator ($\lambda_{300\text{nm}}$).

Interpretations

- Case 1: If the metagenomic DNA has migrated slower than the fosmid DNA control, there is a need to shear it because the size is more than 10 kb using pipetting several times (≈ 50 times) with a micropipette and small tips and test the size again.
- Case 2: If metagenomic DNA migrates faster than fosmid DNA control, it means that it was too much sheared (< 40 kb), in this case, the metagenomic DNA isolation process needs to be repeated.
- Case 3: If more than 10% of the metagenomic DNA migrates with fosmid DNA control, it is ready to proceed to the next step.

3.9.2 End-Repair of Insert DNA

Procedure

The following steps are to generate blunt-ended, 5'-phosphorylated metagenomic DNA:

1. Thaw and thoroughly mix all reagents listed below before dispensing. Place on ice and add the reagents (present in CopyControl Fosmid Library construction) sequentially.
 - 8 μl 10X End-Repair Buffer
 - 8 μl 2.5 mM dNTP mix
 - 8 μl 10 mM ATP
 - up to 20 μg insert DNA (around 0.5 $\mu\text{g}/\mu\text{l}$)
 - 4 μl End-Repair Enzyme Mix
 - 80 μl Total reaction volume
2. Incubate at room temperature for 1 h.
3. Incubate at 70 °C for 10 min to inactivate the End-Repair Enzyme.
4. Add 15 μl of 6X loading dye to the end repair reaction tube and store at -20 °C or proceed to the next step.

3.9.3 Size Selection of Metagenomic DNA Inserts

Procedure

1. Test the size using 1% LMP gel electrophoresis by comparing end-repaired DNA fragments to fosmid control DNA.
2. Cut only the marker, fosmid control DNA and slit of end-repaired metagenomic DNA part of the gel and stain it in EtBr solution to visualize and select the location of metagenomic DNA with desired size (Fig. 3.6).
3. Transfer the gel slices to tarred tubes. At this stage, samples can be stored at 4 °C to -20 °C for up to 1 year.

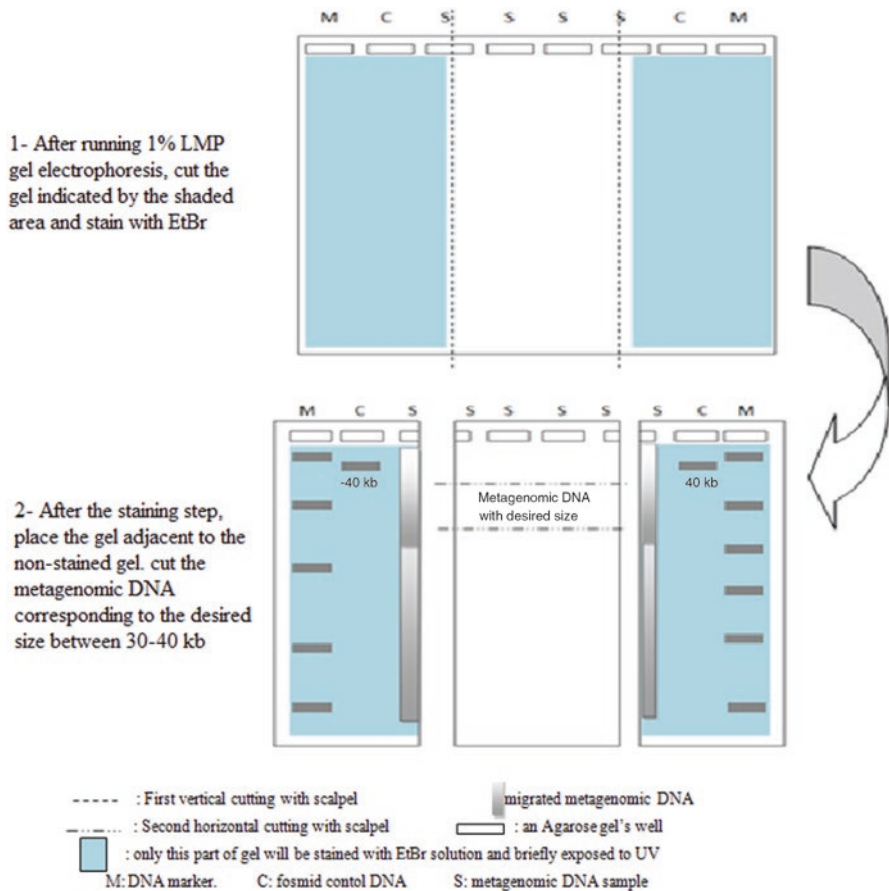


Fig. 3.6 Size selection of end-repaired metagenomic DNA with 1% LMP gel electrophoresis comparing to fosmid control DNA

3.9.4 DNA Inserts Recovery

Procedure

Before beginning this step, prepare a 70 °C and a 45 °C water bath or other temperature-regulated apparatus.

1. Weigh the tarred tubes containing the gel slices (1 mg of solidified agarose = 1 µl of molten agarose upon melting).
2. Warm the GELase 50X Buffer to 45 °C at the same time melt the LMP agarose by incubating the tubes at 70 °C for 10–15 min and then quickly transfer them to 45 °C.
3. Calculate and add the appropriate volume of warmed GELase 50X Buffer to 1X final concentration and then carefully add 1 µl of GELase enzyme to the tube for each 100 µl of melted agarose. Keep the melted agarose solution at 45 °C and gently mix the solution. Incubate the solution at 45 °C for at least 1 h.
4. Transfer the reaction to 70 °C for 10 min to inactivate the GELase enzyme.
5. Remove 500 µl aliquots of the solution into sterile microcentrifuge tubes.
6. Chill the tubes in an ice bath for 5 min and then microcentrifuge at maximum speed for 20 min. Carefully remove the upper 90%–95% of the supernatant which contains the DNA and transfers it to a sterile microcentrifuge tube.
7. The following sub-steps are to recover the DNA:
 - (a) Add 1/10 volume of 3 M sodium acetate and mix gently.
 - (b) Add 2.5 volumes of ethanol. Cap the tube and mix by gentle inversion.
 - (c) Allow precipitation to proceed for 10 min at room temperature.
 - (d) Centrifuge the precipitated DNA for 20 min in a microcentrifuge at top speed.
 - (e) Carefully aspirate the supernatant from the pelleted DNA.
 - (f) Wash the pellet twice with cold, 70% ethanol, repeating steps (d) and (e), using care not to disrupt the DNA pellet.
 - (g) After the second 70% ethanol wash, carefully invert the tube and allow the pellet to air-dry for 5–10 min.
 - (h) Gently resuspend the DNA pellet in TE buffer.
8. Determine the DNA concentration by fluorometry.

3.9.5 Ligation of Metagenomic DNA to pCCIFOS with Ligase Enzyme

Procedure

1. Determine the approximate number of CopyControl fosmid clones that is needed for the library to ensure that all DNA sequences are available in the constructed library. The number of fosmid clones required needs to be determined using this equation.

$$N = \ln(1-P)/\ln(1-f)$$

Where N is the required number of clones, P is the desired probability and f is the proportion of the genome contained in single clone.

Set up a 20 μ l ligation using all of DNA (or 10 μ l ligation with half volumes)

2 μ l 10X Fast-Link Ligation Buffer

2 μ l 10 mM ATP

2 μ l CopyControl pCC1FOS (0.5 μ g/ μ l)

x μ l concentrated insert DNA (approximately 0.5 μ g total DNA)

2 μ l Fast-Link DNA Ligase

y μ l sterile water for a total of 20 μ l

2. Also, set up a 10 μ l ligation using 2 μ l of control DNA in the kit for ligation control (present in the Kit).
3. Incubate at 16 $^{\circ}$ C overnight using a thermocycler.
4. Prepare 2 flasks of supplemented LB broth for the next step (see Appendix B).
5. Add a single colony of EPI300 in 1 of these flasks, and a culture of the phage control plating strain LE392MP in the other.
6. Incubate in a shaking incubator at 37 $^{\circ}$ C overnight.
7. The next day, inactivate the ligase at 70 $^{\circ}$ C for 10 min and freeze at -20 $^{\circ}$ C.

3.9.6 *Lambda Packaging*

Procedure

1. Thaw on the ice, one tube of the MaxPlax lambda packaging extract.
2. Set a water bath to 30 $^{\circ}$ C and label one 1.5 ml microcentrifuge tube per sample and place on ice.
3. (Thaw ligations if frozen). Add 10 μ l ligation to the labeled tube and 25 μ l phage to this tube as well.
4. Prepare one tube with 1 μ l control ligation from the Kit and 2.5 μ l phage.
5. Briefly, spin down the tubes and incubated at 30 $^{\circ}$ C for 2 h.
6. After 1 h, thaw the same tube of Packaging Extract on ice for 30 min.
7. When the time of incubation is complete, add another 25 μ l phage to the tube and add 2.5 μ l phage to the control tube, spin down and incubate at 30 $^{\circ}$ C for another 90 min.
8. Inoculate the second flask of LB with 3 ml of overnight culture, and incubated at 37 $^{\circ}$ C with shaking until it reaches log phase (see Appendix D for bacterial growth measurement).
9. Dilute the phage packaging reaction by adding 150 μ l Phage Dilution buffer. Flick to mix and briefly centrifuge and add only 15 μ l to the control tube.

3.9.7 Transformation in EPI300T1R Plating Cells

Procedure

1. Transfer 150 μl of diluted phage to a new tube, add 4 ml of EPI300T1^R cell culture and incubated at 37 °C for 20 min without shaking. For the ligation control, mix 10 μl phage and 300 μl EPI300T1^R cells.
2. On labeled, pre-warmed LB + chloramphenicol large plates, plate 50 μl , and 10 μl . Spread using glass spreader. Incubate upside down at 37 °C overnight.

3.10 Titer Test

In order to test the cloning technique success and the proximal number of metagenomic DNA colonies, a titer test has been carried out before the lambda packaging step. At this point, the fosmid clones can be packaged using a small amount of ligation and 200 μl cells to test the packaging efficiency by calculating a titer (see Appendix E).

3.11 Preparation of Metagenomic DNA Libraries Stock

The following protocol is for the preparation of the metagenomic DNA libraries stock and long-term storage with glycerol at -80 °C. If there is a plan to screen these libraries, replicates of the transformed bacteria into special 384-well plates should be conducted, and save the libraries stock.

Procedure

1. Prepare standard 384-well microplates with LB + 10% glycerol (around 80 μl per well).
2. Hand-pick each colony from large petri dish into one well and be sure that the swab or tooth-pick to hand-pick each colony is used only once.

3.12 Preparation of Metagenomic DNA Libraries for High-Throughput Screening

To screen the libraries for a special activity, replicates of the transformed bacteria in new microplates should be carried out. It is important to choose the type of microplates compatible to the screening method. For example, in the case of high-throughput screening of POME metagenomic libraries for cellulose-degrading enzyme bioprospecting with fluorescent substrates, black microplates for fluorescent detection should be used.

Procedure

1. Prepare 384-well plates with LB media + antibiotic (chloramphenicol) + arabinose (check for the correct vector-antibiotic-inducer requirements).
2. Hand-inoculate transformed *E. coli* from libraries stock to the high-throughput screening plates (preserve information of each clone, see Appendix F).
3. Incubate for 18 h at 37 °C.
4. Measure the bacterial growth before the screening.

At the end of this stage, the metagenomic libraries will be ready for high-throughput screening.

3.13 Appendices: Preparations, Calculations, and Measurements

3.13.1 Appendix A: Metagenomic DNA Isolation

Ethidium bromide 1% stock solution use 1 μ l of stock solution for each 100 ml of 1% agarose solution.

3.13.2 Appendix B: Metagenomic Library Construction

1. TAE buffer for electrophoresis
 - A 50X 1 liter stock solution
 - 242 g Tris base
 - 57.1 ml acetic acid
 - 100 ml 0.5 M EDTA
- Adjust pH to 8.5 with KOH solution. Store at room temperature.
2. LB broth medium: 1 liter
 - 10 g Bacto tryptone
 - 5 g yeast extract
 - 10 g NaCl
 - Medium is supplemented with MgSO₄ to a final concentration of 10 mM
- Store at room temperature.
3. Phage dilution buffer PDB (pH 8.3)
 - 10 mM Tris-HCl
 - 100 mM NaCl
 - 10 mM MgCl₂
- Store at room temperature.

4. LB broth agar

- 10 g Bacto tryptone
 - 5 g yeast extract
 - 10 g NaCl
 - Medium is supplemented with MgSO_4 to a final concentration of 10 mM
 - 15 g agar
- Dry the plates at room temperature and then store at +4 °C.

5. Chloramphenicol:

- 25 mg/ml
 - 100% Ethanol
- Store at -20 °C.

3.13.3 Appendix C: Test Antibiotic

Plate 25 μl of ligation control. Also plate out 50 μl of plain EPI300T1^R from the original flask, on one plate. This is a control for the antibiotics in the plate, and nothing should grow.

3.13.4 Appendix D: Measurement of Bacterial Growth

1. To measure bacterial growth, prepare 1 blank cuvette with 600 μl dH₂O and 300 μl LB broth. Label the top of the cuvette as you may need the blank several times.
2. After 1 h of incubation, dilute the culture 1 in 3, i.e., 600 μl dH₂O with 300 μl culture. Measure OD₆₀₀.
3. The desired undiluted OD reading is ~0.8-1. (If OD is greater than 1, start a new inoculation into the appropriate LB).
4. Measure after 1 h, and then every 15 min until the appropriate cell density is attained.

3.13.5 Appendix E: Ligation Titer Calculation Based on the Colonies Counted

Calculation: Colonies counted \times dilution factor \times total ligation \times phage dilution = colonies counted \times dilution factor \times 20 μl \times 2.

This gives total titer in cfu for using all the ligation, example:

if the number of count is 100 cells and it was a ¼ dilution plated:

$$100 \text{ colonies} \times 4 \times 20 \times 2 = 16000 \text{ cfu}$$

3.13.6 Appendix F: Microplates Labeling

Proper labeling is necessary for the inventory of metagenomic libraries. Try to find a clear style of labeling because with hundreds or thousands of microplates it will not be easy to identify the location of positive clones in the moment of screening, for example:

Source of metagenomic DNA/Number of microplate/date.

3.13.7 Others

1. Prepare high-molecular-weight genomic DNA from the organism using the MasterPure™ DNA Purification Kit or standard methods. Resuspend the DNA in TE buffer at a concentration of 0.5 µg/µl. This DNA will be referred to as the “insert DNA” throughout the write-up.
2. The EPI300T1^R plating strain is supplied as a glycerol stock. Prior to beginning the CopyControl Fosmid Library Production procedure, streak out the EPI300T1^R cells on an LB plate. Do not include any antibiotic in the medium. Grow the cells at 37 °C overnight, and then seal and store the plate at 4 °C. The day before the Lambda Packaging reaction, inoculate 50 ml of LB broth + 10 mM MgSO₄ + 0.2% maltose with a single colony of EPI300T1^R cells and shake the flask overnight at 37 °C.

References

- Carola S, Rolf D (2011) Metagenomic analyses: past and future trends. *Appl Environ Microbiol* 77(4):1153–1161
- Cowan D, Meyer Q, Stafford W, Muyanga S, Cameron R, Wittwer P (2005) Metagenomic gene discovery: past, present and future. *Trends Biotechnol* 23(6):321–329
- Handelsman J, Rondon MR, Brady SF, Clardy J, Goodman RM (1998) Molecular biological access to the chemistry of unknown soil microbes: a new frontier for natural products. *Chem Biol* 5:R245–R249
- Kauffmann IM, Schmid RD, Schmitt J (2004) DNA isolation from soil samples for cloning in different hosts. *Appl Microbiol Biotechnol* 64:665–670
- Kennedy J, O’Leary ND, Kiran GS, Morrissey JP, O’Gara F, Selvin J, Dobson ADW (2011) Functional metagenomic strategies for the discovery of novel enzymes and biosurfactants with biotechnological applications from marine ecosystems. *J Appl Microbiol* 111:787–799

- Praveen K, Yasuhisa A (2012) Strategies for discovery and improvement of enzyme function: state of the art and opportunities. *Microb Biotechnol* 5:18–33
- Rees HC, Grant S, Jones B, Grant WD, Heaphy S (2003) Detecting cellulase and esterase enzyme activities encoded by novel genes present in environmental DNA libraries. *Extremophiles* 7:415–421
- Sabree ZL, Rondon MR, Handelsman J (2009) Metagenomics. In: Schaechter M (ed) *Encyclopedia of microbiology*, 3rd edn. Elsevier, Amsterdam
- Voget S, Leggewie C, Uesbeck A, Raasch C, Jaeger KE, Streit WR (2003) Prospecting for Novel Biocatalyst in a Soil Metagenome. *Appl Environ Microbiol* 7:6235–6242. Epicentre: <http://www.epibio.com/>

Chapter 4

Thermotolerant Bacteria Producing Fibrinolytic Enzyme



Azura Amid and Nurul Aqilah Ab. Shukor

Abstract Fibrinolytic enzyme is very useful protease in degrading fibrin for the treatment of thrombosis. Producing the fibrinolytic enzyme at industrial scale involves many steps that require the identified enzyme to be resistant to high temperature, especially during the drying process. Therefore, a thermotolerant enzyme is an advantage, and it is possible to identify this kind of enzyme by isolating the thermotolerant microbe from the hot spring. Thus, this chapter discusses the procedure to isolate fibrinolytic producing-bacteria from a hot spring.

Keywords Thermotolerant · Fibrinolytic · Fibrinogen · Thermophilic · Caseinolytic

4.1 Introduction

An unchecked alteration of fibrinogen to fibrin leads to thrombosis within the blood vessels. In general, there are four treatment options for thrombosis: surgery, anti-platelets, anticoagulants and fibrinolytic enzymes. Enzymes have many industrial and medical applications. They act as biocatalysts and allow complex reactions to occur everywhere and anytime in life. The enzymes produced by the human body are either digestive or systemic. Digestive enzymes work in the eponymous system where they break down food for easier absorption. Amylase, pepsin, and lactase – which break down starch, proteins, and fats respectively – are the most common digestive enzymes. Similarly, systemic enzymes, also called metabolic enzymes, work in the blood, tissues, and cells of the body systems. Some important systemic enzymes include proteases and catalases. Fibrinolytic enzymes, which are proteases, have the ability to degrade fibrin and can be extracted from plants, animals as well as microorganisms. In the past few years, many new fibrinolytic enzymes have been extracted from various types of microorganisms in the soil (Raju and Divakar

A. Amid (✉) · N. A. A. Shukor
Department of Biotechnology Engineering, Faculty of Engineering, International Islamic University Malaysia, Kuala Lumpur, Malaysia
e-mail: azuraamid@iium.edu.my

2013; Mukherjee and Rai 2011), oceans (Huang et al. 2013; Mahajan et al. 2012), fermented food (Jeong et al. 2015; Afifah et al. 2014; Sanusi and Jamaluddin 2012) and fish products (Vijayaraghavan and Vincent 2014; Prihanto et al. 2013; Montriwong et al. 2012).

Thermophilic bacteria are classified into moderate or extreme thermophiles. They thrive in temperatures exceeding 60 °C (Bruins et al. 2001; Sellek and Chaudhuri 1998; Synowiecki 2010) and are usually able to produce thermophilic enzymes owing to the nature of their habitat.

4.2 Principles

The skim milk test, which involves the usage of an agar made of skim milk, was used to identify protease-producing bacteria. If a bacterium expresses proteases, it will be able to break down casein (milk protein) in skim milk and use the resulting amino acids for its growth. Proteases make the agar clear as the opaque characteristic of the proteins is lost.

Fibrinolysis is the breaking down of fibrin and usually involves the enzymatic action of plasmin. Hence, plasmin is a fibrinolytic agent. Normally, fibrinolytic-producing organisms are isolated by surface plating on a fibrin agar medium. Fibrinolytic hydrolyze fibrin and result in clear zones on the agar plate.

4.3 Objective of Experiment

This experiment aims to isolate thermotolerant bacteria from hot springs and screen for thermotolerant bacteria that produce fibrinolytic enzymes.

4.4 Materials and Methods

4.4.1 Equipment (Table 4.1)

Table 4.1 Equipment used for this project

| No | Equipment | Aims of usage |
|----|------------------------|--|
| 1 | Weighing balance | To read absorbance at 600 nm |
| 2 | Incubator shaker | To ferment culture |
| 3 | Water bath | To maintain objects at the desired temperature |
| 4 | Spectrometer (A600 nm) | To read absorbance at 600 nm |
| 5 | pH meter | To read pH |
| 6 | Centrifuge | To separate supernatant fluid from precipitate |
| 7 | Pipette | To add solution into micro- centrifuge tubes |

4.4.2 Chemicals and Reagents (Table 4.2)

Table 4.2 Chemicals used for this project

| No | Chemicals | Manufacturer |
|----|-------------------------------|-------------------------------|
| 1 | Nutrient broth | Sigma-Aldrich, St. Louis, USA |
| 2 | Skim milk | OXOID |
| 3 | Nutrient agar | OXOID |
| 4 | Bradford reagent | Bio Basic, Canada |
| 5 | Bovine serum albumin (BSA) | Merck, Germany |
| 6 | L-tyrosine | Sigma-Aldrich, St. Louis, USA |
| 7 | Casein from bovine | Sigma-Aldrich, St. Louis, USA |
| 8 | Trichloroacetic acid | Sigma-Aldrich, St. Louis, USA |
| 9 | Folin's phenol reagent | Sigma-Aldrich, St. Louis, USA |
| 10 | Anhydrous sodium carbonate | Sigma-Aldrich, St. Louis, USA |
| 11 | Fibrinogen from bovine plasma | Sigma-Aldrich, St. Louis, USA |
| 12 | Thrombin from bovine plasma | Sigma-Aldrich, St. Louis, USA |
| 13 | Plasmin from human plasma | Sigma-Aldrich, St. Louis, USA |

4.4.3 Methodology

4.4.3.1 Isolation

1. Soil samples are collected from a hot spring using a sterilized 50 ml tube and spatula.
2. Temperature and pH values of the samples are immediately recorded using a thermometer and pH indicator respectively. All samples are transported without temperature control and analyzed within 24 h.
3. 1 g of the soil samples are added to 100 ml of distilled water to make soil suspensions. The samples are incubated at 53 for 1 h in a shaking incubator.
4. 2.8 g of nutrient agar powder is weighed and dissolved in 100 ml of distilled water on a hot plate. The solution is stirred vigorously and later sterilized in an autoclave for 15 min at 121. The solution is allowed to cool, after which it is dispensed in Petri dishes and allowed to solidify.
5. 10 μ l of the soil suspensions are spread onto the triplicate nutrient agar. The suspensions are incubated at 53°C for 24 h.
6. The growth colonies are stored as stock cultures in nutrient broth containing 30% glycerol at -80°C for further studies. The growth colonies are taken from the glycerol stock and will be cultured in 5 ml nutrient broth medium for acclimatization purposes.

4.4.3.2 Cell Morphology by Gram Staining

1. All isolated strains are grown on nutrient agar plates at 53°C for 24 h.
2. Sterile techniques are used to prepare a bacterial smear. A drop of water is placed on a slide, and bacteria are added to it by using a sterile cooled loop.
3. The bacteria are mixed and spread in a circular pattern using the inoculating loop. The smear is allowed to air-dry before it is heat-fixed.
4. The smear is flooded with crystal violet and allowed to stand for 1 min before the dye is washed off with tap water. Gram's iodine is then added and left for 1 min before it is washed off with tap water. Next, the smear is decolorized with 95% ethyl alcohol (ethanol). The alcohol is added drop by drop until no more crystal violet is washed out from the smear (after about 30 s). After that, the smear is gently washed with tap water. Counterstaining is done by adding safranin for 45 s and washing the slide with tap water afterwards.
5. The smear is blot-dried with blotting paper and examined under a light microscope via oil immersion technique.

4.4.3.3 Cell Motility by Hanging Drop Method

1. Using a cotton swab, a ring of petroleum jelly is applied around the depression of a glass slide.
2. A loopful of culture is placed at the center of a clean coverslip using sterile techniques.
3. The depression slide is placed over the coverslip with the concave surface facing down so that the depression covers the drop of culture.
4. The slide is pressed gently to form a seal between the slide and the coverslip. The slide is quickly turned over so that the drop continues to adhere to the inner surface of the coverslip.
5. The slide is examined under a light microscope. Initially, the drop culture is visualized under the low-power objective (10X), and the area of illumination is reduced by adjusting the condenser. This step is repeated using the high-power objective (40X).

4.4.3.4 Skim Milk Agar

1. 2% of distilled skim milk solution and 25 g of nutrient agar are mixed to give 1000 ml of skim milk agar for enzymatic screening.
2. The respective isolates are spread in a single line on the plates and are incubated at 53°C for 24 h.
3. Comparisons between the proteolytic potential of the isolates are made based on the diameters of the zones of casein hydrolysis and individual colonies. The diameters of the zones of hydrolysis are measured to the nearest mm.

4. The growth colonies are stored as stock cultures in nutrient broth containing 30% glycerol at -80°C for further studies. The growth colonies are taken from the glycerol stock and will be cultured in 5 ml nutrient broth medium for acclimatization purposes.

4.4.3.5 Caseinolytic Assay

1. Enzymatic assay, with casein as a substrate, is done to confirm for caseinolytic activities.
2. 1 ml of 0.65% (w/v) casein is added to each of several 15 ml tubes, which are then placed in a water bath at 37°C for about 5 min.
3. 0.2 ml of enzyme solution is added to the casein solution and is mixed by swirling. It is incubated at 37°C for exactly 10 min, after which 1 ml of 110 mM trichloroacetic acid (TCA) is added to stop the reaction. The mixture is swirled and then incubated at 37°C for about 30 min. Distilled water is used as a blank.
4. Each solution is centrifuged to yield the supernatant fluid needed for the next step. 1.25 ml of 500 mM Na_2CO_3 is pipetted and 0.5 ml of supernatant added into a 2 ml centrifuge tube. Then, 0.25 ml of 0.5 M Folin and Ciocalteu's phenol reagent (F-C) are immediately added to more consistent results.
5. The released tyrosine due to caseinolytic activity is measured at 660 nm absorbance (A_{660}) in suitable vials. A standard graph for tyrosine with five replications of different tyrosine concentrations against net absorbance at 660 nm is prepared. Caseinolytic activity is calculated by comparing with the tyrosine standard.
6. Enzyme activity is calculated by using equation below:

$$\text{Enzyme activity } U / ml = \frac{(\mu\text{mole tyrosine equivalent released}) \times (\text{total volume})}{(\text{Enzyme solution}) \times (\text{Colometric volume}) \times (\text{time})}$$

7. The specific activity of the enzyme is calculated by using the following equation:

$$\text{Specific activity } \frac{U}{\mu\text{g}} = \frac{\text{Enzyme activity } (U / ml)}{\text{Total protein } (\mu\text{g} / ml)}$$

4.4.3.6 Fibrin Plate

1. 6 ml of 0.6% fibrinogen in 0.1 M phosphate buffer at pH 7.4 is mixed with 6 ml of 1.5% agarose in the same buffer containing 10 NIH units of human thrombin.
2. The reagents are mixed gently and then poured in a Petri plate of diameter 90 mm. It is allowed to stand for 1 h at room temperature before use.

3. Holes of diameter 2 mm are made in the fibrin agar, into which 4 μl of crude enzymes are loaded. The fibrin agar plates are then incubated at 37°C for 2 h.
4. The diameters of clear zones are measured to determine the intensity of fibrinolytic activity with plasmin as a standard.

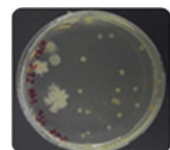
4.4.3.7 Fibrinolytic Assay

1. 45 μl of 0.6% fibrinogen and 5 μl of 0.01 NIH units/ μl of thrombin are mixed in 0.2 ml centrifuge tubes and are allowed to stand for 1 h to form fibrin clots.
2. 40 μl of 0.1 M phosphate buffer at pH 7.4 and 10 μl of crude enzymes are added to the fibrin clots and then incubated at 37°C for 3 min in a water bath.
3. The reaction is stopped by adding 10% trichloroacetic acid.
4. The mixture is kept at room temperature for 20 min before being centrifuged at 15,000 x g for 15 min.
5. The amount of tyrosine released due to fibrinolytic activity is measured at 280 nm absorbance (A_{280}).
6. A standard graph is prepared for plasmin (with five replications involving different plasmin concentrations) against the amount of tyrosine released.
7. Fibrinolytic activity is calculated by comparing with the plasmin standard.
8. Fibrinolytic activity of 1 plasmin unit (PU) is defined as the A_{280} equivalent of perchloric acid-soluble products released from fibrinogen in a reaction volume of 100 μl by NIH units of plasmin in 30 min at pH 7.4 and 37°C. One A_{280} is equivalent to 167 plasmin units (PU) in the above-defined conditions.

4.5 Results and Discussion

The primary stage in the development of an industrial fermentation process involves the isolation of strains which are capable of producing the target product in commercial yields. Screening of a large number of microorganisms is an important step in selecting highly potent microbial cultures for various uses. Samples were collected from Selayang Hot Spring, Selangor, Malaysia. 27 colonies of thermotolerant bacteria were isolated in pH 7 nutrient agar plates which were incubated at 53 °C for 24 h (Fig. 4.1). As per the results, 19 colonies of thermotolerant bacteria showed proteolytic activity when cultured on skim milk agar. The protease-secreting thermotolerant bacteria were then classified into four groups based on their colonial and bacterial morphologies. All of them were motile, cocci in shape and were

Fig. 4.1 Growth of isolated thermotolerant bacteria



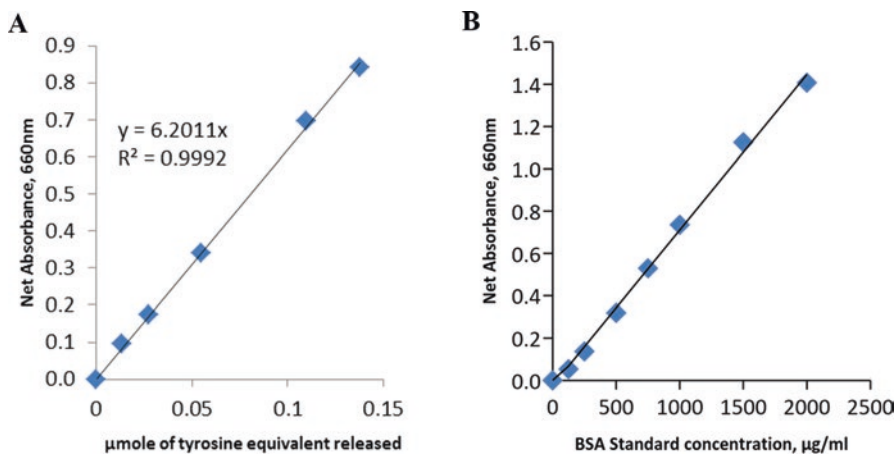


Fig. 4.2 Standard curve for casein (a) and total protein (b) assays

Table 4.3 Specific activity of caseinolytic assays

| Strain | Enzyme activity (U/ml) | Protein content (mg protein/ml) | Specific activity (U/mg protein) |
|--------|------------------------|---------------------------------|----------------------------------|
| HSP03 | 0.127 | 0.101 | 1.253 |
| HSP22 | 0.117 | 0.108 | 1.083 |
| HSP23 | 0.140 | 0.093 | 1.503 |
| HSP24 | 0.117 | 0.103 | 1.139 |
| HSP25 | 0.113 | 0.105 | 1.071 |
| HSP26 | 0.131 | 0.100 | 1.307 |

arranged in four ways: single, diplococci (pairs), streptococci (chains) and staphylococci (clusters). HSP04 and HSP11 strains were Gram-positive bacteria while the others Gram-negative.

Normally, fibrinolytic organisms are isolated by surface plating on a fibrin agar medium with subsequent screening for the desired characteristics. Proteolytic enzymes of bacteria do not automatically degrade fibrin, so fibrinolytic bacteria are needed. However, the number of species of fibrinolytic bacteria known to date is much smaller than that of proteolytic bacteria. Based on the results, HSP03, HSP22, HSP23 HSP24, HSP25 and HSP26 strains were showed fibrinolytic activity when tested with fibrin plate assay (Table 4.3). HSP23 showed an ability to degrade fibrin, giving rise to a clear zone diameter of 1.5 cm (Fig. 4.3). It is interesting to note that similar to proteolytic activity, HSP23 also showed high fibrinolytic activity with 33.543 U/mg protein (Table 4.4).

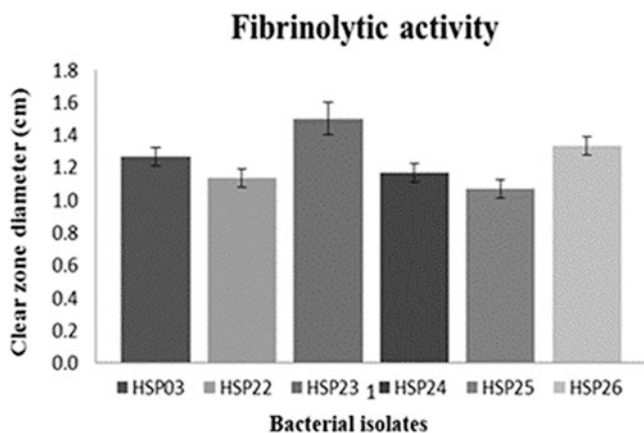


Fig. 4.3 Fibrinolytic activity based on fibrin plates containing various strains from soil of hot springs

Table 4.4 Specific activity from different fibrinolytic enzyme-producing strains

| Strain | Enzyme activity (U/ml) | Protein content (mg protein/ml) | Specific activity (U/mg protein) |
|--------|------------------------|---------------------------------|----------------------------------|
| HSP03 | 2.836 | 0.101 | 27.940 |
| HSP22 | 2.527 | 0.108 | 23.364 |
| HSP23 | 3.134 | 0.093 | 33.543 |
| HSP24 | 3.116 | 0.103 | 30.330 |
| HSP25 | 0.965 | 0.105 | 9.152 |
| HSP26 | 3.025 | 0.100 | 30.238 |

4.6 Conclusion

The search for promising strains of fibrinolytic protease producers is a continuous process. Thus, with the availability of thermostable bacteria, the production of fibrinolytic enzymes has a number of new applications. Although it is believed that such enzymes can provide tremendous economic benefits, achievement of the minimum production quantity required by industries remains a challenge.

References

- Afifah DN, Sulchan MS, Yanti D, Suhartono MT, Kim JH (2014) Purification and characterization of a fibrinolytic enzyme from bacillus pumilus 2.g isolated from gembus, an Indonesian fermented food. *Prev Nutr Food Sci* 19(3):213–219
- Bruins ME, Janssen AEM, Boom RM (2001) Thermozyymes and their applications. *Appl Biochem Biotechnol* 90:155–186

- Huang S, Pan S, Chen G, Huang S, Zhang ZLY, Liang Z (2013) Biochemical characteristics of a fibrinolytic enzyme purified from a marine bacterium, *Bacillus subtilis* HQS-3. *Int J Biol Macromol* 62:124–130
- Jeong S, Heo K, Park JY, Lee KW, Park J, Joo SH, Kim JH (2015) Characterization of AprE176, a fibrinolytic enzyme from *Bacillus subtilis* HK176. *J Microbiol Biotechnol* 25(1):89–97
- Mahajan PM, Nayak S, Lele SS (2012) Fibrinolytic enzyme from newly isolated marine bacterium *Bacillus subtilis* ICTF-1: media optimization, purification and characterization. *J Biosci Bioeng* 113(3):307–314
- Montriwong A, Kaewphuak S, Rodtong S, Roytrakul S, Yongsawatdigul J (2012) Novel fibrinolytic enzymes from *Virgibacillus halodenitrificans* SK1-3-7 isolated from fish sauce fermentation. *Process Biochem* 47:2379–2387
- Mukherjee AK, Rai SK (2011) A statistical approach for the enhanced production of alkaline protease showing fibrinolytic activity from a newly isolated Gram-negative *Bacillus* sp. strain AS-S20-1. *N Biotechnol* 28(2):182–189
- Prihanto AA, Darius, Firdaus M (2013) Proteolytic and fibrinolytic activities of halophilic Lactic Acid Bacteria from two Indonesian fermented Foods. *J Microbiol Biotechnol Food Sci* 2(5):2291–2293
- Raju EVN, Divakar G (2013) Screening and isolation of fibrinolytic protease producing bacteria from various regions in Bangalore. *Scholars Acad J Pharm (SAJP)* 2(1):27–30
- Sanusi NA, Jamaluddin H (2012) Purification of fibrinolytic enzyme from *Bacillus* Sp. Isolated from Budu. *J Technol* 59:63–68
- Sellek GA, Chaudhuri JB (1998) Biocatalysis in organic media using enzymes from extremophiles. *Enzymes Microb Technol* 25:471–482
- Synowiecki J (2010) Some application of thermophiles and their enzymes for protein processing. *Afr J Biochem Res* 9(42):7020–7025
- Vijayaraghavan P, Vincent SGP (2014) Statistical optimization of fibrinolytic enzyme production by *Pseudoalteromonas* sp. IND11 using cow dung substrate by response surface methodology. *Springerplus* 3(60): <https://doi.org/10.1186/2193-1801-3-60>

Chapter 5

Chemical Mutation Method for High CO₂-Requiring-Mutants of the Cyanobacterium *Synechococcus* sp. PCC 7002



Ummi Syuhada Halmi Shari, Azlin Suhaida Azmi, and Azura Amid

Abstract High carbon dioxide and others greenhouse gas emissions have caused the increasing of global temperature, leading to a significant rise in sea level, thus, disturbing the balance of ecosystems. These have encouraged researchers to explore several methods to reduce and mitigate CO₂ from atmosphere and one of the methods is by using microalgae to capture and utilize CO₂ from atmosphere or directly from flue gas. This biological method is economically feasible and environmentally sustainable alternative technology as the CO₂ will be consumed during photosynthesis, thus released oxygen and produced valuable biological products. Numerous studies on mutagenesis of cyanobacteria have greatly emerged purposely to change their genetic material specifically by altering the mechanism in cyanobacteria in order to increase the ability for carbon dioxide uptake. One of the mutagenesis methods is by random mutagenesis using chemical mutagen. It has been proven to be able to produce high CO₂-requiring-mutant of cyanobacteria. In this chapter, a modified of chemical mutation method using ethyl methanesulfonate based on Price and Badger (1989), is presented to randomly mutated *Synechococcus* sp. PCC 7002.

Keywords Chemical mutation · Mutants · *Cyanobacterium synechococcus* · Global warming · Greenhouse gas

5.1 Introduction

Increased of atmospheric carbon dioxide (CO₂) has contributed to a major challenge in global sustainability particularly on global warming. This has increased the concerns over greenhouse gases (GHG) emissions, as CO₂ is one of the anthropogenic

U. S. H. Shari · A. S. Azmi (✉) · A. Amid
Department of Biotechnology Engineering, Faculty of Engineering, International Islamic University Malaysia, Kuala Lumpur, Malaysia
e-mail: azlinsu76@iium.edu.my

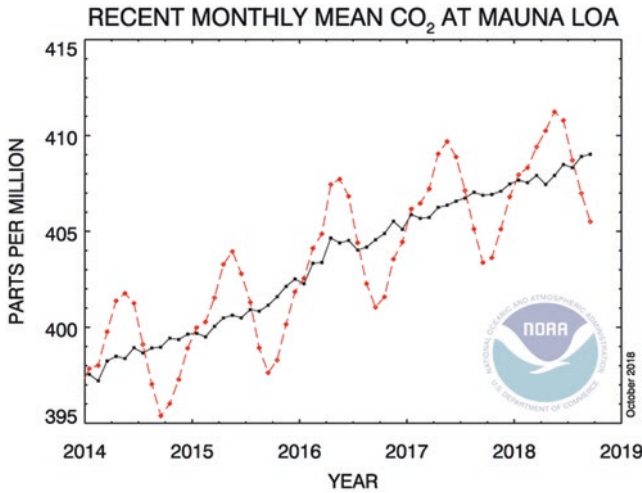


Fig. 5.1 Dashed red line with diamond symbols represents the monthly mean values, centered on the middle of each month. The black line with the square symbols represents the same, after correction for the average seasonal cycle. <https://www.esrl.noaa.gov/gmd/ccgg/trends/>

GHG. The data recorded by Earth System Research Laboratory (ESRL) showed that CO₂ emission had been reported to increase every year globally as shown in Fig. 5.1 (ESRL 2018). The graph shows the monthly mean of CO₂ emission globally averaged over marine surface sites.

High CO₂ and others GHG emissions have caused the increasing global temperature, leading to a significant rise in sea level, thus, disturbing the balance of ecosystems, causing the extinction of fauna species and changing the nature's pattern (Sudhakar et al. 2011). These have encouraged researchers to explore several methods to reduce and mitigate CO₂ from the atmosphere and one of the methods is by using microalgae to capture and utilize CO₂ from the atmosphere or directly from flue gas. This biological method is economically feasible and environmentally sustainable alternative technology as the CO₂ will be consumed during photosynthesis and will be released during combustion of biofuels produced (Kumar et al. 2010). Henceforth, CO₂ fixation by photoautotrophic algae cultures is the alternative way to alleviate the greenhouse gases in the atmosphere.

5.2 Cyanobacteria

Cyanobacteria, also known as blue-green algae, have been investigated recently for many purposes. Photosynthetic green plant poses higher growth rate as compared to plants (Machado and Atsumi 2012). Moreover, they are widely distributed on earth, exist naturally in water, hence have no issue on food vs. crop competition for diverse utilizations (Rosgaard et al. 2012). They are unique creatures as they have the

abilities to absorbing the sunlight energy for photosynthesis process, at the same time; they are able to absorb CO₂ and releasing oxygen, simultaneously. Many recent studies have suggested that cyanobacteria could be considered as a solution for the reduction of the atmospheric CO₂ level (Morais and Costa 2007; Yoo et al. 2010; Anjos et al. 2013). Cyanobacteria possess extremely effective single cell CO₂ concentrating mechanism (CCM) whose function is to maximize the intracellular CO₂ concentration around Rubisco, the CO₂ fixing enzyme.

Numerous studies on mutagenesis of cyanobacteria have greatly emerged purposely to change their genetic material specifically by altering the mechanism in cyanobacteria to increase the ability for carbon dioxide uptake. Random mutagenesis using chemical mutagen has been proven to be able to produce high CO₂-requiring-mutant of cyanobacteria (Price and Badger 1989)

5.3 Mutagenesis in Cyanobacteria

Mutagenesis is referred as the exposure or treatment of the biological material to a mutagen (Rieger et al. 1976). This will cause a mutation where a sudden, heritable, and detectable change in genetic material occurs. A mutagen is an agent that induces genetic mutation, which can be categorized into physical mutagen and chemical mutagen. Physical mutagens include electromagnetic radiation; such as gamma (γ) rays, X-rays, and ultraviolet (UV) light; and particle radiation, such as fast and thermal neutrons, beta and alpha particles (Kodym and Afza 2003). Chemical mutagens act as alkylating agents, cross-linking agents, and polycyclic aromatic hydrocarbons (PAHs). Various types of documented chemical mutagens are: ethyl methanesulphonate (EMS), methyl methanesulphonate (MMS), N-methyl-N'-nitro-N-nitrosoguanidine (MNNG) and mitomycin C. Based on the previous study, EMS (CH₃SO₂OC₂H₅) is the most frequent chemical mutagen that had been used on cyanobacteria for CO₂ mitigation research (Price and Badger 1989; Yu et al. 1994; Wu et al. 2000; Kao et al. 2012). The chemical mutagen such as EMS alkylates guanine, leading to the mispairing of guanine (G) with thymidine (T), instead of cytosine (C). The resulting point mutations are mainly lack of plastoquinone (PQ), demonstrating that plastoquinone GC to AT transitions (McCarthy et al. 2004, Halmi Shari et al. 2014). PQ is a quinone molecule involved in the electron transport chain in the light dependence reactions of photosynthesis. The concentration of chemical mutagen used, time and temperature incubation affect the degree of mutagenesis.

5.4 Objective of Experiment

This experiment aims to mutate the marine microalgae strain of *Synechococcus* sp. PCC 7002 using ethyl methanesulfonate (EMS).

5.5 Materials and Methods

5.5.1 Materials

All consumables and equipment in this procedure are listed in Tables 5.1 and 5.2.

Environmental Safety & Health (ESH) Considerations and Hazards

Mutagen EMS is volatile at room temperature and highly toxic. Thus, it is important to go through the material safety data sheet (MSDS) and perform a proper risk assessment before carrying out this experiment.

Table 5.1 List of consumable and the usage

| No | Consumable | Usage |
|----|--|--|
| 1 | Pipettes (200 μ L, 1 mL) | To add any solution into cuvette |
| 2 | Centrifuge Tube micro 1.5 mL conical bottom snap cap with gear rim | Use for volumetric analysis |
| 3 | Syringe filter 13 mm 0.22 μ m (N6) disposable | To filter the air flow |
| 4 | Gas refill labogaz France | Use for heating, sterilization, and combustion |
| 5 | Petri dish diameter 90 mm plastic, local sterile | Use to culture cell |

Table 5.2 List of equipment use during the procedure

| No | Equipment | Usage |
|----|--|--|
| 1 | Weighing balance (Mettler Toledo) | To weigh chemicals and other important materials |
| 2 | Air pump (SuperXX Air Pump) | To mix equally between nutrient and cells in the shake flasks |
| 3 | UV – VIS Spectrophotometer | To read absorbance at 630 & 640 nm |
| 4 | Laminar flow hood (ESCO) | To prepare sample and other preparation with sterilized handling |
| 5 | Dryer (Memmert) | To dry the algal biomass at 80 °C |
| 6 | Autoclave (ASTELL model SWIFTLOCK AUTOCLAVE 130 L) | To autoclave the media, sterilize glasswares |
| 7 | Centrifuger Eppendorf (Centrifuge 5804) | To harvest biomass from media, to separate pellet and supernatant. |
| 8 | Water bath (Memmert) | To boil the water at certain temperature |
| 9 | CO ₂ sensor | To measure the input & output of CO ₂ gaseous (%) |
| 10 | Purified CO ₂ Gas | To supply carbon sources |
| 11 | Lamp (Aquarium lamp: XiLong). (Model : XL-11W) | To provide light intensity |
| 12 | Light meter (Mini Light Meter : CENTER 337) | To detect the intensity of light (LUX) |
| 13 | Flowmeter (purchased for Stable Arm Sdn Bhd) | To control the air flow (air range: 0.6-6 LPM) |

5.5.2 Methodology

5.5.2.1 Culture Medium

The medium composition was based on culture ATCC medium 957.

1. Trace metal solution was prepared in 1 L distilled water in a Duran bottle. The trace metal composition is shown in Table 5.3.
2. The solution was sterilized in an autoclave.
3. The solution temperature was cooled down to 30 °C.
4. The resulting solutions were stored in a chiller unit, until further use.
5. In a different 1 L graduated flask, all chemicals were added to the right composition as shown in Table 5.4.
6. The pH of the culture medium was adjusted to 8.5 with the addition of potassium hydroxide (KOH) before autoclaving.
7. The solution was mixed, and the volume was raised up to 1L with distilled water.
8. The medium was autoclaved at 121 °C for 15 min for sterilization purpose.
9. About 1 mL of the trace metal solution prepared in Step 1, was added to the medium.
10. After the temperature was reduced to around 35 °C, 20 µg/L of vitamin B12 was added to the medium.
11. The medium was stored in a chiller for later use.

Table 5.3 Trace metal solution (1 L)

| Compound | Composition |
|---|-------------|
| H ₃ BO ₃ | 2.86 g |
| MnCl ₂ .4H ₂ O | 1.81 g |
| ZnSO ₄ .7H ₂ O | 0.222 g |
| CuSO ₄ .5H ₂ O | 0.079 g |
| CO(NO ₃) ₂ | 49.4 mg |
| Na ₂ MoO ₄ .2H ₂ O | 0.039 g |
| dH ₂ O | 1 L |

Table 5.4 Composition of ATCC medium 957 (1 L)

| Components | Composition |
|--|-------------|
| Magnesium sulfate.7H ₂ O | 0.04 g |
| Calcium chloride. 2H ₂ O | 0.02 g |
| Sodium nitrate | 0.75 g |
| Potassium phosphate dibasic | 0.02 g |
| Citric acid | 3.0 mg |
| Sodium carbonate | 0.02 g |
| Distilled water | 250 ml |
| Seawater | 750 ml |
| Ferric ammonium citrate | 3.0 mg |
| Ethylenediaminetetraacetic acid (EDTA) | 0.5 mg |

5.5.2.2 ATCC 957 Agar

1. ATCC medium (~ 8.5%) supplemented with 1.5% agar and 5 mM sodium thiosulfate was prepared.
2. The solution was stirred on a hot plate at 50 °C in order to dissolve it.
3. The dissolved solution was autoclaved at 121 °C for 15 min.
4. The agar solution was removed from the autoclave, and the temperature was reduced to 50 °C.
5. The solution was poured into a petri dish.
6. The solution was then allowed to solidify under the UV light (Caution!).

5.5.2.3 Chemical Mutation

The method was based on Prices and Badger (1989) with some modifications.

1. About 1 mL of cells was combined with 1 mL of phosphate buffer solution containing 0.01 M ethyl methylsulphonate (EMS).
2. The cells were mixed and incubated in the dark for 45 min at a temperature of 37 °C.
3. Inactivation of the mutagen was achieved by adding 10 mL of sodium thiosulphate (pH 8).
4. The cells were vortex-mixed after the inactivation of the mutagen.
5. The suspension was centrifuged at a speed of 4000 rpm for 5 min, and the cells (pallet) were then collected.
6. The cells were suspended in 1 mL of medium.
7. Step 5 and 6 were repeated to ensure that the mutagen has been fully removed and inactivated. Summary of the steps is shown in Fig. 5.2.

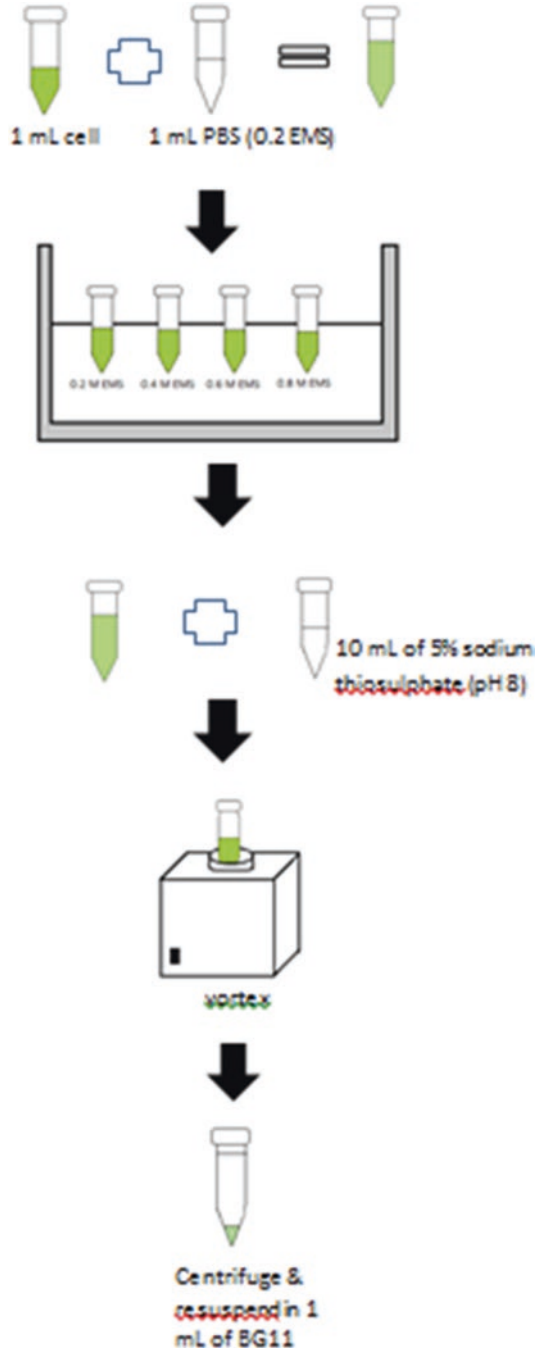
Caution: The experimental procedures that involved the use of EMS should be conducted in a fume hood. The waste-containing EMS should be collected separately from other chemicals.

Note: EMS is mutagenic, tetragenetic and carcinogenic component. Sodium thiosulphate should be used to neutralize any EMS spillage and to neutralize treatment solution after mutagenesis.

5.5.2.4 Isolation of Mutants

1. After washing from mutagenesis method, the mutated cells were grown in culture medium with 5% CO₂ or at any desired CO₂ concentration for 30 min, twice every day, in the presence of ampicillin and light in a few days until the green color appeared.
2. The cells were washed and plated on agar plates containing ATCC medium 957.
3. Incubation of the mixture was carried out with 5% CO₂ under a constant light intensity of 4000 lux at a temperature of 37 °C until the colonies are visible.

Fig. 5.2 Outline of procedure to mutant cells by using EMS



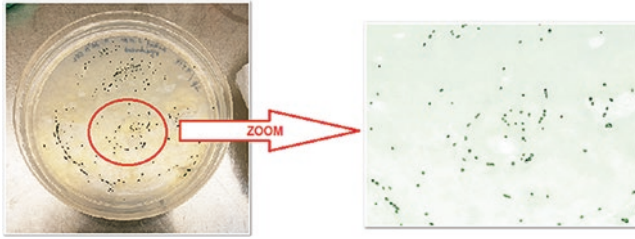


Fig. 5.3 Colonies of EMS treated *Synechococcus* sp. PCC 7002 on ATCC 957 solid agar medium

4. The colonies were screened on the duplicate plate.
5. Selected colonies were incubated for further analysis.

Note: Microalgae that was isolated from freshwater required 3–7 days to form visible colonies on agar with inorganic nutrients. However, the marine strains grew much slower than that of the freshwater strains. It took at least 15 days for the colonies of marine microalgae to appear (He et al. 2012).

5.6 Results

Figure 5.3 shows the colonies of EMS-treated *Synechococcus* sp. PCC 7002 on ATCC 957 solid agar medium after 3 weeks of incubation.

5.7 Discussion

The green, plant-like growth of single colonies, which is spotted on the agar medium, confirmed the photosynthesis process occurred naturally in the mutated species (Fig. 5.3). A slightly slower growth was observed for the first time based on the appearance of the single green colony after 3 weeks of incubation. This occurrence was due to the adaptation of mutated species to the new environment after the EMS treatment. The growth of mutated colony was then observed to become normal like wild strain, only after the second and third incubations on the solid agar. The wild strain of *Synechococcus* sp. PCC 7002 appeared as a green single colony after one to two weeks of incubation on solid agar medium. The observation on the mutant to CO₂ uptake was identified in the next experiment. Ten mutant strains of *Synechococcus* sp. PCC 7002 were isolated and subjected to the different level of CO₂ challenge in order to identify their potential to the CO₂ uptake.

5.8 Conclusion

A mutagenesis process on *Synechococcus* sp. PCC 7002 by ethyl methane sulfonate (EMS) has been presented. The mutagenesis that was performed with the lowest concentration of EMS needs to be subjected to the next experiment to identify the mutant ability to uptake the CO₂ uptake.

Questions

1. Differentiate between mutant, mutagenesis and mutagen.
2. In general, describes how EMS induces mutation.
3. State one chemical that can neutralize EMS.
4. Explain how mutagenesis could affect the CO₂ uptake

References

- Anjos M, Fernandes BD, Vicente AA, Teixeira JA, Dragone G (2013) Optimization of CO₂ biomitigation by *Chlorella vulgaris*. *Bioresour Technol* 139:149–154
- ESRL (2017) Recent global CO₂, NOAA/ESRL. Available at <https://www.esrl.noaa.gov/gmd/ccgg/trends/> (12/05/2017)
- Halmi Shari US, Azmi AS, Amid A, Raus RA, Muyibi SA, Jimat DN (2014) Mutagenesis on cyanobacteria for high CO₂ uptake: a review. *J Pure Appl Microbiol* 8:761–768
- He M, Li L, Liu J (2012) Isolation of wild microalgae from natural water bodies for high hydrogen producing strains. *Int J Hydrog Energy* 37(5):4046–4056
- Kao CY, Chiu SY, Huang TT, Dai L, Wang GH, Tseng CP, Chen CH, Lin CH (2012) A mutant strain of microalga *Chlorella* sp. for the carbon dioxide capture from biogas. *Biomass Bioenerg* 36:132–140
- Kodym A, Afza R (2003) Physical and chemical mutagenesis methods. *Mol Biol* 236:189–204
- Kumar A, Ergas S, Yuan X, Sahu A, Zhang Q, Dewulf J, Malcata XF, Langenhove H (2010) Enhanced CO₂ fixation and biofuel production via microalgae: recent developments and future directions. *Trends Biotechnol* 28:371–380
- Machado IMP, Atsumi S (2012) Cyanobacterial biofuel production. *Biotechnology* 162(1):50–56
- McCarthy SS, Kobayashi MC, Niyogi KK (2004) White mutants of *Chlamidomonas reinhardtii* are defective in phytoene synthase. *Genet Soc Am* 168:1249–1257
- Morais MGD, Costa JAV (2007) Isolation and selection of microalgae from coal fired thermoelectric power plant for biofixation of carbon dioxide. *Energy Convers Manag* 48:2169–2173
- Price GD, Badger MR (1989) Two phenotypes that accumulate inorganic carbon but are apparently unable to generate CO₂ within the carboxysome. *Plant Physiol* 91:514–525
- Rieger R, Michaelis A, Green M (1976) *Glossary of genetics and cytogenetics*. Springer Verlag, New York
- Rosgaard L, Alice JDP, Jacob HJ, Frigaard N, Sakuragi Y (2012) Bioengineering of carbon fixation, biofuels, and biochemicals in cyanobacteria and plants. *Biotechnology* 162(1):134–147
- Sudhakar K, Suresh S, Premalatha M (2011) An overview of CO₂ mitigation using algae cultivation technology. *Int J Chem Res* 3(3):110–117
- Wu T, Liu Y, Song L (2000) Selection & ultrastructural observation of a high-CO₂-requiring mutant of cyanobacteria *Synechococcus* sp. PCC7942. *Acta Bot Sin* 42(2):116–1221

- Yoo CS, Jun SY, Lee JY, Ahn CY, Oh HM (2010) Selection of microalgae for lipid production under high levels carbon dioxide. *Bioresour Technol* 101:S71–S74
- Yu J, Price GD, Badger MR (1994) A mutant isolated from the cyanobacterium *Synechococcus* PCC7942 is unable to adapt to low inorganic carbon conditions. *Plant Physio* 4:605–611

Chapter 6

Identification of Fatty Acid Methyl Ester in Palm Oil Using Gas Chromatography-Mass Spectrometer



Sarina Sulaiman

Abstract Biodiesel or Fatty Acid Methyl Ester (FAME) is a non-toxic, biodegradable alternative fuel that is easy to produce and process from vegetable oil or animal fats. In this chapter, identification of Fatty Acid Methyl Ester in palm oil biodiesel using GCMS has been studied. The main component existed in FAME are Caprylic acid C8:0, Capric acid C10:0, Myristic acid C14:0, Palmitic acid C16:0, Stearic acid C18:0, Oleic acid C18:1, Arachidate acid C20:0 and Docosanoic acid C22:0.

Keywords Fatty acid methyl ester · Palm oil · Gas chromatography-mass spectrometer · Biodiesel · Transesterification · Vegetable oil · Coconut waste · Egg shell · Heterogeneous catalyst · Chromatogram

6.1 Introduction

Biodiesel is a non-toxic, biodegradable alternative fuel that is easy to produce and process from vegetable oil or animal fats. It can be used in any diesel engine without any modifications. It typically produces around 60% less carbon dioxide than petroleum-based diesel, as it is produced from atmospheric carbon dioxide via photosynthesis in plants. Since biodiesel can be used in some diesel engines, the renewable fuel can directly replace petroleum products, decreasing the country's dependency on imported oil (Ong et al. 2011).

Biodiesel or fatty acid methyl ester (FAME) can be produced by transesterification of vegetable oils with alcohols. Transesterification process involves the reaction of alcohol, such as methanol and ethanol, with vegetable oils or fats as feedstocks, with the presence of a catalyst. The transesterification process can be optimized

S. Sulaiman (✉)

Department of Biotechnology Engineering, Kulliyah of Engineering, International Islamic University Malaysia, Kuala Lumpur, Malaysia
e-mail: sarina@iium.edu.my

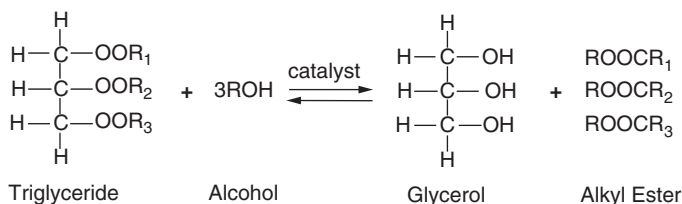
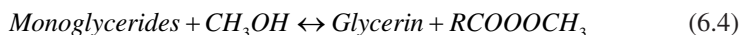
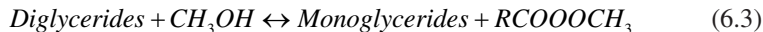
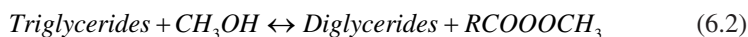
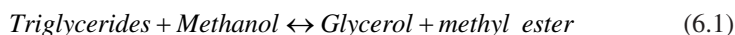


Fig. 6.1 Transesterification process

based on the reaction conditions such as the type of alcohol, reaction temperature, oil to alcohol ratio, catalyst loading, and reaction time. In the reaction, three units of alkyl esters are produced from one triglyceride molecule. A byproduct, glycerol, is also produced in a molar ratio of 1:1 of glycerol to triglyceride, further adding to the value of processing oils (Yan et al. 2010). Figure 6.1 presents the reaction of transesterification process.

This well-established process which was introduced in the nineteenth century has been used to exploit the fatty acid and triglyceride content of a variety of natural oils for biodiesel production over the years (Yan et al. 2010).



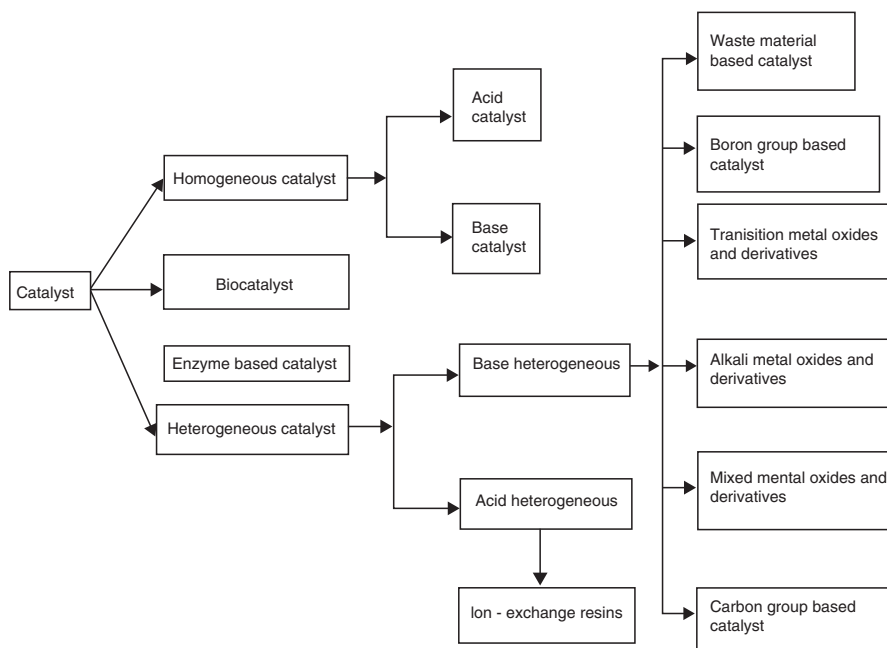
In principle, transesterification is a reversible reaction, although, in the production of biodiesel, the back reaction does not occur or is negligible because the glycerol formed is not miscible with the product, leading to a two-phase system. Equations 6.1, 6.2, 6.3 and 6.4 show the step by step of production of biodiesel from triglyceride to fatty acid methyl ester and glycerin. The stoichiometry of the reaction is 3:1 molar ratio of alcohol to oil, to produce three moles of biodiesel and one mole of glycerol.

The palm oil is derived from the seed of the palm, and its tree grows up to 20–30 m tall (Ong et al. 2011). The palm fruit is reddish, about the size of a plum, and grows in large bunches. Oil is extracted from fruit and kernel of the oil palm. For every 100 kg of fruit bunches, typically 22 kg of palm oil and 1.6 kg of palm kernel oil can be extracted. As altitude increases, biodiesel fueling leads to shorter combustion duration and better engine performance (Mofijur et al. 2013). Table 6.1 shows the properties of palm oil (Noiroj et al. 2009). The density and kinematic viscosity of palm oil is 0.901 g/mL and 40.5155 cSt, respectively.

There are several of types of catalyst have been used in biodiesel production. As illustrated in Fig. 6.2, the catalyst can be classified into three types. All catalysts have their advantages and disadvantages related to biodiesel production.

Table 6.1 Properties of palm oil

| Properties | Value |
|--------------------------|---------|
| Density @ 27 °C, g/mL | 0.901 |
| Kinematic viscosity, cSt | 40.5155 |
| Free Fatty Acid, % | 0.3579 |
| Moisture content, ppm | 452.8 |

**Fig. 6.2** Classification of catalysts. (Singh and Singh 2010)

The conventional process of biodiesel production in the transesterification of oils or fats uses a homogeneous catalyst (Viriya-Empikul et al. 2010). There are several homogeneous acids or base catalysts involve in preparation for biodiesel production such as potassium hydroxide and carbonate, and sodium and potassium alkoxides. The use of a heterogeneous catalyst is the key to all the problems and drawbacks of using a homogeneous catalyst (Li et al. 2011). Successful ventures were reported on the utilization of waste chicken egg shell, oyster shell, mud crab shell, golden apple snail, and mollusk shell as cheap resources of calcium oxide (CaO) for the application as low cost heterogeneous catalyst for biodiesel synthesis (Boey et al. 2009; Chakraborty and Das 2012; Nakatani et al. 2009; Viriya-Empikul et al. 2010; Wei et al. 2009).

Calcium oxide is a solid base catalyst that is used in the biodiesel production. Among the alkaline earth metal oxides, CaO is the most widely used catalyst for transesterification process, and as high as 98% FAME yield is possible during the

first cycle of reaction (Veljković et al. 2009). Balakrishnan et al. (2013) also reported the use of calcium oxide as a solid base catalyst from construction waste material in the synthesis of methyl ester, which obtained a yield of 88% (Balakrishnan et al. 2013). Apart from that, Wei et al. (2009) used waste eggshell as a low-cost solid catalyst (CaO) for biodiesel production and the obtained yield exceeded 95% with optimal condition of 9:1 molar ratio of methanol to oil, 3 wt% of eggshell-derived catalyst (calcined at 1000 °C), 65 °C reaction temperature, and 3 h of reaction time.

In this study, identification of FAME in palm oil biodiesel was conducted using gas chromatography-mass spectrometer (GCMS). The palm oil went through transesterification process and catalyzed by a mixture of solid coconut waste and eggshell to produce biodiesel.

6.2 Objectives

The objectives of this study are:

1. To produce fatty acid methyl ester (FAME) from palm oil
2. To identify fatty acid methyl ester (FAME) in palm oil biodiesel using GCMS (Tables 6.2, 6.3 and 6.4).

6.3 Materials

Table 6.2 Consumable item

| No | Equipment | Usage |
|----|----------------------|----------------------------------|
| 1 | Pipettes tips (1 mL) | To add any solution into GC vial |

Table 6.3 Equipment

| No | Equipment | Usage |
|----|---|--|
| 1 | Büchner filter system attached to vacuum pump | To filter the sample |
| 2 | Refrigerated recirculating water bath | To reduce the temperature of the reactor |
| 3 | Heating hot plate stirrer and bar | To increase the temperature of the solvent |

Table 6.4 Chemicals and reagents

| No | Equipment | Usage |
|----|-----------------------------|--------------------------|
| 1 | Methanol (analytical grade) | Merck (Malaysia) |
| 2 | n-Hexane (GC analysis) | Merck (Malaysia) |
| 3 | Standard FAME | Sigma-Aldrich (Malaysia) |

6.4 Methodology

6.4.1 Catalyst Preparation

1. Coconut waste and eggshells which are low-cost heterogeneous catalysts were selected.
2. Then, it was dried in hot air oven at 100 °C for overnight.
3. Then, both were calcined in a furnace at a temperature of 800 °C for 4 h.
4. A sieve tray with a size of <math><212\ \mu\text{m}</math> was used to sieve the catalysts.

6.4.2 Transesterification

1. The transesterification process was conducted using a reactor. A hot digital magnetic stirrer was used to control the temperature and mixing intensity.
2. Ten grams of palm oil was weighed. The catalysts were varied in the range of 4–10 wt%.
3. The reaction temperature was varied at 55, 60, and 65 °C and the reaction time was fixed at 120 min.
4. After the reaction, the mixture was transferred to a separating funnel, allowing the glycerol and the catalyst to separate from the biodiesel.
5. The glycerol layer and the biodiesel layer were drained separately and collected before purification processes.
6. The catalyst was separated from the glycerol by vacuum filtration through a filter paper.
7. The biodiesel layer was washed with warm water to remove all the excessive catalysts.

6.4.3 GCMS Identification

1. The biodiesel composition was analyzed using HP 6890 Gas Chromatogram Mass Spectrometer (GCMS) equipped with an automated split injector (Agilent 7683 automatic sample).
2. The sample (0.1 mL) was diluted with 3.9 mL of n-hexane, and 1 μL of sample was injected into DB 23 column.
3. Oven temperature was set to 50 °C for 1 min before increasing it to 175 °C at a rate of 4 °C/min. Then it was increased to 235 °C at a rate of 4 °C/min and held for 5 min.

Table 6.5 Conditions for fatty acid methyl ester analysis

| Agilent 6890 GC | |
|----------------------|---|
| Inlet | Split |
| Detector | FID |
| Automatic sampler | Agilent 7683 |
| Liner | Split line |
| Column | DB 23: 60 m × 0.248 mm × 0.15µm |
| Inlet temperature | 250 °C |
| Injection volume | 1 µL |
| Split ratio | 1/50 |
| Carrier gas | Helium |
| Head pressure | Constant pressure mode at 230 kPa |
| Oven temperature | 50 °C for 1 min, 25 °C/min to 175 °C, 4 °C/min to 230 °C, 5 min |
| Detector temperature | 280 °C |
| Detector gases | Hydrogen: 35 mL/min |
| | Air: 350 mL/min |
| | Helium: 30 mL/min |

- The inlet and detector temperatures were set at 250 and 280 °C, respectively. The column is a 60 m × 0.248 mm × 0.15 µm DB 23 capillary column (J&W Scientific, USA). Purified helium was used as the carrier gas.
- Table 6.5 summarizes the conditions used during GC analysis.

6.4.4 GCMS Identification

- The standard mixture of fatty acid was obtained from Sigma-Aldrich.
- The fatty acid methyl ester analysis was conducted by using the mixture of standards at five different concentrations.
- Each sample was injected three times to obtain a precise result.
- The method in Section 4.2 was used to construct the calibration curve.
- Five calibration curves of methyl palmitate, stearate, oleate, linoleic, and linoleate were obtained. The yield of biodiesel was calculated based on the fatty acid methyl esters (FAME) and presented by Eq. 6.5.

$$FAME\ yield = \frac{Total\ FAME(g)}{Amount\ of\ oil\ used(g)} \times 100\% \quad (6.5)$$

6.5 Flow of Experiment

6.5.1 Transesterification (Fig. 6.3)

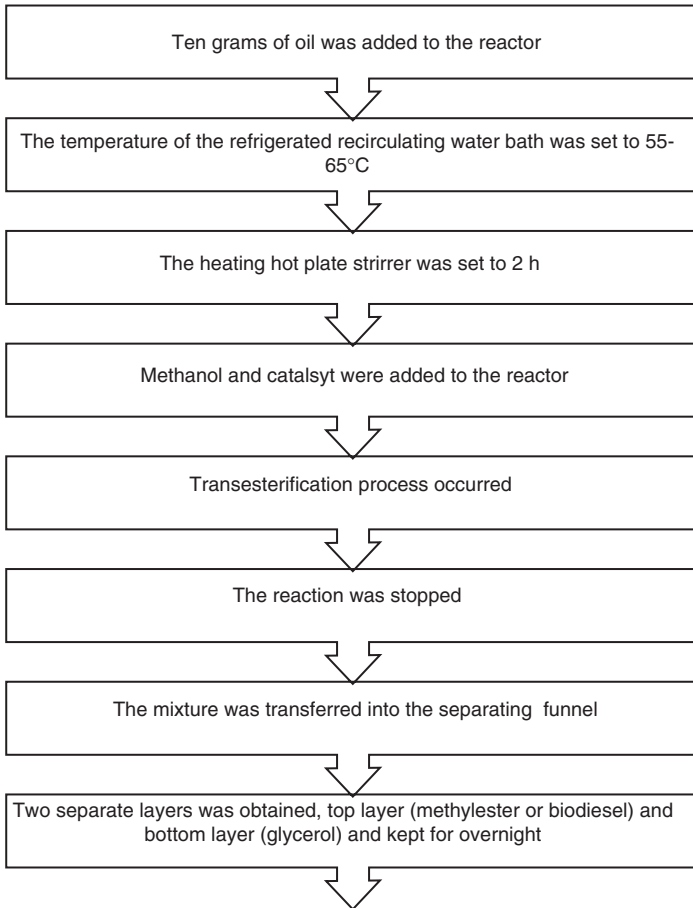


Fig. 6.3 Transesterification flow diagram

6.5.2 Identification of Fame (Fig. 6.4)

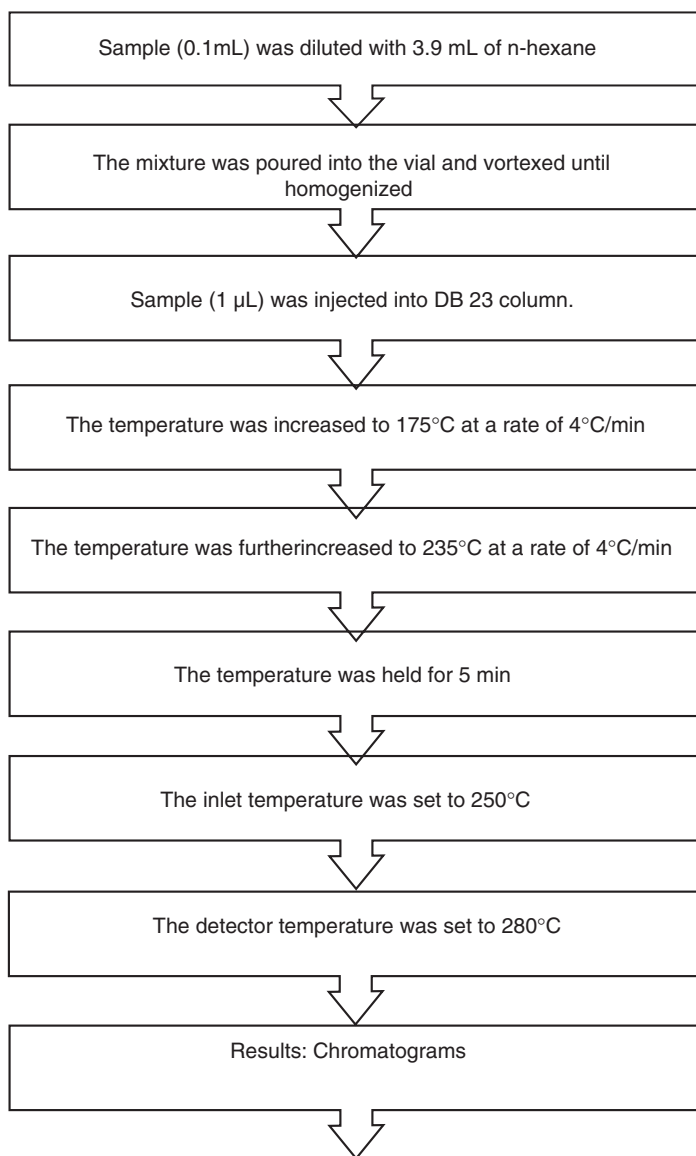


Fig. 6.4 FAME identification flow diagram

6.6 Results and Discussion

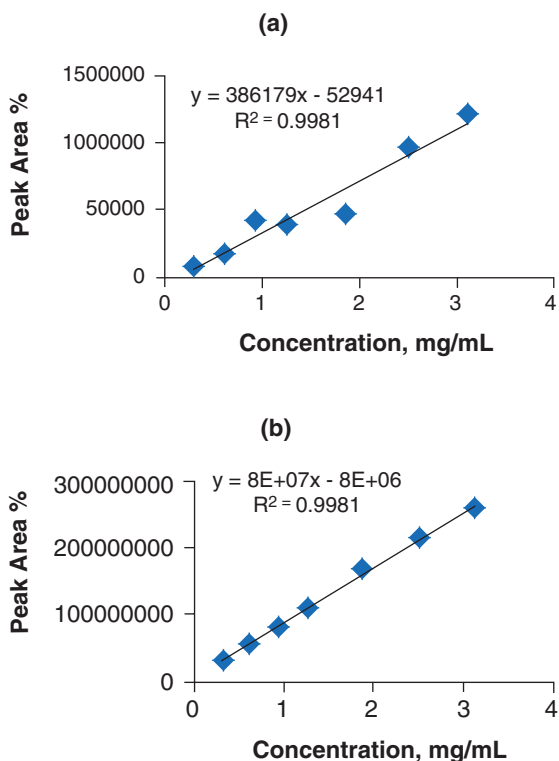
6.6.1 Calibration Curve

Figures 6.5 and 6.6 show the calibration curve obtained for palmitic acid (C16:0), stearic acid (C18:0), oleic acid (C18:1), linoleic acid (C18:2), and linolenic acid (C18:3). Correlation coefficients of all fitted calibration curves were excellent. The total FAME concentration is calculated by summing the concentrations obtained for the five specified FAMES using the specified calibration ranges.

6.6.2 Identification of FAME Using GCMS

The sample of biodiesel was analyzed using GCMS to identify the components of FAMES. Figure 6.7 shows the chromatogram of palm oil biodiesel. The main components in biodiesel are caprylic acid (C8:0), capric acid (C10:0), myristic acid (C14:0), palmitic acid (C16:0), stearic acid (C18:0), oleic acid (C18:1), arachidate acid (C20:0), and docosanoic acid (C22:0). Table 6.6 summarizes and compares the

Fig. 6.5 Calibration curves for (a) C16:0 and (b) C18:0



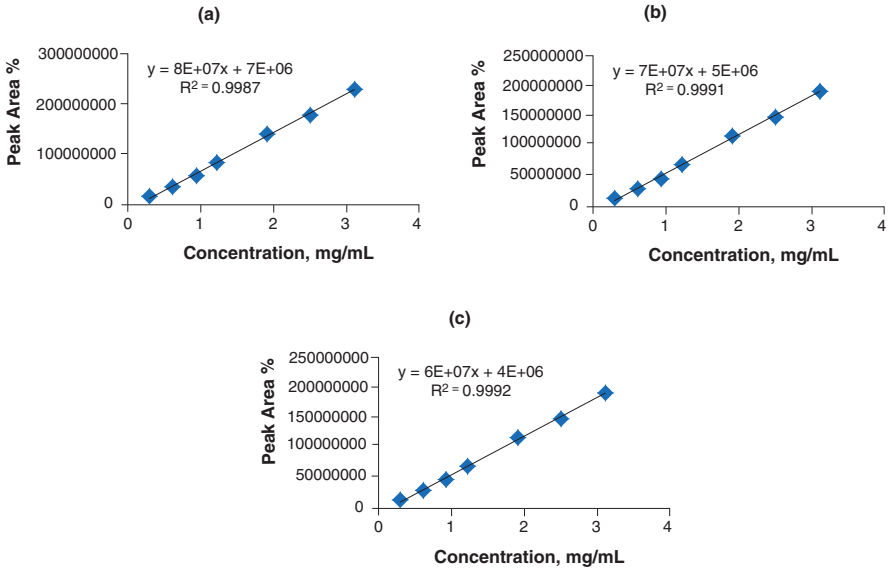


Fig. 6.6 Calibration curves for (a) C18:1, (b) C18:2, and (c) C18:3

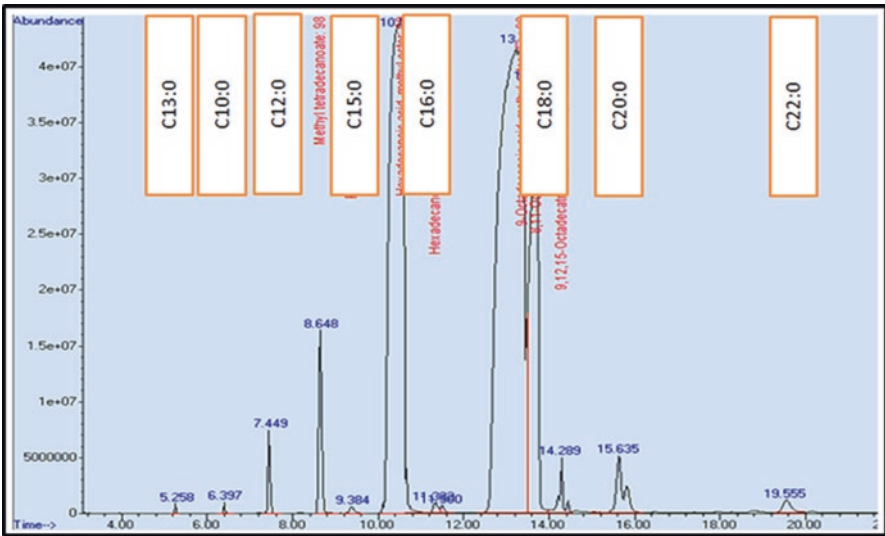


Fig. 6.7 Chromatogram of palm oil biodiesel

composition of methyl esters and their respective areas of another study (Darnoko and Cheryan 2000; Maycock 1987). The areas of palmitic and stearic acid are the highest with 28.94 and 63.22%, respectively. These results are in agreement with other studies (Darnoko and Cheryan 2000; Maycock 1987).

Table 6.6 Composition of methyl ester

| Compound | Area (%) (this work) | Area (%) (Darnoko and Cheryan 2000; Maycock 1987) |
|------------------------|----------------------|---|
| Caprylic acid, C8:0 | 0.04 | – |
| Capric acid, C10:0 | 0.74 | – |
| Myristic acid, C14:0 | 2.20 | 1.08 |
| Palmitic acid, C16:0 | 28.94 | 43.79 |
| Stearic acid, C18:0 | 2.81 | 4.42 |
| Oleic Acid, C18:1 | 63.22 | 39.90 |
| Arachidate acid, C20:0 | 1.64 | 0.38 |
| Behenic acid, C22:0 | 0.41 | – |

6.7 Conclusion

In this study, biodiesel production using palm oil has been successfully carried out. The transesterification of palm oil catalyzed by a mixture of solid coconut waste and eggshell has produced high-quality biodiesel. The CaO synthesized from the mixture of solid coconut waste, and eggshell was identified to assist the conversion of triglycerides to fatty acid methyl ester (FAME).

The identification of fatty acid methyl ester (FAME) in palm oil biodiesel using GCMS has identified the main components are caprylic acid (C8:0), capric acid (C10:0), myristic acid (C14:0), palmitic acid (C16:0), stearic acid (C18:0), oleic acid (C18:1), arachidate acid (C20:0), and docosanoic acid (C22:0).

Acknowledgment This research was funded by FRGS grant (FRGS 13-079-0320) from the Government of Malaysia.

References

- Balakrishnan K, Olutoye M, Hameed B (2013) Synthesis of methyl esters from waste cooking oil using construction waste material as solid base catalyst. *Bioresour Technol* 128:788–791
- Boey P-L, Maniam GP, Hamid SA (2009) Biodiesel production via transesterification of palm olein using waste mud crab (*Scylla serrata*) shell as a heterogeneous catalyst. *Bioresour Technol* 100(24):6362–6368
- Chakraborty R, Das SK (2012) Optimization of biodiesel synthesis from waste frying soybean oil using fish scale-supported Ni catalyst. *Ind Eng Chem Res* 51(25):8404–8414
- Darnoko D, Cheryan M (2000) Kinetics of palm oil transesterification in a batch reactor. *J Am Oil Chem Soc* 77(12):1263–1267
- Li Q, Zheng L, Cai H, Garza E, Yu Z, Zhou S (2011) From organic waste to biodiesel: black soldier fly, *Hermetia illucens*, makes it feasible. *Fuel* 40:1545–1548
- Maycock JH (1987) Extraction of crude palm oil. In: Gunstone FD (ed) *Palm oil*, vol 15. Wiley, New York, pp 29–38 *Crit Rev App Chem*
- Mofijur M, Masjuki H, Kalam M, Atabani A, Shahabuddin M, Palash S, Hazrat M (2013) Effect of biodiesel from various feedstocks on combustion characteristics, engine durability and materials compatibility: a review. *Renew Sust Energ Rev* 28:441–455

- Nakatani N, Takamori H, Takeda K, Sakugawa H (2009) Transesterification of soybean oil using combusted oyster shell waste as a catalyst. *Bioresour Technol* 100(3):1510–1513. <https://doi.org/10.1016/j.biortech.2008.09.007>
- Noiroj K, Intarapong P, Luengnaruemitchai A, Jai-In S (2009) A comparative study of KOH/Al₂O₃ and KOH/NaY catalysts for biodiesel production via transesterification from palm oil. *Renew Energy* 34(4):1145–1150
- Ong H, Mahlia T, Masjuki H, Norhasyima R (2011) Comparison of palm oil, *Jatropha curcas* and *Calophyllum inophyllum* for biodiesel: a review. *Renew Sust Energ Rev* 15(8):3501–3515
- Singh SP, Singh D (2010) Biodiesel production through the use of different sources and characterization of oils and their esters as the substitute of diesel: a review. *Renew Sust Energ Rev* 14(1):200–216
- Veljković VB, Stamenković OS, Todorović ZB, Lazić ML, Skala DU (2009) Kinetics of sunflower oil methanolysis catalyzed by calcium oxide. *Fuel* 88(9):1554–1562
- Viriya-Empikul N, Krasae P, Puttasawat B, Yoosuk B, Chollacoop N, Faungnawakij K (2010) Waste shells of mollusk and egg as biodiesel production catalysts. *Bioresour Technol* 101(10):3765–3767
- Wei Z, Xu C, Li B (2009) Application of waste eggshell as low-cost solid catalyst for biodiesel production. *Bioresour Technol* 100(11):2883–2885
- Yan S, Dimaggio C, Mohan S, Kim M, Salley SO, Ng KS (2010) Advancements in heterogeneous catalysis for biodiesel synthesis. *Top Catal* 53(11–12):721–736

Chapter 7

Procedure to Develop Binodal Curve and Phase Diagram for Aqueous Two-Phase System



Zatul Iffah Mohd Arshad and Azura Amid

Abstract Purification of protein is normally involved an expensive downstream processing step. For large scale manufacturing facilities, identification of an economical procedure is the most advantage. Aqueous Two-Phase System (ATPS) is a technique that suitable to be used in extracting protein from the mix culture supernatant. The process is also economical. However, there are a few tricky parts that the researchers need to master before this technique can be applied. Therefore, this chapter presents the step by step procedure in optimizing this technique.

Keywords Purification · Recombinant protein · Biodal curve · Solvent-solvent extraction

7.1 Introduction

Aqueous two-phase system (ATPS) is formed by mixing two incompatible polymers (polyethylene glycol/dextran) or one polymer and a salt (polyethylene glycol/salt), and in an equilibrium condition, these mixtures separate into two distinct phases. The phase diagram is a unique system, and under a specific condition of pH, temperature, or salt concentration, it is needed to facilitate the use of aqueous two-phase for protein purification. The binodal curve is a curve that separating between one phase and two phases system. The construction of binodal curve is important for the extrapolation of volume ratio for aqueous two-phase separation. The concentration, pH, volume ratio and tie line length are determined after choosing the phase-forming component. The published phase diagram reported by other researchers may have a variation in the material to be separated, the molecular weight of the polymer, concentration and temperature which eventually cause a movement of the binodal position and therefore, it can be used as a reference for the starting point

Z. I. M. Arshad · A. Amid (✉)

Department of Biotechnology Engineering, Faculty of Engineering, International Islamic University Malaysia, Kuala Lumpur, Malaysia
e-mail: azuraamid@iium.edu.my

preparation of ATPS. This chapter presents laboratory procedures for the construction of binodal curve for PEG1500 and determination of tie-line length (TLL) and volume ration (VR).

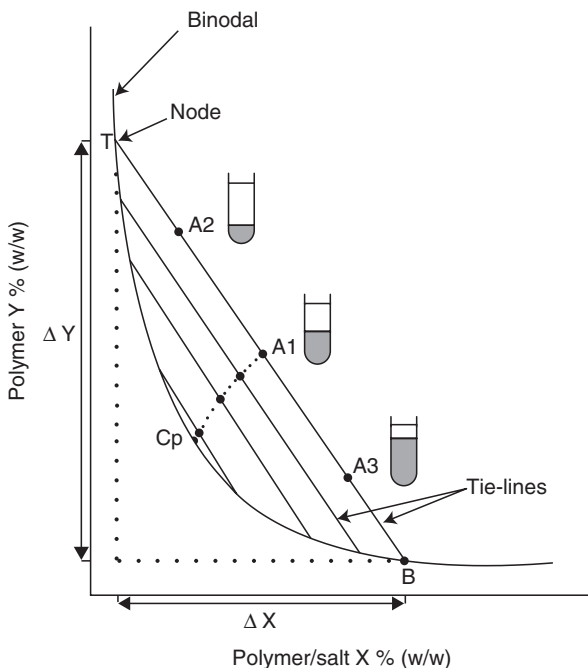
7.2 Binodal Curve and Phase Diagram

The bimodal curve separate two regions of component concentration between two phases (above the curve) and one phase (below the curve). The tie-line connects two nodes on the binodal which represent the final concentration of top and bottom phases. The nodes along the tie-line have different composition and volume ratio while the nodes in the critical point have an equal volume ratio in the top and bottom phases as illustrated in Fig. 7.1 (Kaul 2000; Raja et al. 2011). In order to evaluate the purification efficiency, the specific activity (SA) and purification factor (PF) recovered at the top, and bottom phase was calculated according to the equation below:

$$SA = \frac{EAe}{TPe} \tag{7.1}$$

$$PF = \frac{SAe}{SA_t} \tag{7.2}$$

Fig. 7.1 Phase diagram. A1, A2, and A3 represent the total composition (●) of three systems lying on the same tie-line with different volume ratios. The nodes T and B (■) represent the final concentration of the top and bottom phase, respectively. The Cp represents the critical point that is obtained by extrapolation (.....) through the midpoints of tie-lines. The Δy and Δx denote the concentration difference of component x and y (Kaul 2000)



Where E_{Ae} , T_{Pe} , is the enzyme activity and total protein of each phase, respectively. The S_{Ae} is an SA of each phase, and S_{Ai} is an initial SA of crude lysate. The partition coefficient (KE) and volume ratio (VR) was defined as

$$KE = \frac{At}{Ab} \quad (7.3)$$

$$VR = \frac{Vt}{Vb} \quad (7.4)$$

Where At and Ab are the enzyme activity in the top and bottom phase, respectively. The Vt and Vb are the volumes of the top and bottom phase, respectively.

7.3 Objective of Experiment

This experiment aims to construct a binodal curve for PEG1500 and determine the tie line length (TLL), volume ratio (VR), partition coefficient (KE) and purification fold (PF) of recombinant bromelain.

7.4 Materials and Methods (Tables 7.1a, 7.1b and 7.1c)

1. Stock solutions for PEG1500 are prepared by weight using weighting balance. For 250 g stock, weight 125 g of PEG1500 and mix with 125 g of distilled water.
2. Stock solutions for potassium phosphate buffer at pH 7.0 are prepared by weight using weighting balance. For 500 g stock, weight 153.75 g of dipotassium phosphate and 96.25 g of potassium dihydrogen phosphate and mix with 250 g of distilled water.
3. In a test tube, different concentration of 500 g potassium phosphate buffer stock, pH 7.0 starting from 1% (w/w) is added to 50% (w/w) of 250 g PEG1500 stock and 20% (w/w) of lysate r-bromelain. Top-up the weight balance with distilled water until achieving a total weight of 2 g.
4. The process is repeated by increasing the percentage of potassium phosphate buffer until 25% (w/w).
5. Next, 45% (w/w) of PEG1500 will be used to test on a different percentage of potassium phosphate buffer.

Table 7.1a List of consumable items

| No | Item | Usages |
|----|------------------------------|----------------------------------|
| 1 | Pipettes (200 μ L, 1 mL) | To add any solution into cuvette |
| 2 | Tube (2 mL) | To do the ATPS process |

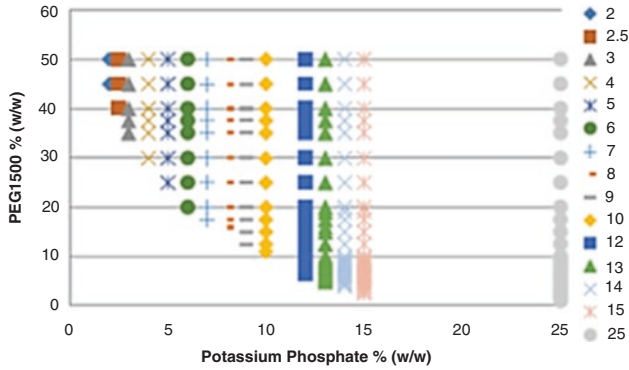


Fig. 7.2 Graphical representation of binodal curve construction for system contain potassium phosphate/PEG1500, pH 7.0

Table 7.3 The end nodes for the construction of phase diagram for potassium phosphate/PEG1500, pH 7

| Potassium Phosphate, pH 7.0% (w/w) | PEG1500% (w/w) |
|------------------------------------|----------------|
| 2 | 45 |
| 2.5 | 40 |
| 3 | 35 |
| 4 | 30 |
| 5 | 25 |
| 6 | 20 |
| 7 | 18 |
| 8 | 16 |
| 9 | 13 |
| 10 | 11 |
| 12 | 7 |
| 13 | 5 |
| 14 | 4 |
| 15 | 3 |
| 25 | 1 |

11. The tie-line length (TLL) can be estimated graphically by using volume ratio since the length of segment AVR, and BVR is one and it can be expressed in units of % (w/w) and can be calculated using equation as follows:

$$TLL = \sqrt{\Delta X^2 + \Delta Y^2} \tag{7.5}$$

where ΔX and ΔY are the difference between salt and PEG concentration, respectively.

12. The standard salt conductivity and refractive index curves (Figs. 7.4 and 7.5) are used to determine the concentration of salt and PEG at the end of each tie-line (Fig. 7.3).

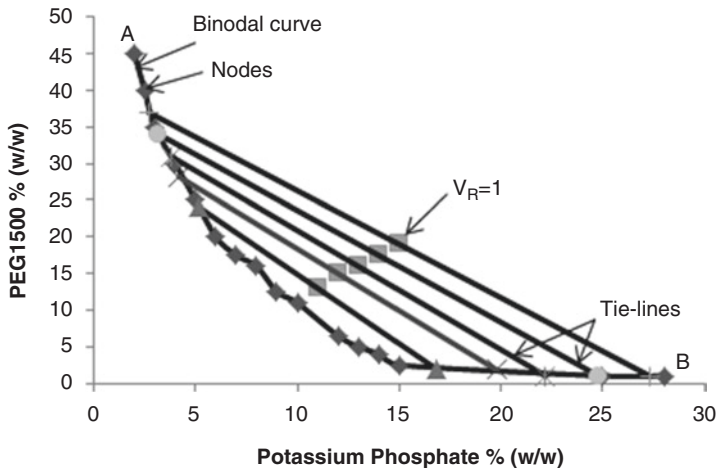


Fig. 7.3 Phase diagram for a system containing potassium phosphate /PEG1500, pH 7.0. The nodes A and B denote \blacklozenge that represents the final concentration of the top and bottom phase respectively. The sign of \blacksquare represents the volume ratio (V_R) which equal to one

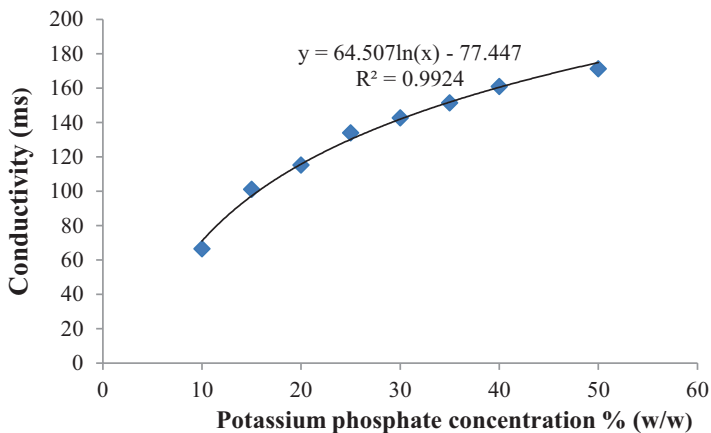


Fig. 7.4 Standard curve for potassium phosphate buffer at pH7.0

7.5 Discussion

The composition of potassium phosphate and PEG1500 at VR equal to one is shown in Table 7.4. There was no obvious trend of the values of SA, KE, and PF when the tie line length (TLL) was elevated. For this study, the recombinant bromelain showed the highest specific activity (SA), partition coefficient (KE) and purification factor (PF) from the system of 11% (w/w) potassium phosphate and 13%(w/w)

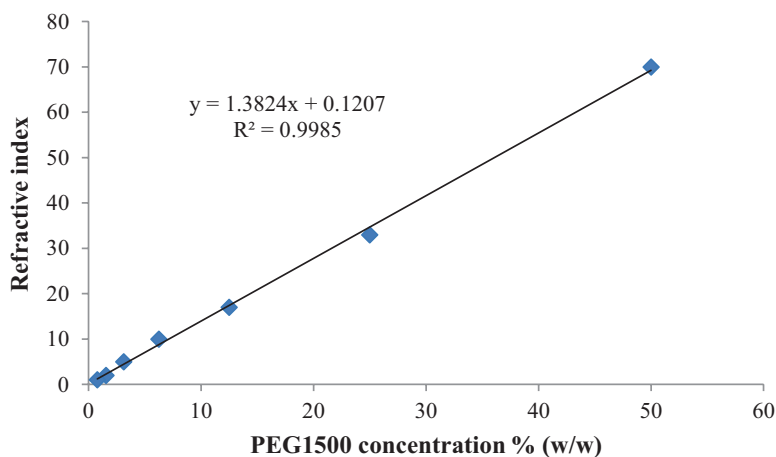


Fig. 7.5 Standard curve for polyethylene glycol 1500

Table 7.4 The effect of molecular weight of PEG at $V_R = 1$ to the partition coefficient (KE) and purification fold (PF)

| MW of PEG | Composition PP/PEG at $V_R = 1$ | SA | KE | PF |
|-----------|---------------------------------|-------|-------|-------|
| 1500 | 11/13 | 0.397 | 0.613 | 0.727 |
| | 12/15 | 0.204 | 0.315 | 0.123 |
| | 13/16 | 0.031 | 0.047 | 0.051 |
| | 14/17.5 | 0.091 | 0.141 | 0.142 |
| | 15/19 | 0.302 | 0.46 | 0.137 |

*PP is potassium phosphate and PEG is polyethylene glycol

PEG1500. When the tie-line increased from the concentration of 11 to 14% (w/w) of potassium phosphate, major amount of proteins recovered in the top phase due to the increase of ionic strength in the bottom phase (González-Valdez et al. 2013). However, the total proteins other than recombinant bromelain will also partition to the top phase, thereby decrease its SA, PF and KE results.

7.6 Conclusion

A separation process for the purification of recombinant bromelain ATPS extraction method is presented. With a 13% (w/w) of PEG1500/11% (w/w) of potassium phosphate solution (pH 7.0), recombinant bromelain with a purification factor of 0.727, specific activity of 0.397unit/mg and 0.617 of partition coefficient was obtained. The construction of binodal curve allows the exploitation of ATPS parameter and improves the purification of recombinant bromelain.

References

- González-Valdez J, Rito-Palomares M, Benavides J (2013) Effects of chemical modifications in the partition behavior of proteins in aqueous two-phase systems: A case study with RNase A. *Biotechnol Prog* 29(2):378–385. <https://doi.org/10.1002/btpr.1684>
- Kaul A (2000) The phase diagram. In: Hatti-Kaul R (ed) *Aqueous two-phase systems: methods and protocols*, vol 11. Humana Press, Totowa, pp 11–21
- Raja S, Murty VR, Thivaharan V, Rajasekar V, Ramesh V (2011) Aqueous two phase systems for the recovery of biomolecules – a review. *Sci Technol* 1(1):7–16. <https://doi.org/10.5923/j.scit.20110101.02>

Chapter 8

Technique to Produce Catalyst from Egg Shell and Coconut Waste for Biodiesel Production



Sarina Sulaiman and Nur Syakirah Talha

Abstract Many studies have been conducted to develop low cost catalysts to reduce the production cost. Several catalysts such as homogeneous/heterogeneous acid catalysts, homogeneous/heterogeneous base catalysts and biocatalysts (enzymes) have been studied and applied in the synthesis of biodiesel. Base-catalyzed transesterification is commonly used in commercial production because of high FAME yield in short reaction time and the reaction can be done in mild conditions as compared to acid-catalyzed transesterification. In the present study, egg shell and coconut waste were synthesized using calcination method at 800 °C for 4 h. SEM micrographs prove that the mixture of catalyst shows a bigger surface area. This result is expected to increase the yield of biodiesel. It can be concluded that biodiesel was produced successfully using palm oil and mixed catalysts.

Keywords Catalyst · Coconut waste · Biodiesel · Waste catalyst · Calcination · Characterization · Egg shell · Scanning electron microscopy · Restaurant Waste · Transesterification

8.1 Introduction

In biodiesel production, there are three categories of catalysts that are commonly used such as alkalis, acids, and enzymes (Canakci and Van Gerpen 1999; Nelson et al. 1996; Shimada et al. 1999). However, the use of homogeneous alkaline catalysts will lead to soap formation, the catalyst cannot be reused, and produce large amount of wastewater hence increase the cost for biodiesel production. So one way to overcome this problem is by using heterogeneous catalyst. Waste materials such as coconut waste and egg shells are examples of heterogeneous catalysts which can be utilized as catalyst for biodiesel production. This chapter focuses on the technique to produce catalyst from waste e.g. coconut waste.

S. Sulaiman (✉) · N. S. Talha
Department of Biotechnology Engineering, Kulliyah of Engineering, International Islamic University Malaysia, Kuala Lumpur, Malaysia
e-mail: sarina@iium.edu.my

8.2 Literature Review

Heterogeneous catalysts are the opposite of homogeneous catalysts. By definition, the heterogeneous catalyst is a catalyst that occupy different phase with the reactants. The simplification and the reusability of the heterogeneous catalysts make it better than homogenous catalysts (Obadiyah et al. 2012; Moradi and Mohammadi 2014). Calcium oxide which is a heterogeneous catalyst that exhibits excellent potential in the transesterification reaction. This catalyst is also cheap, low methanol solubility, non-corrosive, environmental friendly and can be reused many times. According to Obadiyah et al. (2012), calcium compounds such as calcium nitrate, calcium carbonate, calcium phosphate and calcium hydroxide can be synthesized to produce calcium oxide. Moreover, some natural sources such egg shells, shrimp, osyter and crab shells also can be synthesized to produce calcium oxide (Obadiyah et al. 2012).

Currently, many researches were being conducted on different types of heterogeneous catalysts such as oxides, hydrotalcides and zeolites (Atadashi et al. 2013). Formerly, oxides of alkali and oxides of alkaline earth metals supported over large surface area were mostly used as heterogeneous catalysts (Atadashi et al. 2013). In addition, Esterfip-H process is applied for the commercialization of biodiesel production with heterogeneous catalyst which avoids the need for the catalyst recovery or aqueous treatment stages (Atadashi et al. 2013). Besides, high biodiesel yields and direct production of salt-free glycerol with more than 98% purity can be obtained from the Esterfip-H process.

Transesterification is an endothermic reaction. Therefore, high temperature is appropriate for biodiesel production (Talha et al. 2017). Rise in temperature permits the reactant to be more dissolved that consequently results on higher reaction rate (Talha et al. 2017). In a study by Norzita Ngadi et al. (2017), the optimum temperature for biodiesel yield was found to be at 50 °C for cockle shells catalyst whereas 60 °C for commercial calcium oxide (Ngadi et al. 2017). It is also mentioned that the optimum temperature for shell derived calcium oxide catalyst in previous works was in the range of 50–60 °C. In another study by Buasri et al. (2013), the optimum temperature for the transesterification of palm oil using mussel, cockle and scallop shells was 65 °C. However, in a study conducted by Talha et al. (2017), the optimum temperature for the transesterification of mixture solid coconut waste and eggshells was found at 95 °C.

Most of the literatures reported the use of heterogeneous base catalyst at lower reaction temperature (less than 65 °C). Temperature above 70 °C resulted in lower yield as methanol evaporates at 65 °C (Jagadale and Jugulkar 2012). In addition, alkaline catalyst was successfully proven to provide higher yield compared to acid-catalyst which needs more vigorous reaction condition including higher temperature during transesterification (Lam et al. 2010).

8.3 Catalyst from Waste

Heterogeneous catalyst is promising catalyst that will reduce the high production cost of biodiesel, making it competitive with petro-diesel fuels. Therefore, a lot of studies were carried out concerning the improvement of environmentally friendly and cost-effective heterogeneous catalysts for biodiesel production. The utilization of waste heterogeneous catalysts such as cockle, crab, egg and shrimp shells has become the recent interest.

Narzita Ngadi et al. (2017) used palm oil as raw material and heterogeneous catalyst was derived from cockle waste shell for biodiesel production. In the study, it was agreed that the optimum condition to achieve maximum biodiesel yield (73.95%) is when the reaction temperature was 50 °C, reaction time of 1 h with 9:1 methanol to oil ratio. Moradi and Mohammadi (2014) used the waste coral as catalyst in biodiesel production with soybean oil as the feedstock. In the study, the transesterification was carried out with calcination temperature, methanol to soybean oil ratio and catalyst loading has been selected as the variable. The optimum conditions were at calcination temperature of 900 °C, catalyst loading of 6 wt% and methanol to oil ratio of 12:1. In the study, the waste catalyst was capable to be reused up to 4 times without significant loss in activity (Moradi and Mohammadi 2014).

In this study, the duck and egg shells waste was used to synthesize calcium oxide catalyst (Buasri et al. 2013). Duck and chicken egg shells catalyst were used to carry out transesterification of palm oil and the highest yields of 92.92 and 94.49% were obtained respectively. Gryglewicz (1999) used rapeseed as the feedstock for the transesterification. The study is performed to examine heterogeneous catalyst of particular calcium compound to produce biodiesel through transesterification of rapeseed. It is found that particular calcium compounds can be used as catalyst effectively to produce biodiesel from rapeseed (Gryglewicz 1999).

Vyas et al. (2009) reported the use of *Jatropha* oil as the raw material to produce biodiesel and the transesterification reaction was carried out using alumina loaded with potassium nitrate as solid base catalyst (Vyas et al. 2009). Vyas et al. (2009) has agree that the 84% conversion of methyl ester was achieved under the conditions of 70 °C, 12:1 methanol to oil ratio, 6 h reaction time, 600 rpm agitation speed and 6 wt.% catalyst loading. Sun et al. (2010) uses sunflower oil as raw material to produce biodiesel. Transesterification has been carried using heterogeneous catalyst of zirconium dioxide (ZrO_2) supported lanthana (La_2O_3) and the highest biodiesel yield was at 84.9% (Sun et al. 2010). The optimum condition was found at 600 °C calcination temperature and 21 wt.% catalyst loading with reaction time was fixed at 4 h. On top of that, Azis et al. (2015) also uses *Jatropha* oil for biodiesel production and 94% of conversion is achieved using cockle shells derived catalyst with optimum condition of 1.5 wt. % catalyst loading and 700 °C calcination temperature (Azis et al. 2015).

8.4 Objectives

The objectives of this study are

- (a) To produce catalyst from coconut waste and eggshell for biodiesel production.
- (b) To characterize the catalyst.

In this study, solid coconut waste and eggshell will be synthesized to produce biodiesel. This technique is widely used in the biodiesel industry.

8.5 Raw Material

Solid coconut waste and eggshell were collected from restaurants (Tables 8.1 and 8.2).

Table 8.1 Equipment

| No | Equipment | Usage |
|----|---|---|
| 1 | Büchner filter system attached to vacuum pump | To filter the catalyst |
| 2 | Heating hot plate stirrer and stirrer bar | To mix vigorously the transesterification process |
| 3 | Furnace | To calcine the catalyst |

Table 8.2 Chemicals and reagents

| No | Equipment | Usage |
|----|--------------------------|--------------------------|
| 1 | Methanol (AR grade) | Merck (Malaysia) |
| 2 | n-Hexane (GC grade) | Merck (Malaysia) |
| 3 | Standard FAME (GC grade) | Sigma-Aldrich (Malaysia) |

8.6 Methodology

8.6.1 Flow of Experiment

8.6.1.1 Solid Coconut Waste Preparation (Fig. 8.1)

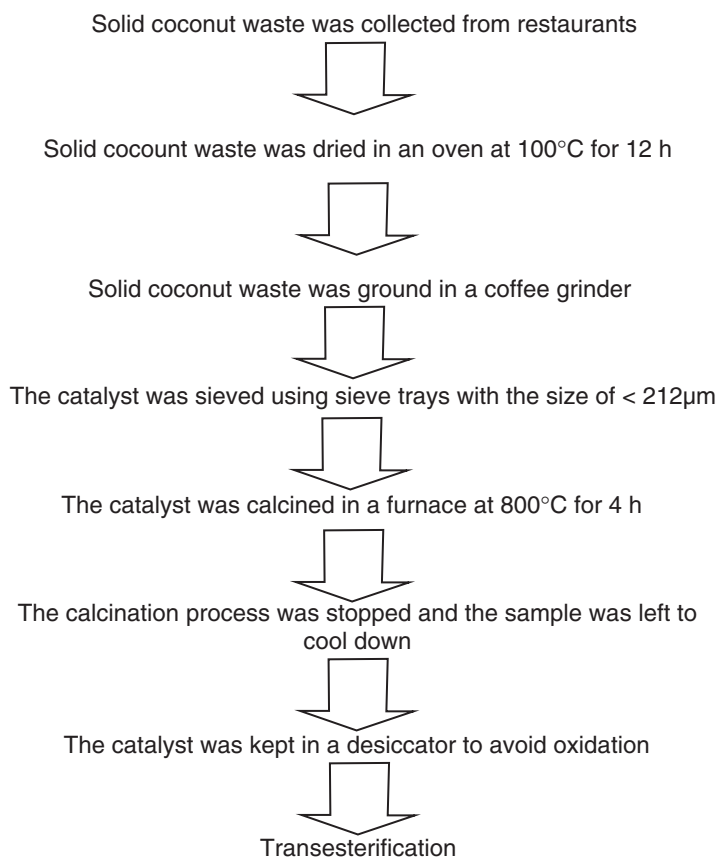


Fig. 8.1 Solid coconut waste preparation flow diagram

8.6.1.2 Eggshell Preparation (Fig. 8.2)

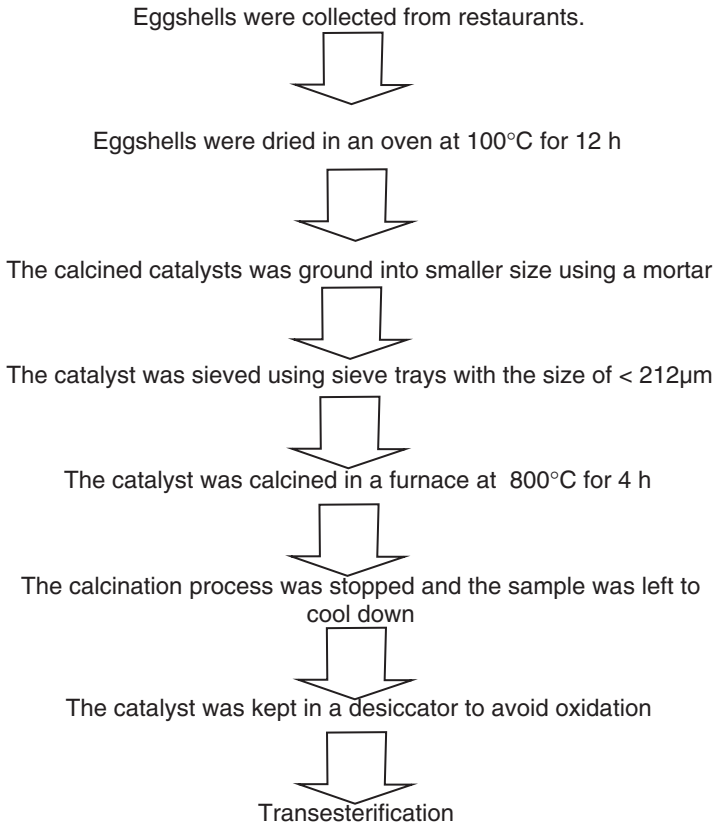


Fig. 8.2 Eggshell preparation flow diagram

8.6.1.3 Catalyst Preparation: Solid Coconut Waste

Solid coconut waste (SCW) before biodiesel production was sieved to eliminate any residual (Sulaiman et al. 2010, 2013a, b).

1. After thorough washing with deionized water, the wastes were filtered and dried in an oven at 90 °C.
2. A highly active solid catalyst was obtained by mixing and well grinding the mixture of SCW and alkaline at 800 °C in air for 4 h (Chen et al. 2013).
3. Crushed and powdered catalysts were sieved and stored in a closed vessel before use.

8.6.1.4 Catalyst Preparation: Eggshell

1. Egg shells were obtained from a local restaurant.
2. The cleaned shells were subsequently dried overnight in an oven at 90 °C before being ground finely to powder form in a grinder.
3. The powder was calcined in a high-temperature muffle furnace at 800 °C for 4 h under static air together with solid coconut waste to observe the influence of the calcination process on the transformation of calcium species into hydroxylapatite.
4. Crushed and powdered catalyst was sieved and stored in a closed vessel before use.

8.6.1.5 Mixture of Solid Coconut Waste and Eggshell and Transesterification

1. The transesterification process was carried out by mixing palm oil, methanol, and catalyst (a mixture of coconut waste and eggshell).
2. The temperature and time for reaction were set at 60 °C and 3 h, respectively.
3. Solid coconut waste (5 wt%) was added to 1 g of eggshell

8.6.2 Catalyst Characterization

1. After calcination procedure was completed, the calcined catalysts were cooled in a desiccator.
2. Scanning electron microscopy (SEM) analysis was conducted to study the morphology of the catalysts.

8.7 Results and Discussion

8.7.1 Catalyst Characterization

The catalysts produced from coconut waste, eggshells, and the mixture of both were analyzed using SEM, and the SEM images were used to observe and compare the catalyst on the basis of their morphology and texture. Based on Fig. 8.3a, with a magnification of 2000 ×, the calcined coconut waste shows bulky substances and irregular rod shape. For comparison, the SEM micrographs of the rice husk ash show that the surface was spherical and it is impermeable porous (Chen et al. 2013). In Fig. 8.3b, with a magnification of 2000×, the eggshells agglomerated with each other, and partly porous nature is observed, which would enhance the catalytic activity. The eggshells

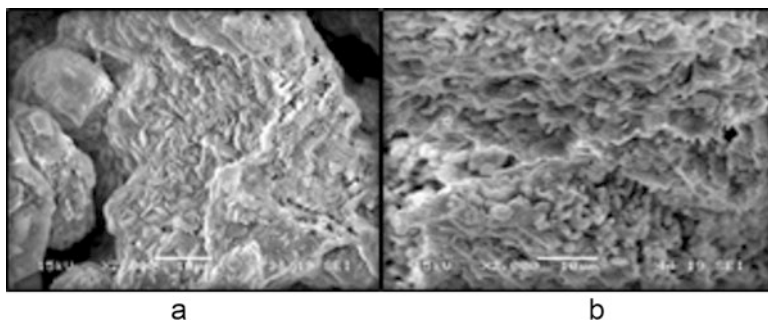
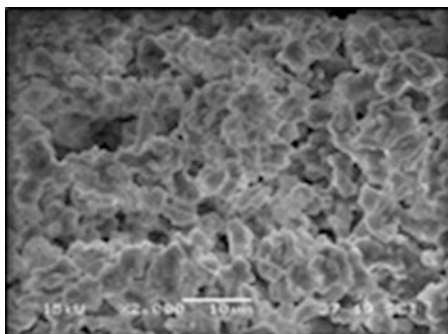


Fig. 8.3 SEM images of after calcination at 900 °C for 4 h (a) coconut waste (b) eggshells powders

Fig. 8.4 SEM image of mixture of coconut waste and eggshell



powder shows smaller particles compared to coconut waste with a slightly wave-like surface. The small size of the catalyst could provide a larger surface area for the catalytic performance. Figure 8.4 shows the irregular rod shape of the mixture of the catalysts. The particles agglomerated with each other to form a big surface area.

8.8 Conclusions

Biodiesel is alternative renewable fuel that has the same chemical and physical property associated with engine operation to petroleum-based fuel. It is produced through the reversible chemical reaction called transesterification where the oil either the vegetable oil or animal fat reacts with the short chain alcohol which is methanol to yield glycerol and methyl ester. This study was performed to beneficially utilize abundant restaurant waste such as coconut waste and eggshell by converting them into valuable catalyst. In the present study, egg shell and coconut waste were synthesized using calcination method. There are many studies were conducted to develop a heterogeneous catalyst which will be cheap and environmentally friendly. SEM micrographs prove that the mixture of catalyst shows a bigger surface

area. This result is expected to increase the yield of biodiesel. It can be concluded that SEM image describes the irregular rod shape of the mixture of the catalysts and the particles agglomerated with each other to form a big surface area.

Acknowledgment The research was funded by FRGS grant (FRGS 13-079-0320) from the Government of Malaysia.

References

- Atadashi IM et al (2013) The effects of catalysts in biodiesel production: a review. *J Ind Eng Chem Kor Soc Ind Eng Chem* 19(1):14–26. <https://doi.org/10.1016/j.jiec.2012.07.009>
- Azis Y, Jamarun N, Arief S, Nur H (2015) Facile synthesis of hydroxyapatite particles from cockle shells (*Anadara granosa*) by hydrothermal method. *J Chem* 31(2)
- Buasri A et al (2013) Application of eggshell wastes as a heterogeneous catalyst for biodiesel production. *Sustain Energy* 1(2):7–13. <https://doi.org/10.12691/rse-1-2-1>
- Canakci M, Van Gerpen J (1999) Biodiesel production via acid catalysis. *Trans Am Soc Agric Eng* 42:1203–1210
- Chen K-T et al (2013) Rice husk ash as a catalyst precursor for biodiesel production. *J Taiwan Inst Chem Eng* 44(4):622–629. <https://doi.org/10.1016/j.jtice.2013.01.006>
- Gryglewicz S (1999) Rapeseed oil methyl esters preparation using heterogeneous catalysts. *Bioresour Technol Elsevier* 70(3):249–253
- Jagdale SS, Jugulkar LM (2012) Review of various reaction parameters and other factors affecting on production of chicken fat based biodiesel. *Int J Mod Eng Res* 2(2):407–411
- Lam MK, Lee KT, Mohamed AR (2010) Homogeneous, heterogeneous and enzymatic catalysis for transesterification of high free fatty acid oil (waste cooking oil) to biodiesel: a review. *Biotechnol Adv Elsevier Inc* 28(4):500–518. <https://doi.org/10.1016/j.biotechadv.2010.03.002>
- Moradi G, Mohammadi F (2014) Utilization of waste coral for biodiesel production via transesterification of soybean oil. *Int J Environ Sci Technol Springer* 11(3):805–812
- Nelson L, Foglia T, Marmer W (1996) Lipase-catalyzed production of biodiesel. *J Am Oil Chem Soc* 73:1191–1195
- Ngadi N et al (2017) Production of biodiesel from palm oil using cockle shell waste as heterogeneous catalyst. *Jurnal Teknologi. Penerbit Utm Press Penerbit Utm Press, Skudai, Johor, 81310, Malaysia* 79(5):183–188
- Obadiah A et al (2012) Biodiesel production from palm oil using calcined waste animal bone as catalyst. *Bioresour Technol Elsevier* 116:512–516
- Shimada Y et al (1999) Conversion of vegetable oil to biodiesel using immobilized *Candida antarctica* lipase. *J Am Oil Chem Soc* 76(7):789–793. <https://doi.org/10.1007/s11746-999-0067-6>
- Sulaiman S, Raman AAA, Aroua MK (2010) Coconut waste as a source for biodiesel production. In *Chemical, biological and environmental engineering (ICBEE), 2010 2nd International Conference on pp 254–256. IEEE*
- Sulaiman S, Abdul Aziz AR, Aroua MK (2013a) Optimization and modeling of extraction of solid coconut waste oil. *J Food Eng* 114(2). <https://doi.org/10.1016/j.jfoodeng.2012.08.025>
- Sulaiman S, Abdul Aziz AR, Aroua MK (2013b) Reactive extraction of solid coconut waste to produce biodiesel. *J Taiwan Inst Chem Eng* 44(2). <https://doi.org/10.1016/j.jtice.2012.10.008>
- Sun H et al (2010) Transesterification of sunflower oil to biodiesel on ZrO₂ supported La₂O₃ catalyst. *Bioresour Technol Elsevier* 101(3):953–958
- Talha NS, Sulaiman S, Azmi AS (2017) High temperature solid-catalyzed in-situ transesterification for biodiesel production. *Jurnal Teknologi*, 79(5–3). <https://doi.org/10.11113/jt.v79.11329>
- Vyas AP, Subrahmanyam N, Patel PA (2009) Production of biodiesel through transesterification of *Jatropha* oil using KNO₃/Al₂O₃ solid catalyst. *Fuel Elsevier* 88(4):625–628

Chapter 9

Carrier-Free Enzyme Immobilization by Cross-Linked Enzyme Aggregates (CLEA) Technology



Faridah Yusof and Soofia Khanahmadi

Abstract Biocatalyst in the form of enzymes is widely used in diverse applications. Unfortunately, free enzymes are quite unstable and may undergo denaturation even under mild conditions, thus hampering their usefulness, and this may lead to higher cost in enzyme based applications. A credible solution is to immobilize the enzymes prior to usages. This procedure was proven to improve the performances in term of stability, activity and selectivity of the enzymes. In addition, separation of product from the used enzyme was made easier and enzyme recyclability was possible. However, carrier-supported enzyme immobilization suffers from many disadvantages, such as large amounts of non-catalytic mass and expensive carrier beads. Thus, to overcome this problem, cross-linked enzyme aggregates (CLEA) has been since widely researched. It involves simple procedure and has many benefits; for example, this procedure does not need purified enzyme. The technique involves an initial precipitation of enzymes using, either organic solvents, salts, non-ionic polymers or acids to obtain aggregates. It is then followed by cross-linking the aggregates by polyfunctional reagents, such as glutaryldehyde, whereby the enzyme molecules react among themselves, leading to the formation of ‘solid biocatalyst’. This chapter aims at deliberating the CLEA technique for enzyme immobilization. Lipase extracted from cocoa pod husk (CPH), an agricultural waste product, has been chosen as the model enzyme, and upon immobilization, the biocatalyst is termed as CLEA-lipase. The production of CLEA-lipase was carried out under an optimum condition and this was followed by experimental comparison with the free-form, on the temperature and pH optima and stabilities. Additionally, recyclability of CLEA-lipase was also studied. Finally, the morphology of the solid biocatalyst, which has bearings towards its activity, was examined by Field Emission Scanning Electron Microscopy (FESEM).

F. Yusof (✉) · S. Khanahmadi
International Islamic University Malaysia, Kuala Lumpur, Malaysia
e-mail: yfaridah@iium.edu.my

Keywords Cross-linked enzyme aggregates (CLEA) · Immobilization · CLEA-lipase · p-nitrophenyl palmitate · p-nitrophenol · Optimum temperature · Optimum pH · Reusability of enzyme · Glutaryldehyde · Ammonium sulphate · Cocoa pod husk · Stability of enzyme

9.1 Introduction

Enzymes are biocatalysts which catalyze most metabolic reactions in living organisms. The enzymes possess desirable qualities which make them appropriate for diverse applications. However, the enzymes are quite unstable, and often denature, even under mild environmental condition. Insufficient enzyme stability under the processing condition and short catalytic lifespan hamper its usefulness; thus elevating the cost of enzyme-based applications. With the advent of biotechnology, it is learned that immobilization of enzyme is a credible solution for most of the problems related to free enzymes. It is a unique tool that improves the performance, stability, activity, and selectivity of the enzyme (Mateo et al. 2007; Rodrigues et al. 2013). Not only immobilization of enzymes can enhance the structural rigidity of the enzyme molecules, thus increasing their stability in response to extreme temperatures and pH's, it can also facilitate easy separation of the catalyst from the product. With this powerful technique, the enzyme can also be recycled several times, extending its usefulness. There are many ways to categorize the available immobilization methods. Accordingly, Chaplin and Bucke (1990) had categorized the methods into four strategies, that is, by adsorption, covalent binding, entrapment and membrane confinement. The different strategies for enzyme immobilization are illustrated in Fig. 9.1.

(a) By adsorption

Adsorption of enzymes onto insoluble supports occurs via different modes such as hydrophobic, van der Waals and ionic interactions. Although the physical links between the enzyme molecules and the support are often very strong, it may be weakened by many factors such as changes in pH, ionic strength and sometimes even upon the introduction of the substrates. The choices of adsorbents are aplenty, such as ion-exchange matrices, porous carbon, clays, hydrous metal oxides, glasses and polymeric aromatic resins, but the choice depends mainly on minimizing the leakage of enzymes from supports during the enzyme use (Chaplin and Bucke 1990).

(b) By covalent binding

Covalent binding is another enzyme immobilization strategy. Covalent bonds that formed between enzymes and insoluble matrices may provide stronger bonds than in adsorption method. There are many functional groups on the enzymes that can form covalent bonds with functional groups that are present on the support materials introduced, however, covalent bonds formation depends upon the

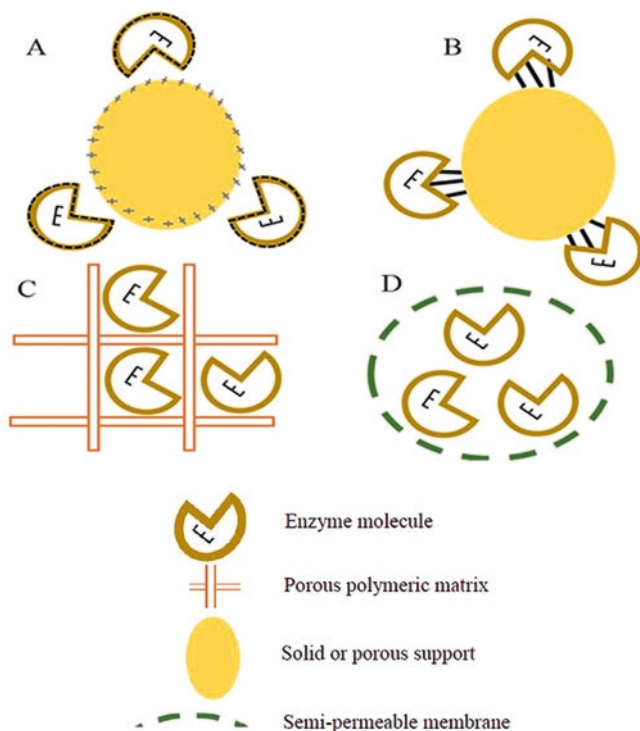


Fig. 9.1 Enzyme Immobilization: (a) by adsorption, (b) by covalent bonding, (c) by entrapment and (d) by membrane confinement. (Adapted from Chaplin and Bucke 1990)

availability and reactivity as well as the stability of the covalent link, once formed. The reactivity of the protein side-chain nucleophiles is determined by their state of protonation (i.e., charged status) and roughly follows the relationship $-S^- > -SH > -O^- > -NH_2 > -COO^- > -OH > > -NH_3^+$ where the charges may be estimated from a knowledge of the pK_a values of the ionizing groups and the pH of the solution (Chaplin and Bucke 1990). Lysine groups on the enzymes are the most likely groups that form covalent bonding with the functional groups on the insoluble supports, especially in slightly alkaline solutions. Moreover, lysine also appears to be only very rarely involved in the active sites of enzymes.

(c) By entrapment

Immobilization of enzyme by entrapment within gels or fibers would be a useful process, especially if it involved low molecular weight substrates and products. However, large substrate molecules will have difficulties in accessing the active sites of entrapped enzymes. The entrapment process may be a purely physical caging or may involve covalent binding. One example of enzyme entrapment is by using calcium alginate, which can be carried out by making up an emulsion of the enzyme

plus sodium alginate, whereby the mixture is then extruded dropwise through a pasture pipette into a gently stirred calcium chloride solution to yield beads of enzymes entrapped in calcium alginate. The beads are washed thoroughly with distilled water to remove non-trapped enzyme or unreacted reagents before it can be used.

(d) By membrane confinement

Enzymes can be immobilized onto semipermeable membranes by several different methods. The enzyme is confined while allowing free passage for the substrates and reaction products. Enzymes can be immobilized on one side of a semipermeable membrane while reactants and products can be present on the same side or the other side. There is another mode of enzyme confinement, that is, by encapsulating the enzyme within small membrane-bound droplets or liposomes. Liposomes are concentric spheres of lipid membranes, surrounding the soluble enzyme and they are formed by the addition of phospholipid to enzyme solutions.

9.2 Cross-Linking of Enzymes

Cross-linking method is another version of enzyme immobilization under the category of covalent binding. It differed from the above already explained under covalent binding, because the covalent bonds in, this case, can either occur between the enzyme and the supports molecules or among the enzyme molecules themselves, assisted by polyfunctional reagents, termed 'cross-linker', such as glutaraldehyde, diazonium salts, hexamethylene diisocyanate and N-N' ethylene bismaleimide. The demerit of using polyfunctional reagent is that they can denature the enzyme. But in the last few decades, enzymes cross-linked to each other have gained much interest due to its simplicity. This 'carrier-free immobilized enzymes' method, such as cross-linked enzyme crystals (CLECs) and cross-linked enzyme aggregates (CLEAs) has several advantages, more so, it does not need support materials, thus considered a cheaper version of the immobilization method. However, the preparation of CLECs is disadvantageous as it requires enzyme in crystallized form, which is often a cumbersome procedure that demands enzyme of high purity. In contrary, it is well-understood that the addition of salts, water-miscible organic solvents or non-ionic polymers, to an aqueous solution of proteins results in precipitation, forming physical aggregates of protein molecules, held together by non-covalent bonds. These phenomena triggered the development of a new family of immobilized enzymes, termed 'cross-linked enzyme aggregates (CLEA).

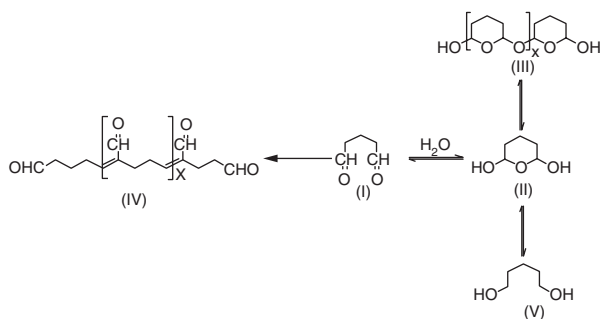


Fig. 9.2 Possible structure of glutaraldehyde in aqueous solution. (Barbosa et al. 2014)

9.2.1 Cross-Linked Enzyme Aggregate (CLEA)

CLEA is the latest mode of enzyme immobilization technique, which emphasized on its carrier-free form of immobilization. A lot of researches has been carried out on this area in recent years, mainly because of its many benefits and simplicity (Sheldon 2007; Sheldon 2011). Carrier bound immobilization was known to have many disadvantages, which is usually associated with large amounts of non-catalytic mass and expensive carrier beads. According to Anbu et al. (2005), CLEA technology may lead to purification of certain proteins when the overall conditions for the precipitation assigned to the target protein are milder than those required for the precipitation of some contaminants. Nevertheless, a very high level of enzyme purification should not be expected (Garcia-Galan et al. 2011). The technique initially involves precipitation of enzyme using organic solvents, salts, non-ionic polymers or acids to obtain aggregates, after which, the aggregates formed are cross-linked by the addition of polyfunctional reagents such as glutaraldehyde which causes the protein molecules to react between themselves. This finally results in the formation of ‘solid biocatalysts.’ Most often, glutaraldehyde has been used because as a reagent; it exhibits the dual function of not just being a cross linker but also has the ability to polymerize (Migneault et al. 2004). During the process of immobilization, the internal structure of the enzyme can be infiltrated by glutaraldehyde which facilitates the reaction of aldehyde group with primarily the amino groups present in the protein, although it may eventually react with other groups (thiols, phenols, and imidazoles) (Migneault et al. 2004; Walt and Agayn 1994; Habeeb and Hiramoto 1968; Wine et al. 2007). Barbosa et al. (2014) proposed some possible glutaraldehyde structures, (Fig. 9.2) as it appears in the solution. However, the exact arrangement of the main structures related to protein cross-linking or enzyme immobilization with regard to glutaraldehyde is still not fully clarified. It is clear that the structure of the glutaraldehyde relevant for the modification of enzymes and supports is not a linear one, but some fairly stable phases. The effectiveness of cross-linking depends upon the content of amine group the enzyme have. Thus, if the enzyme contains less amine group, the cross-linking might not be very effective. In order to overcome this issue, the aggregation can be performed in the presence of certain additives such as

bovine serum albumin (BSA) which contains a large number of amine groups and hence improves the activity and stability of CLEA.

9.3 The Scope of This Chapter

This chapter aims at deliberating the use of CLEA technique to immobilize enzyme. In this chapter, lipase has been chosen to be the model enzyme, thus termed 'CLEA-lipase.' The lipase has been extracted from cocoa pod husk (CPH), an agricultural waste product, easily available in Malaysia. The production of CLEA-lipase was carried out under an optimum condition as described in Yusof et al. (2016) and Khanahmadi et al. (2015) and this was followed by experimental comparison with the free-form, on the temperature and pH optima and temperature and pH stabilities. In addition, the recyclability of CLEA-lipase was evaluated. The morphology of the solid CLEA-lipase, which may have bearings towards its activity, was examined by FESEM.

9.4 Materials and Methods

9.4.1 Materials

The equipment/apparatus needed are spectrophotometer, centrifuge, micropipettes and orbital shaker. The consumable items needed are pipette tips of several dimensions (1 ml and 20 μ l) and Falcon tubes (15 ml). As for the chemicals and reagents, these are needed in the experiments: Glutaraldehyde, *p*-nitrophenyl palmitate (*p*NPP), *p*-nitrophenol, bovine serum albumin (BSA), ammonium sulfate, sodium phosphate, sodium hydroxide, Triton X-100, trizma base and sodium dodecyl sulfate (SDS).

9.4.2 Methods

9.4.2.1 Lipase Activity assay

p-Nitrophenyl palmitate (*p*NPP) was used as the substrate for lipase enzyme activity assay, whereby, the appearance of yellow colored *p*-nitrophenol was monitored by absorbance. A stock substrate solution was made by dissolving 28 mg of *p*-NPP in 100 ml of 1% v/v Triton 100-X and 1.7 ml of 1% (w/v) SDS with stirring and heating. The solution was quite turbid at the beginning of the heating but cleared after a while.

To start the reaction, 1 ml of *p*-NPP stock solution was incubated with 1 ml of 0.1 M Tris-HCl at pH 8.2 and 0.5 ml of enzyme sample in a water bath for 30 min at

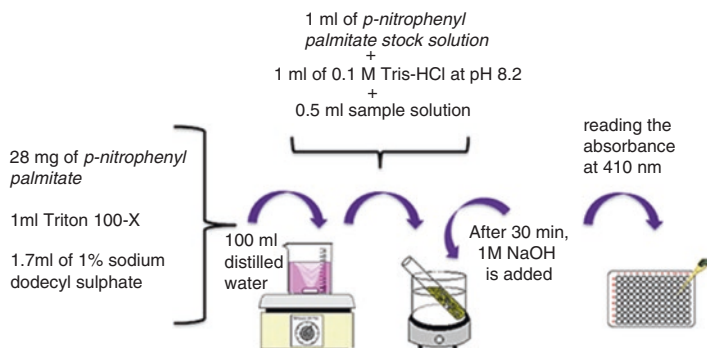


Fig. 9.3 Steps in conducting lipase activity assay

37°C, after which 1 ml of 1 M NaOH was added to stop the reaction. The absorbance of the incubation product was measured by reading the absorbance at 410 nm. The absolute amount of *p*-nitrophenol produced was calculated from a calibration graph constructed with known amounts of *p*-nitrophenol. Figure 9.3 illustrates steps conducted when performing the lipase activity assay. A unit (U) of lipase enzyme activity is defined as the amount of enzyme required to release 1.0 μmol of *p*-nitrophenol per minute under the assay conditions. Lipase activity was calculated as:

$$\text{Lipase activity} = \left(\frac{\text{Units}}{\text{ml}} \right) = \frac{(\text{Absorbance at 410 nm}) \times \text{Total volume of assay (mL)}}{\text{volume of used enzyme (ml)} \times \text{Time of assay (min)} \times 0.0071} \quad (9.1)$$

Where 0.0071 is the slope of the standard calibration curve of *p*-nitrophenol absorbance.

9.4.2.2 Preparation of CLEA-Lipase

Crude lipase enzyme was optimally extracted from CPH (Yusof et al. 2016). The best yield of free lipase, based on regarding activity (11.43 U/ml), was extracted under the following optimum conditions, that is, using 7% (w/v) CPH in 50 mM sodium phosphate buffer at pH 8. The protein content of the crude enzyme extract from CPH was determined by the Bradford assay method (Bradford 1976). A crude enzyme solution of 0.5 ml was poured into a 15 ml Falcon tube. To the enzyme solution, 30% w/v ammonium sulfate (as precipitant), 70 mM glutaraldehyde (as cross-linker) and 0.23 mM BSA (as additive) were added to make the final volume of the solution to 4 ml. The solution was agitated at 200 rpm for 17 h at room temperature. To achieve the best mixing, the tube was inclined at an angle, while agitating as pictured in Fig. 9.4.

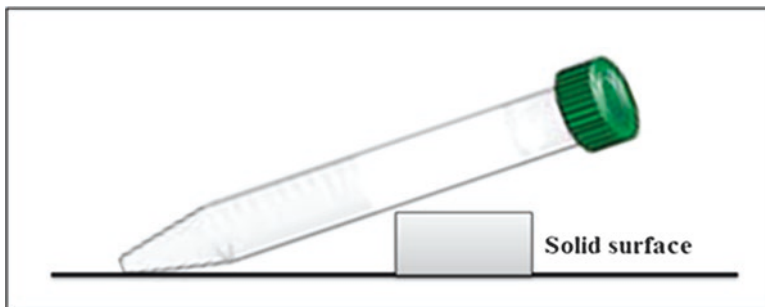


Fig. 9.4 The position of sample on the orbital shaker during CLEA preparation

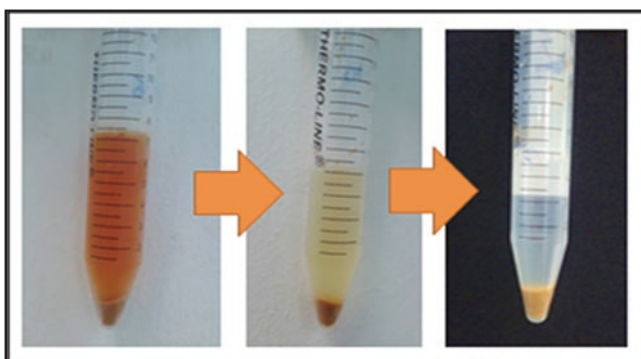


Fig. 9.5 CLEA-lipase was washed and centrifuged three times with distilled water after 17 h incubation time

After 17 h of mixing, 3 ml of water was added and mixed well, and then the mixture was centrifuged at 4000 rpm at 4°C for 30 min. The supernatant was discarded and the residue, which is CLEA-lipase, was washed with water for another three times (Fig. 9.5). The final CLEA-lipase preparation was kept under 5 ml water and stored at 4°C until further use.

9.4.2.3 Effect of CLEA-Lipase Preparation Parameters

Many parameters influenced the final product of CLEA enzymes. In this study, three important parameters were selected, namely, the concentration of ammonium sulfate, glutaraldehyde, and BSA. To determine the effect of these parameters, One-Factor-At-a-Time (OFAT) design of experiment was adopted. OFAT experiment was conducted by varying the value of parameter tested while keeping other parameters constant at its optimum level. The concentration of ammonium sulfate tested were 10, 20, 30, 40 and 50% w/v, glutaraldehyde at 40, 50, 60, 70, and 80 mM, and finally for BSA at 0.018, 0.094, 0.23, 0.28 and 0.37 mM.

9.4.2.4 Optimum Temperature and pH

To determine the optimum temperature for the free and CLEA-lipase the relative activity of the enzyme was assessed after incubation at different temperatures (25–60°C) for 30 min with substrate added, in 50 mM Tris-HCl at pH 8.2. To measure the optimum pH, the relative activity was assessed while incubating the enzymes at optimum temperature (results obtained in the above step), with substrate added at various pH's (5–10).

9.4.2.5 Stability Tests

The temperature stability was determined by measuring the residual activity of free and CLEA enzyme. The preparation was incubated in substrate-free buffer at optimum pH for 30 min at temperatures ranging from 25°C to 60°C. After incubation, the preparation was brought back to room temperature, the thereafter substrate was added, and the normal lipase assay was carried out.

The pH stability test was determined by measuring the residual activity of free and CLEA-lipase by incubating enzyme in the substrate-free buffer at optimum temperature at various pH's ranging from 5 to 10. After 30 min, the substrate was added, and the normal lipase assay was conducted out.

9.4.2.6 Reusability of CLEA-Lipase

The prepared CLEA, after it was first used (first cycle), was washed three times with distilled water and then kept in 5 ml water and stored at 4°C. The enzyme activity was measured after 2 days. This cycle was repeated for another five times. The residual activity was calculated by taking the enzyme activity of the first cycle as 100%.

9.5 Results and Discussion

It has been reported by Garcia-Galan et al. (2011), that the final particle size of CLEA depends on the kind and the amount of precipitant, stirring rate, concentration of glutaraldehyde and also protein concentration. In order to retain the enzyme activity in the final product of CLEA, the entire free enzymes should be precipitated to a significant level. Among the different types of precipitants, ammonium sulfate worked out to be the best for precipitating the entire soluble enzyme (Talekar et al. 2012; Yu et al. 2013). Based on Fig. 9.6a, the production of CLEA-lipase from the crude CPH reached the highest level when the concentration of ammonium sulfate

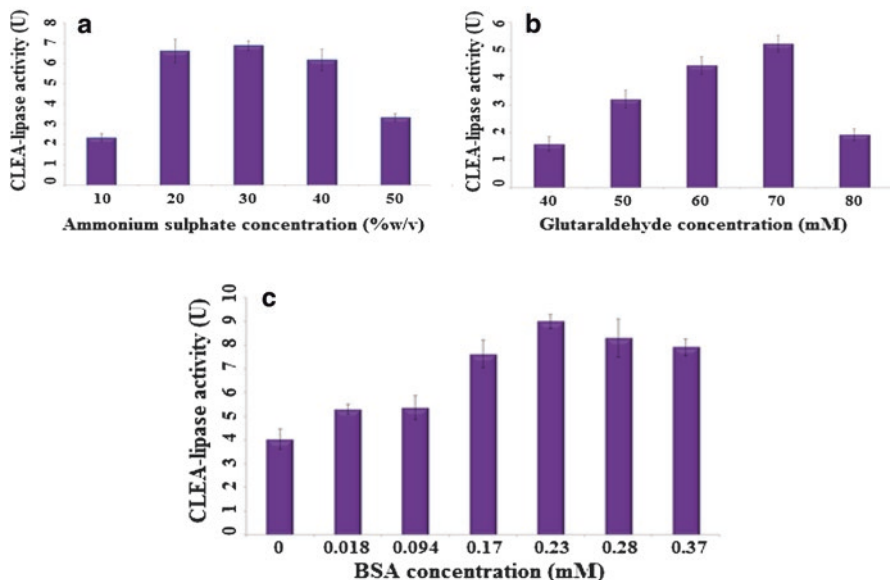


Fig. 9.6 Effect of different concentration of: A. ammonium sulfate (10-50% w/v), B. glutaraldehyde (40-80 mM) and C. BSA (0-0.37 mM) on CLEA-lipase activity from CPH

was 30% (w/v). This means that 30% (w/v) ammonium sulfate concentration was adequate to precipitate most of the lipase out of the solution. Although the addition of more ammonium sulfate will precipitate more protein from the supernatant, which may indicate more free lipase gets involved in forming CLEA (Khanahmadi et al. 2015), high concentration of ammonium sulfate may also lead to protein denaturation that is responsible for loss of enzyme activity (Wang et al. 2011).

The amount of glutaraldehyde concentration needed for maximal lipase activity was determined by testing different concentrations of glutaraldehyde of 40–80 mM. The highest lipase activity of 5.23 U (Fig. 9.6b) was observed at approximately 70 mM glutaraldehyde when the other parameters were set at their optimum level. In general, the reaction of glutaraldehyde molecule with the amine residues present on the CLEA-lipase surface positioned close to the active site could influence (positively/negatively) the lipase activity (Guauque Torres et al. 2014). In the presence of low amount of cross-linkers, the enzyme molecule will leach into the media because the flexible and unstable nature of immobilized enzyme persists for certain duration. Use of an excessive amount of glutaraldehyde is accompanied by the decrease in enzyme activity due to the loss of minimum flexibility required for the enzyme to show its activity (Sheldon 2011).

The addition of BSA as an additive can prevent the formation of clusters in the excess concentration of glutaraldehyde during CLEA formation, which limits the mass transfer process. The positive effect of the presence of BSA is, it provides the lysine residues, which contain amino group side chains that can bind with glutaraldehyde to prevent the denaturation of the targeted protein. However, the downside

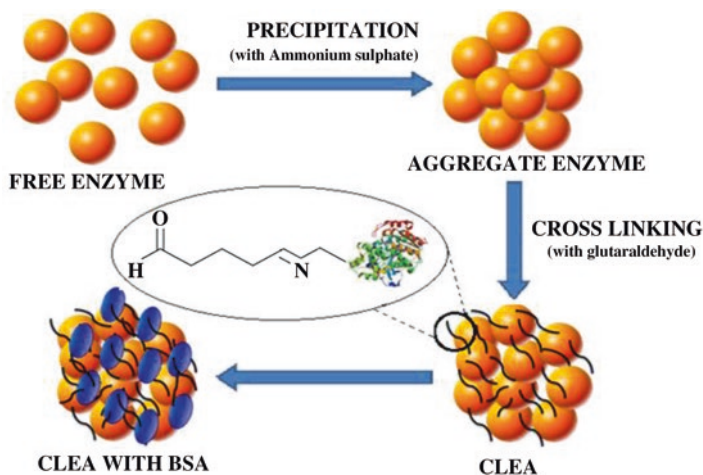


Fig. 9.7 An illustration of CLEA preparation with the addition of BSA as additive. The amine group of enzyme and BSA is reacting with aldehyde group of glutaraldehyde to form cross-linkages

is, the volumetric loading of the target enzyme is decreased by BSA, as the inert protein will occupy a portion of the volume (Caballero Valdés et al. 2011). Figure 9.6c shows the effect of different concentrations of BSA as an additive (0–0.37 mM) on CLEA-lipase activity. A rise in CLEA-lipase activity was seen at levels of BSA ranging from 0 to 0.23 mM while a decrease in activity was observed with subsequent increase in concentrations. The reduction of CLEA activity upon the increase of BSA addition is probably due to an inadequate contact of enzyme-substrate (which is needed in enzyme reaction), because of a shielding effect by BSA molecules (Cabana et al. 2007). Figure 9.7 shows a schematic diagram of CLEA preparation with ammonium sulfate as precipitant and BSA performing as an additive.

The optimum pH for free and CLEA-lipase were 8 and 8.2 respectively (Fig. 9.8). The optimum temperature for CLEA-lipase was found to be 60°C while for free enzyme it was 45°C (Fig. 9.9). It seems that immobilization resulted in different optimum pH and temperature. Immobilization by CLEA technology results in an elevated tolerance of the enzyme against high temperatures, and this phenomena is a very significant property in the industrial settings.

When thermal stability was compared between the free lipase and its CLEA counterparts, CLEA showed more stable over a wide range of temperature tested from 20°C to 60°C, as shown in Fig. 9.10a. Free lipase was partially activated or denatured when incubated at high temperature (Yu et al. 2013). The denaturation was as a result of rupturing of the proteins' secondary, tertiary or quaternary structures which tend to occur at high temperature. Not only that the functional structure of proteins is lost; the active and allosteric sites also lose their functionality, reducing the occurrence of enzyme-substrate binding. From the figures it can be seen that free lipase significantly lost its activities at 60°C, while CLEA-lipase retained its activities as much as 70%.

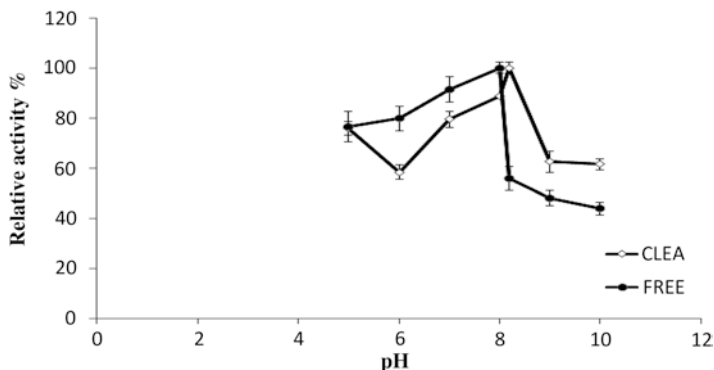


Fig. 9.8 Optimum pH for free and CLEA-lipase obtained from CPH. Reaction condition: 0.5ml crude enzyme (100mM) in different range of pH (5-10) at optimum temperature and incubation time (30 min)

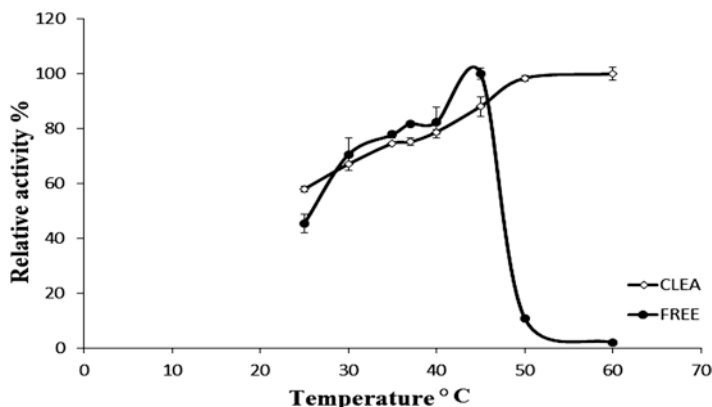


Fig. 9.9 Optimum temperature for free and CLEA-lipase obtained from CPH. Reaction conditions: 0.5 ml crude enzyme in different range of temperature (25-60°C) with Tris-HCl buffer (100 mM, pH 8.2) and incubation time of 30 min

When pH stability was compared, CLEA demonstrated a stability that was significantly higher than the free enzymes within the ranges of pH 5 to 10 (Fig. 9.10b). The higher pH resistance of CLEA towards extreme pH's (acidic and basic) is assumed to be due to the covalent inter-cross-linking through enzyme aggregate that increases the rigidity of enzyme (Yu et al. 2013). The three-dimensional structure of the protein is held together by hydrogen bonds. In a highly acidic (more H⁺ ions) environment, the hydrogen bonding in the free enzyme gets disrupted and results in protein denaturation.

In the industrial settings, to reduce cost, it makes economic sense if enzymes used can be recycled. Immobilization of enzymes allows it to be recycled. Thus, the stability of enzyme is very crucial and should be high enough to allow it to be reused

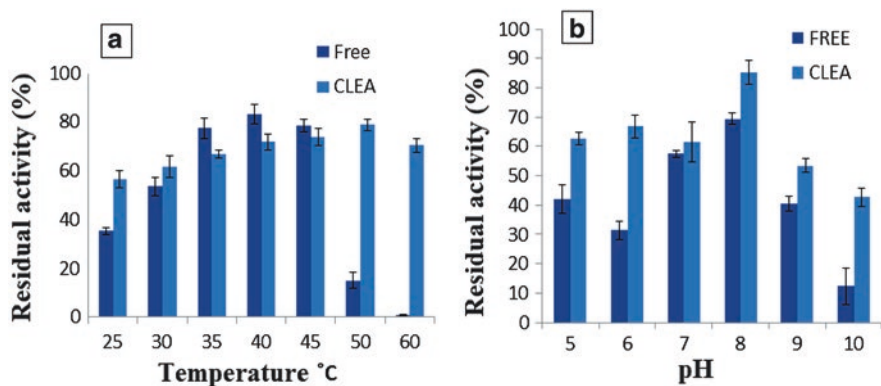


Fig. 9.10 Stabilities of CLEA-lipase and free lipase. (a) Effect of temperature (25-60°C); (b) Effect of pH (100 mM salt buffer pH 5 to 10)

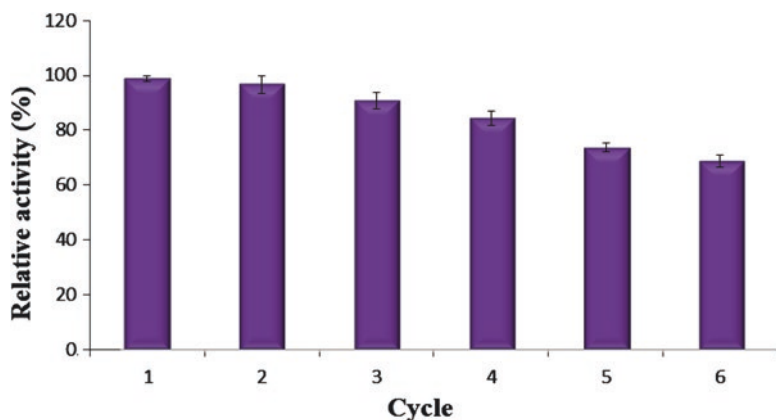


Fig. 9.11 Recyclability Study of CLEA-lipase from CPH

in several cycles (Mateo et al. 2007). Reusability of an enzyme is possible only when the activity is retained even after several reaction cycles (Garcia-Galan et al. 2011). Reusability of CLEA-lipase was studied by carrying out the hydrolysis of *p*-NPP up to six cycles. Repeated use of CLEA-lipase up to three times was possible with loss of only 10% of the initial activity. Figure 9.11 shows that CLEA-lipase was able to retain more than 60% of the initial activity after six batches of reuse.

The shape and size of the particle in CLEA has a good bearing towards the activity of CLEA enzymes, thus needs to be studied in detail. With regard to CLEAs, Schoevaart et al. (2004) have indicated that CLEAs have either a spherical appearance (Type 1) or a less-structured form (Type 2). Schoevaart et al. (2004) reported that the Type 1 aggregates could accommodate a thousand times more enzyme molecules than the Type 2, as the molecules of the Type 1 enzyme are packed in a small

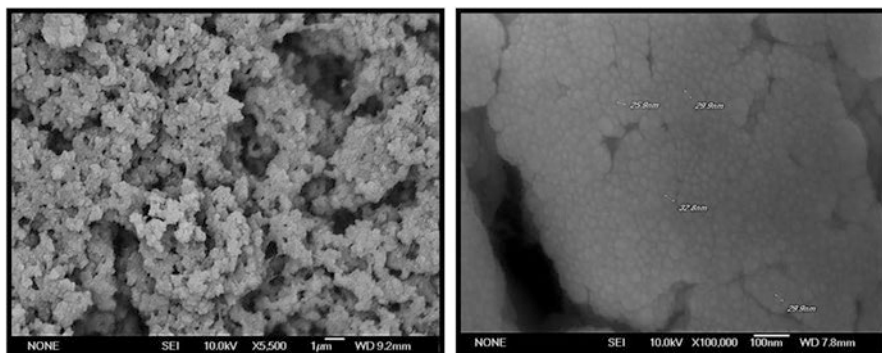


Fig. 9.12 FESEM images of CLEA-lipase from CPH at different magnifications (5500X times and 100000X)

volume. But as surely be ensued, and contrast to the free protein in solution, mass-transport limitations will occur especially with fast reactions. But, when CLEA has finely dispersed in the solution, such as the case when the cross-linking process has ended and subsequently quenched, this effect was observed to be small. Field Emission Scanning Electron (FESEM) micrograph images of CLEA-lipase from CPH, shown in Fig. 9.12, shows that it has a spherical appearance, thus is Type 1 aggregates. The diameter of the CLEA lipase is about 25–32 nm.

9.6 Conclusion

In this chapter, the principle and methodology for the preparation of cross-linked enzyme aggregate (CLEA) were deliberated. As a model enzyme, lipase extracted from CPH was used to elaborate the idea of enzyme self-immobilization. Around 30 mM ammonium sulfate as precipitant, 70 mM glutaraldehyde as cross-linker and 0.23 mM BSA as additives were used for immobilization of lipase obtained from CPH. This study has illustrated the advantages that CLEA technology can offer while taking into account the immobilization method which is simple and sturdy and yields enzymes that are highly stable towards the elevated temperature and extreme pH conditions. In addition, it shows superior retention of activity after six cycles as compared to the free form, which can only be used once.

References

- Anbu P, Gopinath S, Hilda A, Annadurai G (2005) Purification of keratinase from poultry farm isolate-*Scopulariopsis brevicaulis* and statistical optimization of enzyme activity. *Enzym Microb Technol* 36(5):639–647
- Barbosa O, Ortiz C, Berenguer-Murcia Á, Torres R, Rodrigues RC, Fernandez-Lafuente R (2014) Glutaraldehyde in bio-catalysts design: a useful crosslinker and a versatile tool in enzyme immobilization. *RSC Adv* 4(4):1583–1600

- Bradford MM (1976) A rapid and sensitive method for the quantitation of microgram quantities of protein utilizing the principle of protein-dye binding. *Anal Biochem* 72:248–254
- Caballero Valdés E, Wilson Soto L, Aroca Arcaya G (2011) Influence of the pH of glutaraldehyde and the use of dextran aldehyde on the preparation of cross-linked enzyme aggregates (CLEAs) of lipase from *Burkholderia cepacia*. *Electron J Biotechnol* 14(3):1–10
- Cabana H, Jones JP, Agathos SN (2007) Preparation and characterization of cross-linked lactase aggregates and their application to the elimination of endocrine disrupting chemicals. *J Biotechnol* 132:23–31
- Chaplin M, Bucke C (1990) *Enzyme technology*. Cambridge University Press, Cambridge
- García-Galan C, Berenguer-Murcia Á, Fernández-Lafuente R, Rodrigues RC (2011) Potential of different enzyme immobilization strategies to improve enzyme performance. *Adv Synth Catal* 353(16):2885–2904
- Guaque Torres M, Foresti M, Ferreira M (2014) CLEAs of *Candida antarctica* lipase B (CALB) with a bovine serum albumin (BSA) cofeeder core: Study of their catalytic activity. *Biochem Eng J* 90:36–43
- Habeeb AFSA, Hiramoto R (1968) Reaction of proteins with glutaraldehyde. *Arch Biochem Biophys* 126:16–26
- Khanahmadi S, Yusof F, Amid A, Mahmud SS, Mahat MK (2015) Optimized preparation and characterization of CLEA-lipase from cocoa pod husk. *J Biotechnol* 202:153–161
- Mateo C, Palomo JM, Fernández-Lorente G, Guisán JM, Fernández-Lafuente R (2007) Improvement of enzyme activity, stability and selectivity via immobilization techniques. *Enzym Microb Technol* 40(6):1451–1463
- Migneault I, Dartiguenave C, Bertrand MJ, Waldron KC (2004) Glutaraldehyde: behavior in aqueous solution, reaction with proteins, and application to enzyme crosslinking. *BioTechniques* 37(5):790–806
- Rodrigues RC, Ortiz C, Berenguer-Murcia Á, Torres R, Fernández-Lafuente R (2013) Modifying enzyme activity and selectivity by immobilization. *Chem Soc Rev* 42(15):6290–6307
- Schoevaart R, Wolbers M, Golubovic M, Ottens M, Kieboom A, Van Rantwijk F, ... Sheldon R (2004) Preparation, optimization, and structures of cross-linked enzyme aggregates (CLEAs). *Biotechnol Bioeng*, 87(6):754–762
- Sheldon RA (2007) Cross-linked enzyme aggregates (CLEA® s): stable and recyclable biocatalysts. *Biochem Soc Trans* 35(6):1583
- Sheldon RA (2011) Characteristic features and biotechnological applications of cross-linked enzyme aggregates (CLEAs). *Appl Microbiol Biotechnol* 92(3):467–477
- Talekar S, Ghodake V, Ghotage T, Rathod P, Deshmukh P, Nadar S et al (2012) Novel magnetic cross-linked enzyme aggregates (magnetic CLEAs) of alpha amylase. *Bioresour Technol* 123:542–547
- Walt DR, Agayn VI (1994) The chemistry of enzyme and protein immobilization with glutaraldehyde. *TrAC Trends Anal Chem* 13:425–430
- Wang M, Jiang L, Li Y, Liu Q, Wang S, Sui X (2011) Optimization of extraction process of protein isolate from mung bean. *Procedia Eng* 15:5250–5258
- Wine Y, Cohen-Hadar N, Freeman A, Frolov F (2007) Elucidation of the mechanism and end products of glutaraldehyde crosslinking reaction by X-Ray structure analysis. *Biotechnol Bioeng* 98(3):711–718
- Yu CY, Li XF, Lou WY, Zong MH (2013) Cross-linked enzyme aggregates of Mung bean epoxide hydrolases: A highly active, stable and recyclable biocatalyst for asymmetric hydrolysis of epoxides. *J Biotechnol* 166(1):12–19
- Yusof F, Khanahmadi S, Amid A, Mahmud SS (2016) Cocoa pod husk, a new source of hydrolase enzymes for preparation of cross-linked enzyme aggregate. *Springerplus* 57(5):1–18

Chapter 10

Isolation of Microfibrillated Cellulose (MFC) Via Fungal Cellulases Hydrolysis Combined with Ultrasonication



Dzun Noraini Jimat and Aviceena

Abstract Celluloses, the most abundant biopolymers which exist in plant sources are potential materials to be used in manufacturing high performance composites due to their fascinating structure and properties. In plant cell walls, they are embedded in matrix substances such as hemicellulose and lignin. Removal of matrix substances is required before fibrillating the cellulose fibres into nanoscale-sized. The obtained microfibrillated cellulose (MFC) poses different features depending to its origin and degree of initial processing procedures and fibrillation method use. Thus, this chapter explains the isolation steps of microfibril cellulose (MFC) from cocoa pod husk via fungal cellulases hydrolysis combined with ultrasonication. The morphology and structural observation of the MFC of cocoa pod husk (CPH) via scanning electron microscopy images and fourier transform infrared spectroscopy analysis respectively were also showed in this chapter.

Keywords Cellulases · Cocoa pod husk · Fibers · Fourier Transform Infrared · Fungal · Hydrolysis · Microfibrillated cellulose · Scanning electron Microscopy · Ultrasonication

10.1 Introduction

Microfibrillated cellulose (MFC) from biomass has recently gained attention attributed to their low density, high mechanical properties, biodegradable nature, renewability, and appealing economic value (Abdul Khalil et al. 2014). It refers to cellulosic fibrils disintegrated from the plant cell walls (Svagan et al. 2007). The thickness of MFC could, in principle, be as small as 3–10 nm, but is typically in the range of 20–40 nm since it usually consists of aggregates of cellulose microfibrils (Svagan et al. 2007). The production of MFC into nano-scale elements depends on

D. N. Jimat (✉) · Aviceena

Department of Biotechnology Engineering, Kulliyah of Engineering, International Islamic University Malaysia (IIUM), Kuala Lumpur, Malaysia

e-mail: jnoraini@iium.edu.my

the raw materials and the degree of processing and chemical treatments applied prior to mechanical fibrillation. Many studies have been done previously where the nanocellulose fibers were isolated using the combination of mechanical and chemical procedures. Pretreatment prior to the mechanical treatment (refining/homogenizing process) is significantly required to reduce the energy consumption of refining/homogenizing process of the feed material. The energy consumption in the latter process is very high due to the predominating hydrogen bonding between the cellulose microfibrils. Strong acidic or alkaline solutions are often used for pretreatment of lignocellulosic biomass. However, the combination of strongly acidic solutions and sonication leads to aggressive hydrolysis to attack the noncrystalline fractions (Paakko et al. 2007). This results in a mainly low aspect ratio of cellulose I fibril aggregates which leads to mechanically weak gel that is not particularly suitable for mechanical reinforcement (Paakko et al. 2007). The application of enzymatic hydrolysis as an alternative to chemical pretreatment has shown a growing interest due to its highly specific process and can be performed under mild conditions with low energy consumption as well as less corrosive. Many studies have been reported in employing enzymatic hydrolysis using commercial enzyme prior physical process in isolating MCFC (de Campos et al. 2013; Henriksson et al. 2007; Janardhnan and Sain 2006; Monschein et al. 2013; Paakko et al. 2007). In addition, a few studies reported the microbial pretreatment through solid state culture prior to mechanical treatment in defibrillation of lignocellulosic materials. Thus, this chapter explains the isolation steps of microfibril cellulose (MFC) from cocoa pod husk via fungal cellulases hydrolysis combined with ultrasonication.

10.2 Principle

Microfibrillated cellulose is produced by performing mechanical treatment consisting of refining and high-pressure homogenizing process steps. This mechanical treatment results in irreversible changes in the fibers, increasing their bonding potential by modification of their morphology and size (Nakagaito and Yano 2004). Steam explosion and high-intensity ultrasonication are among mechanical treatments used to extract nanocellulose fibers. However, mechanical refining methods tend to damage the microfibril structure by reducing molar mass, and degree of crystallinity or fail to sufficiently disintegrate the pulp fiber (Henriksson et al. 2007). By combining mechanical treatment with chemical or enzymatic pre-treatment, it is possible to reduce the high energy consumption associated with the mechanical treatment to disintegrate the fibers into microfibrillated cellulose. The use of strong acid or alkaline (high concentration) is considered toxic and causes the degradation of cellulose (Abraham et al. 2011). In contrast, the microfibrillated cellulose produced from enzymatically pretreated cellulosic wood fibers yielded a more favorable structure than nanofibers produced by pretreatment of strong acid hydrolysis (Siro and Plackett 2010). Lignocellulose biomass is a cellular complex which consists of cellulose, hemicellulose, and lignin, thus a specific process may be needed

for an effective production of microfibrillated cellulose/nanocellulose. The application of enzymatic hydrolysis as an alternative of chemical pretreatment has growing interest due to its highly specific process and can be performed under mild conditions with low energy consumption as well as less corrosive. This treatment involves a set of cellulases that can be categorized as A- and B- type cellulases (termed cellobiohydrolases), which are able to attack highly crystalline cellulose, and C- and D-type cellulases (termed endoglucanases) which attack the region of low crystallinity in the cellulose fiber. This means that the enzymatic pretreatment is a mild hydrolysis process and the degradation of cellulose can be avoided. This enzymatic pretreatment will also facilitate the subsequent mechanical steps by minimizing the shearing energy through less required passes and preventing the blockage of the homogenizer. Therefore, this study aims to extract microfibrillated cellulose via fungal pretreatment combined with ultrasonication and observe the morphology and structural changes of the extracted microfibrillated cellulose (MFC) via scanning electron microscopy (SEM) and Fourier transform infrared (FTIR) spectroscopy, respectively.

10.3 Objective

The objective of this experiment is to isolate microfibrillated cellulose (MFC) through fungal cellulose hydrolysis and ultrasonication.

10.4 Chemicals and Equipment

All chemicals, consumables, and equipment in this procedure are listed in Tables 10.1 and 10.2.

Table 10.1 List of consumable items

| | |
|----|---|
| 1. | Autoclave bag |
| 2. | Laboratory Parafilm 4 in × 125 ft. roll |
| 3. | Disposable Petri dish |
| 4. | Cotton wool roll |
| 5. | Gauze roll |
| 6. | Sartorius pipette tips 1000 µl |
| 7. | Butane burner Labogaz 206 |
| 8. | Cellulose acetate filter (filter paper), Sartorius Stedim |
| 9. | Whatman filter papers No. 1 (110 mm) |

Table 10.2 List of equipment/apparatus

| | |
|-----|--|
| 1. | Spatula |
| 2. | Inoculating loop |
| 3. | Hockey stick glass rod |
| 4. | Sartorius pipette 100–1000 µl |
| 5. | Mortar and pestle |
| 6. | Magnetic heating plate |
| 7. | Laminar flow cabinet |
| 8. | Incubator shaker |
| 9. | Incubator, Memmert INES00-1406 |
| 10. | Chiller, LinDen-LFC402-30 |
| 11. | Autoclave, Hirayama HV-110 |
| 12. | Weighing balance, Mettler Toledo B204-S |
| 13. | Centrifuge, Hettich Zentrifugen Universal 320R |
| 14. | Vortex mixer, ERLA EVM-600 |
| 15. | Drying oven, Memmert |
| 16. | Ultrasonic, Dismembrator FB-705 |

10.5 Methods

10.5.1 *Preparation of Lignocellulosic Substrate: Cocoa Pod Husk (CPH)*

1. Cocoa pod husk (CPH) was washed and rinsed using tap water to remove any impurities, e.g., dirt, stones, and sand.
2. CPH was cut into the size of 5–7 cm length prior to the drying process.
3. CPH was placed in an oven dryer at 55 °C until constant weight (72 h).
4. The dried CPH was ground at 3500 rpm using a laboratory grinder MF 10 Basic (IKA WERKE) and sieved to get uniform particle size.
5. The granulated CPH was stored in an airtight container at room temperature prior to usage (Table 10.3).

10.5.2 *Preparation of Inoculum (Aspergillus niger)*

1. Potato dextrose agar (PDA) solid media was used to culture *Aspergillus niger* as inoculum for the solid-state fermentation of CPH.
2. The plate culture was incubated in an incubator oven for 7 days.
3. After the seventh days, the *Aspergillus Niger* spores were streaked using an inoculating loop for detachment of spores. Ten milliliters of sterile distilled water was added to the culture plate. The plate was gently swirled, and the spore suspension was transferred into microcentrifuge tubes.

Table 10.3 List of chemicals and reagents

| SSF Media (Basal Media Modified) | | |
|----------------------------------|---|-----------------------------------|
| 1. | Iron(III) chloride | Sigma-Aldrich (Reagent Grade 97%) |
| 2. | Potassium dihydrogen phosphate (KH_2PO_4) | SYSTEM ChemAR (99.5%) |
| 3. | Magnesium sulphate heptahydrate ($\text{MgSO}_4 \cdot 7\text{H}_2\text{O}$) | R&M Chemicals (99.5%) |
| 4. | Sodium nitrate (NaNO_3) | Grade AR – Friedemann Schmidt |
| 5. | Yeast extract | Microbiology Fermitech Merck |
| | Inoculum (<i>Aspergillus niger</i>) Preparation | |
| | Potato dextrose agar | Difco TM |
| | Other chemicals | |
| | Ethanol 95% | HmbG Chemicals |

10.5.3 Solid State Fermentation (Fungal Pretreatment)

1. CPH substrate was placed in a 250-mL conical flask. The layer thickness of the substrate was kept at about 2 mm for an optimum process of fermentation.
2. CPH substrate was soaked with sterilized distilled water for 12 h prior to the inoculation process.
3. Basal media (modified) was prepared to support the growth of the inoculums as described by Oyeleke et al. (2012).
4. Ten milliliters of the basal medium at pH 5 (1:5 ratio of substrate to medium) was added to the CPH substrate followed by 2% (w/w) inoculum suspension.
5. The flasks were incubated at 37 °C for 5 days.
6. At the end of the fermentation process, sodium citrate (pH 4.8, 50 mM) buffer solution was added into the culture to extract the enzyme, and the mixture was centrifuged at 10,000 rpm for 10 min to separate the extracted enzyme and the pellet.

10.5.4 High-Intensity Ultrasonication

1. The pellet (CPH) from SSF was rinsed and filtered thoroughly with sterilized distilled water to separate the fungus from CPH prior to the ultrasonication process.
2. The amplitude of ultrasonicator was set to 85%, and 1/8" microtip probe was used.
3. The pellet of 2.0% (w/w) of solid was mixed with sterilized distilled water was sonicated (placed in a microcentrifuge tube) in three cycles intermittently with a 30s delay between each cycle.
4. The microcentrifuge tubes containing the sample were placed in an ice/water bath throughout the entire ultrasonication process.
5. Then, the sample was centrifuged at 6000 rpm for 10 min to separate the solid (pellet) and the cellulose suspension (supernatant). All samples were kept at -20 °C until further analysis.

10.5.5 Morphology and Structural Analysis

The suspensions of the cellulose fibers before and after the ultrasonication process were subjected to freeze-drying before further analysis. The morphology of the untreated and treated CPH was observed using SEM (SEM-EDX Oxford INCA 400 model, at an acceleration voltage of 10–15 kV).

For Fourier transform infrared (FTIR) spectroscopy analysis, the dried samples were ground into powder and blended with KBr before pressing the mixture into a pellet. The FTIR spectra of the samples were recorded in the range of 400–4000 cm^{-1} .

10.6 Results and Discussion

Figure 10.1 shows the SEM micrographs of the original cocoa pod husk (CPH). Figure 10.2 shows the micrographs of sonicated CPH sample without the fungal cellulases hydrolysis, while Fig. 10.3 shows the micrographs of sonicated CPH with fungal cellulases hydrolysis. The difference morphology of CPH with and without

Fig. 10.1 FE-SEM micrographs at 1000 \times magnification of original cocoa pod husk (CPH)

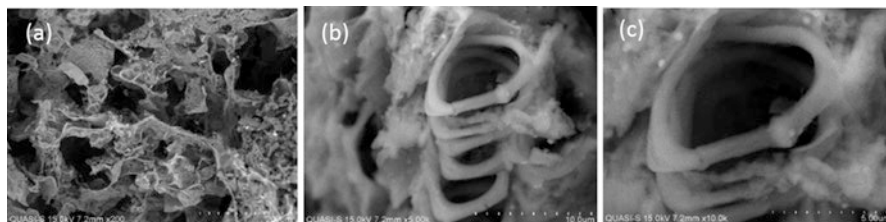
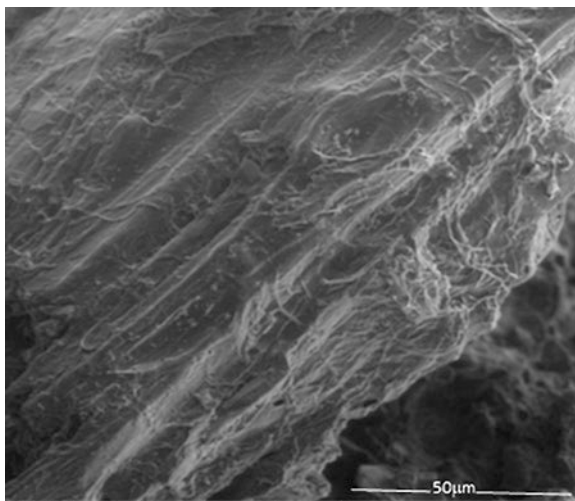


Fig. 10.2 SEM images of sonicated CPH without fungal cellulases hydrolysis under the magnification of (a) 200 \times , (b) 5000 \times , and (c) 10,000 \times

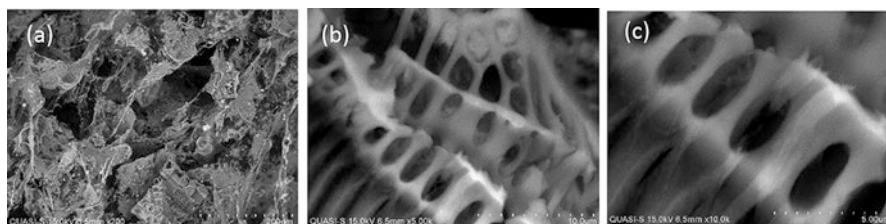


Fig. 10.3 SEM images of fungal-ultrasonicated treated CPH under the magnification of (a) 200 \times , (b) 1000 \times , and (c) 10,000 \times

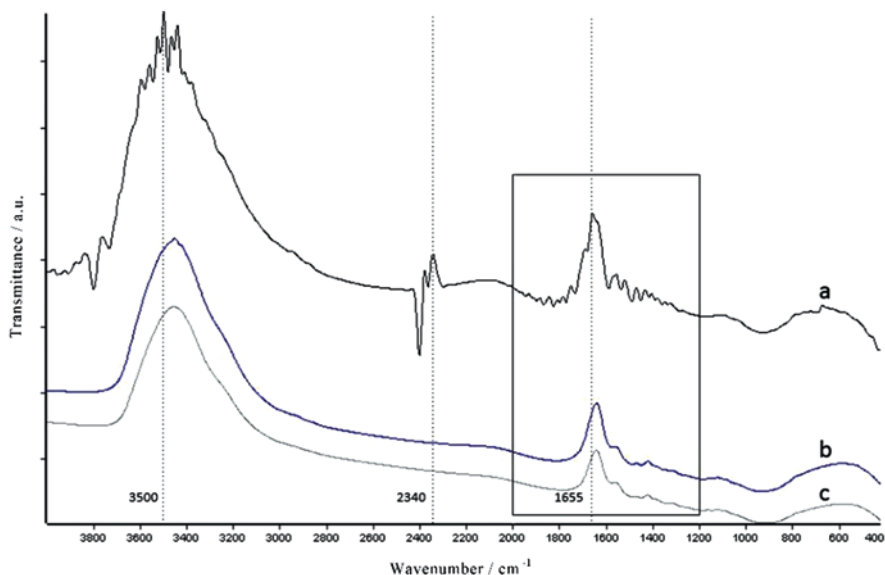


Fig. 10.4 FTIR spectra of (a) the grounded CPH, (b) & (c) the treated CPH

fungal pretreatment before sonication can be seen compared to the untreated CPH (control, CTR) (Fig. 10.1). Only small broken fibers were observed, but no long fibers. A great fibrillation was observed after sonication which indicates that the fungal cellulases hydrolysis facilitates the sonication process of CPH.

FTIR spectra in Fig. 10.4 indicate a prominent change in the functional group of the samples with a notable peak in the range of 3400–3500 cm^{-1} attributed to the vibration of OH-stretching.

Fungal cellulases loosen the cell wall structure that leads to some weak points for the subsequent fibrillation (Hassan et al. 2014). Consequently, it facilitates the refinement by ultrasonication process to defibrillate the CPH fibrils to individualized nanofiber bundles as can be seen at the surface of the substrate (Fig. 10.3). A great diameter reduction of the fibrils was also observed because of the removal of non-cellulosic constituents. It demonstrated that cavitation during sonication effectively opened the structure of the treated CPH, releasing the microfibrils that form the cell wall. The same result was reported by Tonoli and co-workers (2012) (Tonoli et al. 2012). The approximated peak at 1554 cm^{-1} of the raw substrate indicates the presence of lignin. In comparison, the pretreated fungal substrates showed a lower intensity peak and mostly disappeared after the process of ultrasonication. This indicates that most of the lignin and hemicelluloses were removed after the ultrasonication treatment.

10.7 Conclusion

This work shows that the microfibrillated cellulose (MFC) was successfully isolated via the combination of fungal cellulases hydrolysis and ultrasonication. The action of cavitation during sonication effectively opened the structure of the treated CPH, releasing the microfibrils that form the cell wall.

Questions

1. Explain how enzyme could be worked in hydrolyzing lignocellulosic materials.
2. How good enzymatic hydrolysis compare to a chemical in pretreating lignocellulosic materials to extract microcellulose?
3. Which is a cost-effective process for extracting microcellulose; pretreating via pure enzyme or fungus?

References

- Abdul Khalil HPS, Davoudpour Y, Islam MN, Mustapha A, Sudesh K, Dungani R, Jawaaid M (2014) Production and modification of nanofibrillated cellulose using various mechanical processes: a review. *Carbohydr Polym* 99:649–665. <https://doi.org/10.1016/j.carbpol.2013.08.069>
- Abraham E, Deepa B, Pothan LA, Jacob M, Thomas S, Cvelbar U, Anandjiwala R (2011) Extraction of nanocellulose fibrils from lignocellulosic fibres: a novel approach. *Carbohydr Polym* 86(4):1468–1475. <https://doi.org/10.1016/j.carbpol.2011.06.034>
- de Campos A, Correa AC, Cannella D, de M Teixeira E, Marconcini JM, Dufresne A et al (2013) Obtaining nanofibers from curau?? and sugarcane bagasse fibers using enzymatic hydrolysis followed by sonication. *Cellulose* 20(3):1491–1500. <https://doi.org/10.1007/s10570-013-9909-3>
- Hassan ML, Bras J, Hassan EA, Silard C, Mauret E (2014) Enzyme-assisted isolation of microfibrillated cellulose from date palm fruit stalks. *Ind Crop Prod* 55:102–108. <https://doi.org/10.1016/j.indcrop.2014.01.055>
- Henriksson M, Henriksson G, Berglund LA, Lindström T (2007) An environmentally friendly method for enzyme-assisted preparation of microfibrillated cellulose (MFC) nanofibers. *Eur Polym J* 43(8):3434–3441. <https://doi.org/10.1016/j.eurpolymj.2007.05.038>
- Janardhnan S, Sain MM (2006) Isolation of cellulose microfibrils – an enzymatic approach. *Cellulose* 1(2):176–188. <https://doi.org/10.15376/biores.1.2.176-188>
- Monschein M, Reisinger C, Nidetzky B (2013) Bioresource Technology Enzymatic hydrolysis of microcrystalline cellulose and pretreated wheat straw: a detailed comparison using convenient kinetic analysis. *Bioresour Technol* 128:679–687. <https://doi.org/10.1016/j.biortech.2012.10.129>
- Nakagaito AN, Yano H (2004) The effect of morphological changes from pulp fiber towards nano-scale fibrillated cellulose on the mechanical properties of high-strength plant fiber based composites. *Appl Phys Mater Sci Process* 78(4):547–552. <https://doi.org/10.1007/s00339-003-2453-5>
- Oyeleke SB, Oyewole OA, Dauda BEN, Ibeh EN (2012) Cellulase and pectinase production potentials of *Aspegillus Niger* isolated from corn cob. *Bajopas* 5(1):78–83
- Paakko M, Ankerfors M, Kosonen H, Nyakanen A, Ahola S, Osterberg M, Ruokolainen J, Laine J, Larsson PT, Ikkala O, Lindstrom T (2007) Enzymatic hydrolysis combined with mechanical shearing and high-pressure homogenization for nanoscale cellulose fibrils and strong gels. *Biomacromolecules* 8:1934–1941

- Siro I, Plackett D (2010) Microfibrillated cellulose and new nanocomposite materials: a review. *Cellulose* 17(3):459–494. <https://doi.org/10.1007/s10570-010-9405-y>
- Svagan AJ, Azizi Samir MAS, Berglund LA (2007) Biomimetic polysaccharide nanocomposites of high cellulose content and high toughness. *Biomacromolecules* 8(8):2556–2563. <https://doi.org/10.1021/bm0703160>
- Tonoli GHD, Teixeira EM, Corrêa AC, Marconcini JM, Caixeta LA, Pereira-Da-Silva MA, Mattoso LHC (2012) Cellulose micro/nanofibres from Eucalyptus kraft pulp: preparation and properties. *Carbohydr Polym* 89(1):80–88. <https://doi.org/10.1016/j.carbpol.2012.02.052>

Chapter 11

Characterization of Electrochemical Transducers for Biosensor Applications



Farrah Aida Arris, Abdel Mohsen Benoudjit, Fahmi Sanober,
and Wan Wardatul Amani Wan Salim

Abstract Biosensors are devices that detect and report the presence or quantity of a particular analyte. Among the biosensor components, a physicochemical transducer measures physical and chemical changes from analyte-recognition interactions where products, by-products, intermediates, or physical changes are converted into a measurable signal. The character of the transducer determines the performance of a biosensor; hence the characterization of the transduction is crucial in the design of a biosensor. This chapter describes electrochemical characterization of the transducer layer of a biosensor via cyclic voltammetry.

Keywords Biosensors · Chronoamperometry · Cyclic voltammetry · Effective surface area · Electrochemical transducer · Randles-Sevcik

11.1 Introduction

Biosensors are devices that detect and report the presence or quantity of a particular analyte. A more comprehensive definition characterizes a biosensor as “a compact analytical device incorporating a biological or biologically-derived sensing element either integrated within or intimately associated with a physicochemical transducer. The usual aim of a biosensor is to produce either discrete or continuous digital electronic signals which are proportional to a single analyte or a related group of analytes” (Turner et al. 1990). From the definition, a biological or biologically-derived sensing element is any living or non-living biological material that consists of biomolecules (e.g., proteins, DNA, RNA, lipids, sugars, or amino acids), a complex

F. A. Arris · A. M. Benoudjit · F. Sanober · W. W. A. Wan Salim (✉)
Department of Biotechnology Engineering, Faculty of Engineering, International Islamic
University Malaysia, Kuala Lumpur, Malaysia
e-mail: asalim@iium.edu.my

structure (e.g., virus, organelle) or a cell (e.g., bacteria). Analytes, or components in analytical chemistry, are substances or chemical constituents whose properties can be measured (Bartlett 2008). Analytes can consist of toxins, hormones, drugs, neurotransmitters, pathogens, metabolites, or reactants/products/intermediates in a chemical or physical process (Baghayeri et al. 2014). There are five common biosensor types, whose biological element can consist of either an enzyme, an antibody, a single cell, a nucleic acid, or a biomimetic (Luong et al. 2008). Biosensor operation comprises several components: a target molecule (analyte), one or several recognition elements (receptors), a transducer, a detector, a display unit, and an end user (Fig. 11.1). Among the biosensor components, a physicochemical transducer measures physical and chemical changes from analyte-recognition interactions where products, by-products, intermediates, or physical changes are converted into a measurable signal (e.g., current, voltage potential, resistance, mass, refractive index). The character of the transducer determines the performance of a biosensor; hence the characterization of the transduction is crucial in the design of a biosensor.

Currently, transducers come in four varieties, namely optical, piezoelectric, calorimetric, and electrochemical. Figure 11.2 shows existing biorecognition and transduction elements in biosensors.

Optical-based transducers have been widely researched and applied in various biosensors with different types of spectroscopy, such as absorption (Han et al. 2015), fluorescence (Berrettoni et al. 2014) and Raman (Wan et al. 2010). Optical transducers can provide label-free, real-time, simultaneous detection of analytes without the need for complicated chemistry. Existing technologies for optical biosensors are surface plasmon resonance (SPR), chemiluminescence, and fluorescence. Piezoelectric transducers consist of piezoelectric material that vibrates at a natural frequency (An et al. 2014). Contact with a target analyte produces a frequency shift, resulting in a change in current. The magnitude of the current produced and the frequency shift is parameters used to derive the mass of any targeted analyte(s). The two types of piezoelectric sensors are bulk wave (Serhane et al. 2014) and surface acoustic wave (SAW) (Yakovenko 2012). Calorimetric transducers measure changes in temperature as a result of a reaction between the recognition element and the targeted analyte (Vereshchagina et al. 2015). The temperature change is correlated to the concentration of reactants consumed or products formed. Calorimetric biosensors commonly utilize enzymes whose catalytic reactions are often exothermic. Electrochemical transducers convert chemical reactions produced from oxidation and reduction to electrical signals; the product or reactants are correlated to the concentration of the electro-active species (Perumal and Hashim

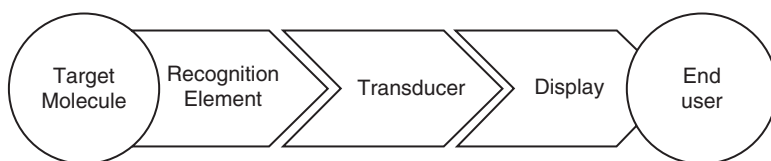
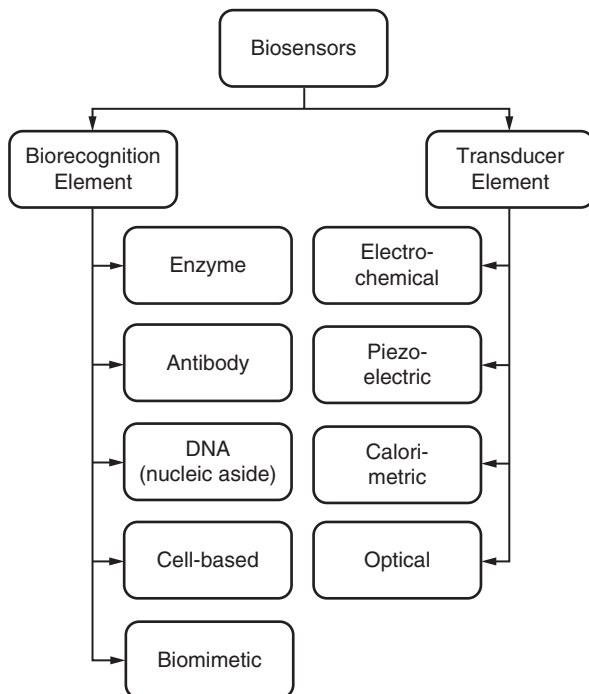


Fig. 11.1 Operational components of biosensors

Fig. 11.2 Categories of biosensors based of biorecognition and transduction elements



2014). Electrochemical sensors have the advantages of simple setup, finely tuned signal that is dependent on the kinetics of the redox reactions, relatively low-cost construction, and potential for miniaturization. Electrochemical measurement comprises amperometric, potentiometric, impedimetric and conductometric forms (Tian et al. 2014).

This chapter will focus on electrochemical transduction for biosensor development and will present the principle of transduction, characterization of electrochemical transducers via cyclic voltammetry (CV), examples of current transducer materials, and methods to fabricate nanostructured electrodes for glucose biosensor development.

11.2 Electrochemical Transducer

An electrochemical transducer converts chemical reactions into measurable electrical signals; the efficiency of conversion is dependent on the redox reaction kinetics of the electroactive species, the material of the transducer, the types of analytes, and environmental factors. Changing the transducer material can help optimize biosensor performance in terms of detection limit, sensitivity, and response time.

11.2.1 Principles of Transduction

In electrochemical transduction, the signal is closely dependent on redox reactions that occur at the solution-electrode interface. Figure 11.3 shows the process that occurs at this interface and the transfer of the redox species to the bulk solution. In solution, ions carry current; hence the kinetics of ion transfer at the electrode-solution interface determines the quality of the measured electrical signal. A redox-reactive species can be oxidized by donating electrons to the electrodes or reduced by receiving electrons from electrode surface. These reduced (R) or oxidized (O) species are constantly shuttled between the electrode surface and the bulk solution; in solution, they are denoted as R^* and O^* . The ions at the electrode-solution interface form a double layer and behave like a parallel-plate capacitor. The capacitive model can be used to study the behavior of electrodes and consequently the measured signals. For a simple parallel plate, the charge Q is proportional to the voltage drop E across the capacitor. The proportionality constant C is the capacitance of the medium.

$$Q = CE \quad (11.1)$$

For the parallel-plate capacitor model, the electrochemical capacitance is described by the Helmholtz model:

$$\frac{C}{A} = \frac{\varepsilon(\varepsilon_0)}{l} \quad (11.2)$$

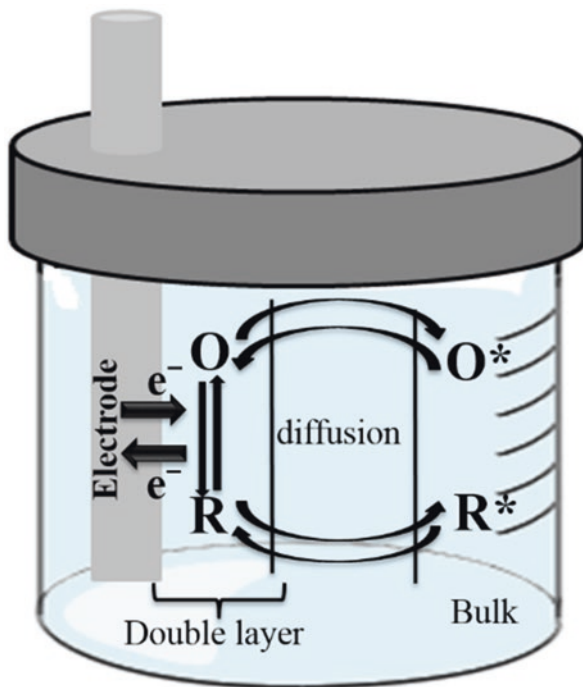
Where C is the capacitance of the medium, A is the area of the electrode, ε is the dielectric constant of the material of a parallel-plate electrode, ε_0 is the permittivity of free space, and l is the distance between the parallel plates of a capacitor. This capacitance model describes the change in current for electrochemical transduction; the magnitude of the current can be derived by differentiating Eq. (11.1) concerning time (t), keeping capacitance (C) constant:

$$\frac{dQ}{dt} = C \frac{dE}{dt} \quad (11.3)$$

Here dQ/dt is current, while dE/dt is the potential scan rate. Hence Eq. (11.3) can be written as follows:

$$i = Cv \quad (11.4)$$

Fig. 11.3 Electrochemical system showing electron transfer at the solution-electrode interface



Where i is the charging current, and v is the scan rate. From Eq. (11.4), the capacitive value can be determined from current and scan rate. In the absence of redox-reactive species, there is no electron transfer at the solution-electrode interface, and i is the only current that will be observed. The equation can be used to explain a popular electrochemical analytical technique called cyclic voltammetry (CV).

11.2.2 Cyclic Voltammetry

CV is a widely used and powerful tool to examine the electrochemical properties of a transducer, by which the kinetics of ion-transfer at the electrode/solution interface can be obtained from one experiment. Conventionally it requires a potentiostat, often in a two- or three-electrode format. A typical three-electrode format (Fig. 11.4) consists of a working electrode (WE), a counter or auxiliary electrode (CE), and a reference electrode (RE).

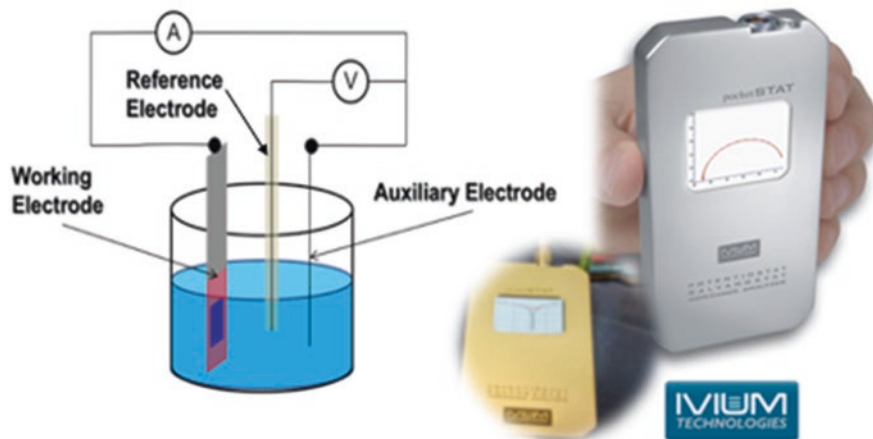
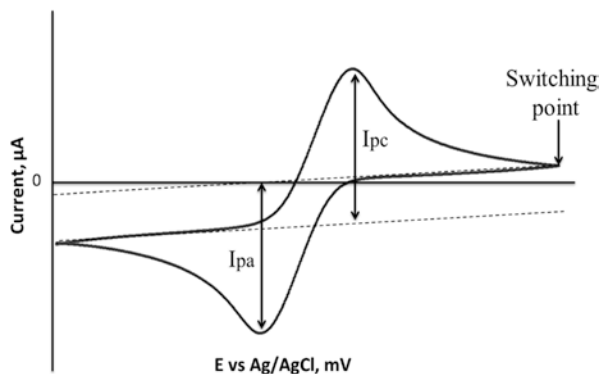


Fig. 11.4 Three-electrode format set-up and a typical potentiostat

Fig. 11.5 Typical CV for the reduction of ferricyanide to ferrocyanide



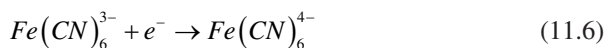
To characterize the effectiveness of a transducer to shuttle ions at the electrode-solution interface, a redox couple that depicts excellent reversibility is often used; one example is a solution of potassium ferricyanide ($\text{K}_3\text{Fe}(\text{CN})_6$). A typical CV curve of the reduction of ferricyanide ($\text{Fe}(\text{CN})_6^{3-}$ to ferrocyanide ($\text{Fe}(\text{CN})_6^{4-}$) is shown in Fig. 11.5; I_{pc} and I_{pa} denote cathodic and anodic peak currents, respectively. The CV curve is governed by the Randles-Sevcik relationship

$$I_p = kn^{3/2} AD^{1/2} C^b v^{1/2} \quad (11.5)$$

where k is a constant equal to 2.69×10^5 ; n is the number of moles of electrons transferred per mole of electroactive species (for example ferricyanide); A is the area of the electrode in cm^2 ; D is the diffusion coefficient of test solution in cm^2/s ; C^b is the solution concentration in mole/l; and ν is the scan rate of the potential in V/s .

Based on the Randles-Sevcik relationship, I_p is linearly proportional to the bulk concentration C^b and the square root of the scan rate, $\nu^{1/2}$. Therefore, the Randles-Sevcik relationship is applicable only when a plot of I_p vs. $\nu^{1/2}$ is linear, which also indicates that the electrode reaction is controlled by diffusion of electroactive species from the bulk solution to electrode surface across a concentration gradient. Another important diagnostic indicator is the magnitude of the peak potential E_p . The E_p value will be independent of the scan rate ν when the rate of electron transfer is fast.

Besides the peak potential, the effective electroactive surface area, A , of a transducer can be calculated using the aforementioned Randles-Sevcik relationship in eq. (11.5) given that the plot of I_p vs. $\nu^{1/2}$ is linear. From the literature, the diffusion coefficient D for the ferricyanide/ferrocyanide couple is typically $6.70 \times 10^{-6} \text{ cm}^2 \text{ s}^{-1}$. For CV using ferricyanide/ferrocyanide, the value of n is equal to one owing to a half-redox reaction.



Rearranging Eq. (11.5) results in

$$A = \frac{I_p}{kn^{3/2} D^{1/2} C^b \nu^{1/2}} \quad (11.7)$$

For a reversible reaction, $I_{pc}/I_{pa} \approx 1$; therefore, I_p in Eqs. (11.5) and (11.7) can be either I_{pc} or I_{pa} . The details of performing a typical CV experiment are outlined in the next section.

11.2.3 Experiment

CV experiments are often carried out by a three-electrode format and a potentiostat. Make sure you read the instructions for using a potentiostat and are trained by your laboratory instructor. An electrochemical cell setup is shown in Fig. 11.4.

11.2.4 Materials (Tables 11.1 and 11.2)

Table 11.1 Consumable Items and equipment

| No | Equipment | Usage |
|----|--------------------------------|---|
| 1 | Weighing boat | To measure potassium ferricyanide mass for redox solution preparation |
| 2 | Weighing balance | To measure potassium ferricyanide mass for redox solution preparation |
| 3 | Potentiostat (e.g. pocketSTAT) | To perform cyclic voltammetry |
| 4 | Glassy carbon electrode (GCE) | To act as working electrode |
| 5 | Platinum electrode | To act as counter or auxiliary electrode |
| 6 | Ag/AgCl electrode | To act as reference electrode |
| 7 | IVIUM software | To perform cyclic voltammetry |

Table 11.2 Chemicals and Reagents

| No | Chemicals | Manufacturer |
|----|------------------------|--------------|
| 1 | Deionized (DI) water | NA |
| 2 | Potassium ferricyanide | R&M |

11.2.5 Methods

1. Polish GCE with 1- μm or smaller alumina particles or a flat polishing kit. Wash the GCE surface with DI water and sonicate the electrode tip in a beaker filled with water for 1 min. Remove the electrode, rinse with DI water, and remove excess water via capillary action with a cleanroom-grade tissue.
2. Prepare 50 and 100 mM ferricyanide solution in 60-ml volumetric flasks.
3. Remove Ag/AgCl reference electrode from saturated 3 M NaCl solution, and clean Pt counter electrode with DI water.
4. Insert the three electrodes at the location as shown in Fig. 11.4 in a beaker filled with ferricyanide solution. Make sure that the ends of the electrodes are immersed in the solution and that they do not touch each other.
5. Place the beaker with the three electrodes on a magnetic stirrer. Add a 1-cm peanut-shaped stirring bar and turn on the stirrer. This step ensures the homogeneity of the ferricyanide solution at the electrode/solution interface and in the bulk solution. Stir for 10 min, and once the stirrer is turned off, remove bubbles by lightly tapping the electrode. If a magnetic stirrer is unavailable, wait for ~ 2 min after each CV scan to ensure equilibrium between the electrode-solution interface and the bulk solution.

- Run a CV scan from initial potential E_i of +600 mV to 0 mV and back to +600 mV at scan rates of 20, 50, 100, 125, 150, and 200 mV/s. Repeat the scans at different rates.
- Label and save each CV scan and ensure that raw data are kept for further analysis.

11.2.6 Results

11.2.7 Discussion of Results

Figures 11.6 and 11.7 depict CV plots for 0.05 M and 0.1 M potassium ferricyanide ($K_3Fe(CN)_6$) solution, respectively, with increasing scan rates of 20, 50, 100, 125, 150 and 200 mV/s. The peak current I_p produced at 200 mV/s is higher than the peak current I_p at 20 mV/s, and this applies for both concentrations (0.1 M and 0.05 M) of ferricyanide solution. The increase in voltage potential applied per unit time increases in current response. For the same scan rate, a higher peak current is measured at a higher concentration (0.1 M), compared to the lower (0.05 M). From this, we can conclude that at higher concentrations of redox solution, more redox species are present and therefore higher current can be generated. Plots of both cathodic and anodic peak currents, I_{pc} and I_{pa} , against the square root of the scan rate, $\nu^{1/2}$, are linear. Therefore, we can conclude that the redox process occurring at the electrode is predominantly diffusion-controlled.

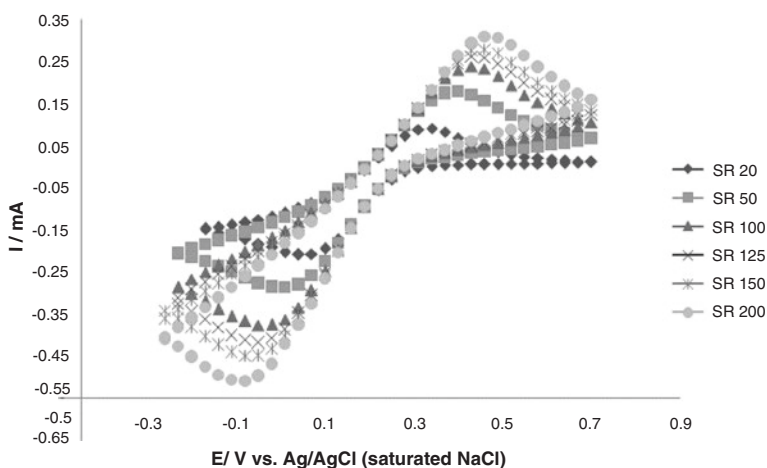


Fig. 11.6 CV for 0.05 M ferricyanide with increasing scan rates of 20, 50, 100, 125, 150 and 200 mV/s

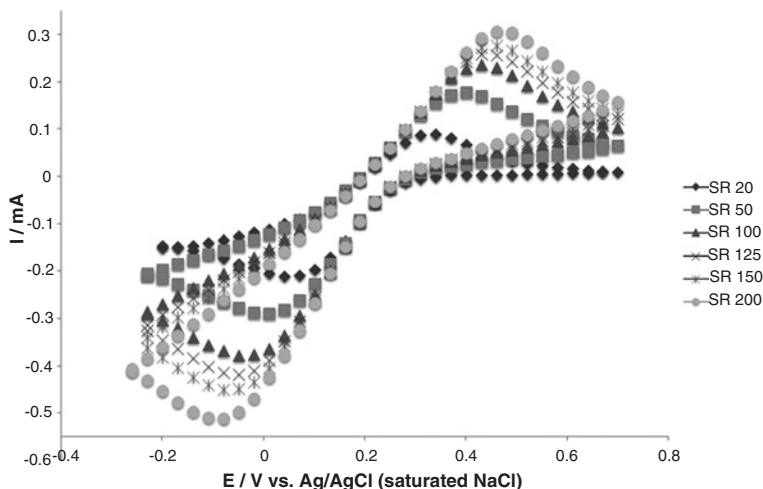


Fig. 11.7 CV for 0.1 M ferricyanide with increasing scan rates of 20, 50, 100, 125, 150 and 200 mV/s

Steps to determine the effective electroactive surface area of electrodes are outlined as follows:

Step 1: Plot CV graph of known concentration and identify I_{pc} and I_{pa} from raw data (Fig. 11.8) and CV. Calculate I_{pc}/I_{pa} ; it should be more or less equal to 1.

Below is an example of 0.1 M potassium ferricyanide ($K_3Fe(CN)_6$) solution with 100 mV/s scan rate.

Step 2: Plot a graph of peak current I_p vs. square root of scan rate, $\nu^{1/2}$. Graph should be linear (Table 11.3).

Step 3: Get slope m from the linear graph of I_p vs. $\nu^{1/2}$ as depicted in Fig. 11.9.

$$y = 1903.1x - 57.903$$

$$I_p = m\nu^{1/2} + c$$

$$m = 1903.1$$

Step 4: Calculate effective surface area (A) from Randles-Sevcik (Eq. 11.5)

$$I_p = kn^{3/2}AD^{1/2}C^b\nu^{1/2} \quad (11.5)$$

From (11.5) we get (11.7)

$$A = \frac{I_p}{kn^{3/2}D^{1/2}C^b\nu^{1/2}} \quad (11.7)$$

From Step 3 $m = \frac{I_p}{\nu^{1/2}}$

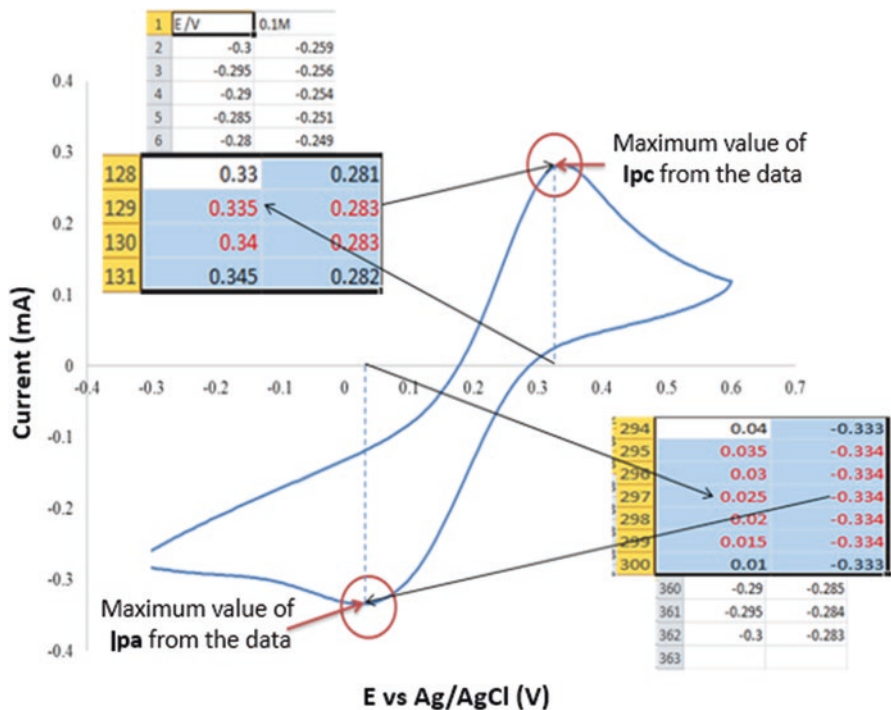


Fig. 11.8 Identification of I_{pc} and I_{pa} from raw data

Table 11.3 Example: Plot a graph of peak current I_p vs. square root of scan rate, $\nu^{1/2}$

| Scan rate, ν (V/s) | SQRT scan rate, $\nu^{1/2}$ (mV/s) ^{1/2} | I_p (μ A) |
|------------------------|---|------------------|
| 0.020 | 0.14 | 160 |
| 0.050 | 0.22 | 410 |
| 0.100 | 0.32 | 580 |
| 0.125 | 0.35 | 630 |
| 0.150 | 0.39 | 680 |
| 0.200 | 0.45 | 750 |

Therefore

$$A = \frac{m}{kn^{3/2} D^{1/2} C^b} \tag{11.8}$$

From (11.8) $A = \frac{1903.1}{2.69 \times 10^5 (1)^{3/2} (6.70 \times 10^{-6})^{1/2} (100)}$

$$A = 0.0273 \text{ cm}^2$$

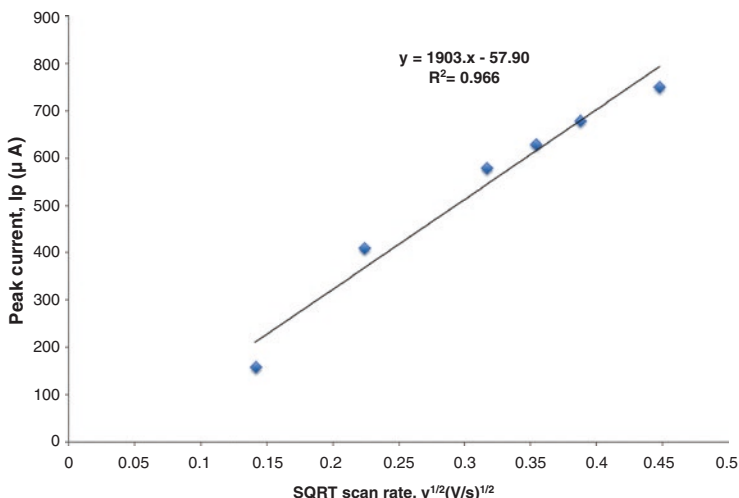


Fig. 11.9 Plot of peak current I_p vs. square root of scan rate, $v^{1/2}$

Hence, electroactive surface area A is 2.73 mm^2 .

Step 5: Compare surface area of the bare electrode (a) (Fig. 11.10) with the calculated electroactive surface area (A) found in Step 4.

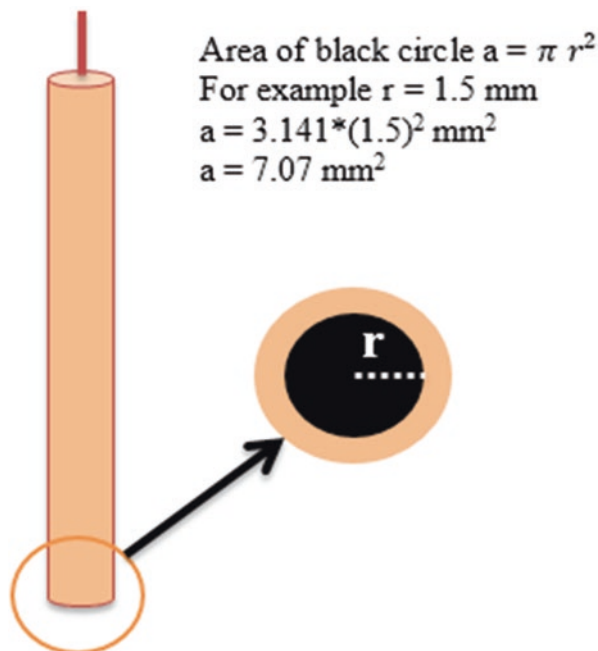
$$\begin{aligned}
 \text{Comparison} &= \frac{a}{A} \\
 &= \frac{2.73}{7.07} \\
 &= 0.39 \times 100\% \\
 &= 39\%
 \end{aligned}$$

From this result, we can conclude that the effective electroactive surface area involved in the reaction is 39% of the surface electrode.

11.3 Transducer Materials

In the development of transducer layers for biosensors, the transducer material selected to interface between the biorecognition element and the detector should enhance electrocatalytic activity, selectivity, sensitivity, and overall performance of the biosensor. Transducer materials are often composites since effective electrocatalytic properties cannot be achieved via one material alone. Composites are a

Fig. 11.10 Area calculation of black circle (a)



combination of two or more distinct materials that possessed very different properties (Royal Society of Chemistry 2015). One of these materials is a matrix or binder that reinforces the composite. Each of the materials in the composite can be easily distinguished as the materials do not combine with or dissolve in each other.

Composites can combine conductive, non-conductive, and semiconductive materials. These materials are often in a nanomaterial format, providing the composites with a large surface-to-volume ratio. Examples of nanomaterials used in composites for transducer fabrication are carbon-derived materials such as carbon nanotubes (CNTs) or graphene, noble or reactive metals, semiconductive materials, and synthetic or natural polymers.

Among the materials mentioned, graphene is one of the most effective nanomaterials used in electrochemical transducer fabrication. Graphene is a two-dimensional, zero-bandgap semiconductor monolayer sheet of sp^2 -bonded carbon atoms, first introduced by Geim and his team in 2004; the discovery led to a Nobel Prize in 2010 (Huang et al. 2011). The carbon atoms in graphene are arranged in a honeycomb lattice, and the material possesses remarkable optical, mechanical, and electrochemical properties. Graphene is one atom thick with a strength 100–300 times that of steel, combined with enhanced electrical conductivity. With its high theoretical specific surface area of $2630 \text{ m}^2 \text{ g}^{-1}$ (Yang and Gunasekaran 2012) and stability at ambient temperature, graphene also exhibits high structural stability and energy storage capability (Singh et al. 2011). Graphene can be functionalized to graphene oxide (GO) to increase its hydrophilicity by the addition of oxygenated functional groups such as carboxyl ($-\text{COOH}$), carbonyl ($-\text{C}=\text{O}$), and hydroxyl

(-OH). Furthermore, graphene can be partially reduced to improve conductivity while maintaining hydrophilicity in aqueous media.

Despite its excellent physical properties, graphene does not possess any catalytic property and therefore cannot be used by itself as a catalyst in electrochemical biosensor development. On the other hand, nanoparticles of noble metals such as silver (Ag), gold (Au), platinum (Pt), iridium (Ir), and palladium (Pd) are known to be excellent catalysts. Therefore, conjugation of noble-metal nanoparticles with graphene in the transducer layer enhances the electroactive surface area as well as electron transfer from biorecognition layer to the electrode surface and subsequently improves transduction. For enzymatic biosensor development, application of metal nanoparticles in a composite can help to protect the enzyme against degradation and environmental conditions as well as prevent enzyme leakage into the measurement solution.

Conjugates of graphene and CNTs, with or without metal or metal oxides, combined with cellulose functioning as matrix or binder can be made into an effective transducer layer that allows bioreceptor immobilization and integration with a detector. Each material in the composites above enhances the optical, electrical, and thermal properties; the enhanced properties contribute to the overall performance of a biosensor. Other examples of composites used for transducer application include conjugates of graphene with conductive polymers such as polypyrrole or polyaniline in cellulose or chitosan matrix; these composites are further decorated with nanoparticles made from noble and reactive metals, or metal oxides such as copper oxide (CuO) and zinc oxide (ZnO).

Gold nanoparticles (AuNPs) are commonly used in graphene composites as a transducer layer for biosensor development, owing to excellent biocompatibility suitable to immobilize various biorecognition elements with electrocatalytic activity. AuNPs are used in transducer layers for detection of glucose (Tabrizi and Varkani 2014), DNA (Shi et al. 2014), uric acid and dopamine (Du et al. 2013), para-aminophenol in paracetamol tablets (Li et al. 2015), and ascorbic acid (Wang et al. 2013a). Silver nanoparticles (AgNPs) have also been used in graphene composites; applications include non-enzymatic hydrogen peroxide (H_2O_2) biosensing (Wang et al. 2013b). Zheng et al. (2011) reported palladium nanoparticles (PdNPs) in chitosan-grafted graphene nanocomposites in the development of glucose biosensors. Gold-palladium nanoparticles (AuPdNPs) have also been studied as complements to graphene in composites in the development of biosensor transducer layers as reported by Yang et al. in 2011.

Apart from noble metals, graphene composites can contain reactive metals in the form of metal oxides such as zinc oxide (ZnO) for the development of glucose biosensors and nonenzymatic hydrogen peroxide sensors (Palanisamy et al. 2012), nickel oxide (NiO) for the development of nonenzymatic glucose sensors (Zhang et al. 2012), and copper oxide (CuO), also for nonenzymatic glucose sensors (Nia et al. 2015).

Finally, the composites above can also be made into wearable and flexible biosensors, where graphene is conjugated with natural or synthetic polymers that may be either conductive or non-conductive. Usage of graphene in cellulose nanofibers

for paper-based biosensor development has been previously reported by Gao et al. (2013), resulting in a flexible transparent electronic device. In addition, Park et al. (2014) reported that thermal conductivity of graphene oxide/polystyrene composites is enhanced by 90% compared to using pure polystyrene, making these composites are suitable for many thermal applications.

11.3.1 Fabrication of a Glucose Biosensor Having a Graphene Composite-Based Transducer

Fabrication of an enzymatic glucose biosensor utilizing reduced graphene oxide (rGO) conjugated with gold nanoparticles (AuNPs) is proposed. Furthermore, this method can also be applied for other composites such as gold-palladium nanoparticles (AuPdNPs). Cellulose nanofibers (CNs) act as a polymer matrix to increase the surface area-to-volume ratio and improve the thermal and mechanical strength of the composite.

11.3.2 Materials (Tables 11.4, 11.5 and 11.6)

Table 11.4 Consumable Item

| No | Equipment | Usage |
|----|---------------|---|
| 1 | Weighing boat | To measure potassium ferricyanide mass for redox solution preparation |
| 2 | Dropper | To drop cast solution onto electrodes |

Table 11.5 List of Equipment

| No | Equipment | Usage |
|----|--|---|
| 1 | Sonicator | To sonicate and clean electrodes |
| 2 | Weighing balance | To measure mass of chemicals |
| 3 | Potentiostat (e.g., pocketSTAT) | To perform cyclic voltammetry |
| 4 | Glassy carbon electrode (GCE) | To act as working electrode |
| 5 | Platinum electrode | To act as counter or auxiliary electrode |
| 6 | Ag/AgCl electrode | To act as reference electrode |
| 7 | IVIUM software | To perform cyclic voltammetry |
| 8 | Optical microscope | To see nanomaterial attachment on electrode surface |
| 9 | Scanning electron microscopy (SEM) | To analyze surface morphology |
| 10 | Fourier transform infrared spectroscopy (FTIR) | To determine functional groups of composites |

Table 11.6 Chemicals and Reagents

| No | Chemicals | Manufacturer |
|----|--|--------------------|
| 1 | Deionized (DI) water | NA |
| 2 | Potassium ferricyanide | R&M |
| 3 | (K ₃ Fe(CN) ₆) | HmbG chemicals |
| 4 | Ethanol | Sigma-Aldrich |
| 5 | Reduced graphene oxide (rGO) | Abalonyx |
| 6 | Graphene oxide (GO) | Sigma-Aldrich |
| 7 | Gold (III) chloride trihydrate (HAuCl ₄ ·3H ₂ O) | Sigma-Aldrich |
| 8 | Sodium borohydride (NaBH ₄) | Riendemann Schmidt |
| 9 | Potassium chloride (KCl) | Chemical |
| 10 | d(+)-Glucose anhydrous | Sigma-Aldrich |
| 11 | Sigmacell cellulose | Sigma-Aldrich |
| 12 | Glucose oxidase (GOx) | Sigma-Aldrich |
| 13 | Glutaraldehyde (GA) | Sigma-Aldrich |
| 14 | Tetraethyl orthosilicate (TEOS) | Sigma-Aldrich |
| 15 | Phosphate buffered saline (PBS) | R&M |

11.3.3 Methods

The step-by-step methodology to synthesize a transducer layer by electrochemical methods and to fabricate a glucose biosensor is as follows:

Step 1: Preparation of glassy carbon electrode (GCE)

1. Polish bare glassy carbon electrode (GCE, 3 mm in diameter, CH Instruments) sequentially with 0.3- μm and 0.05- μm alumina to obtain a mirror-like finish.
2. Sonicate first with absolute ethanol and then with DI water for about 2 min, respectively.
3. Rinse thoroughly with DI water and let dry.

Step 2: Electrodeposition of rGO, AuNPs, and CNs on polished bare GCE

Method 1

1. Drop-cast 3 μL of 1 mg/mL rGO solution on polished GCE.
2. Dry at ambient temperature.
3. Conduct electrochemical deposition via repetitive cyclic voltammetry (CV) scanning from 0 V to -1.5 V at 0.1 V/s in de-aerated 0.05 M PBS (NaHPO₄/NaH₂PO₄), pH 5.0, for 100 cycles.
4. Rinse the modified GCE with DI water and dry at room temperature.
5. Electrodeposit gold nanoparticles (AuNPs) under a constant potential of -0.2 V in a de-aerated precursor solution consisting of 2.5 mM HAuCl₄·3H₂O and 0.1 M KCl for an optimal time of 100 s.

6. Deposit cellulose nanofibers (CNs) using an electrospinning method, in which solutions containing cellulose powder will be used, with voltage strength from 0.7 to 2.5 kV/cm and polymer flow from 1 to 9 mL/min.
7. During experiments, collect samples after 2 min and analyze sample under an optical microscope.

Method 2

1. Drop-cast 2 μL reduced graphene oxide (rGO) on the pre-cleaned GCE and dry in an air oven at 30 °C.
2. Drop-cast 2 μL gold nanoparticles (AuNPs) on top of dried rGO layer on the GCE and let dry in ambient conditions for 24 h.
3. Deposit cellulose nanofibers (CNs) using an electrospinning method, in which solutions containing cellulose powder will be used, with voltage strength from 0.7 to 2.5 kV/cm and polymer flow from 1 to 9 mL/min.
4. During the preliminary test, collect samples after 2 min and analyze sample under an optical microscope.

To perform Step 3, refer to section 2.3.

Step 3: Electrochemical characterization of rGO-AuNP/CN composite layer

1. Perform cyclic voltammetry on the modified transducer layer in a redox-active solution of 2 mM potassium ferricyanide ($\text{K}_3\text{Fe}(\text{CN})_6$) and 1 M potassium nitrate (KNO_3) to determine the oxidation-reduction capability of the sensing layer.
2. Perform potential-step chronoamperometry to characterize the diffusion kinetics of the transducer layer by conducting a potential step from 0.0 to 0.9 V against an Ag/AgCl electrode in 2 mM potassium ferricyanide ($\text{K}_3\text{Fe}(\text{CN})_6$) and 1 M potassium nitrate (KNO_3).

Step 4: Immobilization of glucose oxidase (GOx)

Method 1 – Glutaraldehyde

1. Mix 40 μL of 25 mg/mL BSA, 20 μL of 2.5% glutaraldehyde (GA) and 60 μL of PBS containing 46 mg GOx per ml solution. Dip-coat the modified GCE and allow to sit for 12 h.
2. After 12 h, remove the electrode and air dry for 30 min.

Method 2 – Silica Sol-Gel Encapsulation

1. Dip-coat the modified electrode in PBS containing 46 mg GOx/mL for 1 h.
2. When not in use, store the modified electrode at 4 °C in PBS containing 46 mg GOx/ml.

11.4 Summary of Chapter

A transducer is an integral component of electrochemical biosensors – it connects biorecognition elements and a detector by facilitating the conversion of ions from products or byproducts of chemical reactions to measurable electrons. Selection and

characterization of transducer material are vital for the operation and functionality of biosensors, as this material affects biosensor performance regarding detection limit, response time, sensitivity, and linear range. The principle of electrochemical transduction is introduced followed by the theory and methods of cyclic voltammetry (CV). From CV plots, one can obtain information on the transducer layer: the peak voltage E_p and the effective electrocatalytic surface area. A large surface area provides an effective shuttle of ions at the electrode-solution interface. Potential transducer materials are described followed by methods to fabricate transducer material for glucose biosensor development.

References

- An YK, Kim MK, Sohn H (2014) Piezoelectric transducers for assessing and monitoring civil infrastructures. *Sensor technologies for civil infrastructures: sensing hardware and data collection methods for performance assessment*, pp 1, 86
- Baghayeri M, Zare EN, Hasanzadeh R (2014) Facile synthesis of PSMA-g-3ABA/MWCNTs nanocomposite as a substrate for hemoglobin immobilization: application to catalysis of H_2O_2 . *Mater Sci Eng C* 39:213–220
- Bartlett PN (2008) *Bioelectrochemistry: fundamentals, experimental techniques, and applications*. Wiley, Chichester
- Berrettoni C, Berneschi S, Bernini R, Giannetti A, Grimaldi IA, Persichetti G et al (2014) Optical monitoring of therapeutic drugs with a novel fluorescence-based POCT device. *Proc Eng* 87:392–395
- Du J, Yue R, Ren F, Yao Z, Jiang F, Yang P, Du Y (2013) Simultaneous determination of uric acid and dopamine using a carbon fiber electrode modified by layer-by-layer assembly of graphene and gold nanoparticles. *Gold Bull* 46:137–144
- Gao K, Shao Z, Wu X, Wang X, Li J, Zhang Y, Wang W, Wang F (2013) Cellulose nanofibers/reduced graphene oxide flexible transparent conductive paper. *Carbohydr Polym* 97:243–251
- Han YD, Park YM, Chun HJ, Yoon HC (2015) A low-cost optical transducer is utilizing common electronics components for the gold nanoparticle-based immunosensing application. *Sensors Actuators B Chem* 220:233–242
- Huang X, Yin Z, Wu S, Qi X, He Q, Zhang Q, Yan Q, Boey F, Zhang H (2011) Graphene-based materials: synthesis, characterization, properties, and applications. *Small* 7(14):1876–1902
- Li X, Zhong A, Wei S, Luo X, Liang Y, Zhu Q (2015) Polyelectrolyte functionalized gold nanoparticles-reduced graphene oxide nanohybrid for electrochemical determination of aminophenol isomers. *Electrochim Acta* 164:203–210
- Luong JH, Male KB, Glennon JD (2008) Biosensor technology: technology push versus market pull. *Biotechnol Adv* 26(5):492–500
- Nia PM, Meng WP, Lorestani F, Mahmoudian MR, Alias Y (2015) Electrodeposition of copper oxide/polypyrrole/reduced graphene oxide as a nonenzymatic glucose biosensor. *Sensors Actuators B Chem* 209:100–108
- Palanisamy S, Vilian ATE, Chen S (2012) Direct electrochemistry of glucose oxidase at reduced graphene oxide/zinc oxide composite modified electrode for glucose sensor. *Int J Electrochem Sci* 7:2153–2163
- Park W, Hu J, Jauregui LA, Ruan X, Chen YP (2014) Electrical and thermal conductivities of reduced graphene oxide/polystyrene composites. *Appl Phys Lett* 104:113101
- Perumal V, Hashim U (2014) *Advances in biosensors: principle, architecture and applications*. *J Appl Biomed* 12(1):1–15

- Royal Society of Chemistry (2015). Composites. Retrieved from www.rsc.org/Education/Teachers/Resources/Inspirational/resources/4.3.1.pdf
- Serhane R, Abdelli-Messaci S, Lafane S, Khales H, Aouimeur W, Hassein-Bey A, Boutkedjirt T (2014) Pulsed laser deposition of piezoelectric ZnO thin films for bulk acoustic wave devices. *Appl Surf Sci* 288:572–578
- Shi A, Wang J, Han X, Fang X, Zhang Y (2014) A sensitive electrochemical DNA biosensors based on gold nanomaterial and graphene amplified signal. *Sens Actuator B Chem* 200:206–212
- Singh V, Joung D, Zhai L, Das S, Khondaker SI, Seal S (2011) Graphene based materials: past, present and future. *Prog Mater Sci* 56:1178–1271
- Tabrizi MA, Varkani JN (2014) Green synthesis of reduced graphene oxide decorated with gold nanoparticles and its glucose sensing application. *Sens Actuator B Chem* 202:475–482
- Tian K, Prestgard M, Tiwari A (2014) A review of recent advances in nonenzymatic glucose sensors. *Mater Sci Eng C* 41:100–118
- Turner AP, Karube I, Wilson GS (1990) *Biosensors: fundamentals and applications*. Oxford University Press, Oxford
- Vereshchagina E, Tiggelaar RM, Sanders RGP, Wolters RAM, Gardeniers JGE (2015) Low power micro-calorimetric sensors for analysis of gaseous samples. *Sens Actuators B Chem* 206:772–787
- Wan X, Zhao J, Wang M (2010) A novel design of the sensor head for avoiding the influence of the reflection phase shift in optical current transducer. *Opt Lasers Eng* 48(3):325–328
- Wang C, Ye F, Wu H, Qian Y (2013a) Depositing Au nanoparticles onto graphene sheets for simultaneous electrochemical detection ascorbic acid, dopamine and uric acid. *Int J Electrochem Sci* 8:2440–2448
- Wang MY, Shen T, Wang M, Zhang D, Chen J (2013b) One-pot green synthesis of Ag nanoparticles-decorated reduced graphene oxide for efficient nonenzymatic H₂O₂ biosensor. *Mater Lett* 107:311–314
- Yakovenko VM (2012) Novel method for photovoltaic energy conversion using surface acoustic waves in piezoelectric semiconductors. *Phys B Condens Matter* 407(11):1969–1972
- Yang J, Gunasekaran S (2012) Electrochemically reduced graphene oxide sheets for use in high performance supercapacitors. *Carbon* 51:36–44
- Yang J, Deng S, Lei J, Ju H, Gunasekaran S (2011) Electrochemical synthesis of reduced graphene sheet-AuPd alloy nanoparticle composites for enzymatic biosensing. *Biosens Bioelectron* 29:159–166
- Zhang Y, Wang Y, Jia J, Wang J (2012) Nonenzymatic glucose sensor based on graphene oxide and electrospun NiO nanofibers. *Sens Actuator B Chem* 171–172:580–587
- Zheng Q, Cheng J, Liu X, Bai H, Jiang J (2011) Palladium nanoparticle/chitosan-grafted graphene nanocomposites for construction of a glucose biosensor. *Biosens Bioelectron* 26:3456–3463

Chapter 12

Polymerization Methods and Characterizations for Poly(Lactic Acid) (PLA) Based Polymers



Fathilah Binti Ali and Norshafiq Ismail

Abstract Polymers based from petrochemical have been widely used in various applications due to their availability and lower cost. Products produced from petrochemicals have excellent properties. However their low biodegradability rate had caused terrible environmental problems. Therefore, polymers based on natural resources such as natural polymers, biopolymers, and synthetic polymers are highly in demand as they can be produced from natural sources which means they are sustainable. Apart of that, due to their nature, they are environmentally friendly and biodegradable. There are many types of biopolymers such as cellulose, poly(lactic acid) (PLA), polyhydroxybutyrate (PHB) and much more. Among these biopolymers, PLA has high potential because it has similar properties to conventional polymers such as polystyrene (PS). This polymer is an aliphatic type polyester which can be polymerized from its' monomer, lactic acid. Lactic acid (LA) can be obtained from the fermentation process of natural sources such as starch (Auras R, Harte B, Selke S; *Macromol Biosci* 4(9):835–864, 2004).

Keywords Isocyanate · Chain extender · Chemical structure · Condensation polymerization · Hydrolytic degradation · Lactic acid · Mechanical properties · Poly(lactic acid) · Polymerization · Polyols · Polyurethane · Ring-opening polymerization · Step growth polymerization · Thermal properties

12.1 Introduction

Polymers based from petrochemical have been widely used in various applications due to their availability and lower cost. Products produced from petrochemicals have excellent properties. However their low biodegradability rate had caused terrible environmental problems. Therefore, polymers based on natural resources such as natural polymers, biopolymers, and synthetic polymers are highly in demand as they can be produced from natural sources which means they are sustainable. Apart

F. B. Ali (✉) · N. Ismail
Department of Biotechnology Engineering, IIUM, Kuala Lumpur, Malaysia
e-mail: fathilah@iium.edu.my

of that, due to their nature, they are environmentally friendly and biodegradable. There are many types of biopolymers such as cellulose, poly(lactic acid) (PLA), polyhydroxybutyrate (PHB) and much more. Among these biopolymers, PLA has high potential because it has similar properties to conventional polymers such as polystyrene (PS). This polymer is an aliphatic type polyester which can be polymerized from its' monomer, lactic acid. Lactic acid (LA) can be obtained from the fermentation process of natural sources such as starch (Auras et al. 2004).

Lactic acid can be polymerized into PLA through two different methods as shown in Fig. 12.1; polycondensation or ring-opening polymerization (ROP) of lactic acid. PLA polymerized by polycondensation method usually produces PLA with low molecular weight (Mw). However, during the polymerization of the polymer through polycondensation method, one molecule of water is generated in each step of polymerization. Formation of water in the polymerization vessel cause shorter polymer chain, thus resulting in the low Mw of the polymer. The shorter polymer chains formed through this reaction usually provides the polymer with a higher polydispersity index (PDI). On the other hand, ROP is a method which has an advantage compared to polycondensation where the higher molecular weight of PLA is prepared. This is usually due to controlled reaction of ROP compared to polycondensation method. In addition, polymers prepared by controlled polymerization method generally produces polymer with low PDI. Therefore, PLA prepared through ROP usually has higher Mw and low PDI, which usually used for further polymerization step such as to produce block copolymers (BCP). Therefore, PLA produced through this method can be potentially used for various applications such as lithography and drug delivery.

Lactide monomer which is obtained from lactic acid usually forms in different structures which consisted of L, D, and meso-lactide forms and called as L-lactide, D-lactide and DL-lactide, respectively (Fig. 12.2). Polymerization of these monomers can produce polymers with different properties due to its different stereochemistry; poly(L-lactic acid) (PLLA), poly(D-lactic acid) (PDLA) and poly(DL-lactic acid) (PDLLA). PLLA type homopolymer is a crystalline type polymer whereas PDLA and PDLLA are amorphous type polymers. Crystallites in polymers influences on the properties of polymers. Therefore PLLA has slightly different properties compared to PDLA and PDLLA.

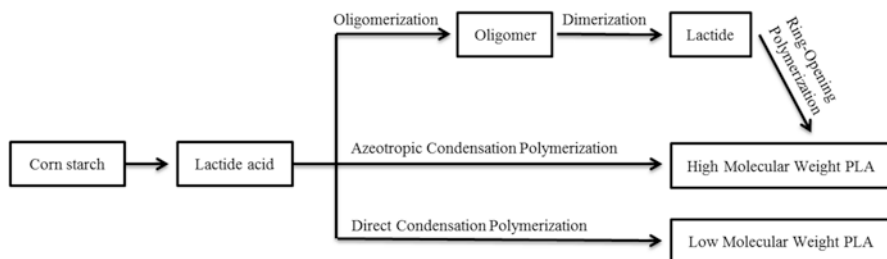
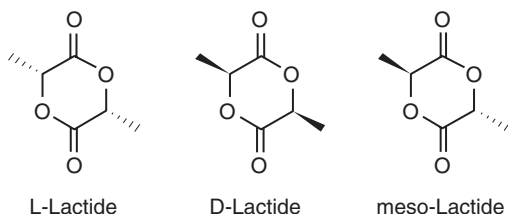


Fig. 12.1 Synthesis methods of PLA

Fig. 12.2 Stereoisomers of lactic acid; L-lactic acid, D-lactic acid and meso-lactide



PLA can be polymerized using the above mentioned steps and this polymer has high mechanical strength, low toxicity and good gas barrier properties. For its biodegradability behavior, PLA has potential and it can be used as environmentally friendly material, especially in packaging materials. However, as mentioned before, PLLA has higher crystallinity and this caused PLLA to be rigid and brittle which limits its usage in packaging application. Therefore, to be used in packaging industry, PLA must have higher elongation with good mechanical strength and this can be achieved through different methods such as blending with other polymers, plasticization of PLA, co-polymerization with different polymers and many more. Among these methods, properties of PLA can be altered through polymerization methods. Through polymerization, the structures of the polymer can be designed and suited according to their desired application.

12.2 Polymerization of PLA

12.2.1 Synthesis of PLA by Condensation Polymerization

PLA can be prepared through two different methods from the lactic acid monomer (Fig. 12.3) which can be produced either by lactic acid or lactide. Polycondensation is performed in bulk by distillation of condensation of water, with or without a catalyst, while vacuum and temperature are progressively increased. This PLA can be used for synthesis of polyurethane. This polymer can be used as it is or coupled with isocyanates, epoxides or peroxide to produce polymers having a range of molecular weights.

12.2.2 Synthesis of PLA by Ring-Opening Polymerization Method (ROP)

The second method is ring opening polymerization of lactide. Ring opening polymerization (ROP) is a type of polymeric reaction where the terminal end of the polymer chain will be activated and act as a reactive center. This reactive site will be used for the addition of monomers which will enhance the polymerization process and

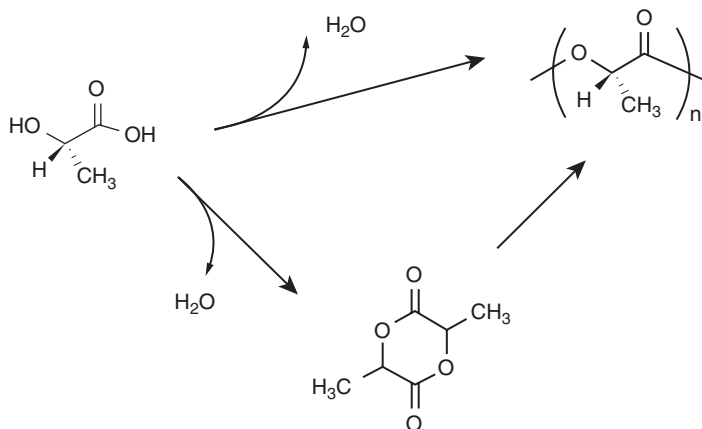


Fig. 12.3 PLA by polycondensation method

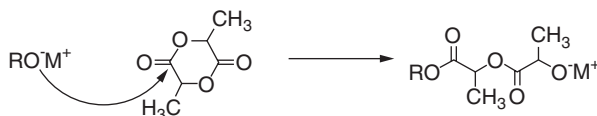


Fig. 12.4 Ring opening polymerization of PLA

form larger polymeric chains. Metals consist of alkoxide are known to be good initiating agent in ROP of lactide and can be used to activate the site as shown in Fig. 12.4. One type of the metal alkoxides is triethylaluminum which has been used for polymerization of PLA where it reacts well with hydroxyl-functionalized polymer (Wang and Hillmyer 2000). PLA produced from this method gave polymer with high molecular weight and low PDI. PLA produced through this method can be used for further polymerization such as for synthesis of block copolymers (BCPs).

12.2.3 Step-Growth Polymerization

In step-growth polymerization method, a polymer is produced when an end chain diol of oligomer reacts with a diisocyanate to provide pre-polymer which is also called as polyurethane (PU) (Fig. 12.5). For an example, ethylene glycol (EG) or different type of diol is added to the isocyanate in the presence of catalyst, a rapid condensation occurs and it gives the pre-polymer. The pre-polymer which has isocyanate at the terminal of the chain, is then can then be reacted with another polyol. In this case, the second polyol function as chain extender and the enhancement of chain extender in the polymer chains substantially give higher performance polymer. The choice of initiator, extender, and molecular weight of the polyol greatly

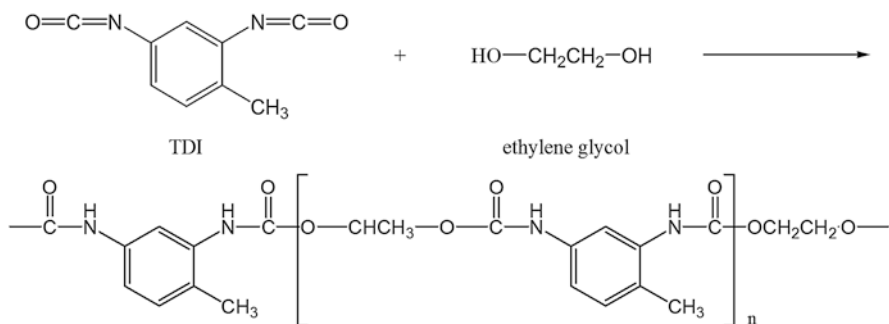


Fig. 12.5 General synthesis scheme of polyurethane

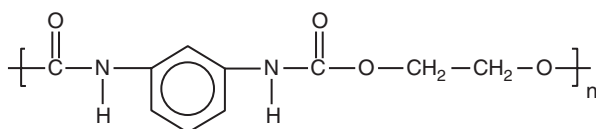


Fig. 12.6 Chemical structure of polyurethane (PU)

affect its physical state, and the physical properties of the polyurethane. PLA based polyurethane using polycaprolactone diol as chain extender was prepared and the properties suit for environmental friendly packaging material (Ali et al. 2014).

12.2.3.1 Chemical Structure

Polyurethane (PU) is a polymer with urethane linkages in their backbone is shown in Fig. 12.6. It is also a compound having one or more of highly reactive isocyanate group ($-\text{N}=\text{C}=\text{O}$) that will react with hydrogen atoms that are attached to atoms which having more electronegative than carbon. It is formed through polyaddition polymerization between isocyanates and polyols which will produce different chemical, physical and mechanical properties depending on their types and characteristics. It also belongs to the class of alternating block copolymers where hard and soft segments alternate along the chain. The soft segments are polyether (mainly prepared from the mixture of propylene oxide and ethylene oxide) and polyester (derived from ethylene glycol and adipic acid). For the hard segment, it is produced from residues of diisocyanates and low molecular weight polyols which is also called as chain extender. Polyurethane properties are strongly dependent on the chemical nature of basic components, also the synthesis and processing conditions. As mentioned before, it is prepared mainly from two compounds which are isocyanates and polyols. The addition of other materials such as chain extenders, surfactants and catalysts are required to aid processing the polymer or to change the properties of the polymer.

12.2.3.2 Isocyanate

The isocyanate is a compound containing the isocyanate group (-NCO) (Fig. 12.7). It is formed through the reaction with a compound containing alcohol (hydroxyl) groups to produce polyurethane polymers. The interaction between hydroxyl and -NCO determine the properties of the PU, in term of its rigidity, mechanical and also tensile properties (Petrović et al. 2002). It also can react with water to form unstable carbamic acid, which consists of carbon dioxide and amines. The released carbon dioxide if trapped within the polymers results in the formation of cell structure, which known as foams. The formation of polyurethane structure needs two or more isocyanate groups on each molecule. There are many commercially available poly- or diisocyanate compound usually used in a production of polyurethane, such as methylene diphenyl diisocyanate (MDI), toluene diisocyanate (TDI) and Hexamethylene diisocyanate (HDI). Methylene diphenyl diisocyanate (MDI) and toluene diisocyanate (TDI) is the most commonly used during the process because of their cost and excellent reactivity. Both of them exhibit a different function to the polyurethane. MDI is commonly used to make flexible foams as well as semi-rigid and rigid polyurethane plastic for construction and insulations. It has relatively low human toxicity and the least hazardous isocyanate but is not benign. Examples for MDI available are 4, 4-, 2, 4-, 2, 2- and polymeric MDI as shown in Fig. 12.7.

Meanwhile, for TDI, it is an aromatic diisocyanate which commonly used in the manufacture of flexible foams such as foam cushions for furniture and automotive components. It is usually produced as a mixture of 2,4- and 2,6- TDI isomers. The isocyanates can be adjusted by partially reacting with polyols or adding other

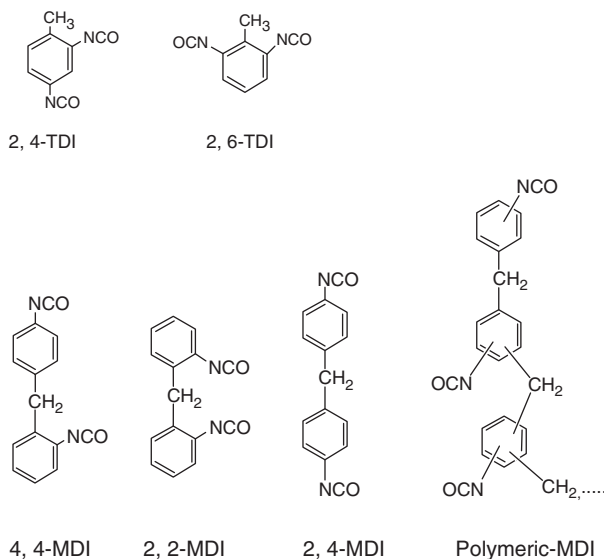


Fig. 12.7 Chemical structure of TDI and MDI

materials to reduce volatility, which also will reduce the toxicity to enhance the properties of polyurethane.

12.2.3.3 Polyols

Polyols are compound with multiple hydroxyl functional groups available for organic reactions. The polyols used in polyurethane production are predominantly hydroxyl-polyethers rather than hydroxyl-polyesters. Soft segment of polyurethane itself is derived from polyols either polyester polyols or polyether polyols. Therefore, the degradation rate can be adjusted through a suitable soft segment. For the production of biodegradable packaging, polyester-polyols is an appropriate choice since it is readily biodegradable instead of polyether-polyols which are resistant to biodegradable (Nakajima-Kambe et al. 1999). It is produced by direct esterification in a condensation reaction. Commonly used biodegradable polyesters are polylactic acid (PLA), polycaprolactone (PCL) and polyglycolide (PGA). It is also can be formed by condensation or step-growth polymerization of diols and a dicarboxylic acid, such as diethylene glycol reacting with phthalic acid (Kadkin et al. 2003) (Fig. 12.8).

Polyether polyols are made by reacting epoxides as a high ring stress and polar character of three-membered epoxy rings to allow cleavage easily with the multi-functional initiator in the presence of a catalyst (Fig. 12.9). Some of the examples are polyethylene glycol and polypropylene glycol. It also can be formed by reacting glycol or polyhydric alcohol with propylene oxide or ethylene oxide to yield a branched molecule contains a plurality of ether linkages and a hydroxyl group. The polyether forming reaction is a strong exothermic polymerization reaction.

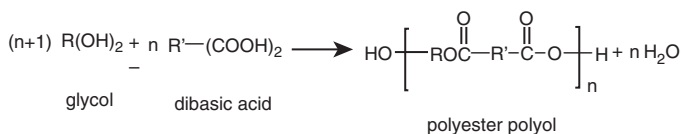


Fig. 12.8 Synthesis of polyester polyol

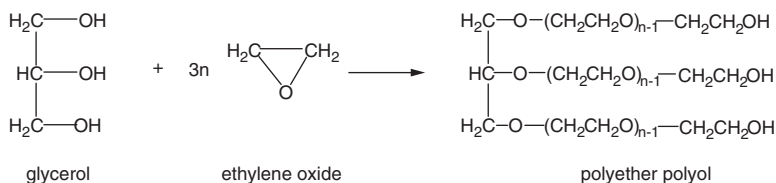
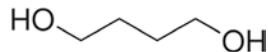


Fig. 12.9 Synthesis of polyether polyol

Fig. 12.10 Chemical structure of 1-4 butanediol



12.2.3.4 Chain Extender

Chain extender plays an important role in the final mechanical properties of the polymer. It incorporates with low molecular weight diols to enhance the elastomeric properties of the resulting polyurethane in terms of polymer morphology, adhesives, elastomers and microcellular foams. The elastomeric properties are derived from chemical dissimilar of hard and soft segment copolymer, such that the urethane hard segment domains serve as cross-links between the amorphous polyether or soft polyester segments. Most commonly used chain extender is an aliphatic of 1-4 butanediol (Fig. 12.10). Introducing chain extender with different rigidity and bulkiness may provide the change in the degree of phase mixing, hard domain structure and hydrogen bonding (Bae et al. 1999).

12.2.4 Controlled Radical Polymerizations (CRP)

Recent developments in controlled radical polymerization methods, such as atom-transfer radical polymerization (ATRP), nitroxide-mediated living polymerization (NMP) and reversible addition-fragmentation transfer (RAFT) can use for the preparation of functional type polymers. This living polymerization method induces uniform chain length as it offers a proper addition to the polymer chains and it means that the polymer's chain growth can be controlled and at the same time obtaining low polydisperse polymers.

12.2.4.1 Atom-Transfer Radical Polymerization (ATRP)

Atom-transfer radical polymerization (ATRP) is also a living radical polymerization assisted with transition metal was discovered by Mitsuo Sawamoto (Kato et al. 1995) and by Krzysztof Matyjaszewski (Wang and Matyjaszewski 1995) in 1995. Figure 12.11 showed block copolymers (BCPs) prepared by ATRP is employed by metal-catalyzed controlled radical polymerizations. Controlled radical polymerization produces linear AB diblock copolymer with narrow molecular weight distribution. This AB BCP can be used for the preparation of ABA triblock copolymer while having a low polydispersity (Yuzo Kotani et al. 1996).

12.2.4.2 Reversible Addition-Fragmentation Transfer (RAFT)

Reversible addition-fragmentation transfer (RAFT) can be used to prepare polymers with pre-determined molecular weight and narrow polydispersity (usually <1.2) (Chen et al. 2015; John Chiefari et al. 1998). The polymerization is carried out

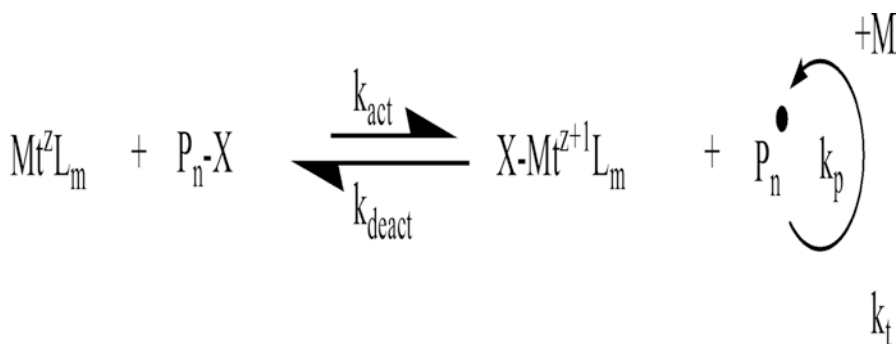


Fig. 12.11 ATRP equilibrium

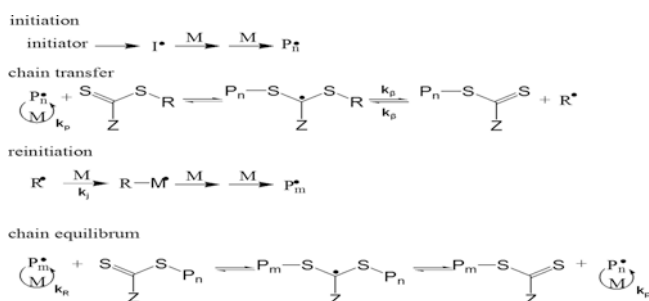


Fig. 12.12 RAFT mechanisms

in the presence of $-\text{SH}$ (thiol) compounds which act as RAFT agent. The polymerization using RAFT agent is shown in Fig. 12.12. The transfer agent $[\text{S}=\text{C}(\text{Z})\text{S}-\text{R}]$ of the RAFT agent plays an important role in polymerizing monomers. Due to the presence of thiol in the polymer chain, polymerization of a second monomer can be continued to give a block copolymer. Diblock copolymers can be prepared using a macro transfer agent (Zalusky et al. 2002). In Fig. 12.12, PLA macro transfer agent was prepared to polymerize styrene with low polydispersity.

12.3 Characterization

12.3.1 Chemical Structure and Molecular Weight

Chemical structures of the polymer can be confirmed using nuclear magnetic resonance (NMR) and ATR-FTIR. The NMR spectra can be obtained using CDCl_3 with a Bruker 400 MHz spectrometer. ATR-FTIR can confirm on the functional group of the polymers. The molecular weight (M_n) and polydispersity index (PDI) of each polymer can be determined using size exclusion chromatography (SEC) (PerkinElmer Series 200), calibrated by polystyrene standards.

12.3.2 Thermal Properties

The thermal properties of the polymers can be determined with a TA Instruments DSC-Q100 between -70 and 180 °C and maintained for 5 min to eliminate thermal history. The first scan is carried out to eliminate the thermal history of the polymer. From the DSC, glass transition temperature (T_g), melting temperature (T_m) and crystallization temperature (T_c) can be obtained.

12.3.3 Mechanical Properties

Tensile properties can be measured using a universal testing machine (INSTRON 5583) at 25 °C with a crosshead speed of 10 mm/min in accordance with ASTM D412 specifications. The samples for tensile measurements can be prepared by compression mold in 1 -mm thick sheets under a pressure of $10,000$ pounds for 5 min at 100 °C.

12.3.4 Polymer Surface Morphology

The field emission scanning electron microscopy (FE-SEM) can be performed to observe the morphology of the tensile-failed samples using a Hitachi S-4800 scanning electron microscope.

12.3.5 Gas Permeability

Gas permeability tests can be performed on a MOCON OX-TRAN 2/21 model in accordance with ASTM D-3985. The gas will penetrate the membrane by a carrier gas (98% N_2 , 2% H_2) at 760 mmHg (test gas, O_2).

12.3.6 Hydrolytic Degradation

Hydrolytic degradation tests can be performed to investigate the biodegradability of the polymer. The polymer samples can be placed in 10 mL of PBS ($pH = 7.4$) at 35 °C, and the hydrolytic degradation should be observed for a month, with measurements taken after 1 , 3 , 5 , 7 , and 30 days. The samples can be removed on the

specified days and washed thoroughly with distilled water, dried in vacuum, and weighted to determine the weight loss, as shown:

$$\text{weight loss}(\%) = \frac{(w_o - w_t)}{w_o} \times 100\% \quad (12.1)$$

where w_o is the initial weight of the samples, and w_t is the weight of the samples after degradation.

12.4 Conclusion

Poly(lactic acid) has high potential to be used in an environmental friendly packaging material, and it can be used to substitute well-known commodity polymers. However, its brittleness limits its use and therefore it can be polymerized to improve its properties. Few methods are suggested for the PLA polymerizations, and its characterizations are recommended.

References

- Ali FB, Kang DJ, Kim MP, Cho CH, Kim BJ (2014) Synthesis of biodegradable and flexible, polylactic acid-based, thermoplastic polyurethane with high gas barrier properties. *Polym Int* 63(9):1620–1626
- Auras R, Harte B, Selke S (2004) An overview of polylactides as packaging materials. *Macromol Biosci* 4(9):835–864. <https://doi.org/10.1002/mabi.200400043>
- Bae JY, Chung DJ, An JH, Shin DH (1999) Effect of the structure of chain extenders on the dynamic mechanical behaviour of polyurethane. *J Mater Sci* 34:2523–2527
- Chen CC, Chen CY, Tsay CY, Wang SY, Lin CK (2015) Influence of Fe₃O₄ nanoparticles on pseudocapacitive behavior of the charge storage process. *J Alloys Compd* 645:250–258. <https://doi.org/10.1016/j.jallcom.2015.04.123>
- John Chiefari YKBC, Ercole F, Krstina J, Jeffery J, Le TPT, Mayadunne RTA, Meijs GF, Moad CL, Moad G, Rizzardo E, Thang SH (1998) Living free-radical polymerization by reversible addition–fragmentation chain transfer: the RAFT process. *Macromolecules* 31:5559–5562
- Kadkin O, Osajda K, Kaszynski P, Barber TA (2003) Polyester polyols: synthesis and characterization of diethylene glycol terephthalate oligomers. *J Polym Sci A Polym Chem* 41:1114–1123
- Kato M, Kamigaito M, Sawamoto M, Higashimura T (1995) Polymerization of methyl methacrylate with the carbon tetrachloride/dichlorotris-(triphenylphosphine)ruthenium(II)/methylaluminum Bis(2,6-di-tert-butylphenoxide) initiating system: possibility of living radical polymerization. *Macromolecules* 28(5):1721–1723. <https://doi.org/10.1021/ma00109a056>
- Nakajima-Kambe T, Shigeno-Akutsu Y, Nomura N, Onuma F, Nakahara T (1999) Microbial degradation of polyurethane, polyester polyurethanes and polyether polyurethanes. *Appl Microbiol Biotechnol* 51(2):134–140
- Petrović ZS, Zhang W, Zlatanić A, Lava CC, Ilavský M (2002) Effect of OH/NCO molar ratio on properties of soy-based polyurethane networks. *J Polym Environ* 10(1–2):5–12. <https://doi.org/10.1023/A:1021009821007>

- Wang Y, Hillmyer MA (2000) Synthesis of polybutadiene-poly lactide diblock copolymers using aluminum alkoxide macroinitiators. Kinetics and mechanism. *Macromolecules* 33(20):7395–7403
- Wang J-S, Matyjaszewski K (1995) Controlled/“living” radical polymerization. Atom transfer radical polymerization in the presence of transition-metal complexes. *J Am Chem Soc* 117(20):5614–5615. <https://doi.org/10.1021/ja00125a035>
- Yuzo Kotani MK, Kamigaito M, Sawamoto M (1996) Living radical polymerization of alkyl methacrylates with ruthenium complex and synthesis of their block copolymers. *Macromolecules* 29:6979–6982
- Zalusky AS, Olayo-Valles R, Wolf JH, Hillmyer MA (2002) Ordered nanoporous polymers from polystyrene-poly lactide block copolymers. *J Am Chem Soc* 124(43):12761–12773. <https://doi.org/10.1021/Ja0278584>

Chapter 13

Polymers in Biosensors



Jia Jia Long, Abdel Mohsen Benoudjit, Farrah Aida Arris, Fathilah Ali, and Wan Wardatul Amani Wan Salim

Abstract Polymers can be conductive or nonconductive, natural or synthetic, and have been widely used in the development of biosensors; polymers can be processed at a large scale at a relatively low cost. Poly (3, 4-ethylenedioxythiophene) polystyrene sulfonate (PEDOT:PSS), PANI, and PPy are widely used in fabricating biosensors owing to their intrinsic conductive property. Although conductivity is crucial in developing biosensors, a large number of nonconductive polymers such as chitin, chitosan, gelatin, dextran, cellulose, and polystyrene also attract interest for their function as support matrices for the immobilization of biomolecules. The nonconductive polymers can be classified into two categories: natural and synthetic. This chapter focuses on the potential use of polymer composites in biosensors.

Keywords Biosensors · Block copolymers · Composite · Conductive polymers · Non-conductive polymers · Natural polymers · Synthetic polymers

13.1 Introduction

Over the last few decades, biosensor-related research has attained extensive growth for various applications. Biomolecule and non-biological material immobilization on biosensor substrates are one of the most important elements in various biosensor research efforts. Immobilization of different biomolecules such as enzymes, proteins, or DNA, and of non-biological material such as polymers, noble metals, carbon-based nanomaterials, and their composites, is becoming inseparable from biosensor development. Various immobilization materials with improved properties of biocompatibility, low toxicity, high affinity, and strong adsorption ability have been utilized for biosensor fabrication (Wang and Uchiyama 2013).

The most important factor that determines the performance of any biosensor is the architecture of materials that results from the immobilization process on elec-

J. J. Long · A. M. Benoudjit · F. A. Arris · F. Ali · W. W. A. Wan Salim (✉)
Department of Biotechnology Engineering, Faculty of Engineering, International Islamic University Malaysia, Kuala Lumpur, Malaysia
e-mail: asalim@iium.edu.my

trode surfaces or specifically on the transducer layer. The surface architecture between the biorecognition element and the analyte is highly significant to determine the performance of a biosensor, as the architecture greatly affects the sensitivity and stability of the biosensor through modifying the performance capability of the transducer surface. (Grieshaber et al. 2008). Enhancement of the transducer surface is especially important in electrochemical biosensors, where the transducer is responsible for facilitating the signal transduction of ions to electrons for electrical measurement. Conductive polymers (CPs) had received considerable interest since the conjugated polymer polyacetylene was discovered in 1977 when CPs were used to conduct electricity through halogen doping (Huang 2006). Furthermore, polymeric materials have the advantage that can be synthesized and processed on a large scale at relatively low cost. The dynamic chemical, electrical, and physical properties of CPs can enhance performance parameters of chemical and biological sensors (Richard et al. 2014). Poly (3, 4-ethylenedioxythiophene) polystyrene sulfonate (PEDOT:PSS), polyaniline (PANI), and polypyrrole (PPy) are widely used in fabricating biosensors owing to their intrinsic conductive property. The high electrical conductivity achieved in organic polymers has directed the synthesis of synthetic metals.

Although conductivity is crucial in developing biosensors, a large number of non-conductive polymers such as chitin, chitosan, gelatin, dextran, cellulose, and polystyrene also attract interest for their function as support matrices for the immobilization of biomolecules. Their advantages encompass excellent biocompatibility, low toxicity, and excellent permselectivity, all of which enhance biosensor performance (Yuqing et al. 2004). Typically, several conductive polymer- and nonconductive polymer-based composites are widely used in biosensors. The non-conductive polymers can be classified into two categories: natural and synthetic. This chapter focuses on the potential use of polymer composites in biosensors.

13.2 Conductive Polymers and Metal Nanoparticles

A conductive polymer is one of the most suitable substrates for metal nanoparticles (MNPs). MNPs have garnered great interest owing to their electrochemical, physical, and nanomaterial characteristics of enhanced electrical properties, large surface-to-volume ratio, increased adsorption, and high surface reactivity (Yao et al. 2013). Owing to these properties, nanoparticles such as noble metal nanoparticles have been widely used in many applications, especially in electrochemical biosensors (Saei et al. 2013; Xue et al. 2014; Yao et al. 2013). Gold nanoparticles (AuNPs) in glucose biosensors function as immobilizer agents (Saei et al. 2013); platinum nanoparticles (PtNPs) and silver nanoparticles (AgNPs) have been integrated into the fabrication of electrochemical biosensors owing to their unique electrical and catalytic properties (Saei et al. 2013; Yao et al. 2013). In addition, multi-MNPs combine the favorable properties of the constituent metals, resulting in a new functional material. Gold (Au) has low catalytic activity compared to platinum (Pt); the

structural and catalytic activity of gold-platinum (Au-Pt) alloys has been extensively studied to enhance synergistic functions (Saei et al. 2013; Cui et al. 2011).

In biosensor development, conductive polymer–metal nanoparticle composites have attracted considerable attention. Saei et al. (2013) reported that PtNPs added to Ppy enhanced the electrocatalytic activity and conductivity of the biosensor transducer system for glucose sensing. Composites consisting of functional graphene sheets and chitosan have shown to provide biosensors with long-term stability and reproducibility (Saei et al. 2013). Poly (3, 4-ethylenedioxy thiophene)–poly (styrenesulfonic acid) and AuNP composites have also been used to enhance transduction of an alcohol biosensor. The performance of the biosensor showed promising results in terms of reproducibility, stability, and sensitivity to ethanol, owing to the increased surface area for enhanced electrochemical signals (Manesh et al. 2008).

13.3 Conductive Polymers and Carbon-Based Materials

The current growth of interest in carbon and polymer-family materials has opened new ways for novel functional nanomaterials (Pham et al. 2011). CPs and graphene composites are promising materials in biosensor development owing to their combined electrochemical and electrical characteristics (Unnikrishnan et al. 2013). Graphene is a two-dimensional, zero-bandgap monolayer sheet of sp^2 -bonded carbon atoms, first introduced by Geim and his team in 2004; the discovery led to a Nobel prize in 2010 (Huang et al. 2011). This carbon-based nanomaterial possesses excellent physical, chemical, mechanical, electrical, optical, thermal, and catalytic properties, and is often called as a wonder material by researchers. With its high theoretical surface area of approximately $2630 \text{ m}^2/\text{g}$ (Yang et al. 2012b; Yang and Gunasekaran 2012), and good biocompatibility similar to that of noble metal nanoparticles, graphene is an excellent candidate as transducer material in biosensors (Pham et al. 2011; Tabrizi and Varkani 2014; Unnikrishnan et al. 2013). On the other hand, PPy, a conductive polymer with a conductivity range of 10^2 to $7.5 \times 10^3 \text{ S/cm}$, has been widely characterized for biosensor fabrication. A combination of PPy and reduced graphene oxide (rGO), a form of functionalized graphene, along with copper oxide (CuO) (PPy/rGO/CuO as composite) was used in the development of a non-enzymatic glucose sensor. The sensor showed a linear range of 0.1–100 mM ($R^2 = 0.991$) for glucose sensing, which is higher than most of the existing non-enzymatic glucose biosensors. The sensor also showed a limit of detection (LOD) as low as $0.03 \text{ }\mu\text{M}$, at a signal-to-noise ratio of 3. Additionally, the sensor exhibited remarkable reproducibility, stability and selectivity properties, which qualifies CuO, Ppy, and rGO composite as transducer material for non-enzymatic glucose sensors (Nia et al. 2015).

Before the discovery of graphene, carbon nanotubes (CNTs) were extensively researched as transducer material for biosensors. A CNT can be pictured as a sheet of graphene rolled into cylindrical shape. It possesses unique properties such as high electrical conductivity, strong adsorptive ability, and excellent electrocatalytic

activity. Moreover, CNTs can promote electron transfer of electroactive species over a wide range, which is favorable to enhance the performance of biosensors. A glucose biosensor containing carboxylated multi-walled carbon nanotubes (MWNTs) modified with glucose oxidase (GOx) and an overlying tetramethyl orthosilicate (TMOS) layer demonstrated optimum efficacy in terms of enhanced current density ($18.3 \pm 0.5 \mu\text{A}/\text{mM cm}$), linear range (0.0037–12 mM), detection limit (3.7 μM), coefficient of variation (2%), response time (less than 8 s), stability, selectivity, and reproducibility. Hydrogen peroxide (H_2O_2) response tests showed that the improved performance is due to an increase in enzyme loading and therefore can be applied for various biosensing applications (Shi et al. 2011).

13.4 Natural Nonconductive Polymer-Based Composites

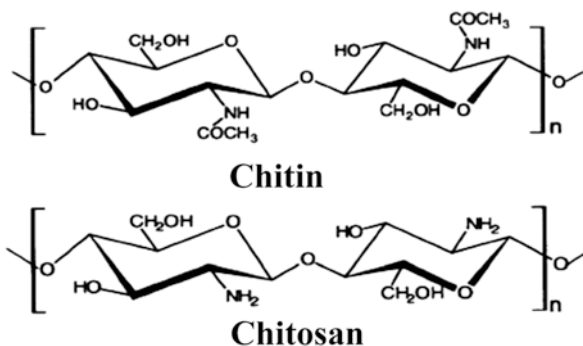
Over the history of biosensor application, natural polymers have continuously attracted a lot of attention owing to their properties, including biodegradability, biocompatibility, permselectivity, and environmental friendliness. Among natural polymers, chitosan and cellulose are widely used for various biosensor applications. In addition, dextran-based composites and gelatin/collagen-based composites are also commonly used in biosensor fabrication.

13.4.1 Chitin- and Chitosan-Based Composites

Chitosan (CS) is a non-acetylated or partially de-acetylated chitin found in the exoskeleton of crustaceans, such as crabs, shrimp, and insects, as well as in fungal cell walls, and the structure of CS is shown in Fig. 13.1 (Luo et al. 2010). Chitin and chitosan possess appealing physical and biological features. Their biodegradability, biocompatibility, antibacterial activity, and wound-healing capacity have attracted intense attention. As frequently used biomaterials, chitin and chitosan have the potential to be applied in several fields such as drug release, tissue engineering, wound dressing, cosmetics, biosensors, and medical implants (Ding et al. 2014).

In biosensor application, chitin- and CS-based composites have garnered interest owing to their unique properties, including a high surface area-to-volume ratio, which increases the number of binding sites available for biomolecule immobilization, as well as faster mass-transfer rates, which results in lower limits of detection and faster detection rates (Ding et al. 2014). Composites of metal, metal oxides, and magnetic nanoparticles with a CS matrix open up a new approach for modifying the electrode surface. Wang et al. in 2013 reported the fabrication of an amperometric glucose biosensor based on silver nanowires (AgNWs), CS, and glucose oxidase (GOx) film. In this work, CS was used as an immobilization matrix for immobilizing GOx on the AgNW surfaces based on its excellent film-forming ability, good biocompatibility, and high mechanical strength. The biosensor reported a linear

Fig. 13.1 Chemical structures of chitin and chitosan

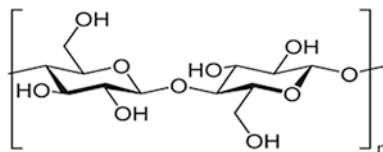


range of 10 M to 0.8 mM, indicating a high sensitivity with a low detection limit (Wang et al. 2013).

Another important characteristic of CS is the chemical structure, which has intrinsic oxygen- and nitrogen-based functional groups that can be used as target points for covalent modification. A graphene-CS nanocomposite was successfully synthesized and utilized to fabricate a DNA-based electrochemical biosensor for the detection of typhoid, which is presented by an *S. typhi*-specific DNA probe (Singh et al. 2013). This DNA biosensor exhibited a lower detection limit of 10 fM in phosphate buffer and 100 fM in spiked serum, and good stability (stable up to 15 days, with about 10% loss in the signal after 30 days, when stored at 4 °C, which loss is attributed to the biodegradability of chitosan). The excellent performance of the biosensor is attributed to the large surface area-to-volume ratio and good electrochemical activity of graphene oxide (GO), combined with the good biocompatibility of chitosan, which improves the DNA immobilization and enhances electron transfer between the DNA and the indium tin oxide (ITO) electrode surface (Singh et al. 2013).

Carbon nanotubes (CNTs) are also widely used in chitosan-based composites for biosensors owing to their excellent properties (Chawla et al. 2011). In the research reported by Diaconu et al. in 2010, a multi-walled carbon nanotube/chitosan (MWCNT/CS) composite deposited on a gold electrode was introduced to evaluate total polyphenolic content from in-vitro cultivated plants. The electrodeposition of MWCNT/CS film on the gold electrode surface led to a two-fold increase in current intensity as a result of an increased electroactive area, as well as providing a proper environment for enzyme immobilization to preserve enzyme catalytic specificity. The biosensor showed a limit of detection of 2.33×10^{-7} mol/L, a linear response range from 9.1×10^{-7} to 1.21×10^{-5} mol/L and a sensitivity of 846 $\mu\text{A}/\text{mmol}$ (Diaconu et al. 2010). The modified electrode also displayed characteristics of fast response time, highly competitive detection limit, and good reproducibility towards rosmarinic acid and other phenolic acids.

Fig. 13.2 Chemical structure of cellulose



13.4.2 Cellulose-Based Composites

Cellulose, as shown in Fig. 13.2, a straight-chain polymer consisting of a linear chain of several hundred to many thousand β (1 \rightarrow 4)-linked d-glucose units, is an important structural component of the primary cell wall of green plants, as well as the most abundant organic polymer. It is traditionally used to produce paper, pulp, and textiles. Cellulose has many advantages, such as abundance, biodegradability, biocompatibility, renewability, high Young's modulus, dimensional stability, and low thermal expansion coefficient (Kim et al. 2014).

To enhance cellulose properties in terms of chemical stability, electrical conductivity, and photocatalytic activity for sensor application, cellulose-based composites have been widely studied by adding conductive materials to a cellulose matrix (Kim et al. 2014). Mahadeva et al. in 2013 introduced an inexpensive, flexible, and disposable tin oxide (SnO_2) and cellulose nanocomposite-based conductometric urea biosensor. Tin(II) oxide (SnO_2) is an electrical conductor widely used for sensor applications. In this research, a thin layer of SnO_2 was coated on regenerated cellulose films via a liquid-phase deposition technique (LPD). The result was a uniform and homogeneous deposition of a well-grown SnO_2 coating on the cellulose surface, as well as the presence of nanopores all over the SnO_2 coating, observable through SEM and TEM images. This cellulose/ SnO_2 nanocomposite-based urea biosensor was prepared by immobilizing urease on the SnO_2 layers via a physical absorption method. In general, the resulting biosensor showed a linear response up to 42 mM; it was also found that the proposed sensor exhibited the same level of sensitivity for seven (7) days (Mahadeva et al. 2013). Furthermore, Mahadeva et al. also demonstrated a humidity and temperature sensor by introducing a biodegradable and flexible nanocomposite consisting of a nanoscale polypyrrole (PPy) as a humidity- and a temperature-sensitive layer formed on a cellulose surface via in-situ polymerization. The sensor showed good linearity as well as superior reversibility with good response and recovery behavior (Mahadeva and Kim 2013).

13.4.3 Dextran-Based Composites

Dextran, a complex branched glucan composed of chains of varying lengths, is a highly hydrophilic natural polymer that has a protective effect against the denaturation of an enzyme by creating a water structure around the enzyme without any alteration in enzyme conformation (Satvekar et al. 2014). In the research of

Altikatoglu et al. reported in 2010, covalent conjugation of GOx with different molecular weights of dextran in various molar ratios was investigated; results showed that the conjugate enhanced the stability of an enzyme against temperature and pH (Altikatoglu et al. 2010). In addition, dextran has many advantages that are promising for biosensor applications, including biodegradability, chemical inertness, biocompatibility, and good film formation (Satvekar et al. 2014). Dextran-based polymers have become a popular material for immobilization matrices used in biosensors owing to their non-specific interaction with biomolecules and their hydrophilic properties. Naghib et al. fabricated a bio-electrochemical sensor by immobilizing phenylalanine dehydrogenase on a bio-functionalized polymeric film for direct, cost-effective, and rapid determination of l-phe for diagnosis of phenylketonuria (PKU). In this work, the modified materials are made up of dextran, polyvinylpyrrolidone (PVP), bovine albumin serum (BSA) protein, glutaraldehyde (GA), and immobilized phenylalanine dehydrogenase (PHD). Comparison of electrochemical behavior among the different dextran/PVP/PHD, dextran/PVP/BSA/PHD, dextran/PVP/GA/PHD, and dextran/PVP/BSA/GA/PHD composites showed that the sensitivity of the dextran/PVP/BSA/GA/PHD-modified electrode towards l-phe is 7.73 mA/M cm^2 , and the linear range spans the concentration of l-phe from 0 to 6 mM with a correlation coefficient of 0.993 ($y = 2.192 \times + 1.58$, $R^2 = 0.993$). In addition, the modified electrode also showed desirable stability, retaining approximately 90% of the initial response and its reliability confirmed after 16 days (Naghib et al. 2012).

13.4.4 Gelatin- and Collagen-Based Composites

Gelatin, which is widely used in immobilization matrices for the preparation of biosensors, is a water-soluble and natural polymer product obtained by partial hydrolysis of collagen extracted from the skin, bones, and connective tissues of animals. Gelatin is an example of a physically cross-linked hydrogel; the hydrophilic groups or domains that are hydrated make gelatin a suitable matrix for the entrapment of biomolecules because of its excellent biocompatibility (De Wael et al. 2011). In general, advantages of gelatin for the fabrication of electrodes are (1) good property for dispersing the modified electrode materials; (2) high adhesion ability for bonding different types of small particles; (3) intrinsically high biocompatibility that can provide a favorable environment for an enzyme to maintain high activity. Its gel-forming ability with extremely heterogeneous and hydrophilic polymer networks makes it ideal for the preparation of electrochemical biosensors (TermehYousefi et al. 2015; De Wael et al. 2012; Wang et al. 2014).

A novel hydrogen peroxide biosensor was fabricated based on the immobilization of horseradish peroxidase (HRP) by cross-linking on a glassy carbon electrode (GCE) modified with cobalt oxide (Co_3O_4) nanoparticles, multi-walled carbon nanotubes (MWCNTs), and gelatin composite. In this work, gelatin was applied as a dispersive agent to obtain stable MWCNTs dispersions. Next, Co_3O_4 nanoparticles

were incorporated into the MWCNTs/gelatin film in order to increase the electron transfer. The proposed biosensor showed optimum response within 5 s at pH 7.0, a linear response range of $7.4 \times 10^{-7} - 1.9 \times 10^{-5}$ M with a detection limit of 7.4×10^{-7} M, as well as good stability (90% of its original sensitivity after storage for 1 week) (Kaçar et al. 2014).

Collagen is one of the main classes of natural extracellular matrix structural proteins and commonly used as a biomaterial in a variety of tissue applications owing to its excellent biocompatibility. A hydrogen peroxide (H_2O_2) biosensor based on hemoglobin (Hb)/collagen/CNT composite nanofibers was fabricated by electrospinning in order to enhance the sensitivity and detection limit by taking advantage of the subtle electronic properties of CNTs, the excellent biocompatibility of collagen as a natural polymer, and the high specific surface area and three-dimensional porous structure of electrospun nanofibers. In particular, collagen as a natural polymer has good biocompatibility and can be a suitable matrix and favorable microenvironment for Hb immobilization. The resulting biosensor showed a steady-state response of current in a good linear relationship with the concentration of H_2O_2 ranging from 5.0 μM to 200 μM ($R^2 = 0.999$). In addition, the modified electrode also showed a good detection limit of 0.91 μM toward H_2O_2 , as well as retaining 90% response to H_2O_2 after storage in 0.10 M phosphate buffer solution at 4 °C for 3 weeks (Li et al. 2014).

13.5 Synthetic Nonconductive Polymer-Based Composites

Synthetic polymers present a large variety of immobilization opportunities owing to the range of possible physical and chemical structures. Some functional groups of synthetic polymers are promising as matrices for physical entrapment and as support for covalent coupling during the immobilization procedure. Among the numerous synthetic polymers, polystyrene-based composites and nafion-based composites are two main types of materials widely used in biosensor development.

13.5.1 Polystyrene-Based Composites

Polystyrene, a synthetic aromatic polymer made from the monomer styrene, has attracted attention as an excellent sensing material owing to its excellent properties, including high surface activity, good biocompatibility, high organization, and uniformity, which could provide a desirable microenvironment to immobilize biomolecules and facilitate direct electron transfer between a protein and the underlying electrode. Polystyrene sulfonate (PSS) is a linear polymer derived from polystyrene and contains sulfonic acid or sulfonate functional groups. It is widely used in combination with some conductive polymers or nanomaterials in biosensor applications owing to its excellent solubility. Xu et al. in 2010 applied a PEDOT:PSS-gold (Au)

nanocomposite as biomaterial for horseradish peroxidase (HRP) immobilization, as this nanocomposite has excellent aqueous compatibility and biocompatibility. In this study, PSS was used as the charge-balancing dopant during polymerization to synthesize PEDOT: PSS, resulting in a water-soluble matrix with good conductivity, good film-forming properties, biocompatibility, and excellent stability. The biosensor showed excellent electrocatalytic ability towards hydrogen peroxide (H_2O_2); response currents showed a linear relation with H_2O_2 concentration from 2.0×10^{-7} to 3.8×10^{-4} mol/L, and the detection limit was 1.0×10^{-7} M (with a signal-to-noise ratio of 3). Furthermore, the formal Michaelis–Menten constant was 0.78 mmol/L, indicating aqueous compatibility and good biocompatibility of this composite, which can provide an ideal microenvironment for HRP immobilization and retain high bioactivity (Xu et al. 2010).

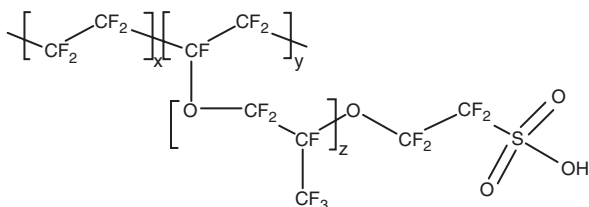
13.5.2 Nafion-Based Composites

Nafion, which is composed of a mainly hydrophobic backbone (CF_2 groups) and hydrophilic chains (SO_3 groups), just as shown in Fig. 13.3, is usually utilized as a perfluorosulfonated cation-exchange polymer. It is commonly used in the fabrication of biosensors for its good chemical and thermal stability, excellent biocompatibility, and ability to resist interference from anions and biological macromolecules.

Nasirizadeh et al. in 2015 constructed an electrochemical biosensor based on immobilization of catalase and toluidine blue (TB, a phenothiazine dye) on a gold electrode (AuE) coated with nafion film, which helped to enhance the stability of the biosensor and its ability to resist interference from anions. Differential pulse voltammetry (DPV) showed that the calibration plots were linear within two ranges (1.0–21.5 μM , 21.5–115.0 μM), and the detection limit of H_2O_2 was 0.25 μM . The diffusion coefficient of H_2O_2 was calculated as 1.48×10^{-6} cm^2/s using chronoamperometric results. The results displayed excellent catalytic activity for the reduction of H_2O_2 , attributed to the synergistic effects between TB and catalase at the AuE/nafion (Nasirizadeh et al. 2015).

Choi et al. (2011) fabricated a flow-injection amperometric glucose biosensor based on reduced graphene oxide (rGO)/nafion hybrids. In this work, compared to rGO alone, rGO/nafion hybrids showed higher current responses and lower peak-to-peak potential separation (ΔE_p) for the redox process of $[\text{Fe}(\text{CN})_6]^{3-/4-}$ owing to the

Fig. 13.3 Chemical structure of nafion



large accessible surface area and capacitance that was improved by nafion. Moreover, the value of the diffusion coefficient of the rGO/nafion hybrid was evaluated to be $9.5 \times 10^{-6} \text{ cm}^2 \text{ s}^{-1}$, which is about three-fold higher than that of the rGO electrode. This hybrid biosensor showed a fast response time of $\sim 3 \text{ s}$, a sensitivity of $3.8 \mu\text{A}/\text{mM cm}^2$, a limit of detection of $170 \mu\text{M}$, and a linear detection range of $2\text{--}20 \text{ mM}$ for the flow-injection amperometric detection of glucose (Choi et al. 2011).

13.5.3 Polyvinylpyrrolidone-Based Composites

Polyvinylpyrrolidone (PVP), also commonly called polyvidone or povidone, is a water-soluble polymer made from the monomer N-vinylpyrrolidone. For the investigation of a biosensor, it is usually used as a dispersant for other materials in a composite or acts as a reducing and stabilizing agent for AuNP synthesis. It is also used as a matrix for immobilizing biomolecules or nanomaterials owing to its ability to prevent nanoparticle aggregation and the excellent compatibility with metal NPs (Sophia and Muralidharan 2015).

Sophia & Muralidharan described a simple, novel, and convenient approach for preparing an enzyme-free biosensor using gold nanoparticles for the electroanalytical determination of H_2O_2 . In order to prevent particle growth and aggregation of AuNPs, PVP was used as a dispersant and suitable matrix based on its excellent adsorption properties and excellent compatibility. A well-defined linear current response to H_2O_2 concentration in the region of $0.8\text{--}80 \mu\text{M}$, with a high correlational coefficient of 0.99 and a detection limit of $0.7 \mu\text{M}$ were observed. The fabricated sensor showed good reproducibility, long-term stability, and high selectivity in the presence of common electroactive species such as ascorbic acid (AA), uric acid (UA), and 4-acetamidophenol (AP) (Sophia and Muralidharan 2015).

Yang et al. (2012a) constructed an H_2O_2 and glucose sensor by dropping a polyvinylpyrrolidone (PVP) and silver nanowire (AgNW) composite onto the surface of a glassy carbon electrode (GCE). In this study, AgNWs were prepared through a polyol process using PVP as protection agent. The resultant non-enzymatic based H_2O_2 biosensor showed a fast amperometric response time of less than 2 s; the catalytic current was linear for concentrations of H_2O_2 ranging from $20 \mu\text{M}$ to 3.62 mM , with a detection limit of 2.3 mM , at a signal-to-noise ratio of 3. In addition, the resulting glucose biosensor constructed by immobilizing glucose oxidase (GOx) on the surface of the PVP-AgNW/GCE exhibited a linear relationship between the catalytic current and a glucose concentration range from 2 to 20 mM; the sensitivity of the glucose detection was $22.43 \mu\text{A}/\text{mM cm}^2$. This glucose biosensor was also investigated for glucose detection in human blood serum and showed a sensitivity of $15.86 \mu\text{A}/\text{mM cm}^2$ with good selectivity and stability (Yang et al. 2012a).

13.5.4 *Block Copolymer-Based Composites*

Block copolymers (BCPs), which are comprised of at least two different immiscible polymers joined by covalent bonds, have drawn immense interest for their potential applications. The dissimilar blocks can be separated into distinct domains with controllable dimensions and functionalities (Tseng and Darling 2010). The simplest BCPs are linear diblock copolymers, comprised of two distinct polymer chains connected at their ends to form a linear chain. Diblock copolymers are able to form lamellae, cylinders, spheres, or more complicated structures depending on the ratio of each polymer. They have been applied in various nanotechnological applications in several different fields, including nanostructured membranes, BCP templates for nanoparticle synthesis, photonic crystals, high-density information-storage media, and nanomedicine (Auriemma and De Rosa 2011).

BCP-based nanostructures that depict natural assemblies regarding their complexity and functionality have also been investigated regarding their response to external stimuli; such polymers include the poly(N-isopropylacrylamide)-based copolymer PDMA and PVP-based copolymers. The stimulus-responsive nanostructures, which are also referred to as “smart,” “intelligent,” or “environmentally sensitive” nanostructures, are systems that exhibit changes in response to physical stimuli such as heat and light, or to chemical stimuli such as pH and chemical substances (Auriemma and De Rosa 2011). In particular, the intelligent, responsive polymers on gold nanoparticles show a hydrophilic-hydrophobic phase transition due to the stimulus, which provides the potential to be nanocarriers for catalysts or dyes. Usually, the response of the smart polymer is reversible, giving the smart composites. The researchers categorized the stimuli-responsive polymers into two types: thermo-sensitive polymers and pH-responsive polymers. Furthermore, BCP and gold nanocomposites can be soluble in different solvents depending on the solubility of the outside polymer shells, which provides the possibility for application of drug delivery based on the phase transition between water and oil phases (Li et al. 2009).

Over the past few years, a diblock copolymer–hybridized gold nanoparticle has attracted considerable interest in investigating the morphology of the composites and their dependence on different ratios of gold nanoparticles and diblock copolymers. In actuality, the polymer grafted onto the surface of gold nanoparticles can not only improve the stability of the gold cores but also functionalize the gold surface through the outside polymer shells. There are three approaches, usually called direct-synthesis, “graft-to,” and “graft-from” methods via a gold-sulfur bond, to prepare smart nanocomposites of intelligent polymers and gold nanoparticles (Li et al. 2009). In order to examine the phase behavior of the BCP/gold nanoparticle composite, some papers applied different methods of preparation: ex-situ synthesis and in-situ synthesis. In the first method, the formation of gold nanoparticles is within the BCP microdomains, in which the monomers are preloaded with metal salt and the preformed polymer phase acts as a micro-reactor for metal and metal oxide nanoparticles from precursors that are transformed into the desired nanopar-

ticles by a series of appropriate reactions (Sarkar and Alexandridis 2012). This method attracts attention because the particle size and morphology can be controlled with relative ease. The functional groups of the host BCPs play an important role in determining the overall characteristics of the BCP-based composite by determining the polymer capacity to bind with metal ions, metal complexes, or other precursor ions containing the target metal (Lin et al. 2010). The ex-situ method of synthesis can be performed by first synthesizing the inorganic nanoparticles, and then dispersing them in a polymer solution or three-dimensional matrix. This method is popular because it does not set a limitation on the nature of the nanoparticles and host polymer to be used. However, the challenge is the difficulty of forming a homogeneous and well dispersed inorganic material in the polymer (Sarkar and Alexandridis 2012). Similar to the preparation of gold nanoparticle (AuNP)/ polystyrene-*b*-poly(4-vinylpyridine) (PS-*b*-P4VP) composites, this research introduced 3-*n*-pentadecylphenol (PDP) as the small molecule linker with the P4VP block of the PS-*b*-P4VP chain based on the hydrogen bond between the pyridine group of P4VP and the phenol group of PS, forming a PS-*b*-P4VP(PDP) comb-like supramolecule. The AuNPs can be preferentially localized at the interface between the P4VP domain at the particle surface and the surrounding water. The structure of the convex lens-shaped particles (CL particles) of PS-*b*-P4VP with highly ordered and oriented nanoporous channels showed promise for optical and biological sensing (Ku et al. 2014).

In general, the BCP/AuNPs or other metal nanoparticle composites with well-defined core/shell nanostructures show potential as nanocarriers for drugs, catalysts, dyes, metal ions, or biomolecules, based on the tunable internal structures, shapes, and surface properties (Li et al. 2009). Furthermore, the nanocomposites consisting of an outside polymer tunnel structure around gold cores can be utilized as a suitable matrix to immobilize enzymes or other molecules based on the different properties of BCPs and gold nanoparticles and used to fabricate biosensors.

13.6 Conclusion

The increasing world market demand for biosensing has brought researchers around the world to a continual search for smart ways to improve the overall performance of a biosensor. This involves sustained effort to find the best electrode fabrication methods using different materials as transducer layer. Among the materials widely used in biosensor, fabrication are polymeric materials. Conductive polymers are mostly used as transducer materials owing to their chemical, electrical and physical properties. Natural and synthetic non-conductive polymers are typically used as support or immobilizer material for non-biological materials such as metal nanoparticles and carbon-based materials (e.g., graphene, CNTs), as well as for biological materials (e.g., enzymes, DNA, proteins, and cells). The combination of polymers with biological and non-biological materials to produce composite-based

biosensors plays an important role in the advancement of biosensors because the most important element that determines the performance of biosensor is the architecture of the materials used as the transducer layer. The incorporation of polymeric materials as composites in biosensors enhances the electrical conductivity of the transducer as well as providing support matrices for the immobilization of biomolecules.

References

- Altikatoglu M, Basaran Y, Arioz C, Ogan A, Kuzu H (2010) Glucose oxidase-dextran conjugates with enhanced stabilities against temperature and pH. *Appl Biochem Biotechnol* 160(8):2187–2197
- Auriemma F, De Rosa C (2011) Nanotechnological applications of block copolymers in biomedicine. *Trop J Pharm Res* 10(1):1–2
- Chawla S, Rawal R, Pundir CS (2011) Fabrication of polyphenol biosensor based on laccase immobilized on copper nanoparticles/chitosan/multiwalled carbon nanotubes/polyaniline-modified gold electrode. *J Biotechnol* 156(1):39–45
- Choi BG, Im J, Kim HS, Park HS (2011) Flow-injection amperometric glucose biosensors based on graphene/Nafion hybrid electrodes. *Electrochim Acta* 56(27):9721–9726
- Cui L, Xu M, Zhu J, Ai S (2011) A novel hydrogen peroxide biosensor based on the specific binding of horseradish peroxidase with polymeric thiophene-3-boronic acid monolayer in hydrophilic room temperature ionic liquid. *Synth Met* 161:1686–1690
- De Wael K, Verstraete A, Van Vlierberghe S, Dejonghe W, Dubruel P, Adriaens A (2011) The electrochemistry of a gelatin modified gold electrode. *Int J Electrochem Sci* 6:1810–1819
- De Wael K, De Belder S, Pilehvar S, Van Steenberghe G, Herrebout W, Heering HA (2012) Enzyme-gelatin electrochemical biosensors: Scaling down. *Biosensors* 2(1):101–113
- Diaconu M, Litescu SC, Radu GL (2010) Laccase–MWCNT–chitosan biosensor—a new tool for total polyphenolic content evaluation from in vitro cultivated plants. *Sensors Actuators B Chem* 145(2):800–806
- Ding F, Deng H, Du Y, Shi X, Wang Q (2014) Emerging chitin and chitosan nanofibrous materials for biomedical applications. *Nanoscale* 6(16):9477–9493
- Grieshaber D, MacKenzie R, Voeroes J, Reimhult E (2008) Electrochemical biosensors—sensor principles and architectures. *Sensors* 8(3):1400–1458
- Huang J (2006) Syntheses and applications of conducting. *Pure Appl Chem* 78:15–27
- Huang X, Yin Z, Wu S, Qi X, He Q, Zhang Q, Yan Q, Boey F, Zhang H (2011) Graphene-based materials: Synthesis, characterization, properties, and applications. *Small* 7(14):1876–1902
- Kaçar C, Dalkiran B, Erden PE, Kiliç E (2014) An amperometric hydrogen peroxide biosensor based on Co₃O₄ nanoparticles and multiwalled carbon nanotube modified glassy carbon electrode. *Appl Surf Sci* 311:139–146
- Kim JH, Mun S, Ko HU, Yun GY, Kim J (2014) Disposable chemical sensors and biosensors made on cellulose paper. *Nanotechnology* 25(9):092001
- Ku KH, Shin JM, Kim MP, Lee CH, Seo MK, Yi GR, Kim BJ (2014) Size-controlled nanoparticle-guided assembly of block copolymers for convex lens-shaped particles. *J Am Chem Soc* 136(28):9982–9989
- Li D, He Q, Li J (2009) Smart core/shell nanocomposites: intelligent polymers modified gold nanoparticles. *Adv Colloid Interf Sci* 149(1):28–38
- Li J, Mei H, Zheng W, Pan P, Sun XJ, Li F, Guo F, Zhou HM, Ma JY, Xu XX, Zheng YF (2014) A novel hydrogen peroxide biosensor based on hemoglobin-collagen-CNTs composite nanofibers. *Colloids Surf B Biointerfaces* 118:77–82

- Lin T, Li CL, Ho RM, Ho JC (2010) Association strength of metal ions with poly (4-vinylpyridine) in inorganic/poly (4-vinylpyridine)-b-poly (ϵ -caprolactone) hybrids. *Macromolecules* 43(7):3383–3391
- Luo L, Li Q, Xu Y, Ding Y, Wang X, Deng D, Xu Y (2010) Amperometric glucose biosensor based on NiFe₂O₄ nanoparticles and chitosan. *Sensors Actuators B Chem* 145(1):293–298
- Mahadeva SK, Kim J (2013) Porous tin-oxide-coated regenerated cellulose as disposable and low-cost alternative transducer for urea detection. *IEEE Sens J* 13(6):2223–2228
- Mahadeva SK, Ko HU, Kim J (2013) Investigation of cellulose and tin oxide hybrid composite as a disposable pH sensor. *Int J Res Phys Chem Chem Phys* 227(4):419–428
- Manesh K, Santhosh P, Gopalan A, Lee K (2008) Electrocatalytic oxidation of NADH at gold nanoparticles loaded. *Talanta* 75:1307–1314
- Naghib SM, Rabiee M, Omidinia E, Khoshkenara P, Zeini D (2012) Biofunctionalization of dextran-based polymeric film surface through enzyme immobilization for phenylalanine determination. *Int J Electrochem Sci* 7(1):120–135
- Nasirizadeh N, Hajjiosseini S, Shekari Z, Ghaani M (2015) A novel electrochemical biosensor based on a modified gold electrode for hydrogen peroxide determination in different beverage samples. *Food Anal Methods* 8(6):1546–1555
- Nia PM, Meng WP, Lorestani F, Mahmoudian MR, Alias Y (2015) Electrodeposition of copper oxide/polypyrrole/reduced graphene oxide as a nonenzymatic glucose biosensor. *Sensors Actuators B Chem* 209:100–108
- Pham T, Choi B, Lim K, Jeong Y (2011) A simple approach for immobilization of gold nanoparticles on graphene oxide sheets by covalent bonding. *Appl Surf Sci* 257:3350–3357
- Richard B, Nigel JC, Sarah HC (2014) Review Conductive polymers: Towards a smart biomaterial for tissue. *Acta Biomater* 10:2341–2353
- Saei A, Najafi-Marandi P, Abhari A, de la Guardia M, Dolatabadi A (2013) Electrochemical biosensors for glucose based on metal nanoparticles. *TrAC Trends Anal Chem* 42:216–227
- Sarkar B, Alexandridis P (2012) Self-assembled block copolymer-nanoparticle hybrids: Interplay between enthalpy and entropy. *Langmuir* 28(45):15975–15986
- Satvekar RK, Rohiwal SS, Raut AV, Karande VA, Tiwale BM, Pawar SH (2014) A silica-dextran nanocomposite as a novel matrix for immobilization of horseradish peroxidase, and its application to sensing hydrogen peroxide. *Microchim Acta* 181(1–2):71–77
- Shi J, C Claussen J, S McLamore E, ul Haque A, Jaroch D, R Diggs A, D Porterfield M (2011) A comparative study of enzyme immobilization strategies for multi-walled carbon nanotube glucose biosensors. *Nanotechnology* 22:355502
- Singh A, Sinsinbar G, Choudhary M, Kumar V, Pasricha R, Verma HN, Arora K (2013) Graphene oxide-chitosan nanocomposite based electrochemical DNA biosensor for detection of typhoid. *Sensors Actuators B Chem* 185:675–684
- Sophia J, Muralidharan G (2015) Gold nanoparticles for sensitive detection of hydrogen peroxide: a simple non-enzymatic approach. *J Appl Electrochem* 45:1–9
- Tabrizi MA, Varkani JN (2014) Green synthesis of reduced graphene oxide decorated with gold nanoparticles and its glucose sensing application. *Sensors Actuators B Chem* 202:475–482
- TermehYousefi A, Bagheri S, Kadri NA, Mahmood MR, Ikeda S (2015) Constant glucose biosensor based on vertically aligned carbon nanotube composites. *Int J Electrochem Sci* 10:4183–4192
- Tseng YC, Darling SB (2010) Block copolymer nanostructures for technology. *Polymers* 2(4):470–489
- Unnikrishnan B, Palanisamy S, Chen SM (2013) A simple electrochemical approach to fabricate a glucose biosensor based on graphene-glucose oxidase biocomposite. *Biosens Bioelectron* 39:70–75
- Wang X, & Uchiyama S (2013) Polymers for biosensors construction. In *State of the art in biosensors* general aspects. InTech.
- Wang L, Gao X, Jin L, Wu Q, Chen Z, Lin X (2013) Amperometric glucose biosensor based on silver nanowires and glucose oxidase. *Sensors Actuators B Chem* 176:9–14

- Wang Y, Li T, Zhang W, Huang Y (2014) A hydrogen peroxide biosensor with high stability based on gelatin-multiwalled carbon nanotubes modified glassy carbon electrode. *J Solid State Electrochem* 18(7):1981–1987
- Xu J, Peng R, Ran Q, Xian Y, Tian Y, Jin L (2010) A highly soluble poly (3, 4-ethylenedioxythiophene)-poly (styrene sulfonic acid)/Au nanocomposite for horseradish peroxidase immobilization and biosensing. *Talanta* 82(4):1511–1515
- Xue K, Zhou S, Shi H, Feng X, Xin H, Song W (2014) A novel amperometric glucose biosensor based on ternary gold nanoparticles/polypyrrole/reduced graphene oxide nanocomposite. *Sensors Actuators B Chem* 203:412–416
- Yang J, Gunasekaran S (2012) Electrochemically reduced graphene oxide sheets for use in high performance supercapacitors. *Carbon* 51:36–44
- Yang X, Bai J, Wang Y, Jiang X, He X (2012a) Hydrogen peroxide and glucose biosensor based on silver nanowires synthesized by polyol process. *Analyst* 137(18):4362–4367
- Yang X, Chen H, Li J, Xu M (2012b) Chemical methods for graphene synthesis. In: Xu Z (ed) *Graphene: properties, synthesis and applications*. Nova Science Publishers, Inc, New York, pp 101–124
- Yao Y, Wen Y, Zhang L, Xu i, Wang Z, Duan X (2013) A stable sandwich-type hydrogen peroxide sensor based on immobilizing horseradish peroxidase to a silver nanoparticle monolayer supported by PEDOT: PSS. *Int J Electrochem Sci* 8(7):9348–9359
- Yuqing M, Jianrong C, Xiaohua W (2004) Using electropolymerized non-conducting polymers to develop enzyme amperometric biosensors. *Trends Biotechnol* 22(5):227–231

Chapter 14

Characterization of Conformational and Oligomeric States of Proteins



Fazia Adyani Ahmad Fuad

Abstract Oligomerization and conformational changes of proteins in solutions are advantageous for their structural and functional control. The advancement in biophysical characterization analyses, such as Size Exclusion Chromatography coupled with Multi-Angle Light Scattering (SEC-MALS) has shed lights in understanding the underlying mechanisms of actions for protein molecules. This chapter focuses on three types of protein analysis; SEC-MALS, native PAGE and continuous enzymatic assays of the bacterially expressed cofactor-independent phosphoglycerate mutase from *Leishmania mexicana* (Lm-iPGAM), which was shown to exist in different oligomeric and conformational states in solution. The outcome of this analyses has paved the way towards understanding the behavior of Lm-iPGAM in solution, which is important for further structural and functional studies.

Keywords Protein conformations and oligomeric states · Multi-Angle Light Scattering (SEC-MALS) · Native PAGE · Continuous enzymatic assays · *Leishmania mexicana* · Cofactor-independent phosphoglycerate mutase

14.1 Introduction

Flexibility in solutions plays a significant role in the functions of many proteins. Evidence is emerging that oligomerization and conformational changes to proteins in solution offer the potential for structural and functional control, which is deemed important for elucidating the underlying mechanisms of their actions, in particular the role of enzymes in catalysis. Recent developments in biophysical characterization analyses, specifically Size Exclusion Chromatography coupled with Multi-Angle Light Scattering (SEC-MALS), may facilitate characterization of different protein forms and oligomeric states in solution. Owing to its ability to determine the absolute molecular masses of proteins, SEC-MALS provides the means for

F. A. A. Fuad (✉)

International Islamic University Malaysia, Kuala Lumpur, Malaysia

e-mail: fazia_adyani@iium.edu.my

distinguishing the conformational transitions and domain motions of proteins in the absence of calibration curves, comprising a series of globular proteins as standards. This chapter focuses on three types of protein analysis, namely (i) SEC-MALS; (ii) native PAGE; and (iii) continuous enzymatic assays of the bacterially expressed cofactor-independent phosphoglycerate mutase from *Leishmania mexicana* (Lm-iPGAM), which reportedly exists in different oligomeric and conformational states in solution (Fuad 2012; Blackburn et al. 2014). Lm-iPGAM is a potential drug target. However, while its closed form crystal structure has been determined in the presence of the substrate 3-phosphoglycerate (Nowicki et al. 2009), knowledge of its open conformation is limited. Consequently, the search for potential drug candidates through structure-based drug design experiments has been hindered thus far. The aim of this study was to distinguish the different oligomeric and conformational states of Lm-iPGAM, following an earlier work involving ion-exchange chromatography, based on which this enzyme was separated into three distinct peaks, as shown in Fig. 14.1.

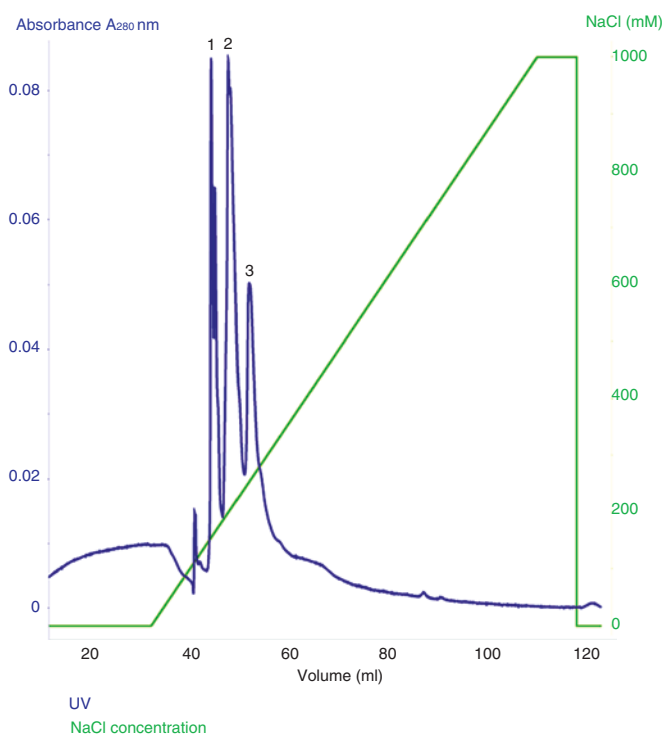


Fig. 14.1 The three protein peaks (P1, P2 and P3) eluted from the ion-exchange chromatography column

14.2 Objectives

The objective of these experiments was twofold, namely:

1. To characterize the multiple conformational and oligomeric states of bacterially expressed *Lm*-iPGAM in solution.
2. To determine the specific activities of the three different forms of *Lm*-iPGAM.

14.3 Sec-Mals Analysis

The separation of proteins by their shapes and sizes referred to as SEC or gel filtration, is a routine technique employed in the laboratory not only for purification or buffer exchange purposes but also as an analytical method to characterize macromolecules in a solution. When performing separation, the matrix, which comprises of globular particles selected by their chemical and physical properties, must be packed into a column. Separation involves both a mobile and a stationary phase, whereby the former is at the liquid containing multiple components outside the porous matrix, and the latter is the liquid, namely the buffer, inside the pores. In a sample containing multiple components, differences in sizes or molecular weights are manipulated to isolate one or more components. Molecules larger than the matrix pores cannot disseminate into the pores and thus pass through the column earlier. On the other hand, smaller molecules can enter the pores and are eluted later.

In a standard SEC approach, the molecular weights of these molecules are relatively determined by comparing the elution volumes of the particles to a calibration curve providing pertinent data for a range of protein standards with varying molecular weights. On the other hand, SEC-MALS combines conventional SEC with laser light scattering (LS), refractive index (RI), and ultraviolet (UV) detection techniques. Consequently, molecular weight determination is independent of calibration curves and the incorporation of radioactive or fluorescent tags. Its further advantage stems from not destroying the analyzed samples (Folta-Stogniew and Williams 1999). A schematic diagram showing the analysis principles is presented in Fig. 14.2.

The SEC-MALS benefits from the linear relationship between the amounts of LS with the weighted-average molar mass of the molecules (MW) and solute concentration (c). This correlation is derived from Zimm's formalism of the Rayleigh-Debye-Gans scattering model for dilute polymer solutions (Folta-Stogniew and Williams 1999). The relationship between the excess scattered light and MW is given by the following expression:

$$\frac{K^*c}{R(\theta)} = \frac{1}{MW.P(\theta)} + 2A_2c \quad (14.1)$$

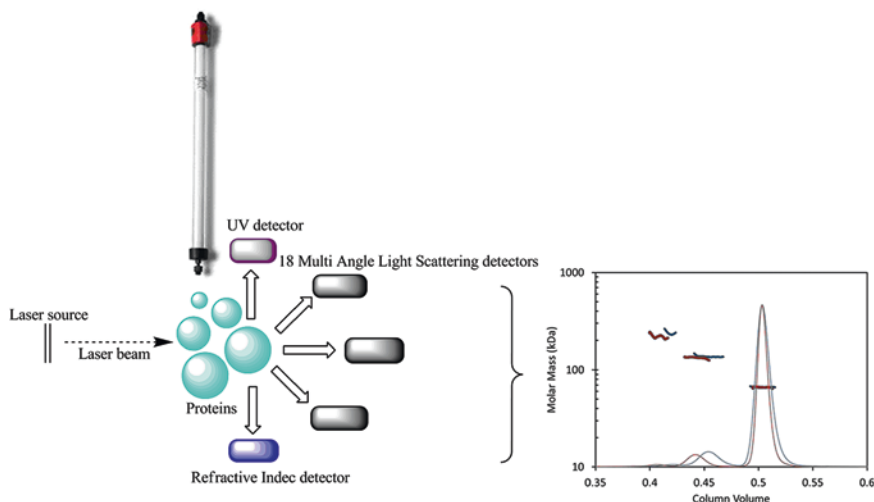


Fig. 14.2 The principle of SEC-MALS analysis. By using a SEC column, the proteins can be separated based on their shapes and sizes. The light scattered from the molecules is detected by 18 MALS detectors, as well as by UV and RI detectors. This strategy allows the protein MWs to be determined directly by calculating the amount of light scattered at each detected angle

where

- $R(\theta)$ excess intensity of scattered light at DAWN detector angle θ
- c sample concentration (g/mL)
- MW molecular weight
- A_2 second virial coefficient ($\text{ml}\cdot\text{mol}/\text{g}^2$)
- K^* optical parameter equal to $4\pi^2 n^2 (\text{dn}/\text{dc})^2 / (\lambda_0^4 N_A)$
- n solvent refractive index
- dn/dc refractive index increment
- N_A Avogadro's number
- λ_0 wavelength of the scattered light in vacuum (cm)

By solving Eq. 14.1, the MWs of protein molecules can be determined directly from the scattered light measurements, on the condition that the eluted protein concentrations are determined independently. ASTRA software (Wyatt Technology Corp., Santa Barbara, CA) allows application of four fitting methods, namely Zimm, Debye, Berry, and Random Coil (Folta-Stogniew and Williams 1999; Andersson et al. 2003), when solving Eq. 14.1. According to Folta-Stogniew and Williams 1999, all four methods yield similar results for small molecules (rms radius $r < 10$ nm) and proteins with MW < 500 kDa. It is noteworthy that, apart from the MWs of the molecules, the different conformations could also be distinguished by analyzing the elution volumes of the molecules that correspond to similar MWs, but with ~ 0.5 ml difference in the elution volume.

14.3.1 Materials and Equipment

1. Eppendorf tubes
2. Syringe (1 ml)
3. Ettan™ Liquid Chromatography (LC) (GE Healthcare)
4. DAWN HELIOS II™ multiangle light scattering (MALS) and an Optilab® T-rEX refractometer (Wyatt Technology Corp., Santa Barbara, CA)
5. Superdex 200 10/300 GL column (GE Healthcare)
6. Triethanolamine-HCl (TEA-HCl)
7. Sodium chloride (NaCl)

14.3.2 Methods

1. Connect the Ettan™ LC (GE Healthcare) to a DAWN HELIOS II™ multiangle light scattering (MALS) instrument (with 18 detectors) and an Optilab® T-rEX refractometer (Wyatt Technology Corp., Santa Barbara, CA), controlled by the ASTRA light scattering software version 5.3.4 (Wyatt Technology Corp., Santa Barbara, CA).
2. Attach a Superdex 200 10/300 GL to Ettan™ LC and equilibrate with 20 mM TEA-HCl pH 7.6 and 20 mM NaCl for two column volumes (CV) with a flow-rate maintained at 0.5 ml/min.
3. Load 100 μ l of 1 mg/ml purified a protein that has been separated by ion-exchange chromatography onto the column.
4. Monitor protein elution by absorbance at $\lambda = 280$ nm with a flow rate maintained at 0.5 ml/min for 50 min.
5. Following a Debye fitting method incorporated into the ASTRA light scattering software version 5.3.4, the intensity of the Rayleigh Scattering will indicate the MWs of the eluted proteins. Repeat this analysis in triplicate.

14.3.3 Results and Discussion

Different elution volumes were observed for each peak (Fig. 14.3). A single sharp peak eluting at ~ 13.9 ml was discerned for P1. A subsequent run for P2 resulted in a spectrum exhibiting a major peak eluting at ~ 13.4 ml, which indicated a larger species, corresponding to the open conformation of the enzyme. Nevertheless, both samples showed the existence of a monomeric species in the solution. However, the presence of dimeric species was confirmed in P2 through an elution at 11.6 ml. In contrast, P3 revealed the existence of multiple forms of LmiPGAM, as indicated by peaks at ~ 11.6 ml and 13.4 ml, along with a shoulder at 13.9 ml, in

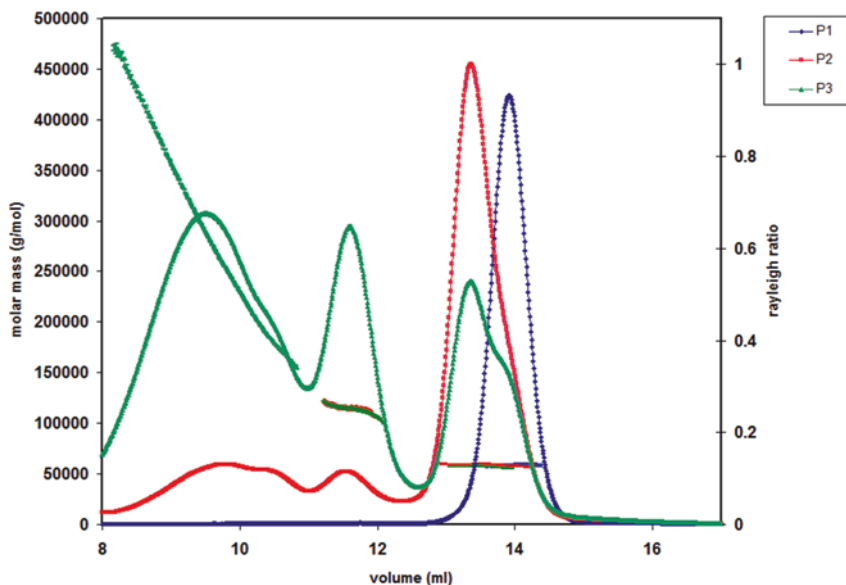


Fig. 14.3 SEC-MALS analysis of the P1, P2 and P3 protein samples, where the presence of monomeric species was inferred from the major peaks eluting in the 13–15 ml range (as indicated by the horizontal lines). P3 spectrum indicated the presence of dimeric species in the peak eluting at ~11.6 ml, while a tetramer was observed in the peak eluting at ~9.7 ml. The molecular masses are represented by the horizontal lines corresponding to the colors of each peak. The horizontal lines for the peaks located at 13–15 ml confirm that the masses are consistent throughout the elution peak. However the vertical components of the lines pertaining to the peaks at 11.6 ml and 9.7 ml imply changes in molecular mass across the elution peak. Thus, it can be posited that the peak eluting at ~9.7 ml likely contains a mixture of tetramer and aggregated materials

Table 14.1 The calculated MWs and predicted conformational states of protein samples P1, P2, and P3 from SEC-MALS analysis

| Samples | Molecular weights | Oligomeric states | Conformational states |
|---------|-------------------|-------------------|-----------------------|
| P1 | 58.2 | Monomer | Closed |
| P2 | 59.1 | Monomer | Open |
| P3 | 114.9 | Dimer | Closed/open |

addition to heterogeneous protein eluting at ~9.7 ml. The MWs of these protein peaks, as calculated by ASTRA™ software (Wyatt Technology), are presented in Table 14.1.

The first sample, P1, produced a single peak eluting at ~13.9 ml with a calculated molecular mass of 58.2 kDa, which corresponds to a monomeric *Lm*-iPGAM. Monodispersity was observed, and the peak homogeneity indicated the presence of a single species in the solution. The delayed elution volume (13.9 ml) indicated a

smaller hydrodynamic size, which may correspond to the closed conformation of the enzyme. The elution of P2 resulted in a major peak eluting at ~13.4 ml, corresponding to a monomer at 59.1 kDa. This finding suggested the presence of a dimeric form of the enzyme in the sample, as indicated by a small peak eluting at ~11.6 ml, corresponding to the molecular mass of 114.9 kDa. The heterogeneous protein eluting before 11 ml may correspond to a mixture of higher-order oligomers and aggregated proteins. The major peak was slightly asymmetric with a right-hand edge, indicating that the *Lm*-iPGAM in this peak might contain a small amount of the closed form in addition to the predominantly open form. On the other hand, P3 contained multiple forms of *Lm*-iPGAM, as indicated by two peaks, at ~11.6 ml and 13.4 ml, respectively, along with a shoulder at 13.9 ml, in addition to the heterogeneous protein eluting at ~9.7 ml. The *Lm*-iPGAM molecules eluting at 13.4 ml and 13.9 ml were monomeric (56.9 kDa), and were presumably in the open and closed form, respectively. The *Lm*-iPGAM eluting at 11.6 ml had a mass of 113.7 kDa, corresponding to a dimer, whereas the protein eluting at ~9.7 ml corresponded to a tetramer (265.5 kDa). However, the vertical line pertaining the molecular mass was broad, which may indicate that, apart from a higher-order oligomer, this sample may also contain aggregates. This observation strongly suggests that *Lm*-iPGAM, apart from being a monomer, may be present in a dimeric state in solution, as inferred from the properties of P2 and P3 (Fuad 2012; Blackburn et al. 2014).

14.4 Native Page Analysis

Polyacrylamide gel electrophoresis (PAGE) is an advantageous protein separation technique, as it is based on the uniform pore size of the gel. Native PAGE allows proteins to be separated in the absence of sodium dodecyl sulphate (SDS) into their different conformations and surface net charges. Nevertheless, it is often onerous to interpret the results unambiguously since protein mobility may reflect both its conformation and surface net charge. The pI of the proteins also contributes to the success of this analysis. Proteins with pI above the pH of the PAGE running buffer migrate back into the upper buffer chamber, indicating that this analysis is not appropriate for these proteins (Fuad 2012). Hence, it is vital to ensure that the conditions for such analysis are suitable for a particular protein. In this study, the pI of 5.62 pertaining to His-tagged *Lm*-iPGAM and the pH = 8.3 of the PAGE running buffer indicate that native PAGE could appropriately be employed to analyze the differences in the conformational or oligomeric states of the three *Lm*-iPGAM samples: P1, P2, and P3.

14.4.1 Materials and Equipment

1. Eppendorf tubes
2. Electrophoresis apparatus
3. Gel documentation system
4. 30% acrylamide
5. 10% ammonium persulphate (APS)
6. TEMED
7. Tris-base
8. Glycine
9. Glycerol
10. Dithiothreitol (DTT)
11. Coomassie R-250
12. Methanol
13. Distilled water
14. Glacial acetic acid

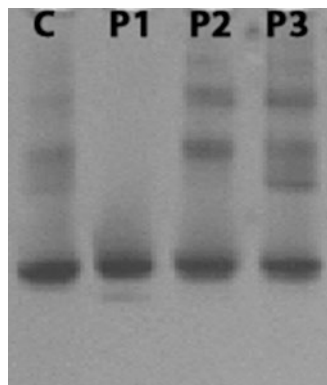
14.4.2 Method

1. Prepare 9% polyacrylamide gel (30% acrylamide, 10% APS, TEMED, resolving and stacking buffers containing Tris-base with pH adjusted to 6.8 and 8.8, respectively).
2. Prepare the running buffer containing 250 mM Tris and 2 M glycine pH 8.3
3. Mix 5 μ l of 5–10 μ g proteins with 5 μ l of 2X loading buffer containing Tris-base buffer pH 6.8 and 10% glycerol, and add 1 mM of freshly prepared DTT.
4. Load protein samples into the gel wells. The electrophoresis will be conducted in the cold room at 4 °C and will run at 100 V for 130 min.
5. Upon staining with Coomassie staining solution (Coomassie R-250, methanol, distilled water and glacial acetic acid), followed by destaining with distilled water, analyze the gel by using a gel documentation system.

14.4.3 Results and Discussion

P1 was observed as a single prominent band, in contrast to P2 and P3, which comprised of additional multiple upper bands (Fig. 14.4). A further additional band was noted in P3 relative to P2. In line with the SEC-MALS analysis findings, the upper bands in P2 and P3 are expected to correspond to different conformations as a result of distinct charge distribution on the surface of the protein molecules, and higher molecular masses due to different oligomeric states. The control (C) also showed

Fig. 14.4 Electrophoretic analysis of protein samples P1, P2 and P3. A 9% native PAGE gel is shown with 5–10 μg samples of each protein fraction. C is a control sample of pure *Lm*-iPGAM without an additional ion-exchange step



the presence of multiple bands, which formed a pattern similar to that observed in P3, indicating that the ion-exchange step was vital for separating the *Lm*-iPGAM into its different conformations and oligomeric states.

14.5 Continuous Coupling Enzyme Assay

The significance of the characterization of the three peaks depends on activity measurements. This evaluation aims to ensure that all peaks are active and do not exhibit a loss of activity due to, for example, an incorrectly folded protein. In this particular experiment, a continuous enzyme assay will be employed, in which the activity of *Lm*-iPGAM will be monitored by observing the decrease in the NADH absorbance at A_{340} nm. Since *Lm*-iPGAM activity cannot be measured in isolation, three coupling enzymes (enolase, pyruvate kinase and lactate dehydrogenase) will also be included in the reaction mixture, thus directing the reaction towards the forward direction in glycolysis. As empirical evidence indicates that Co^{2+} is essential for the activation of *Lm*-iPGAM, this experiment will be conducted in the presence of cobalt chloride.

14.5.1 Materials and Equipment

1. Jasco V-550 UV-VIS spectrophotometer
2. Cuvette
3. TEA-HCl
4. Cobalt chloride (CoCl_2)
5. 3-phosphoglycerate (3PGA)
6. Magnesium chloride (MgCl_2)

7. Potassium chloride (KCl)
8. Nicotinamide adenine dinucleotide (NADH)
9. Adenosine diphosphate (ADP)
10. Enolase from baker's yeast (ENO)
11. Pyruvate kinase from rabbit muscle (PYK)
12. Lactate dehydrogenase from rabbit muscle (LDH)

14.5.2 Method

1. Prepare 10X assay buffer containing 100 mM TEA-HCl buffer pH 7.6, 1.5 mM 3PGA, 5 mM MgCl₂, 50 mM KCl, 0.2 mM NADH, 1 mM ADP, 2 units of ENO from baker's yeast, and 4 units and 6 units of PYK and LDH, respectively, from rabbit muscle.
2. Incubate *Lm*-iPGAM with 0.1 mM CoCl₂ at 25 °C for 15 min, 1, 3, 6, 9, 18, 24 and 48 h.
3. Add 10 µl samples containing 0.2 mg/ml protein into a cuvette to produce 1 ml of a final reaction mixture containing the enzymatic assay chemicals indicated above.
4. Place the cuvette in the spectrophotometer. Monitor the oxidation of NADH by the decrease in absorbance at A₃₄₀ nm.
5. Determine the rate of reaction from the change of absorbance/minute. By using the rate of reaction, calculate the specific enzyme activity, expressed in U/mg (one unit corresponds to the conversion of 1 µmol of substrate min⁻¹ mg⁻¹ protein under standard conditions).

14.5.3 Results and Discussion

The results depicted in Fig. 14.5 reveal an interesting pattern, whereby the activities of each *Lm*-iPGAM increased hyperbolically and displayed significant differences in the trend of activity increment. Although the initial activities of the three samples were similar (20, 19.8 and 15.9 U/mg for P1, P2, and P3, respectively), P1 exhibited a significant increase throughout the incubation period, compared to P2 and P3. After 48 h, P1 activity reached a "plateau" or stationary phase, indicating that the maximum activity of the purified enzyme has almost been obtained.

Both P2 and P3, on the other hand, required longer incubation to reach their maximum activity levels. These observations indicate a distinctive regulation of activity for P1 relative to P2 and P3. The variation may stem from the flexibility of the protein in the vicinity of the active site, where the catalytic site of *Lm*-iPGAM is located in the cleft between two functional domains. This consequently resulted in the active and inactive states of the enzyme. The active state may be correlated to

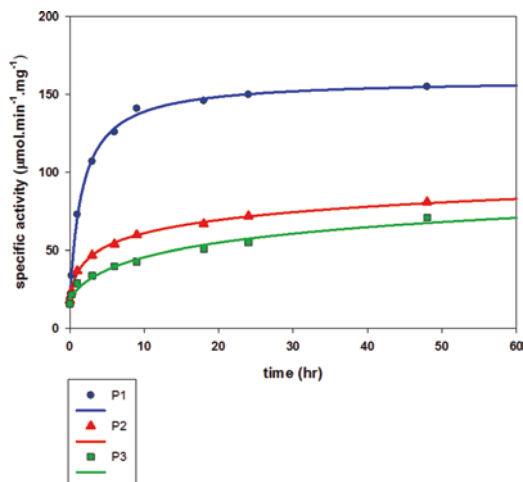


Fig. 14.5 The specific activities of P1, P2 and P3 after incubation with 0.1 mM Co. The specific activity was found to be similar prior to incubation, but was significantly enhanced during the incubation period, especially for P1. The maximum value for P1 is calculated at 159.8 U/mg, whereas P2 and P3 maximum values were off-scale, suggesting that the activity was too slow and could not be measured in the period designated for the experiment

the closed conformation of the enzyme, which may exist in the presence of the substrate 3PGA, as well as divalent metals occupying the metal sites. The open-form conformation, on the other hand, may be indicative of the inactive state of the enzyme in the absence of ligand, which can be either the substrate or the metal. While most enzyme-catalyzed reactions occur at a rapid rate, this result revealed that this is not the case for the *Lm*-iPGAM in P2 and P3. This finding may indicate that major molecular and conformational changes in the structure take place during catalysis (Fuad 2012).

14.6 Conclusion

The different oligomeric and conformational states of *Lm*-iPGAM have been successfully characterized by using SEC-MALS, native PAGE, and continuous enzyme assay. These analyses, SEC-MALS in particular, provide a solution to the difficulties in distinguishing different states of proteins in solution. The presence of multiple forms and oligomeric states of *Lm*-iPGAM, with distinct Co²⁺-regulated activities, are perceptible through these experiments, thus improving the understanding of the behavior of this protein in solution.

References

- Andersson M, Wittgren B, Wahlund KG (2003) Accuracy in multiangle light scattering measurements for molar mass and radius estimations. Model calculations and experiments. *Anal Chem* 75(16):4279–4291
- Blackburn EA, Fuad FAA, Morgan HP, Nowicki MW, Wear MA, Michels PAM, Fothergill-Gilmore LA, Walkinshaw MD (2014) Trypanosomatid phosphoglycerate mutases have multiple conformational and oligomeric states. *Biochem Biophys Res Commun* 450(2):936–941
- Folta-Stogniew E, Williams KR (1999) Determination of molecular masses of proteins in solution: implementation of an HPLC size exclusion chromatography and laser light scattering service in a core laboratory. *J Biomol Tech* 10(2):51–63
- Fuad FAA (2012) Effects of metal ions on the structural and biochemical properties of trypanosomatid phosphoglycerate mutases. PhD thesis. Institute of Structural and Molecular Biology, School of Biological Sciences. University of Edinburgh, UK
- Nowicki MW, Kuaprasert B, McNaie IW, Morgan HP, Harding MM, Michels PAM, Fothergill-Gilmore LA, Walkinshaw MD (2009) Crystal structures of *Leishmania mexicana* phosphoglycerate mutase suggest a one-metal mechanism and a new enzyme subclass. *J Mol Biol* 394:535–543

Chapter 15

Skim Latex Serum as an Alternative Nutrition for Microbial Growth



Vivi Mardina and Faridah Yusof

Abstract Malaysia is one of the biggest producers of natural rubber. The fresh latex, tapped from the rubber tree (*Hevea brasiliensis*), known as field latex, is a cloudy white and viscous liquid containing rubber fraction and non-rubber components. As a basic raw material in rubber processing, fresh field latex undergoes a series of procedures during its conversion to either dry rubber, or high concentrated latex. To prepare high concentrated latex, ammonia is usually added to the field latex upon reaching the factories to prevent coagulation. Ammoniated latex will then undergo centrifugation which yield high concentrated latex and a by-product named 'skim latex'. Skim latex is considered as low value by-product and usually discarded as waste effluent. However, it must be first treated in the oxidation treatment pond, before the clearer water can be released into the main waterways. In Malaysia, the discharged water must meet the strict requirements of MS ISO/IEC 17025:2005. Eventually, the rubber manufacturers have to spend a lot of money for waste management and effluent treatment of skim latex. Therefore, utilization of this wasteful skim latex is one of the economic saving measures and may minimize the environmental problems. This chapter aims at deliberating the use of the serum of skim latex as an alternative nutrition for culturing microorganism. As a model microorganism, this study has selected to use *Bacillus licheniformis* (ATCC 12759). Skim latex serum was used as the basal media, supplemented by some selected medium composition (lactose, galactose, casein, KH_2PO_4 , MgSO_4 and LB broth) for the production of extracellular protease. At the end of the study, it was demonstrated that skim latex serum is able to fulfill a criteria as an efficient culture media due to its abundance, low cost, stable in quality and having a stimulatory effect on bacterial growth. Therefore, valorization of this wasteful skim latex into protease enzyme is hoped to be an introduction for further inventions relating to processes suitable for microbial culturing.

V. Mardina · F. Yusof (✉)
International Islamic University Malaysia, Kuala Lumpur, Malaysia
e-mail: yfaridah@iium.edu.my

Keywords *Hevea brasiliensis* · Skim latex · Serum · Concentrated latex · *Bacillus licheniformis* · Protease · Casein · Tyrosine · Bradford method · Microbial growth · Nutrition · Natural rubber · Effluent

15.1 Introduction

Malaysia is one of the biggest producers of natural rubber. The fresh latex, tapped from the rubber tree (*Hevea brasiliensis*), known as field latex, is a cloudy, white and viscous liquid containing 30–45% weight rubber fraction, consisting of *cis*-(1–4)-polyisoprene molecules and about 60–70% weight of non-rubber comprising mainly of proteins, lipids, quebrachitol, carbohydrates and inorganic ions (Rattanaphan et al. 2012). Table 15.1 represents the composition of field natural rubber latex (Jayanthi and Sankaranarayanan 2005; Ochigbo et al. 2011; Ochigbo and Luyt 2011).

As a basic raw material in rubber processing, fresh field latex undergoes much procedures during its conversion to either dry rubber or high concentrated latex, whereby, the processing usually involves three methods: centrifugation, creaming, and evaporation (Veerasamy et al. 2008; Veerasamy and Ismail 2012). Some of the processes have been carried out by a chemical treatment that poses a lot of negative impact on the environment (Hien and Thao 2012).

To prepare high concentrated latex, ammonia is added to the latex upon reaching the factories to prevent coagulation. Ammoniated latex then undergoes centrifugation which yields high concentrated latex, containing around 60% dry rubber contents (DRC). This technique produces ‘skim latex’ as a by-product with 3–7% DRC. Figure 15.1 illustrates the process involves in producing high concentrated latex from fresh latex that results in skim latex as a by-product. Factories and manufacturers throw away skim latex as waste effluent, but firstly it has to be treated in the oxidation treatment pond before the clearer water can be released into the main waterways (Rattanaphan et al. 2012). In Malaysia, the discharged water must meet the strict requirements of MS ISO/IEC 17025:2005. In the end, the rubber manufacturers have to spend a lot of money for waste management and effluent treatment of skim latex

Table 15.1 Composition of field NR latex. (Jayanthi and Sankaranarayanan 2005)

| Component | Composition (%) |
|------------------|-----------------|
| Rubber particles | 30–40 |
| Serum or water | 55–65 |
| Carbohydrate | 1–2 |
| Protein | 2–3 |
| Resins | 1.5–3.5 |
| Glycosides | 0.1–0.5 |
| Ash | 0.5–1.0 |

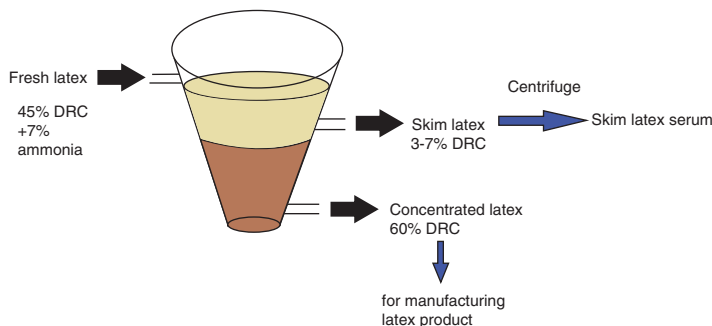


Fig. 15.1 Illustration of high concentrated latex production with by-production of skim latex

(Mohamed and Yusof 2014). Therefore, utilization of this wasteful skim latex is one of the economic saving measures and may minimize the environmental problems.

At this point, it is important to differentiate between ‘latex serum’ and ‘skim latex serum.’ ‘Latex serum’ is the supernatant obtained after ‘fresh latex’ centrifugation; while ‘skim latex serum’ is the supernatant obtained after ‘skim latex’ centrifugation. The main difference between them, is that skim latex is ammoniated with pH around 11 with about 3–7% DRC, whereas, the pH of fresh latex is about 7 with about 45% DRC. Nevertheless, except ammonia in skim latex, it is presumed that the contents of both are similar. Both ‘fresh latex’ and ‘skim latex’ have been the subjects of many types of researches, as indicated.

15.2 Utilization of Skim Latex

As illustrated in Table 15.2, skim latex contains various organic compounds that enable its valorization into value-added products. There are two alternative ways to make use of skim latex:

- I. Some fine biochemicals can be extracted from skim latex, such as quebrachitol (McGavack and Binmore 1930; Veerasamy et al. 2008), carotenoid (Tri-Panji and Suharyanto 2001), hevein (Soedjanaatmadja et al. 1995), hevamine, (Tata et al. 1983), Cathepsin G (Yusof, et al. 2006), superoxide dismutase (Yusof and Abdullah 1997) and lipase (Yusof et al. 1998; Mohamed and Yusof 2014).
- II. Alternatively, skim latex can be used to support the production of many useful products such as single cell protein (Mahat and MacRae 1991), protease (Mardina et al. 2015), bioplastic (Tang et al. 1999), as fertilizer (Eifediyi et al. 2012; Orhue and Osaigbovo 2013) and a medium to culture fish (John 1978).

Table 15.2 Average chemical composition of skim latex serum. (Ismail and Mohd Noor 2011)

| Components | Content (%) |
|---------------------|---------------|
| Proteins | 1–1.1 |
| Sugars | 0.40 |
| Free amino acids | 0.13–0.018 |
| Other organic acids | 0.04 |
| Formic acid | 0.012 |
| Nitrogenous bases | 0.06–0.08 |
| Inorganic anions | Trace amounts |
| Metallic ions | Trace amounts |
| Uncoagulated rubber | 1 |

15.2.1 Extraction of Useful Biochemical from Skim Latex

One of the fine biochemicals which has been successfully extracted from the latex serum is quebrachitol, an optically active cyclitol or cyclic polyol. It was found as the largest component in latex serum (McGavack and Binmore 1930) and had been used as feedstock for the production of many bioactive materials (Kiddle 1995). Veerasamy et al. (2008) from the Rubber Research Institute of Malaysia (RRIM) had efficaciously extracted quebrachitol from latex serum by an economical means. Another product which has been isolated from latex is hevamine (Tata et al. 1983), a member of one of the several families of plant chitinases and lysozyme that are important for plant defense against bacteria and fungi. A useful protease which behaves like Cathepsin G, named Hevea Cathepsin G, is one of the enzymes that can be recovered from the skim latex serum (Yusof, et al. 2006) whereby, in human, Cathepsin G is a lysosomal enzyme contained in cytotoxic cells which are known as a member of the serine protease family, mostly present in azurophilic granules of neutrophils, and comprises up to 18% of the azurophil granule proteins (Shafer et al. 2002). Another enzyme which has been detected and studied in natural rubber latex is superoxide dismutase (SOD) (Yusof and Abdullah 1997). SOD catalyzes the dismutation of superoxide ions into hydrogen peroxide and oxygen during the oxidative energy process (Chi et al. 2001), where, in the presence of catalase, the hydrogen peroxide is converted to harmless water molecules. Yusof et al. (1998) have extracted and purified ‘a patatin-like protein’ from the latex serum of *Hevea brasiliensis*, which played an inhibitory role in *in-vitro* rubber biosynthesis. This protein has a lipid acyl hydrolase activity, a subtype of lipase which supposedly plays a role in the defense mechanism against plant parasites. Subsequently, Mohamed and Yusof (2014) had optimized the extraction and purification conditions of this same enzyme from the skim latex serum. Furthermore, Soedjanaatmadja et al. (1995) isolated protein, hevein, an N-acetyl-D-glucosamine (GlcNAc) specific lectin from the effluent of rubber factory that presumably has antifungal properties.

15.2.2 Use of Latex Serum to Support the Production of Other Useful Products

It has been proven in many researches that skim latex serum was able to support the production of many useful products. This is because, upon the coagulation of skim latex, the content of the serum, which consists of N, Mg, P, K, Mg, Fe, Mn, Zn, are essential elements for plant growth (Eifediyi et al. 2012). This effluent has been shown to support the growth of fodder, for instance, Napier grass (*Pennisetum purpureum*), which has responded favorably to this effluent application by notably increased production (Tan et al. 1979). The serum also has a high water content that can be usefully applied in moisture deficit areas during the dry season. In the study, a mixed effluent of block rubber, crumb lump and skim latex serum in the ratio of 8:4:3 was applied at 1 cm rain equivalent per month (r.e.m), or skim latex serum alone at 0.25 cm r.e.m. results in an increased yield of up to 200% over control especially during dry weather. John (1978) had also indicated that the effluent from rubber factories could be used to irrigate oil palm field; the effluent is beneficial both as a source of nutrient and water supply, resulting in increased yield. Eifediyi et al. (2012) have evaluated the effect of rubber effluent on the growth and yield of cucumber (*Cucumis satives* L), whereby, their findings showed that rubber effluent at 150,000 L/ha results in the growth of cucumber with the highest vegetative traits. Similarly, Orhue and Osaigbovo (2013) investigated the effect of the rubber factory effluent on the chemical properties of soil and early growth of maize (*Zea mays* L) and concluded that the effluent that contains vital plant nutrients could be used as fertilizer for the growth of maize.

Besides using skim latex effluent to enrich the soil for plant growth, John (1978) has also shown that the stabilization pond that was used to treat the effluent from the block rubber factory was suitable for the propagation of a variety of freshwater fishes. Fishes derive their food mainly by feeding on green algae which thrive well under the Malaysian climatic conditions. *Tricpodus leeri* grew to about 35 g in 6 months, while *Clarias sp.* rise from about 10–85 g in 4 months. A fairly rapid growth was also observed with *Talapia sp* and *Ophiocephalus sp.* These investigations indicated that it is possible to convert the polluting protein and other waste in the rubber factory effluent into algae protein, and in turn to edible fish protein.

Because of the presence of various compounds (Table 15.2) and metal elements (Table 15.3) as reported by John (1978), many researchers have reported the successful use of skim latex serum or latex serum as a substitute to various nutritive compounds for the cultivation of microorganisms. Mardina et al. (2015) had successfully cultivated a protease secreting *Bacillus licheniformis* in a media supplemented with skim latex serum, where, skim latex serum has replaced the function of lactose, casein, KH_2PO_4 and MgSO_4 . Tri-Panji and Suharyanto (2001) reported that latex serum supplemented with salt minerals could enhance the growth of *Spirulina platensis* to produce single cell protein (SCP) and γ -linolenic acid (GLA). Kresnawaty et al. (2008) studied the optimization of indole acetic acid (IAA) production by *Rhizobium sp* which was cultured in concentrated latex with tryptophan

Table 15.3 The elements of effluent from concentrated and Ribbed Smoked Sheet (RSS) latex (John 1978)

| Elements | Type of effluent | |
|------------|-------------------------------|----------------|
| | From concentrated latex (ppm) | From RSS (ppm) |
| Copper | 0.7 | 0.1 |
| Calcium | 0.7 | 0.1 |
| Iron | 26 | 0.4 |
| Potassium | 110 | 63 |
| Magnesium | 268 | 4.5 |
| Sodium | 35 | 6.3 |
| Phosphorus | 268 | 8.2 |
| Rubidium | 0.7 | 0.3 |
| Silicon | 27 | 0.3 |

*Ba, Co, Cr, Mo, Ni, Pb, Al are found only in trace

supplementation. Furthermore, Siswanto (1999) had used skim latex serum as a substitute to casein, for culturing *Bacillus subtilis*, *Bacillus megaterium* and *Bacillus licheniformis*, to produce protease. In this case, LB media concentrated tenfold without casein was added to the skim latex serum at the ratio of 1:10 (v/v). Nuradibah (2012) has reported the utilization of skim latex serum as a sole media to culture *Rhizopus oligosporus* for bioprotein production that may be used as animal fodder. Likewise, Iyagba et al. (2008) had reported that rubber effluent could be used as a growth media for aerobic heterotrophic bacteria including *Bacillus sp*, *Staphylococcus*, *Aerobacter*, *Streptococcus*, *Aeromonas*, *Micrococcus*, *Pseudomonas*, and *Corynebacterium*. And lastly, Tang et al. (1999) reported that the rubber latex effluent which has been treated anaerobically produced two useful organic acids, acetic and propionic, which were then utilized for the production of polyhydroxyalkanoates (PHA).

15.3 Scope of This Chapter

This chapter aims at deliberating the use of skim latex serum as an alternative nutrition for culturing microorganism. In this study, *Bacillus licheniformis* (ATCC 12759) was used as a model microorganism. Skim latex serum was used as the basal media, supplemented by some selected medium composition (lactose, galactose, casein, KH_2PO_4 , MgSO_4 and LB broth) for the production of the extracellular protease at a bench scale level experiments, in 100 ml incubating media and cultivated in 250 ml Erlenmeyer flasks. The concentration of medium composition and skim latex serum in each sample are illustrated in Table 15.4.

Table 15.4 Comparison study of protease production in different concentration of skim latex serum in the fermentation culture

| Component | Sample 1 | Sample 2 | Sample 3 | Sample 4 |
|---|----------|----------|----------|----------------|
| Skim latex serum % (v/v) | 50 | 10 | 70 | – ^a |
| Lactose % (v/v) | 1.0 | – | – | – |
| Galactose % (v/v) | 1.0 | 1.0 | 1.0 | 1.0 |
| Casein % (v/v) | 0.0 | 0.5 | – | – |
| K ₂ HPO ₄ % (g/l) | 0.5 | 0.0 | – | – |
| MgSO ₄ . 7H ₂ O % (g/l) | 0.5 | 0.5 | – | – |
| LB broth % (v/v) | 0.0 | 0.0 | 1.0 | 1.0 |
| Inoculums size % (v/v) | 1.0 | 1.0 | 4.0 | 4.0 |
| pH | 7 | 11 | 5.5 | 5.5 |
| Agitation (rpm) | 50 | 250 | 75 | 75 |
| Temperature (°C) | 35 | 35 | 35 | 35 |
| Incubation period (h) | 24 | 24 | 24 | 24 |

^awhere skim latex serum was replaced by distilled water

15.3.1 Materials and Methods

15.3.1.1 Materials

(a) Raw material

Skim latex was collected from the Mardec Industrial latex Sdn Bhd. in Tapah, Perak, Malaysia. It was kept in the clean plastic containers and stored at 4°C for further study.

(b) Microorganism and maintenance of culture

Bacillus licheniformis (ATCC 12759) was cultured in the sterilized skim latex serum. The culture is routinely maintained on nutrient agar medium at 37°C for 24 h and stored at 4°C (Ahmed and Abdel Fattah 2010; Akcan 2012).

(c) Experimental Apparatus, consumable items and chemicals

Equipment, consumable items, and chemicals used in this study are itemized in Tables 15.5, 15.6, and 15.7 accordingly.

15.3.1.2 Methods

An overview of the experimental studies and procedures are described in Fig. 15.2.

Table 15.5 List of equipment

| Equipment | Model | Use |
|--------------------------------|--|--|
| UV-spectrophotometer | Anthelie junior (SECOMAM) | Measuring absorbance of protein, bacteria and enzyme activity |
| Incubator shaker | MaxQ: 4000 (Barnsted) | Shaking the Erlenmeyer flasks containing bacteria and skim latex serum fortified media |
| Weighing balance | Mettler college balance, B204-S | Weighing chemicals |
| Vortex mixer | EVM-60 (ERLA) | Mixing solution |
| pH meter | MP 220 (Mettler Todelo) | Adjusting chemical pH |
| Hot plate and magnetic stirrer | EMS-HP-7000 (ERLA) | Stirring chemicals to achieve uniform mixtures |
| Incubator | Incucell | Incubating enzyme |
| Autoclave | Hirayama | Sterilizing media |
| Dryer | FFD 720 (Protech) | Sterilization of all materials used |
| Laminar air-flow cabinet | ERLA CFM 4 | Culturing <i>B. licheniformis</i> (ATCC 12759), preparing inoculums and culture media. |
| Centrifuge | 5804 R (Eppendorf) and Sorvall suspended fixed angle rotor | Centrifuging filtrate sample to separate substrate and pellet for the enzyme and protein assay |
| | Avanti® J-E centrifuge | |
| Water bath | WB 22 (Memmert) | Analytical incubation |
| -20°C fridge | MDF-U531 (Sanyo) | Storing protein and enzyme for further use |
| -80°C fridge | | Storing the stock culture in 80% glycerol |
| Chiller | Lin den | Storing chemical and enzyme sample for as short period |

15.3.1.2.1 Preparation of Skim Latex Serum

Serum from skim latex was prepared using a method suggested by Ismail and Mohd Noor (2011). The skim latex was first coagulated by adding 10% acetic acid until the pH of the latex effluent is decreased to 5. It was followed by centrifugation at a speed of 10,000 x g for 30 min in Avanti® J-E centrifuge, whereby the coagulated rubber was separated from the serum. The serum was subsequently filtered using a 0.2 µm polystyrene membrane for sterilization. Figure 15.3 shows the pictorial steps in preparing the sterilized skim latex serum.

Table 15.6 List of consumable items

| |
|--|
| Conical flasks (100 – 500 ml) |
| Beakers (100 – 1000 ml) |
| Eppendorf pipettes (20 µl, 100 µl and 1000 µl) |
| Aluminium foil |
| Whatman No.1 Filter Paper |
| Funnel |
| Measuring cylinder (25 – 500 ml) |
| Tips (20 µl – 1000 µl) |
| Schott bottles (100 – 2000 ml) |
| Glass rod |
| Weight boat |
| Spatula |
| Test tube |
| Cotton gauze |
| Parafilm |
| Disposable cuvettes |
| Tissue culture plate |
| 0.2 µm polystyrene membrane filter unit |
| Wire inoculating loopful |
| Snake Skin™ pleated dialysis tubing |

Table 15.7 List of chemicals

| |
|--|
| Propagation of <i>Bacillus licheniformis</i> (ATCC 12759)/inoculum preparation |
| Glycerol |
| Nutrient agar |
| Nutrient broth |
| To pretreat skim latex and protease production medium: |
| Acetic acid glacial |
| Lactose |
| Galactose |
| Casein |
| Dipotassium hydrogen phosphate (K_2HPO_4) |
| Magnesium sulphate heptahydrate ($MgSO_4 \cdot 7H_2O$) |
| LB broth |
| HCl |
| Potassium hydroxide (NaOH) |
| Protease assay: |
| Tris buffer |
| Casein |
| L-tyrosine |
| Trichloroacetic acid (TCA) |
| Folin phenol reagent |
| Sodium carbonate (Na_2CO_3) |
| Protein determination: |
| Bovine serum albumin (BSA) |
| Protein dye reagent |
| Sodium acetate (Na_2CO_3) |

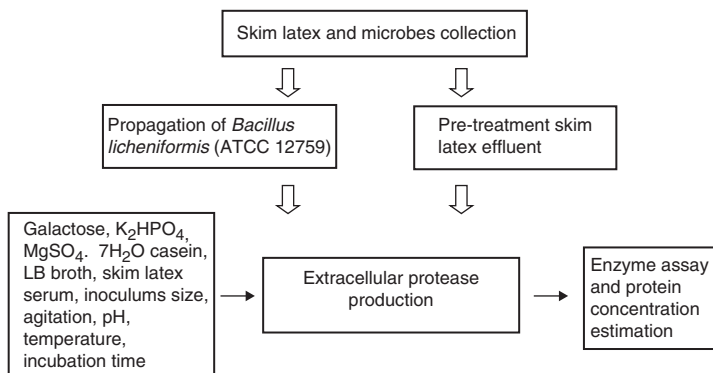


Fig. 15.2 An overview of experimental strategy

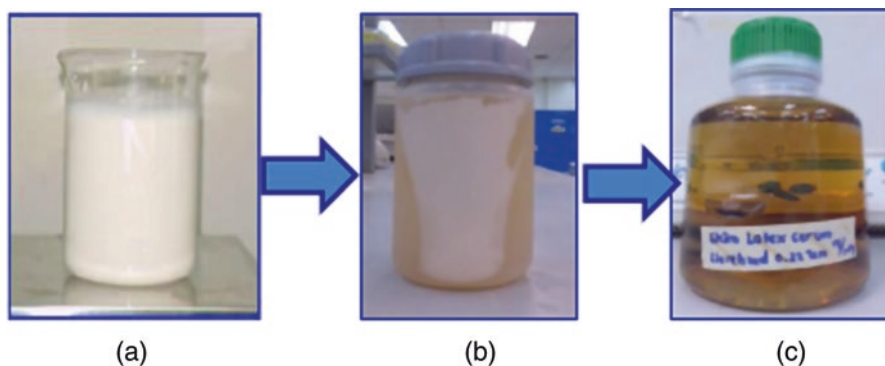


Fig. 15.3 Pretreatment of skim latex effluent into the sterilized latex serum, (a) skim latex effluent, (b) Skim latex after centrifugation, (c) sterilized skim latex serum

15.3.1.2.2 Inoculum Preparation

The microbial strain obtained from ATCC is in a lyophilized form. For propagation, 1 ml of nutrient broth was added to the freeze-dried pellet, and the entire content was mixed to form a suspension, which was transferred into a test tube containing 5 ml nutrient broth. Then, several drops of suspension were inoculated into the nutrient agar plate by spreading method, and it is allowed to cultivate at 30°C for 24 h, as recommended by the supplier. Preserving bacteria culture for long-term storage was prepared in 80% sterile glycerol as attached in Table 15.8.

Inoculum preparation was performed by inoculating a 24 hour-old loopful of the bacteria into 100 ml sterilized nutrient broth inoculum medium. The inoculated broth was incubated overnight at 30°C in an orbital shaker at 140 rpm for the propagation of bacteria growth up to 10^{8-10} cell/ml (Nadeem et al. 2008; Ahmed and Abdel Fattah 2010). Microbial cell count was determined according to the method described by Yousef and Carlstrom (2003).

Table 15.8 Preserving bacteria culture

| |
|---|
| In order to ensure the viability of bacteria (ATCC 12759), preservation of bacteria for long-term storage is required. The method of preservation is given below: |
| Pick a single colony from bacterial plate and transfer to 30 ml of LB media |
| Culture the bacteria for 14–16 h or overnight (ON) at 37°C and 250 rpm |
| Label 2.0 ml tube and put it on ice (throughout the procedure, maintain the tube on ice) |
| Add 1.8 ml ON culture to the labeled 2.0 ml tube |
| Spin at 13,000 rpm for 1 min and discard the supernatant |
| Add 200 µl fresh LB to the pellet and vortex to resuspend the pellet |
| Add 500 µl 80% sterile glycerol to the resuspended pellet and invert the tube to mix |
| Transfer the tube to –70 °C for long term storage |

15.3.1.2.3 Bacteria Culture Using Skim Latex Serum

The potential of skim latex serum as an alternative nutrition toward the growth of *Bacillus licheniformis* (ATCC 12759) was studied by comparing the culture media with different concentration of the selected medium composition that was predicted to play an important role in accelerating microbial growth. The established design has already been presented in Table 15.4. The skim latex serum fortified media was supplemented by lactose, galactose, casein, K_2HPO_4 , $MgSO_4$ and LB broth. After 24 h of the incubation period, the production medium was centrifuged at a speed of 10,000xg for 10 min at 4°C in the 5804 R Eppendorf centrifuge. The supernatant was collected followed by the determination of protease enzyme activity and protein content.

15.3.1.2.4 Protease Activity Assay

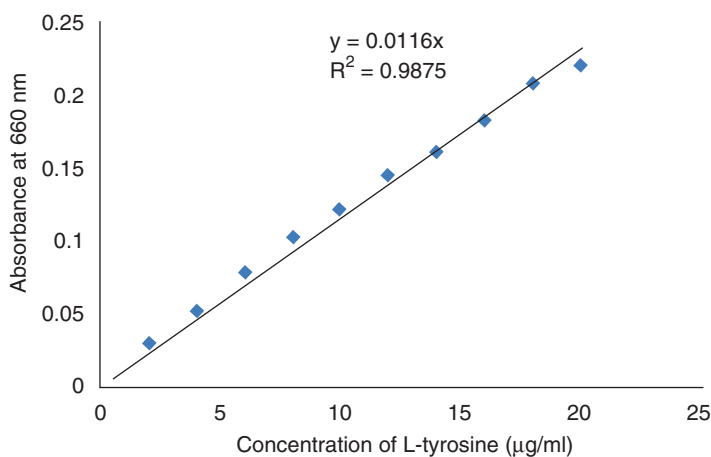
Protease assay was determined by the casein digestion method as suggested by Padmapriya et al. (2012). A 2.5 ml of 1% (w/v) casein (prepared in 50 mM of tris buffer, pH 8) was equilibrated to 37°C for 5 min prior adding 0.5 ml of crude enzyme. The solution was mixed by swirling and incubated for 10 min in 37°C water bath. The enzyme reaction was stopped by adding 2.5 ml of 0.11 M trichloroacetic acid, then allowed to stand at room temperature for 45 min. The supernatant was collected by centrifugation at 10,000xg for 10 min at 4°C. Subsequently, color development was achieved by mixing 1 ml supernatant with 2.5 ml of 0.5 M Na_2CO_3 and 0.5 ml of 0.1 N Folin Ciocalteu's phenol reagent for 30 min. Ultimately, the OD of the mixed solution was measured at 660 nm against the blank sample without incubation.

The L-Tyrosine standard curve was prepared by varying the tyrosine concentration in a mixture of dH_2O , sodium carbonate and Folin & Ciocalteu's Phenol reagent (Table 15.9). The absorbance reading was taken at 660 nm. The relationship between

Table 15.9 Mixture compositions of L-tyrosine standard curve

| Reagent | Tyrosine (μl) | dH ₂ O (μl) | Na ₂ CO ₃ (ml) | Folin Reagent (ml) | Total Volume (ml) |
|---------|----------------------------|-------------------------------------|--------------------------------------|--------------------|-------------------|
| Blank | – | 1000 | 2.5 | 0.5 | 4 |
| Std 1 | 10 | 990 | 2.5 | 0.5 | 4 |
| Std 2 | 20 | 980 | 2.5 | 0.5 | 4 |
| Std 3 | 30 | 970 | 2.5 | 0.5 | 4 |
| Std 4 | 40 | 960 | 2.5 | 0.5 | 4 |
| Std 5 | 50 | 950 | 2.5 | 0.5 | 4 |
| Std 6 | 60 | 940 | 2.5 | 0.5 | 4 |
| Std 7 | 70 | 930 | 2.5 | 0.5 | 4 |
| Std 8 | 80 | 920 | 2.5 | 0.5 | 4 |
| Std 9 | 90 | 910 | 2.5 | 0.5 | 4 |
| Std 10 | 100 | 900 | 2.5 | 0.5 | 4 |

Std - Standard

**Fig. 15.4** Standard calibration curve for L-tyrosine for protease activity assay

the absorbency and the amount of L-tyrosine will be plotted as y/x line plot as shown in Fig. 15.4.

Protease activity and protease specific activity are calculated as follows:

$$\text{Protease activity} \left(\frac{\text{Units}}{\text{ml}} \right) = \frac{\text{Tyrosine released} (\mu\text{mole}) * \text{Total volume of assay} (\text{mL})}{\text{volume of used enzyme} (\text{mL}) * \text{Time of assay} * \text{volume} (\text{mL})} \quad (15.1)$$

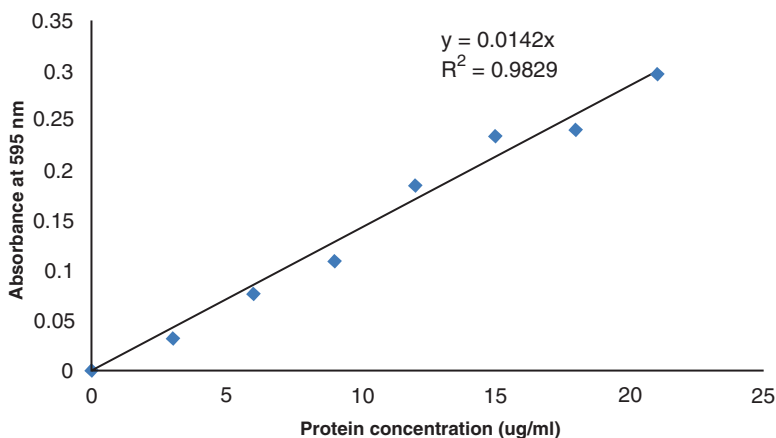
$$\text{Protease specific activity} \left(\frac{\text{Units}}{\text{mgprotein}} \right) = \frac{\text{units} / \text{mLenzyme}}{\text{mgprotein} / \text{mLenzyme}} \quad (15.2)$$

15.3.1.2.5 Protein Concentration

The protein concentration of enzyme sample is needed to aid in the calculation of protease specific enzyme activity. The protein content of the extract was determined according to the procedure described by Bradford method using bovine serum albumin (BSA) as standard (Bradford 1976). A protein standard curve was established by preparing mixtures of 0.1 mg/ml stock BSA, 0.1 M sodium acetate pH 4.5, and Bio-Rad protein Dye reagent. The absorbency was taken for 30, 60, 90, and 120, 150, 180, and 210 μ l from BSA stock solution completed to the 1 ml total volume of mixture solution by adding 200 μ l Bio-Rad protein Dye reagent and a buffer solution (Table 15.10). The relationship between absorbency at 595 nm and protein concentration was plotted as y/x line plot as shown in Fig. 15.5. Subsequently, the average of triplicate absorbance reading at 595 nm wavelength was plotted to determine the protein concentration from crude protease enzyme.

Table 15.10 Preparation of BSA standard curve

| Tube | 0.1 mg/ml stock BSA solution(μ l) | 0.1 M sodium acetate, pH 4.5 (μ l) | Bio-Rad Protein Dye Reagent (μ l) |
|------|--|---|--|
| 1 | 0 | 800 | 200 |
| 2 | 30 | 770 | 200 |
| 3 | 60 | 740 | 200 |
| 4 | 90 | 710 | 200 |
| 5 | 120 | 680 | 200 |
| 6 | 150 | 650 | 200 |
| 7 | 180 | 620 | 200 |
| 8 | 210 | 590 | 200 |

**Fig. 15.5** Standard calibration curve for BSA for protein concentration determination

15.4 Results and Discussion

Skim latex serum has been proven to be a potential substrate as a growth medium for microbial fermentation processes (Mardina et al. 2015; Ishizaki 1991; Tri-Panji and Suharyanto (2001); Kresnawaty et al. (2008); Siswanto (1999); Nuradibah (2012). The serum is rich in various organic compounds that are stated in Table 15.2 and Table 15.3. In the microbiological industry, bacteria have been allowed to grow with the supply of various nutrition elements typified by amino acids, vitamins, minerals and combination. Thus, on the basis of nutrients requirement for the microbial growth, carbon, hydrogen, oxygen, nitrogen, sulfur, potassium, phosphorus and magnesium were found as major elements that are needed in concentration of more than 10^{-4} M (Bhunja et al. 2012; Stanbury et al. 2003). Physical parameters involving temperature, initial pH, inoculums size, dissolved oxygen, agitation and incubation time also affect the culture system.

Therefore, this study has selected six medium compositions (lactose, galactose, casein, KH_2PO_4 , MgSO_4 and LB broth) and five culture conditions (inoculums size, agitation rate, pH, incubation temperature and incubation period) for growing the *Bacillus licheniformis* (ATCC 12759) on skim latex serum as the basal medium. Lactose and galactose serve as the carbon source, while casein and LB broth were considered as sources of nitrogen. KH_2PO_4 and MgSO_4 were the sources of minerals. The chosen factors have been predicted to play an important role in accelerating the bacteria growth and enhancing the production of the protease enzyme. The influences of medium compositions and culture conditions were examined in the established design (Table 15.4), carried out in triplicates. Galactose (1% v/v), incubation temperature (35°C) and incubation period (24 h) were kept constant for all samples.

Results for the experiments are given in Fig. 15.6. Protease activity varied from 0.4 U/ml to 19.33 U/ml. In order to show the significant effect of skim latex serum

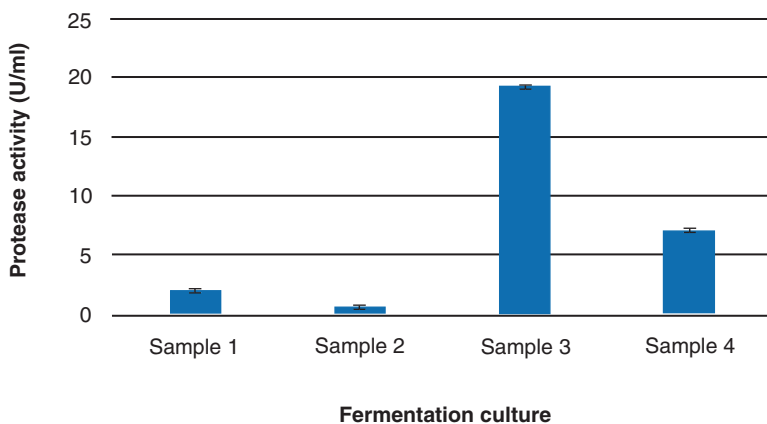


Fig. 15.6 Protease activity (U/ml) for fermentation culture, Samples 1–4 with different concentration of skim latex serum

as an alternative nutrition for microbial growth, the discussion would first highlight Samples 1 and 2, followed by the discussion relating to results from Samples 3 and 4. Sample 1 which has higher level in some variables, namely, skim latex serum (50% v/v), lactose, (1% v/v), KH_2PO_4 (0.5% w/v), pH 7 and agitation rate of 50 rpm, shows higher protease enzyme activity than Sample 2, which lacked lactose and KH_2PO_4 . No LB broth was added for both Samples 1 and 2, however, 0.5% (v/v) casein was added to Sample 2. Both yielded low enzyme activities which could be related to insufficient organic nitrogen sources (absent of LB broth that has a composition of 1% yeast extract, 0.5% peptone, 0.5% NaCl), and insufficient skim latex serum that is rich in protein and carbohydrate sources for microbial growth and to produce the yield. Further on, the study examined skim latex serum's ability to assist bacterial growth without the supplementation of lactose, casein, KH_2PO_4 , and MgSO_4 but with a higher concentration of skim latex serum, as shown in Sample 3. The results showed that using 70% (v/v) skim latex serum but supplemented only with galactose (1%, v/v) and LB broth (1%, v/v) resulted in an increase of protease activity, ninefolds and threefolds higher compared to Samples 1 and 4 respectively. This means that skim latex serum has a high content of nutrition elements for bacteria. It might replace the function of lactose, casein, KH_2PO_4 and MgSO_4 as sources of carbohydrate, protein as well as trace elements respectively. The presence of ash components from skim latex serum in growth medium helps to boost up product formation in fermentation. It may act as an inducer for enzyme production (Mardina et al. 2015; Sevinc and Demirkan 2011; Tunga et al. 2001).

This finding is in accordance with Ishizaki et al. (1995) who investigated the presence of skim rubber serum powder in culture media of *Bifidobacterium*, an aerobic gram-positive bacterium. Their result showed that supplement of 1% natural rubber serum powder (NRSP) in the medium had a remarkable growth-promoting effect on all species of these bacteria tested. Furthermore, this finding is also in agreement with work carried out by Siswanto (1999) who reported the isolation of *Bacillus sp.* from coagulated rubber particles. Their study substituted 0.5% casein in LB liquid medium with cytosolic serum of fresh latex or skim latex at the ratio of 1:10 (v/v). In the study, it was observed that the capacity of *Bacillus sp.* to produce protease in the LB media containing protein from skim latex serum, heated to 70°C, was slightly higher than the control media (LB containing casein, LBC). This indicated that skim latex serum might be used as an alternative nitrogen source for *Bacillus sp.*

15.5 Conclusion

This chapter describes the biotechnological potential of abundantly available agricultural waste as well as the effort to utilize them to produce a value-added product, focusing on protease, which is a very useful industrial enzyme. Skim latex is an effluent originating from the natural rubber factories, which can be further processed to get the skim latex serum. This serum can provide the nutrients

requirement such as protein, saccharides, inorganic salt (K, Mg, Cu, Fe, Na, Ca, and P) and trace elements for microbial growth. It has fulfilled the criteria as an efficient culture media due to its abundance, low cost, stable in quality and having a stimulatory effect on bacterial growth. Therefore, the valorization of this wasteful effluent into protease enzyme is hoped to be an introduction for further inventions relating to processes suitable for microbial culturing.

References

- Ahmed SA, Abdel Fattah AF (2010) Production of *Bacillus licheniformis* ATCC 21415 alkaline protease in batch, repeated batch and continuous culture. *Malays J Microbiol* 6(2):156–160
- Akcan N (2012) Production of extracellular protease in submerged fermentation by *Bacillus licheniformis* ATCC 12759. *Afr J Biotechnol* 11(7):1729–1735
- Bhunia B, Basak B, Dey A (2012) A review on production of serine alkaline protease by *Bacillus spp.* *Biochem Technol* 3(4):448–457
- Bradford MM (1976) A rapid and sensitive method for the quantitation of microgram quantities of protein utilizing the principle of protein-dye binding. *Anal Biochem* 72:248–254
- Chi TS, Tung LL, Jong CS (2001) Purification and characterization of black porgy muscle Cu/Zn superoxide dismutase. *Zool Stud* 40(2):84–90
- Eifediyi EK, Ihenyen JO, Ojiekpon IF (2012) Evaluation of the effects of rubber factory effluent on soil nutrients, growth and yield of cucumber (*Cucumis sativus L.*). *Niger Ann Nat Sci* 12(1):21–28
- Hien NN, Thao LT (2012) Situation of wastewater treatment of natural rubber latex processing in the Southeastern region, Vietnam. *J Vietnamese Environ* 2(2):58–64
- Ishizaki A (1991) Bacteria culture and fermentation using the same. United State Patent, 5,026,641
- Ishizaki A, Koike K, Noguchi K, Ando Y (1995) Natural rubber serum powder, an enhancer for the growth of *Bifidobacterium*. *Fac Agric Kyushu Univ* 39(3–4):125–129
- Ismail AI, Mohd Noor Z (2011) Effect of spray drying on protein content of natural rubber serum (NRS). *IIUM Eng J* 12(4):61–65
- Iyagba MA, Adoki A, Sokari TG (2008) Testing biological methods to treat rubber effluent. *Afr J Agric Res* 3(6):448–454
- Jayanthy T, Sankaranarayanan PE (2005) Measurement of dry rubber content in latex using microwave technique. *Meas Sci Rev* 5(3):50–54
- John CK (1978) Waste originating from agriculture and forestry. Lecture presented at the FAO/SIDA workshop on aquatic pollution in relation to protection of living resources, scientific and administrative basis for management measures. Food and agriculture organization of the United Nations. *Aquatic Ecology*, pp 1–458
- Kiddle JJ (1995) Quebrachitol: a versatile building block in the construction of naturally occurring bioactive materials. *Chem Rev* 95(6):2189–2220
- Kresnawaty I, Andanawarih S, Suharyanto, Tri-Panji (2008) Optimization and purification of IAA produced by *Rhizobium sp* in latex serum media supplemented with tryptophan from chicken manure. *Menara Perkebunan* 76(2):74–82
- Mahat MS, MacRae IC (1991) *Rhizopus oligosporus* grown on natural rubber waste serum for production of single cell protein: a preliminary study. *World J Microbiol Biotechnol* 8(1):63–64
- Mardina V, Yusof F, Alam MZ (2015) Statistical optimization of physicochemical factors for protease production by *Bacillus licheniformis* on skim latex serum effluent fortified media,

- Journal of Engineering Sciences and Technology. Special Issue 6 on The 27th Symposium of Malaysian Chemical Engineers (SOMChe 2014) in conjunction with the the 1st Regional Symposium of Chemical Engineering (RSCE 2014), pp 42–52
- McGavack J, Binmore GB (1930) Method for recovering quebrachitol from rubber latex serum, US Patent 1758616
- Mohamed N, Yusof F (2014) Experimental design and statistical analysis of protein buffer to purify hydrolases from the skim latex of *Hevea brasiliensis*. *Adv Environ Biol* 8(3):672–679
- Nadeem M, Qazi JI, Baig S, Syed QA (2008) Effect of medium composition on commercial important alkaline protease production by *Bacillus licheniformis* N-2. *Food Technol Biotechnol* 46(4):388–394
- Nuradibah MA (2012) Preliminary study on the production of bioprotein from skim latex serum and process growth optimization. Retrieved November, 15, 2013. <http://hdl.handle.net/123456789/27661>
- Ochigbo SS, Luyt AS (2011) Mechanical and morphological properties of film based on ultrasound treated titanium dioxide dispersion/natural rubber latex. *Int J Lamposite Mat* 1(1):7–13
- Ochigbo SS, Araga RAL, Suleiman MAT (2011) Comparison of two creaming methods for preparation of natural rubber latex concentrates from field latex. *Afr J Agric Res* 6(12):2916–2919
- Orhue ER, Osaigbovo AU (2013) The effect of rubber effluent on some chemical properties of soil and early growth of maize (*Zea mays L.*). *Bayero J Pure Appl Sci* 6(1):164–168
- Padmapriya B, Rajeswari T, Nandita R, Raj F (2012) Production and purification of alkaline serine protease from marine *Bacillus species* and its application in detergent industry. *Eur J Appl Sci* 4(1):21–26
- Rattanaphan O, Danwanichakul D, Danwanichakul P (2012) Reduction of protein content in skim rubber via both extractions in skim latex and from rubber films. In: 1st Mae Fah Luang University International Conference, pp 1–7
- Sevinc N, Demirkan E (2011) Production of protease by *Bacillus sp. N-40* isolated from soil and its enzymatic properties. *Biol Environ Sci* 5(14):95–103
- Shafer WM, Katzif S, Bowers S (2002) Tailoring an antibacterial peptide of human lysosomal cathepsin G to enhance its broad-spectrum action against antibiotic-resistant bacterial pathogens. *Curr Pharm Des* 8(9):695–702
- Siswanto (1999) Characterization of protease from *Bacillus sp* isolated from natural rubber coagulum. *Menara Perkebunan* 67(2):26–36
- Soedjanaatmadja UMS, Subroto T, Beintema JJ (1995) The effluent of natural rubber factories is enriched in the antifungal protein hevein. *Bioresour Technol* 53:39–41
- Stanbury PF, Whiteker A, Hall SJ (2003) Principle of fermentation technology, 2nd edn. Butterworth–Heinemann, New York
- Tan HT, Pillai KP, Barry DJ (1979) Possible utilization of rubber factory effluent on cropland. In: Proceedings of Rubber Research Institute of Malaysia, Kuala Lumpur, p 154
- Tang SN, Fakhrol-Razi A, Hassan MA, Karim M (1999) Feasibility study on the utilization of rubber latex effluent for producing bacterial biopolymers. *Artif Cells Blood Substit Immobil Biotechnol* 27(5–6):411–416
- Tata SJ, Beintema JJ, Balabaskaran S (1983) The lysozyme of *Hevea brasiliensis* latex: isolation, purification, enzyme kinetics and a partial amino acid sequence. *J Rubb Res Inst Malaysia* 31:35–48
- Tri-Panji, Suharyanto (2001) Optimization media from low-cost nutrient sources for growing *Spirulina plantesis* and caretenoid production. *Menara Perkebunan* 69(1):18–28
- Tunga R, Banerjee R, Bhattacharyya BC (2001) Optimization of some additives to improve protease production under solid state fermentation. *Indian J Exp Biol* 39:1144–1148
- Veerasamy D, Ismail AF (2012) Rehabilitation of fouled membrane from natural rubber skim latex concentration through membrane autopsy and ultra-sonication enhanced membrane cleaning procedure. *Desalination* 286:235–241

- Veerasamy D, Sulaiman NM, Nambiar J, Aziz Y (2008) Environment friendly natural rubber latex concentration by membrane separation technology. Retrieved June 28, 2011. <http://www.membrane.unsw.edu.au/imstec03/content/papers/IND/imstec2008.pdf>
- Yousef AA, Carlstrom C (2003) Chapter 1: Basic microbiological techniques. In: Food microbiology. Wiley, New York, pp 5–12
- Yusof F, Abdullah L (1997) Purification and characterization of superoxide dismutase from *Hevea brasiliensis* latex. In: Proceeding of the 9th national biotechnology seminar, Pulau Pinang, Malaysia, pp 208–212
- Yusof F, Ward MA, Walker JM (1998) Purification and characterisation of an inhibitor of rubber biosynthesis from C-serum of *Hevea brasiliensis* latex. *J Rubber Res* 1(2):95–110
- Yusof F, Amid A, Jimat DN, Nayan MY, Osman NO, Abdullah NAH (2006) Recovery of useful protease, cathepsin G, from the waste skim latex serum of *Hevea brasiliensis*, Kulliyah of Engineering Research and Innovation Exhibition (KERIE 2006), IIUM

Chapter 16

Method for Isolation of Bacterial Strain from Contaminated Soil for Biodegradation of Polycyclic Aromatic Hydrocarbons (PHAs)



Nooraidah Binti Mustaffa, Parveen Jamal, Kola Saheed Olorunnisola, and Abdul Haseeb Ansari

Abstract Continuous release of xenobiotic chemicals to a human environment increasingly predisposes society to significant health-related risks due to their toxicity and long-term presence in the environment. Naturally occurring and manufactured polycyclic aromatic hydrocarbons (PAHs) are categorized based on their teratogenic, mutagenic and carcinogenic properties (Acevedo F, Pizzul L, Castillo Mdel P, Cuevas R, Diez MC; *J Hazard Mater* 185(1):212–219, 2011). Longevity of PHAs in the environment directly depends on their low solubility in water, vapor pressures and high octanol/water partitioning coefficients (Bogan BW, Lamar RT; *Appl Environ Microbiol* 61(7):2631–2635, 1995).

Keywords Phenanthrene · Bioremediation · *Pseudomonas putida* · Xenobiotic chemicals · Environment · Contaminated soil · Polycyclic aromatic hydrocarbons

16.1 Introduction

The continuous release of xenobiotic chemicals to a human environment increasingly predisposes society to significant health-related risks due to their toxicity and long-term presence in the environment. Naturally occurring and manufactured polycyclic aromatic hydrocarbons (PAHs) are categorized based on their teratogenic,

N. B. Mustaffa
Center for Foundation Studies, IIUM, Kuantan, Malaysia

P. Jamal (✉)
Department of Biotechnology Engineering, IIUM, Kuala Lumpur, Malaysia
e-mail: jparveen@iium.edu.my

K. S. Olorunnisola
Biological Sciences Department, Elizade University, Ilara-Mokin, Nigeria

A. H. Ansari
AIKOL, International Islamic University, Kuala Lumpur, Malaysia

mutagenic and carcinogenic properties (Acevedo et al. 2011). Longevity of PHAs in the environment directly depends on their low solubility in water, vapor pressures and high octanol/water partitioning coefficients (Bogan and Lamar 1995).

PAHs have a high affinity for soil organic matters (humus), and this has increased the challenges posed by the accidental release of petroleum products to the environment. In a report, a number of crude petroleum products discharged in error was estimated at over 600,000 metric tons annually with an average of 200,000 metric tons increase in the same duration. This development is a major cause of river, oceanic and underground water contamination and soil pollution (Kumari et al. 2013).

Bioremediation is a biological method for complete mineralization of organic contaminants. The process involves cultivation of microorganisms on contaminated habitat to convert PHAs into benign end products such as carbon dioxide, water, inorganic compounds, and cell protein. However, to effectively rescue contaminated soils and aquatic environments from perpetual damage by PHAs, microbes capable of degrading the high molecular compounds must be isolated from the contaminated soil (Medina-Bellver et al. 2005).

This method has been adopted for remediating plethora of challenges in food and agricultural environments with impressive results. Hence, adoption of similar approach to PHAs devastated environments is touted to provide a potent platform for abatement of water and soil degrading hydrocarbon contaminants.

16.2 Material and Methodology

16.2.1 Materials

All materials and chemicals to be used in the isolation and biodegradation works are as listed in the following Tables 16.1, 16.2 and 16.3. They are tabulated and categorized according to the consumable item, equipment and chemicals.

Table 16.1 Consumable Item

| No | Equipment | Usage |
|----|-----------------------------------|--|
| 1 | Petri dish | To serve as growing media container for microbes |
| 2 | L-shaped rod | To spread serially diluted liquid samples from contaminated soil |
| 3 | Distilled water | To dissolve all reagents |
| 4 | Spatula | To pick required amount of soil samples |
| 5 | Parafilm | To cover petri dish |
| 6 | Bunsen burner | To sterilize inoculating loop |
| 7 | Inoculating loop | To pick viable colonies for sub-culturing |
| 8 | Measuring cylinder | To measure distilled water |
| 9 | Round bottom flask | To prepare chemical reagents |
| 10 | Weighing boat | To weigh solid materials |
| 11 | Pipette (1 mL, 5 mL, 100 μ L) | To add solutions as required |
| 12 | Erlenmeyer flask | To keep the microbial growing media for autoclaving |

Table 16.2 Equipment

| No | Equipment | Usage |
|----|------------------|---|
| 1 | Incubator | To maintain microbial growing conditions |
| 2 | Autoclave | To sterilize materials (glass wares, pipette tips, cotton plugs and liquid media) |
| 3 | Centrifuge | To separate bio-solids |
| 4 | Chiller | To store consumables and microbes |
| 5 | Weighing balance | To measure samples |
| 6 | Laminar flow | To achieve sterile environment for inoculation |
| 7 | Vortex mixer | To mix contaminated soil slurry |

Table 16.3 Chemicals

| No | Chemical reagent | Usage |
|----|------------------|--|
| 1 | Nutrient agar | To grow media for isolating target bacterial cells |
| 2 | Phenanthrene | Chemical for checking the degrading efficiency of microbes |
| 3 | Ethanol | To sterilize lamina flow working space |

16.2.2 Methodology

Soil Samples

Contaminated soil samples were collected from stale areas where spillage had previously occurred. The soil was placed in airtight screwed containers to prevent cross-contamination with unwanted microorganisms. Soil samples were stored at 4 °C in a chiller before and after use (Fig. 16.1).

Preparation of Agar Plates

Nutrient agar was prepared according to manufacturers' instructions and was autoclaved at 121 °C for 15 min. The laminar flow cabinet was prepared by spraying 70% ethanol on the working space, and the airflow was sustained throughout. About 15 ml of sterile nutrient agar was poured into each sterile petri dish and allowed to solidify. The dish covers were slightly opened to prevent condensation which harbors unwanted microorganisms (Fig. 16.2).

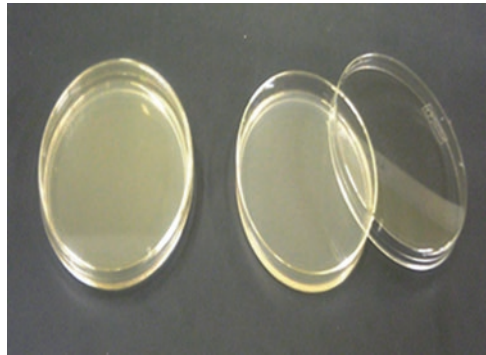
Preparation of Media Broth

The nutrient broth was prepared according to manufacturers' instruction and was autoclaved at 121 °C for 15 min. The laminar flow cabinet was prepared by spraying 70% ethanol on the working space, and the airflow was sustained throughout. About



Fig. 16.1 A contaminated soil

Fig. 16.2 Sterile nutrient agar plates



25 ml of sterile nutrient broth was poured into each Erlenmeyer flask and was allowed to cool to room temperature.

Serial Dilution

About 1–2 g of soil sample was weighed and transferred to clean beaker. A similar amount of sterilized distilled water was added to release the microbes. Additional 1 ml sterilized distilled was added, and the content of the beaker was shaken with a spatula. The soil was allowed to settle while the supernatant was used for serial dilution. The supernatant was diluted from 10^{-1} to 10^{-6} by adding 1 ml of the previous dilution to 9 ml of sterilized distilled water (Fig. 16.3).

Media Inoculation

About 100 μ l of serially diluted samples was transferred aseptically to the sterile petri dish. L-shaped rod was used to spread the samples evenly on the petri dish and was sealed with parafilm. Incubation then was performed at 37 °C for 24 h.

Bacteria Sub-Culturing by Streaking Method

24 h old bacterial cells were sub-cultured by taking 1 loop full of bacterial culture, and streaking was performed by rubbing the cell at a spot closer to the extreme end

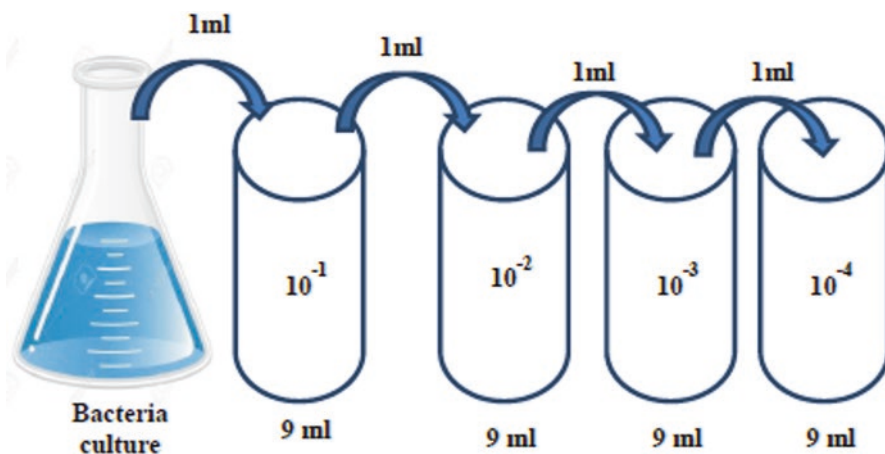


Fig. 16.3 Serial dilution

of the petri-dish and taking several lines out of the cell mass in a zigzag manner. Sub-culturing was carried out several times until a true culture was identified in all sub-culturing process.

Preparation of Seed Culture

A seed culture of true cells was prepared by suspending 1 loop full of cultivated cells in cooled nutrient broth. The flask was corked with a cotton plug to facilitate sterilized gas exchange, and the flask was incubated at 37 °C in an incubator shaker at 150 rpm for 24 h. The flask content was aseptically transferred to sterilized 50 ml plastic tubes and centrifuged at 1000 rpm for 1 min. Then the supernatant was discarded, and 5 ml of sterile nutrient broth was added and vortexed for 30 s. to suspend the cells.

Preparation of PHA

Phenanthrene was used as target PHA. Prepare 0.1 g/l of phenanthrene by dissolving it in acetone and stir vigorously for absolute dissolution.

Testing of PHAs Degradation of Isolated Bacteria

One (1) ml of phenanthrene solution was transferred to a sterile petri dish in order to cover the whole plate. The acetone was allowed to evaporate, and one loop-full of bacterial seed culture was added. After that, the petri-dish was sealed with parafilm and incubated in upside down position at 37 °C for 2–5 days. Successful increase in radial growth of bacteria indicated phenanthrene degradation.

16.3 Results and Discussion

Some of the isolated bacteria strains were able to grow extensively on the phenanthrene contaminated agar plates (Fig. 16.1). The profound growth of the strains signifies degradation and metabolism of the polyaromatic compound. The result

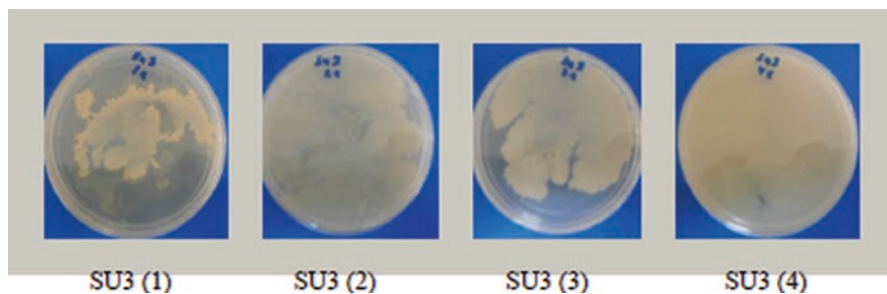


Fig. 16.4 Growth characteristics of isolated SU3 bacteria from contaminated soil on phenanthrene

shows that all SU3 strains grew on the plates. However, SU3 (2) showed more prominence compared to other strains in the group. The use of microbial growth on plates to evaluate their degradation potential of certain soil contaminants have been reported, and the present outcome is similar (Sarfraz Ahmed et al. 2010) (Fig. 16.4).

16.4 Conclusion

Phenanthrene degrading bacteria were successfully isolated through serial dilution of the contaminated soil sample. The capacity of isolated microbes in degrading selected PHA was elucidated qualitatively with the profound metabolism of the soil contaminants.

References

- Acevedo F, Pizzul L, Castillo Mdel P, Cuevas R, Diez MC (2011) Degradation of polycyclic aromatic hydrocarbons by the Chilean white-rot fungus *Anthracophyllum discolor*. *J Hazard Mater* 185(1):212–219
- Bogan BW, Lamar RT (1995) One-electron oxidation in the degradation of creosote polycyclic aromatic hydrocarbons by *Phanerochaete chrysosporium*. *Appl Environ Microbiol* 61(7):2631–2635
- Kumari N, Vashishtha A, Saini P, Menghani E (2013) Isolation, identification, and characterization of oil-degrading Bacteria isolated from the contaminated sites of Barmer, Rajasthan. *Int J Biotechnol Bioeng Res* 4(5):429–436. ISSN 2231-1238, © Research India Publications <http://www.ripublication.com/ijbbr.htm>
- Medina-Bellver JI, Marín P, Delgado A, Rodríguez-Sánchez A, Reyes E, Ramos JL et al (2005) Evidence for in situ crude oil biodegradation after the prestige oil spill. *Environ Microbiol* 7(6):773–779
- Sarfraz Ahmed SA, Nisar MF, Hussain K, Majeed A, Pir Bakhsh Ghumroo SA, Shahzad A, Nawaz K, Ali K (2010) Isolation and characterization of a bacterial strain for aniline degradation. *Afr J Biotechnol* 9(8):1173–1179

Chapter 17

Monitoring the Growth of Plant Cells in Suspension Culture



Noor Illi Mohamad Puad and Tajul Afif Abdullah

Abstract Cell suspension cultures provide a convenient way in understanding the dynamics growth of plant cells. This knowledge is crucial in order to manipulate all parameters related to their growth so that the potential of plants can be fully utilised. Growth can be defined as the increase of cell numbers, size or mass. In a growth cycle, cells will be experiencing four phases which are lag, logarithmic (exponential), stationary and death phase. The information and knowledge gained from growth kinetics parameters provide the basic platform for modelling and predicting the characteristics of cell culture. This chapter describes the procedures for fresh weight, dry weight, TCN, medium conductivity (pH) and residual sugar analysis.

Keywords Plant cell suspension · Cell growth · Fresh weight · Dry weight · Total cell number · Medium conductivity · Residual sugar analysis · *Arabidopsis thaliana* · *Ficus deltoidea*

17.1 Introduction

Plant cell cultures show potential as an alternative for the production of valuable natural products, particularly secondary metabolites that serve as agricultural chemicals, dyes, flavors, and medicinal compounds. Plant cell cultures possess several advantages over intact plants. Suspension culture of plant cells is a technique in which the cells are growing as single cells or cell aggregates suspended in a liquid nutrient medium. The cells in suspension can grow faster in bulk liquid since all the cells are exposed uniformly to the nutrient medium. In addition, the culture conditions can be controlled and modified for optimum growth and production rate even outside the growth season. Suspension cultures are initiated from the callus of plants.

N. I. Mohamad Puad (✉) · T. A. Abdullah
Department of Biotechnology Engineering, Faculty of Engineering, International Islamic University Malaysia, Kuala Lumpur, Malaysia
e-mail: illi@iium.edu.my

The growth of cells in suspension culture can be observed and followed by using several methods during the growth phase. These methods include total cell number (TCN), packed cell number (PCV), fresh weight (FW) and dry weight (DW), cell viability, and medium conductivity. It is recommended to perform any two of the methods to monitor the culture during the growth phase until the cells enter the stationary phase (Evans et al. 2003). Also, consumption of carbon source (residual sugar analysis) and nutrients, uptake of oxygen or production of carbon dioxide can also be complementary methods in monitoring the growth of suspended plant cells. The procedures for FW, DW, TCN, medium conductivity (pH) and residual sugar analysis are further elaborated in this chapter.

17.2 Principles

17.2.1 *Fresh Weight (FW) and Dry Weight (DW) Analysis*

Both of these analyses are the most common and simplest methods to monitor the growth of cells in suspension since no sophisticated equipment is required. Basically, FW is determined by weighing the freshly harvested cells (cells and medium are separated by vacuum filtration (Evans et al. 2003). Using the same cells, dry weight is calculated by drying up the cells for 48 h at 80 °C or until the dry weight becomes consistent. The reading for DW is usually reduced by 90% from that of FW. This shows that approximately 90% of the water content has been removed during the drying process. DW is more reliable than FW since the latter reading might be affected by the removal of water from the sample during the vacuum filtration step.

17.2.2 *Total Cell Number (TCN)*

TCN is usually expressed as the number of cells per unit volume. The device that is used to count the cells is hemocytometer. The diluted sample is loaded into the counting chamber of the hemocytometer and the total number of cells recorded should be greater than 1000 with at least three fields scored. Plant cells in suspension cultures always form cell aggregates and have larger cell sizes, which makes the process cell number calculation difficult. These can be overcome by dispersing the cell aggregates with 10% HCl and 10% chromic acid (Evans et al. 2003) or by using an improved Neubauer type hemocytometer (depth of counting chamber, 0.1 mm) to accommodate the larger cells.

17.2.3 Medium Conductivity (pH)

Medium conductivity is sometimes a convenient method to monitor cell growth and can be regarded as a complement to FW, DW or even TCN. It can be measured by using a conductivity meter. The change of medium conductivity occurs due to the uptake and utilization of electrolytes from the medium, and the value usually drops over the passage of time. The changes in pH reflect various phases of the culture cycle (Evans et al. 2003). Usually, in the early logarithmic phase, the culture is more acidic (pH 3.5–4.5) and returns to pH 5 in the stationary phase. This might be due to the production of protons from metabolic activities and rapid removal of nutrient ions from the medium, such as phosphate, that provide buffering capacity to the medium.

17.2.4 Residual Sugar Analysis

Sucrose is the common carbon source supplied to suspension cultures of plant cells. Sucrose is a disaccharide consisting of two hexoses, glucose, and fructose. It has been reported that for several plant cultures, the enzyme invertase (EC 3.2.1.26) located on the plant cell wall hydrolyzes sucrose into stoichiometrically equal amounts of glucose and fructose (Fowler 1982; Sturm 1999). Then, the plant cells consume these hexoses at different rates with preference to glucose. These trends can also be an indicator that the suspended cells are actively growing and dividing by consuming the hexoses. The common method used to quantify the residual sugars in the plant cell medium is the dinitrosalicylic acid (DNS) method and high-performance liquid chromatography (HPLC). HPLC can conveniently and efficiently quantify 3 different sugars (sucrose, glucose, and fructose) simultaneously, whereas the DNS method might require several steps since the method can only quantify one sugar at a time.

17.3 Objectives

This chapter aims to observe the growth of plant cells in two types of suspension cultures, *Arabidopsis thaliana* (*A. thaliana*) Columbia ecotype and *Ficus deltoidea* (*F. deltoidea*) (Mas cotek). The growth of *A. thaliana* cells in suspension culture is monitored by using FW, DW, and pH analysis while that of *F. deltoidea* is measured by TCN analysis.

17.3.1 *Materials and Methods*

Consumable Items

Whatman No. 1 filter paper, 9 cm in diameter

Micro-centrifuge tubes, 2 mL or centrifuge tubes, 15 mL

Equipment

Fine balance

Glass filter funnel

Buchner flask (with sidearm for vacuum attachment)

Oven set to 80 °C

17.3.2 *Method 1 (Using Filter Paper)*

17.3.2.1 **Fresh Weight**

1. The apparatus setup for this method is shown in Fig. 17.1.
2. Take approximately 25 mL of suspension culture and record its exact volume.
3. Filter the culture through a pre-weighed wet Whatman No.1 filter paper under vacuum by slowly pouring the culture to the center of the filter paper.
4. It takes approximately 20–30 s for the water to drain out.
5. Immediately measure the weight of the wet filter paper with cells.
6. Calculate the fresh weight of cells by subtracting the wet weight of the filter paper alone (B) (which was wetted and weighed previously) from the weight of the filter paper with cells (A) (Eq. 17.1).

$$\text{Fresh weight (g)} = A - B(\text{g}) \quad (17.1)$$

17.3.2.2 **Dry Weight**

1. Use the wet filter paper with the cells that were previously used in the analysis of fresh weight for dry weight analysis.
2. Dry the filter paper with cells in an oven at 80 °C for two nights.
3. After two nights, place the dried filter paper with cells in a desiccator for cooling.
4. Record the dry weight of the filter paper with cells (C). Determine the dry weight of cells by subtracting (D) the dry weight of the filter paper.

$$\text{Dry weight (g)} = C - D(\text{g}) \quad (17.2)$$

Fig. 17.1 The apparatus for filtering cultures and obtaining weight measurements (Puad 2011)



17.3.3 Method 2 (Using a 2 mL Micro-Centrifuge Tube or a 15 mL Centrifuge Tube)

17.3.3.1 Dry Weight

1. Dry the centrifuge tube in an oven at 80 °C for 12 h with its lid closed.
2. Record its weight as W_0 .
3. Stir the suspension culture and transfer 500 μ L of the culture into the pre-dried and pre-weighed centrifuge tube.
4. Centrifuge the tube at 10,000 rpm for 5–10 min. Remove the supernatant (media). Dry the pellet and the tube at 80 °C for 12 h with the lid closed.
5. After 12 h, put the tube in a desiccator for cooling
6. Determine the weight and record it as W_1 . Cell DW is determined as follows:

$$\text{Cell DW} = W_1 - W_2 \quad (17.3)$$

17.3.4 Total Cell Number (TCN)

Consumable Items

Micro-centrifuge tube, 2 mL

Equipment

Pipette

Light microscope

Haemocytometer

Materials and Reagents

Trypan blue

Jones reagent

17.3.4.1 Method

1. Stir the suspension culture well to have a homogeneous mixture. Then, transfer 200 mL of the culture into a microcentrifuge tube.
2. Add 200 mL of 0.02% (v/v) trypan blue into the micro-centrifuge tube. Mix well.
3. Take 10 mL of the mixture and transfer it onto a hemocytometer.
4. The dead cells are indicated by blue color since trypan blue can enter the dead cells, and the viable cells are brown. Equations 17.4 and 17.5 are used to calculate the total cell number:
5. If the cells form clumps/aggregates, transfer 90 mL of the cell suspension into a new micro-centrifuge tube and react with 10 mL of Jones reagent. Mix well.
6. Place the mixture in a water bath at 60 °C for 5–10 min.
7. After that, add 100 mL of trypan blue. Mix well.
8. Repeat steps 3–4 to determine TCN.

$$\frac{\text{Total cells}}{\text{ml}} = \text{Total cell counted} \times \frac{\text{dilution factor}}{5 \text{ squares}} \times 10000 \frac{\text{cells}}{\text{ml}} \quad (17.4)$$

$$\text{Dilution factor} = \frac{(\text{volume of sample} + \text{distilled water added})}{\text{volume of sample}} \quad (17.5)$$

17.3.5 Medium Conductivity (pH)

17.3.5.1 Method

1. Using a pH meter, measure the pH of the filtered culture media.
2. Record the pH reading after the reading of the pH meter becomes stable.
3. Repeat step 2 for an additional 2 times to increase the precision of the reading.

17.3.6 Residual Sugar Analysis

17.3.6.1 Method

1. Filter the defrosted samples (filtered medium) using 0.45 μm cellulose acetate membrane filters (Sartorius).
2. Analyse the residual sugar by using a PL Hi-Plex Ca column (300 \times 7.7 mm) (Polymer labs) with a guard column (Polymer labs).
3. Set the working flow rate of the mobile phase (HPLC grade water) at 0.6 mL/min and the column oven at 85 $^{\circ}\text{C}$ (Shimadzu CTO-6A).
4. Inject each sample twice using auto-injection (Pro Star 410), and detect the peak with the evaporative light scattering detector (ELSD) (PLS-2000).
5. Before that set the evaporation temperature of the ELSD to 90 $^{\circ}\text{C}$ and at 35 $^{\circ}\text{C}$ for nebulization. Set the nitrogen gas flow rate to 1.60 L/min.
6. Analyse the chromatograms with a Prostar/Dynamax System.
7. Before sample analysis, construct a standard curve for each sugar by using different concentrations of sugar, *i.e.*, 1, 2.5, 5 and 10 g/L. The concentration of residual sugars in the samples is determined from the standard curve by comparing the area of the peak. Table 17.1 lists the retention time for each standard sugar (from the mixed sugars sample), while Fig. 17.2 illustrates the peak of sucrose, glucose, and fructose at different concentrations.

17.4 Results and Discussion

17.4.1 Fresh Weight, Dry Weight, and pH of *Arabidopsis thaliana* (*A. thaliana*) *Columbia* (*Col*) Suspension Culture

As shown in Fig. 17.3, the growth of suspended *A. thaliana* cells displays a normal classical sigmoidal curve. It can be observed that the lag phase lasted for 2 days followed by the logarithmic phase that ended on the 8th day. The stationary phase, a phase where all nutrients were depleted, occurred from day 9 to day 11. The cells reached their death phase after 11 days of culture.

Regarding cell concentration, the culture reached the maximum concentration of 10 times the inoculum for which the FW was 252 g/L on day 10 while the DW was

Table 17.1 Retention time for standard solutions of sucrose, glucose and fructose

| Standard | Retention time (min) |
|----------|----------------------|
| Sucrose | 11.132 |
| Glucose | 13.209 |
| Fructose | 15.846 |

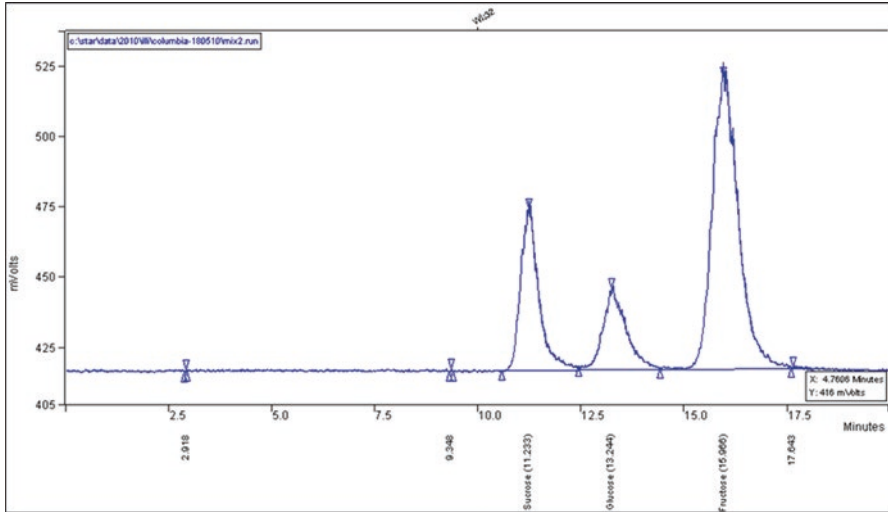


Fig. 17.2 Chromatograms of sugar standards (2.5 g/L sucrose, 1 g/L glucose, 10 g/L fructose) (Puad 2011)

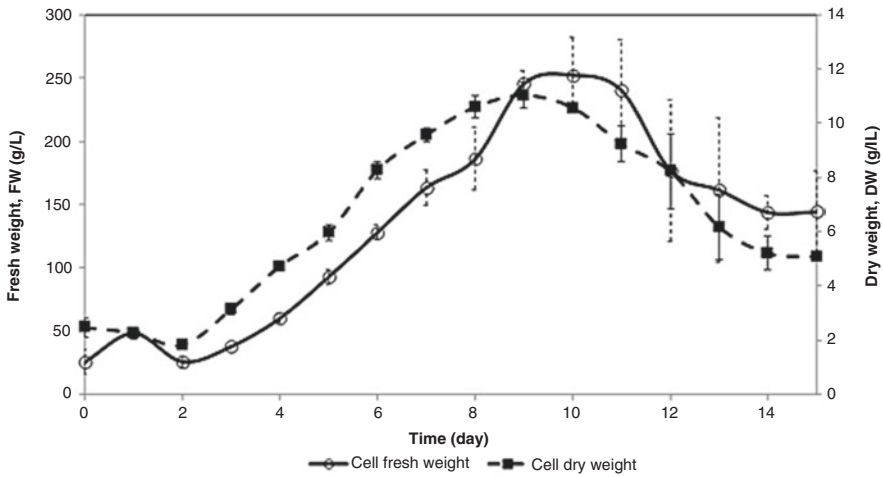


Fig. 17.3 Growth of *A. thaliana* Ler ecotype cells in suspension under continuous light with 10% (v/v) inoculum (Puad 2011)

11 g/L on day 9 (Fig. 17.3). When the cells reached the death phase, both values for FW and DW dropped to almost half of the maximum values.

The ratio of FW and DW seemed to be constant throughout growth, although there were some variations in the ratio towards the end of culture.

In Fig. 17.4, the *A. thaliana* cells grown in the dark and under conditions of cycled light did not differ significantly regarding their growth characteristics.

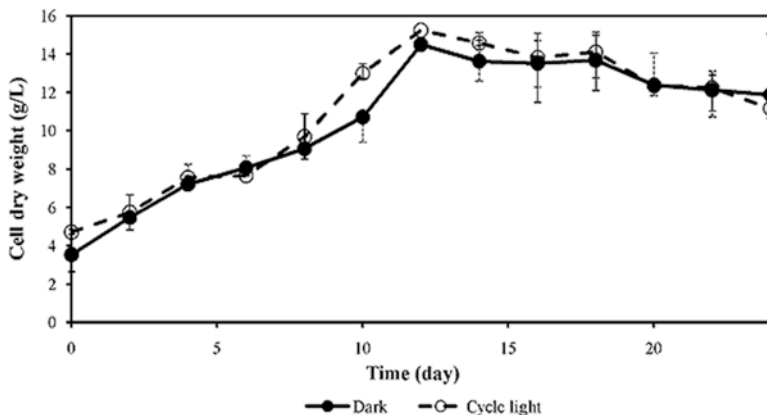


Fig. 17.4 Comparison of growth profiles for Col suspension cells grown in the dark and under conditions of cycled light (Puad 2011)

Table 17.2 Parameters for growth kinetics for Col ecotype cells under different light conditions

| Growth condition | Specific growth rate, μ (h^{-1}) | Sucrose hydrolysis rate ($\text{gL}^{-1} \text{h}^{-1}$) | Glucose uptake rate ($\text{gL}^{-1} \text{h}^{-1}$) | Fructose uptake rate ($\text{gL}^{-1} \text{h}^{-1}$) | Max cell dry weight (gL^{-1}) | Biomass yield (g DW biomass (g total sugar consumed) $^{-1}$) |
|--|---|--|--|---|--|--|
| 10% (v/v) inoculum, cycled light (16 h photoperiod/8 h dark) | 0.004 | 0.470 | 0.058 | 0.042 | 15.247 | 0.375 |
| 10% (v/v) inoculum, continuous darkness | 0.0035 | 0.518 | 0.053 | 0.044 | 14.509 | 0.385 |

Furthermore, both conditions showed a comparable period of growth phase where the cells reached the stationary phase 12 days after inoculation.

Additionally, there were not many differences between the maximum DW values of cells in both cultures. Consequently, their biomass yields were similar (Table 17.2). The Col cells displayed a five-fold increase in biomass. The calculated maximum specific growth rates, μ_{max} were 0.004 h^{-1} and 0.0035 h^{-1} for the cultures grown in cycled light and the dark, respectively.

As shown in Fig. 17.5, sucrose was completely hydrolysed by cell wall invertase into hexoses 96 h after inoculation (4 days). It was also observed that during the sucrose hydrolysis period, the concentrations of glucose and fructose were equal. This is consistent with previous reports that cell wall invertase hydrolyses sucrose into stoichiometrically equivalent amounts of glucose and fructose (Fowler 1982; Sturm 1999).

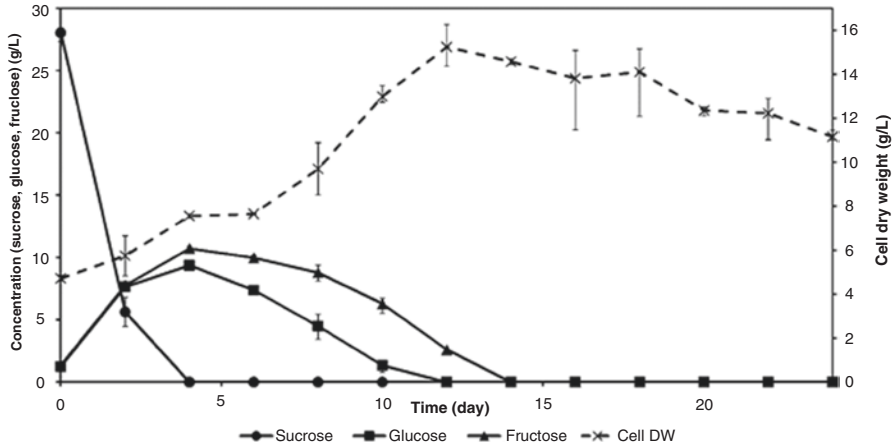


Fig. 17.5 Growth and sugar profiles of suspended Col cells cultured under cycled light conditions with 10% (v/v) inoculum (Puad 2011)

The cells grew at a slower rate during the sucrose hydrolysis period compared to when sucrose hydrolysis was completed, and only hexoses were left in the medium. In cultured rice (*Oryza sativa*) cells, no sucrose was detected at the end of the lag phase (Amino and Tazawa 1988). Only hexoses were present in the medium when the cells entered the exponential growth phase. The same was reported for apple fruit cells (Pareilleux and Chaubet 1980) and *Taxus cuspidata* cells (Son et al. 2000). However, the completion of sucrose hydrolysis is not mandatory for the plant cells to enter the exponential phase since, in *Nicotina tabacum* and *Datura innoxia* suspension cultures, the sucrose hydrolysis occurred during the exponential growth until the cells reached stationary phase (Kato and Nagai 1979; Wylegalla et al. 1985).

Sucrose was hydrolysed slightly faster by the cells grown in the dark (Table 17.2). It can be suggested that the cells grown in cycled light were able to produce sugars via photosynthesis due to the availability of light during the experiment. However, since the cells cultured in the presence of light consisted of both green and yellow cells, photosynthesis probably did not occur at the maximum rate. This may explain why the cells that were grown under cycled light conditions exhausted their carbon sources on the same day as the cells grown in the dark.

Upon the completion of sucrose hydrolysis, Col cells entered their exponential growth phase by consuming both glucose and fructose at different specific rates. Glucose was preferentially consumed over fructose as has been reported for other plant cells, *i.e.*, apple fruit (Pareilleux and Chaubet 1980), *Daucus carota* (Albiol et al. 1993), and *Taxus cuspidata* (Son et al. 2000). Col cells reached their stationary phase on day 12 when all sugars were depleted for both growth conditions (Figs. 17.5 and 17.6). Table 17.2 lists the calculated growth parameters for Col cells in suspension grown under cycled light and dark conditions.

When the cell DW is plotted against pH of the medium (Fig. 17.7), it was observed that the pH increased as the cell phase progressed. This might be due to the release of intracellular metabolites resulting from cell lysis and death.

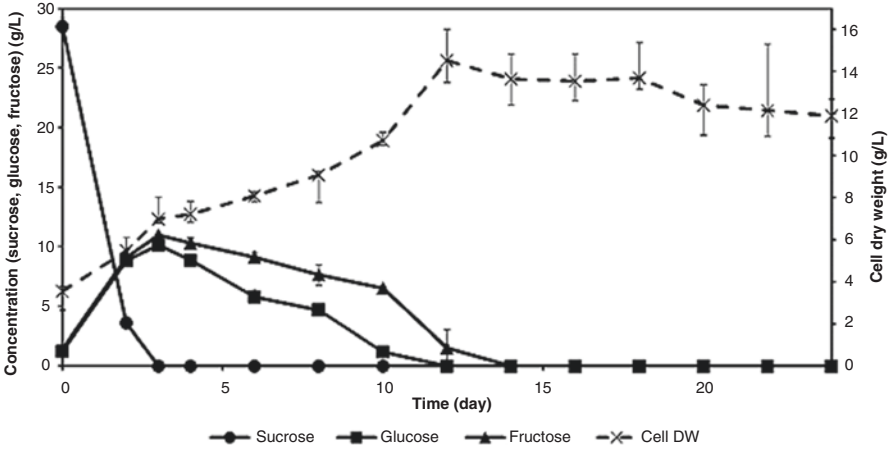


Fig. 17.6 Growth characteristics of suspended Col cells cultured in the dark (Puad 2011)

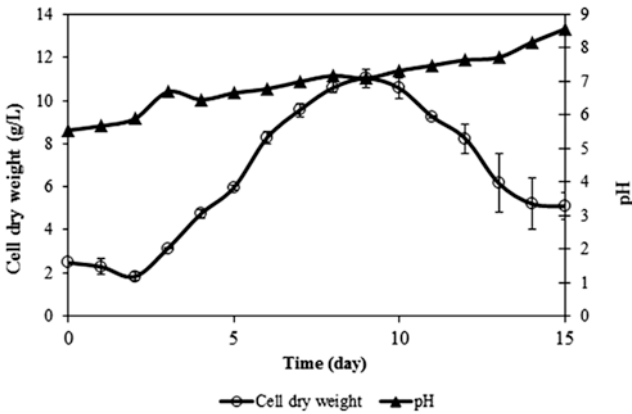
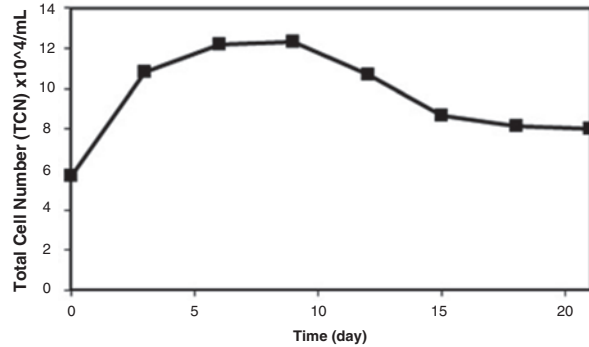


Fig. 17.7 pH reading of *A. thaliana* culture medium throughout various growth phases (Puad 2011)

17.4.2 Total Cell Number of *Ficus deltoidea* (*Mas cotek*) Cells in Suspension Cultures

From the plot of TCN versus time (Fig. 17.8), it can be deduced that the *Mas cotek* cells in culture followed a normal sigmoidal growth curve but the lag phase was not obvious. Perhaps the frequency of sampling could be increased so that the lag phase can be observed. On day 9, the cell number of *Mas cotek* cells in suspension reached the maximum value, which was double that of the initial cell number of 12.3×10^4 cells/mL.

Fig. 17.8 Growth of *Ficus deltoidea* (Mas cotek) cells in suspension



17.5 Conclusions

There are a number of options to monitor the growth of cells in suspension cultures. The most common, simple and convenient method is using the dry weight of cells. Total cell number is also a good choice to quantify the cells, but a good technique should be practised to have accurate and precise readings.

Acknowledgement The authors would like to acknowledge the Ministry of Higher Education in Malaysia for funding this project under the Fundamental Research Grant Scheme (FRGS 14-145-0386).

References

- Albiji J, Robusté J, Casas C, Poch M (1993) Biomass estimation in plant cell cultures using an extended Kalman filter. *Biotechnol Prog* 9(2):174–178
- Amino S-i, Tazawa M (1988) Uptake and utilization of sugars in cultured rice cells. *Plant Cell Physiol* 29(3):483–487
- Evans D, Coleman J, Kearns A (2003) *Plant cell culture: the basics*. Taylor & Francis, London
- Fowler MW (1982) Substrate utilisation by plant-cell cultures. *J Chem Technol Biotechnol* 32(1):338–346
- Kato A, Nagai S (1979) Energetics of tobacco cells, *Nicotiana tabacum* L., growing on sucrose medium. *Appl Microbiol Biotechnol* 7(3):219–225
- Pareilleux A, Chaubet N (1980) Growth kinetics of apple plant cell cultures. *Biotechnol Lett* 2(6):291–296
- Puad NIM (2011) *Modelling the metabolism of plant cell culture* (PhD), University of Manchester
- Son SH, Choi SM, Lee YH, Choi KB, Yun SR, Kim JK et al (2000) Large-scale growth and taxane production in cell cultures of *Taxus cuspidata* (Japanese yew) using a novel bioreactor. *Plant Cell Rep* 19(6):628–633
- Sturm A (1999) Invertases. Primary structures, functions, and roles in plant development and sucrose partitioning. *Plant Physiol* 121(1):1–8. <https://doi.org/10.1104/pp.121.1.1>
- Wylegalla C, Meyer R, Wagner KG (1985) Nucleotide pools in suspension-cultured cells of *Datura innoxia*. *Planta* 166(4):446–451

Chapter 18

Culturing and Maintaining Mammalian Cell Culture



Raha Ahmad Raus, Ghassan Ali Salih, and Mustaffa Nameer Shaban

Abstract Mammalian cell culture refers to culturing mammalian cells in a medium that provide nutrients for cells to be able to grow *in vitro* under environment that closely mimic the *in vivo* conditions. By enabling culturing these cells outside living biological entities, investigation on intra- and intercellular activities and flux; genetic and phenotyping analysis; proteomics, study of toxicology, drug discovery and development can be carried out without manipulation of living animals. In this chapter, detail protocol of media preparation, cell culture maintenance and preservation are elaborated for both types of mammalian cell culture, monolayer or suspension cultures. Determination of number of cells is discussed as well.

18.1 Introduction

The development of mammalian cell culture was established in the early twentieth century where isolation of individual cells from fragments of tissue or organs in the laboratory are carried out to grow mammalian cells. In the early years of tissue culture, the yielded tissue had very limited growth capabilities and number of cell divisions, a condition called Hayflick's Limit (Hayflick and Moorhead 1961). The discovery of HeLa, a unique cervical carcinoma cell line which has limitless lifespan, harvested from a patient called Henrietta Lawson, at John Hopkins Hospital, Baltimore in the 1950s, embarked modern advancement in clinical research for drug development and therapy, where cells can be cultured *in vitro* in large number and stored for a long time (Masters 2002).

Cell culture technology has prompted various fields of cell biology investigation such as the study of intra- and intercellular activities and flux; genetic and phenotyping analysis; proteomics, study of toxicology, drug discovery and development; recombinant protein production, medical diagnosis and treatment (Ozturk and Hu 2005). Significant advancement and development of mammalian cell culture have

R. A. Raus (✉) · G. A. Salih · M. N. Shaban
Department of Biotechnology Engineering, Faculty of Engineering, International Islamic University Malaysia, Kuala Lumpur, Malaysia
e-mail: rahaar@iium.edu.my

enabled researchers to further understand the underlying mechanism of diseases in the search for cure and therapy.

18.2 Mammalian Cell Culture

The use of the mammalian cell culture as a model of physiological function has been criticized due to the uncontrolled microenvironment culture conditions and the requirement of a strict and controlled aseptic procedure to avoid contamination and loss in the cell line (Freshney 2005). Nowadays, with the modern equipped laboratories that ensure the aseptic environment and techniques, it is possible to achieve a cellular microenvironment that closely mimics the *in vivo* conditions. The routine for cell culture maintenance for feeding and subculturing is now conducted in a sterile condition in a biosafety cabinet class 2.

To culture the mammalian cells, the preserved cells is thawed and cultured in the media. Once the cells confluence, they had to be passaged or subcultured. Otherwise it will result in a reduced cellular mitotic index that leads to the death of cells. The cell suspension is then divided into fresh cultures to produce secondary cultures. Once the secondary cultures reach confluency, they must be subcultured to produce tertiary cultures and this will be repeated depending on the need of the study. The passaging time depends on the cellular growth rate and varies among different cell lines.

In general, mammalian cell culture is either in monolayer or suspension cultures. Both techniques involve different protocols for culturing and maintenance. In this chapter, media preparation, cell culture maintenance, preservation, and thawing from a monolayer and suspension stock culture will be elaborated. Determination of number of cells will be discussed as well.

18.3 Media Preparation

Cell culture is a technique to propagate cells under sterile and controlled laboratory condition. It is utilized by the researches to investigate the cellular biological activities, functions, morphologies, and behavior of cells. The most important factor influencing the mammalian cell culture is the choice of the culture medium as the cells require large quantity of simple nutrients for their viability and growth (Eagle 1959). The formulations of the medium should mimic natural conditions that normally happen in the organism to assist their biological activities and viability. There are many different types of culture media available in the market, which vary accordingly to their sugar, protein, minerals supplemented with animal serums, growth factors, and hormones as different types of cell prefer different media formulations for good growth and differentiation (Freshney 2005).

Most cells are cultured in a **basal media** containing nutrient, vitamins, and minerals supplemented with various animal serums such as horse, calf, and fetal bovine. This type of media is called undefined media due to its unknown exact components of the supplemental serum. Examples of readily available cell culture media are Dulbecco's Modified Eagle's Medium (DMEM) (Dulbecco and Freeman 1959), α -Eagle's Minimal Essential Medium (α -MEM) (Eagle 1959), and RPMI 1640 (Moore et al. 1967).

Basal media formulations must consist of the components below:

- Source of energy/carbon – glucose/glutamine
- Building blocks of proteins – amino acids
- Supplementation to support cell survival and growth – vitamin
- Isotonic mixture of ions that functions as cofactors for enzymatic and cellular activities – balanced salt solution
- pH indicator that turn from orange/red at pH 7–7.4 to yellow at acidic pH and purple at basic pH environment
- Buffer – HEPES or bicarbonate to maintain a balanced pH in the media

In the preparation of **complete media**, fetal bovine serum is added into the basal media. Antibiotics such as penicillin and streptomycin and fungicides (e.g., Fungizone) may be added to prevent bacterial and fungi growth. This supplementation is however not recommended due to increased susceptibility of antibiotic resistant bacteria/fungi. Alternatively, glutamine, epithelial growth factor, and cholera toxin can be added into the basal media and the resulting media is said to be defined media. This defined media can be tailor made specific for particular cell types and experimental conditions. In this chapter, preparation of DMEM is described.

Materials and Equipment

1. Dulbecco's Modified Eagle's Medium (DMEM) with glucose, L-glutamine, sodium pyruvate, without sodium bicarbonate (powdered media).
2. Deionized water
3. Sodium bicarbonate
4. 70% (v/v) ethanol
5. One 1-L sterilized bottle
6. Sterile bottle top filter with size porosity 0.22 μ m
7. Biological safety cabinet Type A2

Method

1. Wipe the biological safety cabinet with 70% (v/v) ethanol.
2. Put the sterilized bottle and the bottle top filter in the cabinet.
3. Transfer 950 mL of deionized water into another bottle.
4. Add the powdered media into the bottle and stir it gently until it dissolves.
5. Rinse the DMEM packet with deionized water and transfer it to the rest of the media.
6. Add 3.7 g of sodium bicarbonate to the stirred media and let it dissolves.

7. The final pH of the media should be 7.4. However, the media pH must be adjusted to 0.2–0.3 below the desired pH using 1 M of NaOH or 1 M of HCl. Normally the pH value will increase about 0.1–0.3 upon filtration.
8. Filter the media with bottle top filter into a 1-L sterilized bottle in the cabinet.
9. Label the bottle with the media name, date, and name of the person who prepared the media.
10. Store the media at 4 °C. The media will last longer up until one year if it is stored in the dark at 4 °C.

Notes and Tips

The sterility of the filtered media can be confirmed by checking the color of the prepared media (transfer 5 mL of the media into a 25-cm² T-flask) that is incubated in the CO₂ incubator after three days. If the color turns to cloudy or whitish hyphae is observed in the media, there is bacterial or fungi contamination. The media must be autoclaved before discarded.

18.4 Thawing and Recovering Mammalian Cells from Cryopreservation

Cells thawing from cryopreservation is the most critical procedure in the cell culture routine. It must be done quickly with care. Routinely, cryopreserved cells are stored in complete media containing 5–10% of dimethyl sulfoxide (DMSO) to avoid formation of crystal and degradation of the frozen cellular constituents. Although DMSO is harmful to cells in culture medium, it helps to maintain cellular membrane during the freezing-thawing process. From this procedure, it is estimated that only 50% of the cryopreserved cells will survive. Therefore, a high number of cells (more than 1,000,000 cells/mL) in the cryopreservation will have a high chance for cell survival.

Materials and Equipment

1. Cryopreserved cultures of cells
2. Complete media (DMEM supplemented with 10% fetal bovine serum, FBS)
3. 70% (v/v) ethanol
4. Sterile 25-cm² T-flasks or 60-mm petri plates
5. Sterile centrifugal tubes
6. Sterile serological pipettes
7. Biological safety cabinet Type A2
8. Incubator with 5% CO₂
9. Refrigerated centrifuge
10. Water bath

Method

1. Remove the cryopreserved vials from the $-80\text{ }^{\circ}\text{C}$ freezer or the liquid nitrogen tank. Examine the labels for cell type, passage number, and date of storage to ensure that you have the correct cell line. Warm the frozen vials in the water bath set at $37\text{ }^{\circ}\text{C}$ and ensure that the water in the water bath do not wet the cap of the vials to prevent contamination. The procedure should be done very quickly (about 1–2 min) to prevent the breakage of cellular membrane due to the formation of DMSO crystallization.
2. Remove the vials from the water bath and wipe down well with 70% (v/v) ethanol. Quickly transfer the vials into a biological safety cabinet and mix well with 9 mL of a complete cell culture medium in a 15-mL tube.
3. Close and label the tubes properly. Then using a balanced tube, separate the cells at about $120 \times g$ (1000–1500 rpm) using a refrigerated centrifuge ($4\text{ }^{\circ}\text{C}$) for about 3 min. The cells will separate from the media by forming a pellet at the bottom of the tube. The top clear liquid is called supernatant.
4. Using a sterile pipette, remove the supernatant carefully without affecting the pellet.
5. Then, using another sterile pipette, resuspend the cells pellet with 5 mL of fresh complete medium and transfer the mixture into a culture plate or 25-cm² T-flask containing 5 mL of complete medium.
6. Gently swirl the flask and avoid wetting the flask's cap.
7. Using inverted microscope, observe the cells. You should find many cells are suspended in the media.
8. Put the flask in an incubator with 5% CO₂ at $37\text{ }^{\circ}\text{C}$.
9. Cells may take up about 5–24 h or more to settle and attach to the bottom of the flask and later divide. For those cells that may not survive the freezing-thawing process, they will not attach onto the flask. Therefore, after 24 h, change the cell culture media and replenish with a new culture media.

Notes and Tips

To remove the vials from the $-80\text{ }^{\circ}\text{C}$ freezer or the liquid nitrogen tank, protective clothing or lab coat, gloves, and goggles must be worn.

18.5 Detachment and Subculturing of Mammalian Cells from Flask/Plates

When a cell line is cultured, a lag period after seeding is usually followed by exponential growth called the log phase. When the cell density reaches a level such that all the available cell growth area is occupied (100% confluence), or the media in the flask could no longer support the growth of high cell concentration present in the flask, the cell growth will reduce and greatly decrease; then the medium must be replaced or the culture should be divided (subculture). Subculturing of two types of culture, monolayer and suspension culture are discussed in Sects. 18.5.1 and 18.5.2.

18.5.1 Subculture of Cells in Monolayer Cultures

The first step in cells subculturing from monolayer cell culture is to detach cells from the surface of the primary culture vessel by the use of accutase, trypsin, or mechanical means. This is followed by transferring a fraction of the detached cells to a new culture medium to grow inside a new culture vessel.

Materials and Equipment

1. 100% confluence cultures of cells
2. Complete media (DMEM supplemented with 10% FBS)
3. Sterile serological pipettes
4. Biological safety cabinet Type A2
5. Incubator with 5% CO₂
6. Refrigerated centrifuge
7. Inverted microscope
8. Sterile 25-cm² T-flasks or 60-mm petri plates
9. Phosphate buffer saline (PBS)
10. Accutase or trypsin

Method

1. Discard the medium from the flask containing 100% confluence cultures with a sterile serological pipette. Wash the monolayer cells with 5 mL of 37 °C PBS (for culture in 25-cm² flask) to remove the residual FBS.
2. Add 1 mL of 37 °C accutase/trypsin solution to the culture which covers the adhering cell layer.
3. Place the 25-cm² T-flasks or petri plate in an incubator with 5% CO₂ at 37 °C for 2–3 min. Observe the culture under the microscope to ensure that cells are rounded up and dissociate from the flask surface.
4. Add 8 mL of warm (37 °C) complete medium into the flask. Transfer the cell suspension into sterile centrifuge tubes. Centrifuge the tubes for 5–6 min at 120 × g using a refrigerated centrifuge at 4 °C. Throw away the supernatant that contains accutase or trypsin. Resuspend the cell pellet with 5 mL of complete media.
5. Transfer at least 1 mL of the cell suspension into well labeled culture vessels or flasks.
6. Put 4 mL of fresh complete media into the flask and incubate them in an incubator with 5% CO₂ at 37 °C.
7. In some cases, a fresh media must be fed to the cultures after 3 or 4 days by discarding the old media first.
8. When cultures become confluent, passage the culture by repeating steps 1 to 6.

Notes and Tips

- Cells can be counted using a hemocytometer then diluted to the desired cell concentration therefore a specific number of cells can be transferred to the culture flask.

- For primary cultures and early subcultures, 60-mm petri plates or 25-cm² flasks are generally used. Larger vessels (e.g., 150-mm plates or 75-cm² flasks) may be used for the subsequent subcultures.
- Culture vessels should be labeled with the passage number and date of subculture.
- For culturing cells using 75-cm² culture flasks, 10 mL of medium should be added per flask.
- CO₂ incubators with 5% CO₂ and 4% O₂ should be used because the low oxygen concentration encourages the cell growth and stimulates a good *in vivo* environment of cells.

18.5.2 Subculture of Cells in Suspension Cultures

A suspension culture requires the same incubation condition as in the monolayer culture. Subculturing of suspension cultures is less complicated than subculturing of monolayer cultures because the cells are not adhering to the vessel surface. No detachment or dispersion is needed prior to subculturing.

Materials and Equipment

1. 100% confluence cultures of cells
2. Complete media (DMEM supplemented with 10% FBS)
3. Sterile serological pipettes
4. Biological safety cabinet Type A2
5. Incubator with 5% CO₂
6. Sterile 25-cm² T-flasks
7. 70% (v/v) ethanol
8. Isopropanol
9. Mr. Frosty container

Method

1. Gently take out the flask containing suspension cells from the CO₂ incubator so that the suspension cells that settled at the bottom of the 25-cm² T-flasks are not disturbed.
2. Using sterile serological pipette, remove approximately one-third of the medium from the culture flasks and add an equal volume of 37 °C fresh medium. Gently stir the flask to homogenize the cells with the media.
3. Put back the culture flask into the incubator. If there is less than 20 mL of medium in the flask, place the flask in horizontal position inside the incubator to encourage cell/medium contact. For higher volume, vertical incubation of flask can be applied.
4. Check the culture regularly. Gently swirl and stir to resuspend cells.

5. When suspension cultures reaches confluency ($\sim 2 \times 10^6$ cells/ml), subculturing should be performed as follows:
 - a. Take out the flask from the incubator and gently swirl the flask to distribute the cells evenly in the media.
 - b. Transfer half of the cell suspension volume into a new flask.
 - c. Add 7–10 mL of fresh medium to the new flask and put it back into the incubator.

18.6 Cryopreservation of Mammalian Cells

Cryopreservation of cells involves cell suspension in 10% DMSO in FBS or complete medium to prevent formation of crystal inside the cells and damage to the cells. To maintain cellular viability, the cells have to be placed in a freezing container called Mr. Frosty (Nalgene Ltd, USA) before being placed in a -80 °C freezer. The container is filled with isopropanol to prevent rapid cooling where the temperature is slowly decreasing at the rate of -1 °C/min. During the freezing and thawing, many cells will die. Due to that, higher concentration of 1×10^6 cells/mL is preferred to ensure cell survival.

18.6.1 Cell Cryopreservation of Monolayer Cultures

Materials and Equipment

1. 100% confluence culture of cells
2. Complete media (DMEM supplemented with 10% FBS)
3. Freezing medium (FBS with 10% [v/v] DMSO)
4. Biological safety cabinet Type A2
5. Incubator with 5% CO₂
6. Refrigerated centrifuge
7. Inverted microscope
8. Sterile 25-cm² T-flasks or 60-mm petri plates
9. 70% (v/v) ethanol
10. Phosphate buffer saline (PBS)
11. Accutase or trypsin
12. Sterile serological pipettes
13. Isopropanol
14. Mr. Frosty container

Method

1. Discard the medium from the flask containing 100% confluence cultures with a sterile serological pipette. Wash the monolayer cells with 5 mL of 37 °C PBS (for culture in 25-cm² flask) to remove the residual FBS.
2. Add 1 mL of 37 °C accutase/trypsin solution to the culture which covers the adhering cell layer.
3. Place the 25-cm² T-flasks or petri plate in an incubator with 5% CO₂ at 37 °C for 2–3 min. Observe the culture under the microscope to ensure that cells are rounded up and dissociate from the flask surface.
4. Add 8 mL of warm (37 °C) complete medium into the flask. Transfer the cell suspension into sterile centrifuge tubes and rinse the bottom of the flask two or three times with fresh media to detach the remaining adherent cells. Centrifuge the tubes for 5–6 min at 120 × g using a refrigerated centrifuge at 4 °C. Throw away the supernatant that contains accutase or trypsin. Resuspend the cell pellet with 5 mL of complete media.
5. Count the cells using a hemocytometer (Sect. 18.7) and transfer them into a 15-mL tube.
6. Spin the cell suspension at 120 × g for 3 min at 4 °C to separate the cells from the suspension. Then remove the supernatant and add cell cryopreserved medium containing 10% DMSO in FBS to the pellet. Mix the medium and the pellet well by pipetting up and down slowly. Transfer 1 mL of the mixture into labeled 2-mL cryovials (freezing cells from 25-cm² flask requires 2 mL of freezing solution).
7. Place the vials in Mr. Frosty container for overnight in a –80 °C freezer before storing in a liquid nitrogen tank or in a –140 °C freezer.

18.6.2 Cell Cryopreservation of Suspension Cultures

The method of freezing cells from suspension culture is almost similar to freezing cells from monolayer cultures. The major difference is that the suspension cultures do not require cellular detachment from the surface using accutase or trypsin.

Materials and Equipment

1. Suspension cultures of cells
2. Complete media (DMEM supplemented with 10% FBS)
3. Freezing medium (FBS with 10% [v/v] DMSO)
4. Biological safety cabinet Type A2
5. Refrigerated benchtop clinical centrifuge
6. Sterile 25-cm² T-flasks or 60-mm petri plates
7. 70% (v/v) ethanol
8. Sterile serological pipettes
9. Isopropanol
10. Mr. Frosty container

Method

1. Take out the flask containing suspension cells from the CO₂ incubator
2. Using sterile serological pipette, aspirate the cell suspension from the flask and transfer it into 15-mL sterile centrifuge tubes and spin for 5–6 min at 120 × g using a refrigerated centrifuge at 4 °C. Discard the supernatant and resuspend the cell pellet with fresh complete cell culture media for cell counting.
3. Determine the cell count using a hemocytometer (Sect. 18.7) and subsequently transfer the culture into a 15-mL tube.
4. Centrifuge the cell suspension at 120 × g for 3 min at 4 °C to separate the cell from the suspension. Then remove the supernatant and add cell cryopreserved medium containing 10% DMSO in FBS to the pellet. Mix the medium and the pellet well by pipetting up and down slowly. Transfer 1 mL of the mixture into labeled 2-mL cryovials (freezing cells from 25-cm² flask requires 2 mL of freezing solution).
5. Place the vials in Mr. Frosty container for overnight in a –80 °C freezer before storing in a liquid nitrogen tank or in a –140 °C freezer.

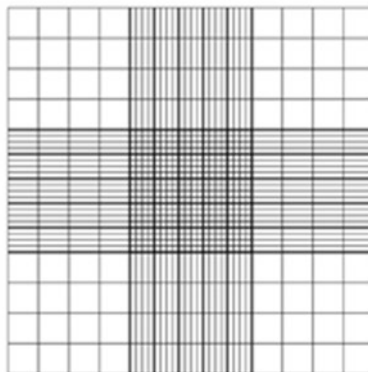
Notes and Tips

- Styrofoam boxes can be used as a substitute to Mr. Frosty (with isopropanol) for freezing cells in a –80 °C freezer for overnight. The cryovials should be covered at all sides in wet wipes/tissues and placed in the container. Label with your name, date, cell type, and passage.
- For routine freezing procedure, estimation of cell concentration can be predicted. Normally, for 100% confluent T25 flask, more than 4 × 10⁶ cells/mL can be harvested and placed in four cryovials with 4 mL of cryopreserved medium (Note that the cell concentration varies with cell types).
- Freezing media of DMSO and FBS can be stored in a refrigerator.
- DMSO is light sensitive. Cover DMSO with aluminium foil to keep it in the dark.

18.7 Mammalian Cell Counting

Cell counting is the most important step in standardization of cell culture. Hemocytometer is a device invented by Louis-Charles Malasses (Verso 1971) to measure cell concentration. It is made of a glass slide with a grid on each half (Fig. 18.1). Each grid is made of nine squares and each square is subdivided into smaller squares. The grid is covered by a cover slip and creates a chamber which can hold up to 0.1 µL of liquid. It is very important to use the hemocytometer cover which is thick and even-surfaced cover slip because ordinary cover slips have uneven surfaces that may cause errors in cell counting. In order to count, a small sample (0.1 µL) of known volume of trypsinized cells will be placed in the hemocytometer chamber. Based on the volume in each square, the concentration of cells can be determined.

Fig. 18.1 Grids in a hemocytometer



Materials and Equipment

1. Suspension cultures of cells
2. 0.4% (w/v) trypan blue solution
3. Hemocytometer with coverslip
4. Hand counter
5. Inverted microscope
6. 70% (v/v) ethanol

Method

1. Prepare a hemocytometer by cleaning its surface and coverslip with 70% (v/v) ethanol.
2. Prepare cell suspension (preparation of cell suspension depends on the type of culture either monolayer or suspension by following the protocols in Sects. 18.5.1 and 18.5.2, respectively).
3. Put trypan blue to the cell suspension on an ordinary slide. Trypan blue will stain dead cells only, thus viable cells can be counted. Mix thoroughly using a pipette and let it stand for 5 min before loading to the hemocytometer.
4. Load the cell suspension to the hemocytometer using a sterile Pasteur pipette at the edge of the hemocytometer counting chamber..
5. Allow the cells to settle for 2–3 min before counting and remove the excess liquid.
6. Count the cells found in the four corners of one counting chamber and also other counting chambers of the hemocytometer (Fig. 18.1).
7. Calculate the cell number using the following equation:

$$\text{Cell number (cells/mL)} = \text{average count per square} \times \text{dilution factor} \times 10^4$$

Notes and Tips

- A hemocytometer is a nonsterile equipment. The pipette used to transport cells to the hemocytometer must not be reused with the original suspension.
- Handle hemocytometers carefully as they are expensive and break if it is drop.
- Make sure the cell suspension is homogenous and not clump by pipetting them up and down to warrantee accurate cell count.
- The viability of cells may deteriorate over time after trypsinized and detach from the flask thus it is vital to fasten the cell counting rather than to have accurate reading.
- Observe your cells in the culture prior trypsinization to ensure a higher number of cells for calculation.
- Trypan blue will stain dead cells only, thus viable cells can be observed as shining under the microscope and can be counted accurately. The trypan blue transverse inside the dead cells through their porous membranes and stain them blue.

References

- Dulbecco R, Freeman G (1959) Plaque production by the polyoma virus. *Virology* 8:396–397
- Eagle H (1959) Amino acid metabolism in mammalian cell cultures. *Science* 130:432–437
- Freshney RI (2005) Culture of specific cell types. Wiley Online Library
- Hayflick L, Moorhead PS (1961) The serial cultivation of human diploid cell strains. *Exp Cell Res* 25:585–621
- Masters JR (2002) HeLa cells 50 years on: the good, the bad and the ugly. *Nat Rev Cancer* 2:315–319
- Moore GE, Gerner RE, Franklin HA (1967) Culture of normal human leukocytes. *JAMA* 199:519–524
- Ozturk S, Hu W-S (2005) Cell culture technology for pharmaceutical and cell-based therapies. CRC Press, Boca Raton
- Verso ML (1971) Some nineteenth-century pioneers of haematology. *Med Hist* 15:55–67

Chapter 19

Integrated Data Analysis Model for Screening Cell Line Producer



Nor Fadhillah Mohamed Azmin

Abstract The complexity of bioprocess data generated from the manufacture of recombinant monoclonal antibodies cell line sparks the chemometrics study of the datasets. The ultimate goal is to form a link between the data and its underlying biological patterns. A concatenated protocol, specifically discrete wavelet transform and multiway principal component analysis techniques, is recommended to successfully extract meaningful information from the complex datasets.

Keywords Cell lines · Monoclonal antibodies · Screening · Selection · Algorithm · Fourier transform infrared (FTIR) · Near infrared (NIR) · Electrospray ionization (ESI-MS) · Principal component analysis (PCA) · Binning · Wavelet transform · Score plot · Loading plot · Contribution plot

19.1 Introduction

The high cost of generating cell lines for recombinant monoclonal antibodies (mAbs) production necessitates the improvements in production techniques to ensure product quality, a reduction in development timelines, and an increase in cost efficiency. Enhancements in the initial steps of the development process would reduce the time from development to commercialization. One of the major challenges in the development process involves the rapid screening and selecting of highly productive and stable cell lines from the transfectant population (Li et al. 2010). Figure 19.1 shows the general procedure for the selection of a recombinant mAbs cell line. In paving the way towards commercialization, one key issue is to identify the criteria that differentiate between high and low producer cell lines.

One approach to expedite the identification process is via selection algorithm. Selection algorithm can be implemented if the spectral measurements of the process or samples are recorded in addition to offline sample analysis (e.g., viable and total

N. F. M. Azmin (✉)

Department of Biotechnology Engineering, Kulliyah of Engineering, International Islamic University Malaysia, Kuala Lumpur, Malaysia
e-mail: norfadhillah@iium.edu.my

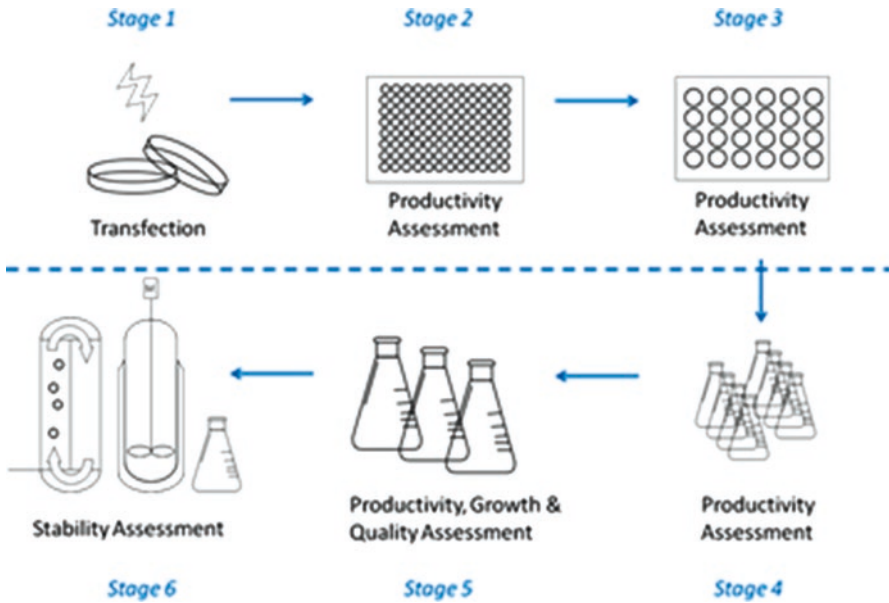


Fig. 19.1 General strategy for recombinant MAb cell line selection

cell count and media components). Some of the popular spectral measurements are Fourier transform infrared (FTIR) spectra, near infrared (NIR) spectra, nuclear magnetic resonance (NMR) spectra, and electrospray ionization-mass spectroscopy (ESI-MS). The selection algorithm is useful in extracting meaningful information from the data set and interpret the information inherent within the data. The extraction of information from a complex data set is related to the technical challenges summarised by Hilario et al. (2006).

This chapter is intended to describe and guide readers to construct a selection algorithm that is useful to identify the criteria of high and low producer cell lines. As an example, the procedures for the construction of selection algorithm applied to ESI-MS data of Chinese hamster ovary (CHO) cell lines will be the case study.

19.2 Objective

The goal of this chapter is to distinguish and characterize the criteria that enable differentiation between high and low producers of CHO cell lines. This approach exploits the concepts of data mining, signal processing, and multivariate statistical data analysis.

19.3 Process Description

The basis of this study is the manufacture of recombinant MAb cell lines. The selection strategy is shown in Fig. 19.1. The host cell line is first transfected with an expression vector. The transfected cell lines are then diluted and cultivated in 96-well plates and screened for highly productive cell lines. The selected cell lines progress to the next stage with non- or low cell line producers being discarded. The selected cell lines are then cultivated in 24-well plates followed by another screening process. The next two stages involve the cultivation of the selected cell lines in shake flasks to mimic a batch process and a fed-batch process. Each stage is followed by a screening process. After the screening process in the fed-batch stage, the selected cell lines are cultured in small-scale bioreactors for cloning purposes, stability assessment, and bioreactor studies. Cell pellets from the small-scale bioreactor stage are collected and analyzed using the liquid chromatography electrospray ionization-mass spectroscopy (ESI-MS) platform.

19.4 Method of The Construction of the Selection Algorithm

The construction of the algorithm and all simulations were carried out on MATLAB platform; utilizing the Wavelet toolbox where necessary.

19.4.1 Preprocessing of Data Matrix

1. Start by converting the files produced by the liquid chromatography electrospray ionization mass spectrometry (LC-ESI-MS) platform from Bruker file format to the mzML file format, which is a universal data format for mass spectrometer output.
2. Align the data from all samples. Note that the ESI-MS generated are of unequal length.
3. Establish the ESI-MS data set for each cell line replicate (Fig. 19.2) as a three-dimensional data set with the following dimensions:
 $\text{Length} \times \text{Width} \times \text{Height} = \text{mass-to-charge ratio of ions (m/z)} \times \text{retention time (t}_R\text{)} \times \text{intensity of the ions (I)}$.
4. Concatenate the three-dimensional data set of each cell line replicate to form a three-dimensional matrix \underline{X} . The convention of matrix is
 $\underline{X} = \text{mass-to-charge ratio of (J)} \times \text{retention time (K)} \times \text{intensity of the ions (I of } C_L\text{)}$.
 Where cell line replicates, $C = 1 \dots L$ (Fig. 19.2).
5. Bin the intensity (I) of the ESI-MS data concerning retention time (t_R) and the mass-to-charge ratio (m/z).

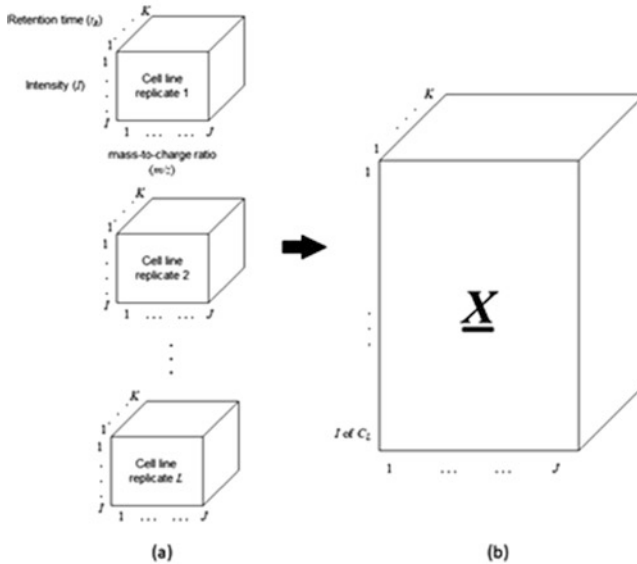


Fig. 19.2 Three-dimensional data matrix of the ESI-MS data

- (a) Determine the bin size such that it is comparable with the spectra peaks width in time and m/z ratio. If the bin size is too large, the binned data may have poor resolution of the peaks (Krishnan et al. 2012)
 - (b) The binning procedure shall be performed by dividing the retention time, t_R , (elution time from the liquid chromatography system) and m/z range into equally spaced intervals.
6. Unfold the three-dimensional data matrix \underline{X} to a two-dimensional data matrix \underline{X} ($C_L \times (I \times J \times K)$), as in Fig. 19.3.
- Note: The rows of \underline{X} represent cell lines and their replicates, and the columns represent the intensity of the ESI spectra after binning on retention time and m/z ratio. This method of unfolding allows the variability in the data to be observed as it accentuates the similarities and dissimilarities between cell lines and also cell replicates (Fig. 19.4).*
7. At this stage, the data matrix \underline{X} requires rescaling due to the differences in units and scales of the variables. There are two well-known methods for rescaling data, which are normalization and standardization. Scaling of the data removes the unwanted variations between measurements whilst retaining the meaningful biological variation (Katajamaa and Oresic 2007).
- (a) In normalization, the numerical variables are scaled in such a way that they are in the range of '0' and '1'. Commonly used normalization formula is expressed in Eq. 19.1:

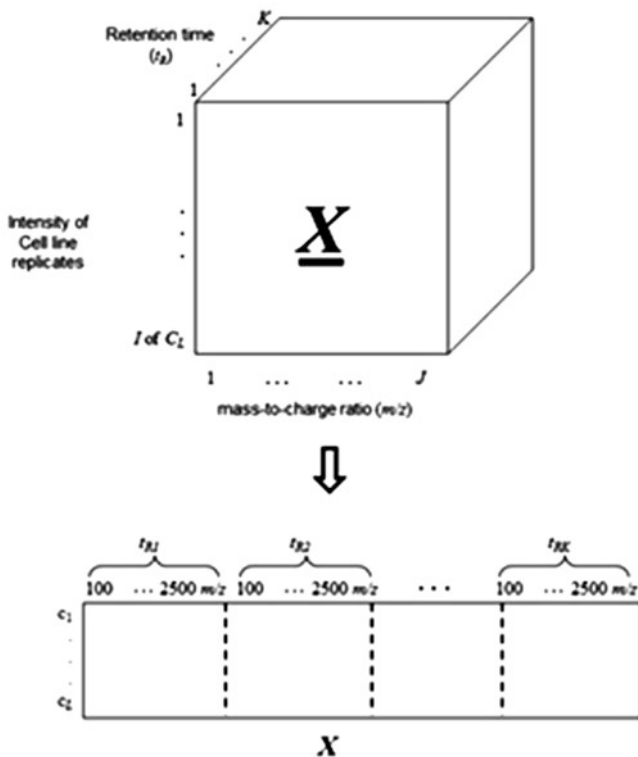


Fig. 19.3 Unfolding of the three dimensional ESI-MS data set to two dimensional matrix after binning on retention time and mass-to-charge ratio



Fig. 19.4 Identify the minimum, maximum, mean and standard deviation of each row

$$X_{\text{new}} = (X - X_{\min}) / (X_{\max} - X_{\min}) \tag{19.1}$$

where

X = current data point

X_{\min} = minimum value of X in the row

X_{\max} = maximum value of X in the row

- (b) In standardization, the data matrix X will be transformed to have zero mean and unit variance by calculating the new data point using Eq. 19.2:

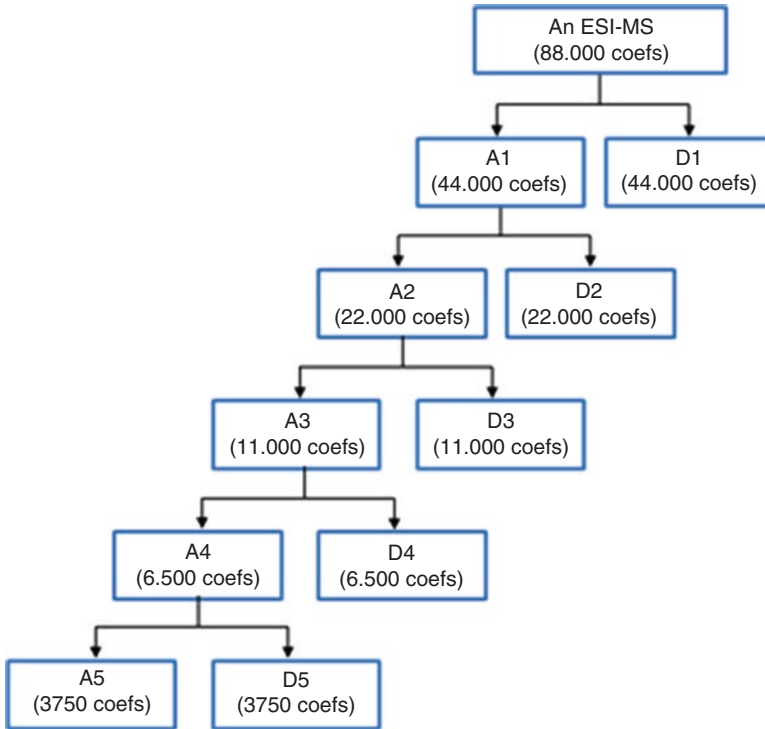


Fig. 19.5 An example of five level of wavelet decomposition of an ESI-MS

$$X_{\text{new}} = (X - \text{mean}(X)) / \text{std}(X) \quad (19.2)$$

where

X = current data point

$\text{mean}(X)$ = mean of the row

$\text{std}(X)$ = standard deviation of the row

8. Apply wavelet transform to the scaled data matrix using a suitable analyzing wavelet and decomposition levels.

Note: This transformation procedure is known as multiresolution wavelet decomposition where it will decompose each spectrum into two types of sub-band, which are a sub-band of useful information or a sub-band of noise, denoted as A and D in Fig. 19.5, respectively. The number of sub-bands depends on the number of decomposition level. For the ESI-MS data in this case study, it was decomposed into five (5) levels. This resulted in six sub-bands which were used for the next step as shown in Fig. 19.5.

9. (Optional) If you have the measurements of the product quality parameters such as total cell density, viable cell density, and glucose concentration, you can use them to classify the cell lines as producers or non-producers. Then you can

randomly divide the cell lines into a training set and a test set where each set shall comprise both producers and nonproducers.

10. Apply principal component analysis (PCA) to each sub-band obtained from the wavelet transform.

Note: This step provides a close inspection of the data at different resolutions.

11. (Optional) It is possible to reconstruct the wavelet sub-bands and subsequently apply PCA. However, this deters close inspection of the data at different resolutions.

19.5 Discussion

Upon completion of the wavelet decomposition and the implementation of PCA, you should be able to analyze the ESI-MS dataset using two approaches. One approach is to combine the PCA results from all sub-bands and generate the common plots for PCA. Another approach is to generate the common PCA plots for each wavelet sub-band.

The common PCA plots include:

- scree plot
- scores plot
- loading plot
- contribution plot

For the scree plot, the number of principal component (PC) retained for combined or individual sub-band may differ due to the percentage of variance explained. It is best to retain the number of PCs which can explain at least 80% of the variance in the dataset. The scree plots will be used to select the number of scores, loading, and contribution plots required for further inspection of the data set.

For the ESI-MS data set used in this case study, some of the observations are:

- The number of principal components retained for each sub-band varies from 6 to 14.
- The contribution plots of the wavelet sub-bands exhibit that most cell lines replicate
- differ from each other despite coming from the same cell lines.
- It is very important to note that the result of the above-mentioned plots may vary depending on the data set in any particular study.

References

- Hilario M, Kalousis A, Pellegrini C, Muller M (2006) Processing and classification of protein mass spectra. *Mass Spectrom Rev* 25(3):409–449.
- Katajamaa M, Oresic M (2007) Data processing for mass spectrometry-based metabolomics. *J Chromatogr A* 1158(1–2):318–328

- Krishnan S, Vogels JT, Coulier L, Bas RC, Hendriks MW, Hankemeier T, Thissen U (2012) Instrument and process independent binning and baseline correction methods for liquid chromatography-high resolution-mass spectrometry deconvolution. *Anal Chim Acta* 740:12–19
- Li F, Vijayasankaran N, Shen A, Kiss R, Amanullah A (2010) Cell culture processes for monoclonal antibody production. *MAbs* 2(5):466–479

Index

A

- Ammonium sulfate, 98–103
- Anabolism, 14
- Aqueous two-phase system (ATPS)
 - binodal curve
 - chemicals, 78
 - composition, 81
 - consumable items, 77
 - equipments, 78
 - graphical representation, 79
 - importance, 75
 - partition coefficient, 77
 - and phase diagram, 78–80
 - purification factor, 76
 - refractive index, 79, 81
 - salt conductivity, 79, 80
 - specific activity, 76
 - tie-line length, 79
 - volume ratio, 77
 - formation, 75
- Arabidopsis thaliana* (*A. thaliana*) suspension culture
 - ecotype cell growth, 210
 - fresh weight, dry weight and pH, 209–213
 - growth and sugar profiles, 211, 212
 - growth kinetics, light conditions, 211
 - intracellular metabolites, 212
 - pH reading, 212, 213
- Arachidate acid, 71, 73
- Aspergillus niger*, 112
- Atmospheric carbon dioxide, 53
- Atom-transfer radical polymerization (ATRP), 146, 147

B

- Bacterial artificial chromosomes (BACs), 26
- Bacterial growth measurement, 40
- Bacterially expressed cofactor-independent phosphoglycerate mutase from *Leishmania mexicana* (Lm-iPGAM), 168, 169, 172, 173, 175–177
- Bacterial strain isolation method from contaminated soil, 197–202
- Halophilic bacteria
 - bile-tolerance, 14
 - BSA, standard curve, 20
 - chemicals and reagents, 15
 - colony and bacterial morphology, 18
 - consumable items, 15
 - crude enzyme preparation, 17
 - culture methods, 14
 - enzymatic activity, 19
 - enzyme assay, 21
 - equipments, 15
 - extracellular protease activity, screening of, 16
 - gram staining, 16–17
 - isolates, activity, 21
 - liquid media (broth), 14
 - materials, 15
 - milk salt agar, 14
 - nutrient agar, 19
 - protease assay, 17–19
 - protein content of samples, 21, 22
 - protein determination, 18
 - for proteolytic activities, 16

- Bacterial strain isolation method (*cont.*)
 spread plate technique, 14
 tyrosine, standard curve, 19, 20
- Bile-tolerance, Halophilic bacteria, 14
- Binning procedure, 230, 231
- Binodal curve for PEG1500
 chemicals, 78
 composition, 81
 consumable items, 77
 equipments, 78
 graphical representation, 79
 importance, 75
 partition coefficient, 77
 and phase diagram
 concentration of salt and PEG, 80
 end nodes for, 79
 system composition for, 78
 purification factor, 76
 refractive index, 79, 81
 salt conductivity, 79, 80
 specific activity, 76
 tie-line length, 79
 volume ratio, 77
- Biodiesel production
 alkaline catalysts, 83
 heterogeneous catalysts
 cockle waste shell, 85
 coconut waste (*see* Coconut waste)
 duck and chicken egg shells, 85
 eggshell waste (*see* Eggshell)
 high temperature, 84
 vs. homogeneous catalysts, 84
 jatropha oil, 85
See also Fatty acid methyl ester (FAME)
- Biomolecules immobilization, 151
- Bioremediation, 198
- Biosensor-related research, 151
- Biosensors
 analytes, 120
 biologically-derived sensing element, 119
 biorecognition and transduction elements,
 120, 121
 conductivity, 152
 immobilization process, 152
 materials architecture, 151
- Block copolymer (BCPs)-based composites,
 161–162
- Blue-green algae, 54–55
- Bovine serum albumin (BSA), 18, 20, 98–100,
 102, 103, 157, 191
- Bradford assay method, 99
- Bradford method, 191
- 1-4 Butanediol, 146
- C**
- Calcination, 85, 87–90
- Calcium oxide, 65, 66
- Calorimetric transducers, 120, 121
- Capric acid, 71, 73
- Caprylic acid, 71, 73
- Carbon-based materials, CPs, 153–154
- Caseinolytic assays, 47, 49
- Cell biology investigation, 215
- Cell counting, mammals, 224–226
- Cell culture technology
 cell biology investigation, 215
 cryopreservation, thawing and recovering
 mammalian cells, 218–219
 detachment and subculturing of
 mammalian cells from flask/plates,
 219–222
 drug discovery and development, 215
 genetic and phenotyping analysis, 215
 intra- and intercellular activities, 215
 in mammals (*see* Mammalian cell culture)
 media preparation
 Dulbecco's Modified Eagle's Medium,
 217
 α -Eagle's Minimal Essential Medium,
 217
 sterility, 218
 medical diagnosis and treatment, 215
 proteomics, 215
 recombinant protein production, 215
 study of toxicology, 215
- Cell DNA repair system, 9
- Cell lines, 215, 216, 219
 producer screening, integrated data
 analysis model, 227–233
- Cell morphology by gram staining, 46
- Cell motility by hanging drop method, 46
- Cellulose-based composites, 156
- Cellulose nanofibers (CNs), 133
- Cell viability and medium conductivity, 204
- Cervical carcinoma cell line, 215
- Chain extender, 146
- Chemical mutagens, 55
- Chemical mutation method
 mutagens, 55
Synechococcus sp. PCC 7002, mutagenesis
 process, 58
- Chinese hamster ovary (CHO) cell lines, 228
- Chitin- and chitosan-based composites,
 154–156
- Chromatogram, 67, 70–72, 209, 210
- Cloning, small-scale bioreactors, 229
- Cockle waste shell, 85

- Cocoa pod husk (CPH), 98, 110, 112, 113, 115
- CO₂ concentrating mechanism (CCM), 55
- Coconut waste, 66, 67, 73
- preparation
- catalyst characterization, 89
 - catalyst preparation, 88
 - chemicals and reagents, 86
 - equipment, 86
 - flow diagram, 87
 - scanning electron microscopy analysis, 89, 90
 - transesterification process, 89
- CO₂ fixation by photoautotrophic algae cultures, 54
- CO₂ mitigation research, 55
- Community genomics, 25
- Condensation polymerization, 141, 142
- Conductive polymers (CPs), 152
- and carbon-based materials, 153–154
 - and metal nanoparticles, 152–153
- Continuous coupling enzyme assay, 175–177
- Contribution plot, PCA, 233
- Controlled radical polymerizations (CRP), 146–147
- Cross-linked enzyme aggregates (CLEAs)
- FESEM images, 106
 - glutaraldehyde in aqueous solution, 97
 - lipase activity assay, 98–99
 - lipase preparation, 99–100
 - materials, 98
 - optimum temperature, 101, 103, 104
 - parameters affecting, 100
 - pH, 101, 103, 104
 - recyclability study of, 105
 - reusability of CLEA-lipase, 101
 - stability tests, 101, 104, 105
- Cross-linked enzyme crystals (CLECs), 96
- Crude enzyme preparation, Halophilic bacteria, 17
- Culture methods, Halophilic bacteria, 14
- CV, *see* Cyclic voltammetry (CV)
- Cyanobacteria, 54–55
- mutagenesis in, 55
 - See also* Cyanobacterium *Synechococcus sp.* PCC 7002, marine microalgae strain
- Cyanobacterium *Synechococcus sp.* PCC 7002, marine microalgae strain
- ATCC 957 agar, 57, 58
 - chemical mutation, 58
 - culture medium, 57
 - equipment use, 56
 - materials, 56
 - mutant isolation, 58–60
 - mutated species adaptation, 60
 - trace metal solution, 57
- Cyclic voltammetry (CV), 123, 134, 135
- electrochemical cell setup, 124, 125
 - experiments, 125
- ## D
- Dextran-based composites, 156–157
- Digestive enzymes
- amylase, 43
 - lactase, 43
 - pepsin, 43
- DNA fragment size and concentration, 34
- DNA inserts recovery, 36
- DNA sequencing, 6
- Docosanoic acid, 71, 73
- Double-stranded deoxyribonucleic acid (dsDNA) vector, 2
- DpnI* endonuclease
- recognition site, 2
 - restriction enzyme digestion, 5
- Drug discovery and development, 215
- Dry weight (DW) analysis, 204, 206
- A. thaliana* suspension culture, 209–213
- Duck and chicken egg shells catalyst, 85

E

Earth System Research Laboratory (ESRL), 54

Ecogenomics, 25

Eggshell, 65–67

 - waste preparation
 - catalyst characterization, 89
 - catalyst preparation, 89
 - chemicals and reagents, 86
 - equipment, 86
 - flow diagram, 88
 - scanning electron microscopy analysis, 89, 90
 - transesterification process, 89

EGuia

 - antibiotic resistance gene (kanamycin), 9
 - DNA sequencing result, 7
 - endoglucanase I, *Fusarium oxysporum*, 7
 - forward (sense) and reverse (antisense) DNA mutagenic primers, 7
 - mutation, 7
 - T224E mutant *vs.* wild type
 - amino acid sequence alignment, 7, 9
 - nucleotide alignment, 7, 8- wild-type, 7

- Electrochemical transducers, 120
 advantages, 121
 chemical reactions into electrical signals, 121
 chronoamperometry, 135
 CV plots, 123–125, 127–130
 electron transfer, solution-electrode interface, 123
 materials, 126, 133, 134
 methods, 126–127, 134–135
 principles of, 122–123
 redox reaction kinetics, electroactive species, 121
- Electrophoretic analysis of protein, 173–175
- Electroporation, 32
- Electrospray ionization-mass spectroscopy (ESI-MS), 228
- End-repair of insert DNA, 32–35
- Enrichment strategies, metagenomic DNA, 25–30
- Environmental genomics, 25
- Environmental safety & health (ESH)
 considerations and hazards, 56
- Enzyme immobilization
 adsorption, 94
 covalent binding, 94–95
 cross-linking
 CLEAs (*see* Cross-linked enzyme aggregates (CLEAs))
 CLECs, 96
 entrapment, 95–96
 membrane confinement, 96
- Enzymes
 biocatalysts, 43
 immobilization (*see* Enzyme immobilization)
 industrial and medical applications, 43
- EPI300T1R plating strain, 41
 cell transformation, 38
- Esterfip-H process, 84
- Ethyl methanesulfonate (EMS), 55
Synechococcus sp. PCC 7002, mutagenesis process
 ATCC 957 agar, 57, 58
 chemical mutation, 58
 culture medium, 57
 equipment use, 56
 materials, 56
 mutant isolation, 58–60
 mutated species adaptation, 60
 trace metal solution, 57
- F**
- Fatty acid methyl ester (FAME)
 advantages, 63
 catalyst types, 64, 65
 flow diagram, 70
- GCMS
 calibration curve, 71
 catalyst preparation, 67
 chemicals and reagents, 66
 chromatogram of palm oil, 72
 consumable item, 66
 equipment, 66
 identification, 67–68
 methyl ester composition, 73
 transesterification process, 67, 69
- palm oil
 chromatogram (*see* Gas chromatography-mass spectrometer (GCMS))
 extraction, 64
 properties, 65
 transesterification (*see* Transesterification process)
- Fermented food halophilic bacteria, 14
- Fibrinogen to fibrin, 43
- Fibrinolysis, 44
 activity, fibrin plates, 49, 50
 assay, 48
 enzymes, 43–44
- Fibrinolytic assay, 48
- Fibrinolytic enzymes
 fibrin degradation, 43
 from microorganisms
 in fermented food, 44
 in fish products, 44
 in oceans, 44
 in soil, 43
- Fibrinolytic-producing organisms, 44
- Ficus deltoidea cells, suspension cultures, total cell number, 213, 214
- Field emission scanning electron (FESEM), 106
- Field natural rubber latex
 ammonia, 180
 by-production of skim latex, 180, 181
 composition, 180
- Fitting methods, 170
- Forward and reverse primers, 4, 5
- Fourier transform infrared (FTIR)
 spectroscopy analysis, 114, 116, 228

Fresh weight (FW) analysis, 204, 206, 207
 A. thaliana suspension culture, 209–213
Functional metagenomic approach, 24–26
Fungal cellulose hydrolysis, 115
 nanocellulose fibers, 110
 with ultrasonication
 chemicals, consumables and
 equipment, 111, 112
 methods, 112–114
Fungal pretreatment, 114
Fusarium oxysporum, 2, 7, 9

G

Gas chromatography-mass spectrometer
 (GCMS)
 calibration curve, 71
 catalyst preparation, 67
 chemicals and reagents, 66
 chromatogram of palm oil, 72
 consumable item, 66
 equipment, 66
 identification, 67–68
 methyl ester composition, 73
 transesterification process, 67, 69
Gas permeability tests, 148
Gelatin-and collagen-based composites,
 157–158
Genetic and phenotyping analysis, 215
Global warming, 53
Glucose biosensor, 134
 fabrication, graphene composite-based
 transducer, 133
Glutaraldehyde, 96–103
Gram staining
 Halophilic bacteria, 16–17
 thermotolerant bacteria, cell morphology,
 46
Greenhouse gases (GHG) emissions, 53

H

Halophiles isolation, *see* Halophilic bacteria
Halophilic bacteria
 isolation of
 bile-tolerant, 14
 BSA, standard curve, 20
 chemicals and reagents, 15
 colony and bacterial morphology, 18
 consumable items, 15
 crude enzyme preparation, 17

 culture methods, 14
 enzymatic activity, 19
 enzyme assay, 21
 equipments, 15
 extracellular protease activity,
 screening of, 16
 gram staining, 16–17
 isolates, activity, 21
 liquid media (broth), 14
 materials, 15
 milk salt agar, 14
 nutrient agar, 19
 protease assay, 17–19
 protein determination, 18
 for proteolytic activities, 16
 spread plate technique, 14
 tyrosine, standard curve, 19, 20
 protein content of samples, 21, 22
 salt-tolerant enzymes, 13
Halotolerant proteases, 14
Hanging drop method, 46
Health-related risks, 197
Helmholtz model, 122
Heterogeneous catalysts, 65, 67
 biodiesel production
 cockle waste shell, 85
 coconut waste (*see* Coconut waste)
 duck and chicken egg shells, 85
 eggshell waste (*see* Eggshell)
 high temperature, 84
 vs. homogeneous catalysts, 84
 jatropha oil, 85
Hevea brasiliensis (Rubber tree), 180, 182
 concentrated latex production, 180, 181
 See also Skim latex serum
High-intensity ultrasonication, 114
High-throughput screening, metagenomic
 DNA libraries, 38–39
Homogeneous catalyst, 65
Hydrolysis reaction, 14
Hydrolytic degradation tests, 148–149

I

Inoculum preparation, 112
Integrated data analysis model, 227–233
Isocyanate, 144–145

J

Jatropha oil, 85

L

- Lambda packaging, 37
- Library construction parameters, metagenomic DNA, 39–40
 - apparatus, instruments, chemicals and biochemicals, 27–29
 - clones number, 26
 - cloning vector, 26
 - DNA extract, 25
 - gene target size, 26
 - for high-throughput screening, 38–39
 - metagenomic DNA extraction, 29–32
 - methods of, 29
 - molecular cloning, 32–38
 - pre-extraction, 25
 - sample enrichment, 29
 - stock preparation, 38
 - test antibiotics, 40
 - titer test, 38
 - using enriched metagenomic DNA, 27
 - using metagenomic DNA, 27
- Ligation titer calculation, colonies, 40–41
- Lignocellulosic substrate preparation, 112
- Lipase activity assay, 98–99
- Liquid chromatography electrospray
 - ionization-mass spectroscopy (ESI-MS) platform, 229
- Loading plot, PCA, 233

M

- mAbs, *see* Monoclonal antibodies (mAbs)
- Mammalian cell culture
 - aseptic environment and techniques, 216
 - cellular microenvironment, 216
 - cryopreservation
 - of monolayer cultures, 222–223
 - of suspension cultures, 223–224
 - detachment and subculturing of mammalian cells from flask/plates
 - in monolayer cultures, 220–221
 - in suspension cultures, 221–222
 - development of, 215
 - feeding and subculturing maintenance, 216
 - in monolayer/suspension cultures, 216
 - physiological function, 216
- Medium conductivity, 205, 208
- Metabolic enzymes
 - in blood, 43
 - catalases, 43
 - in cells, 43
 - proteases, 43
 - in tissues, 43

- Metagenomic DNA extraction
 - approaches and methods, 30, 31
 - chemical method for lysis, 29–30
 - freeze-thawing and sonication methods, 29–30
 - mechanical methods, 29–30
 - Meta-Genomic DNA isolation Kit, 30
 - procedure, 30–32
- Metagenomic DNA isolation, 39
- Metagenomic DNA libraries
 - cellulose-degrading enzymes, 24–25
 - construction parameters, 25–26, 39–40
 - using enriched metagenomic DNA, 27
 - using metagenomic DNA, 27
 - enzymatic activities, 24
 - from palm oil mill, 24–25
 - pre-DNA extraction, 24
 - See also* Library construction parameters, metagenomic DNA
- Metagenomics, 24
 - chaperones, 25
 - cultivation-independent assessment, 25
 - culture-independent novel strategy, 25
 - DNA extraction (*see* Metagenomic DNA extraction)
 - DNA isolation, 39
 - DNA libraries (*see* Metagenomic DNA libraries)
 - function-based, 25
 - genomic analysis of microorganisms DNA, 25
 - inducers, 25
 - library construction parameters, 25–26
 - post-translationally acting factors, 25
 - precursors, 25
 - ribosome binding site, 25
 - secretion mechanisms, 25
 - self-maintenance, cell host, 25
 - sequence-driven analysis, 25
 - transcription factors, 25
- Metal nanoparticles, CPs, 152–153
- Microbial growth, nutrition, *see* Skim latex serum
- Microbial resources, 24
- Microfibrillated cellulose (MFC)
 - biodegradable nature, 109
 - cellulosic fibrils, 109
 - economic value, 109
 - Fourier transform infrared spectroscopy, 111
 - isolation, fungal cellulose hydrolysis and ultrasonication, 111–114
 - lignocellulose biomass, 110–111

- mechanical properties, 109
- mechanical treatment, 110
- renewability, 109
- scanning electron microscopy, 111
- Microplates labeling, 41
- Molecular cloning, metagenomic DNA
 - DNA inserts recovery, 36
 - electroporation, 32
 - end-repair of insert DNA, 34
 - EPI300T1R plating cell transformation, 38
 - fragment size and concentration, 34
 - genetic information, 32
 - inserts, size selection of, 35
 - in vivo* amplification method, 32
 - Lambda packaging, 37
 - ligase enzyme, 32
 - low melting point agarose gel electrophoresis, 32
 - to pCC1FOS
 - into EPI300T1R host cell transformation, 32, 33
 - with ligase enzyme, 36–37
 - phage infection, 32
 - protein expression, 32
 - randomly-sheared repair, 32
 - small bore pipette tip, 33
- Monoclonal antibodies (mAbs)
 - cell line selection, 227, 228
 - data matrix preprocessing, 229–232
 - manufacture of, 229
 - production, 227
 - selection algorithm, construction method, 229–233
 - selection strategy, 229
- Mutagenesis, 1
 - in Cyanobacteria, 55
- Mutagenic primer design, 4
- Myristic acid, 71, 73
- N**
- Nafion-based composites, 159–160
- Naturally occurring amino acids, 11
- Natural nonconductive polymer-based composites
 - cellulose-based composites, 156
 - chitin-and chitosan-based composites, 154–156
 - dextran-based composites, 156–157
 - gelatin-and collagen-based composites, 157–158
- Natural rubber, *see Hevea brasiliensis* (Rubber tree)
- Near infrared (NIR spectra), 228
- Nick repair, 5–7
- p*-Nitrophenol, 98, 99
- Nuclear magnetic resonance (NMR) spectra, 228
- Nucleobases, 10
- O**
- Oleic acid, 71, 73
- One-Factor-At-a-Time (OFAT) experiment, 100
- Optical-based transducers, 120, 121
- P**
- Packed cell number (PCV), 204
- PAGE, *see* Polyacrylamide gel electrophoresis (PAGE)
- PAHs, *see* Polycyclic aromatic hydrocarbons (PAHs)
- Palmitic acid, 71, 73
- Palm oil
 - chromatogram (*see* Gas chromatography-mass spectrometer (GCMS))
 - extraction, 64
 - properties, 65
- Parallel-plate capacitor model, 122
- Partition coefficient, 77, 80, 81
- PCA, *see* Principal component analysis (PCA)
- Phage infection, 32
- Phenanthrene degrading bacteria, 201, 202
- Physical mutagens, 55
- Piezoelectric transducers, 120, 121
- Plant cell suspension, 203
 - materials and methods, 206
 - medium conductivity, 208
 - residual sugar analysis, 209
 - total cell number, 208
 - using filter paper
 - dry weight, 206
 - fresh weight, 206, 207
 - using micro-centrifuge tube/centrifuge tube, dry weight, 207
- Plasmid, site-directed mutagenesis on, 2–3
- Plasmin, 44
- p*-nitrophenyl palmitate (*p*NPP), 98–99
- Point mutation, threonine to glutamic acid at position 224 (T224E), 7–9
- Polyacrylamide gel electrophoresis (PAGE), 173–175

- Poly(lactic acid) (PLA) based polymers
 polymerization methods
 condensation polymerization, 141
 CRP, 146–147
 ROP, 141–142
 step-growth polymerization method, 142–146
 synthesis methods, 140
 Polycondensation/ring-opening polymerization (ROP) of lactic acid, 140, 142
 Polycyclic aromatic hydrocarbons (PAHs)
 affinity for soil organic matters, 198
 carcinogenic properties, 197–198
 degradation testing, isolated bacteria, 201
 materials
 agar plate preparation, 199, 200
 bacteria sub-culturing by streaking method, 200–201
 contaminated soil samples, 199, 200
 media broth preparation, 199
 media inoculation, 200
 PHA degradation testing, isolated bacteria, 201
 PHA preparation, 201
 seed culture preparation, 201
 serial dilution, 200, 201
 microbial growth, 202
 mutagenic properties, 197–198
 preparation, 201
 soil degrading hydrocarbon contaminants, 198
 teratogenic properties, 197–198
 water abatement, 198
 Polydispersity index (PDI), 140
 Polymerase chain reaction (PCR), 1, 4–6
 Polymerization methods, PLA
 CRP, 146–147
 step-growth polymerization method, 142–146
 synthesis, condensation polymerization, 141
 synthesis, ROP, 141–142
 Polymers
 chemical structures, 147
 gas permeability tests, 148
 hydrolytic degradation tests, 148–149
 mechanical properties, 148
 molecular weight, 147
 petrochemicals, 139
 polymer surface morphology, 148
 tensile properties, 148
 thermal properties, 148
 types, 140
 Polystyrene-based composites, 158–159
 Polyurethane, 142
 chemical structure, 143
 general synthesis scheme, 142, 143
 Polyvinylpyrrolidone-based composites, 160
 Potato dextrose agar (PDA), 112
 Principal component analysis (PCA), 233
 contribution plot, 233
 loading plot, 233
 score plot, 233
 scree plot, 233
 Protease assay, Halophilic bacteria, 17–18
 Proteases, hydrolytic enzymes, 13
 Protein analysis
 continuous enzymatic assays, 168
 ion-exchange chromatography, 168
 Lm-iPGAM, 168, 169
 native PAGE, 168
 SEC-MALS, 168
 structure-based drug design, 168
 Protein conformations and oligomeric states, 167–169, 172–175, 178
 Protein determination, Halophilic bacteria, 18
 Protein expression, 32
 Proteomics, 215
 Purification factor (PF), 76, 77, 80, 81
- R**
 Randles-Sevcik relationship, 124, 125, 128
 Rayleigh-Debye-Gans scattering model for dilute polymer solutions, 169
 Recombinant bromelain, 77, 80, 81
 Recombinant protein production, 215
 Residual sugar analysis, 205, 209
 Restaurant waste, 86–90
 Reversible addition-fragmentation transfer (RAFT), 146–147
 Ribbed Smoked Sheet (RSS) latex, 184
 Ring-opening polymerization (ROP) of lactic acid, 140–142
 Rubber tree (*Hevea brasiliensis*), 180
- S**
 Score plot, PCA, 233
 Scree plot, PCA, 233
 Secondary metabolites, 203
 Sequence-driven metagenomic approach, 24, 25
 Site-directed mutagenesis (SDM), 1
 DNA sequencing confirmation, 6
 DpnI digestion, 5
 equipment, 4
 flow of, 3
 materials and skills, 3
 mutagenic primer design, 4
 PCR, 4–5

- on plasmids, 2–3
 - template preparation, 4
 - transformation, 5–6
 - Size exclusion chromatography coupled with
 - multi-angle light scattering (SEC-MALS), 167
 - elution volumes, 171
 - Lm*-iPGAM molecules, 173
 - materials and equipment, 171
 - methods, 171
 - principle of, 169, 170
 - protein separation, 169
 - Skim latex serum
 - bacteria culture, 189
 - biochemical extraction, 182
 - chemicals, 185, 187
 - composition, 181, 182
 - concentrated latex production, 180, 181
 - consumable items, 185, 187
 - equipments, 185, 186
 - experimental studies and procedures, 185, 188
 - in fermentation culture, 184, 185
 - inoculum preparation, 188, 189
 - L-Tyrosine standard curve, 189, 190
 - materials, 185
 - methods, 185–191
 - microbial fermentation processes, 192
 - nitrogen source, *Bacillus*, 193
 - polyhydroxyalkanoates production, 184
 - preparation of, 186, 188
 - pretreatment of, 188
 - products production, 183
 - protease activity
 - assay, 189–190
 - and protease specific activity, 190, 192
 - protease production, 184
 - protein concentration determination, 191
 - stabilization pond, 183
 - testing, 44
 - utilization of, 181
 - waste effluent, 180
 - Skim milk test, 44
 - Sodium dodecyl sulfate (SDS), 98, 173
 - Sodium phosphate, 98, 99
 - Solid biocatalysts, 97
 - Solid state fermentation, 114
 - Specific activity (SA), 76, 77, 80, 81
 - Spread plate technique, Halophilic bacteria, 14
 - Stearic acid, 71, 73
 - Step-growth polymerization method, 142–146
 - 1-4 butanediol, 146
 - chain extender, 146
 - isocyanate, 144–145
 - polyols, 145
 - polyurethane
 - chemical structure, 143
 - general synthesis scheme, 142, 143
 - Suspension culture of plant cells, 203
 - Synthetic nonconductive polymer-based composites
 - block copolymer-based composites, 161–162
 - nafion-based composites, 159–160
 - polystyrene-based composites, 158–159
 - polyvinylpyrrolidone-based composites, 160
 - Systemic enzymes, *see* Metabolic enzymes
- ## T
- Thermophilic bacteria, moderate/extreme thermophiles, 44
 - Thermotolerant bacteria
 - casein and total protein assays, 49
 - growth of, 48
 - industrial fermentation process, 48
 - isolation, fibrinolytic enzyme
 - caseinolytic assay, 47
 - cell morphology by gram staining, 46
 - cell motility by hanging drop method, 46
 - chemicals and reagents, 45
 - equipment, 44
 - fibrinolytic assay, 48
 - fibrin plate, 47–48
 - methodology, 45
 - skim milk agar, 46–47
 - Thrombosis
 - anticoagulants, 43
 - antiplatelets, 43
 - fibrinolytic enzymes, 43
 - surgery, 43
 - treatment options, 43
 - Tie-line length (TLL), 77, 79, 80
 - Titer test, 38
 - Total cell number (TCN), 204, 208
 - of *Ficus deltoidea* cells, suspension cultures, 213, 214
 - Transducers
 - calorimetric, 120
 - electroactive surface area, 125, 128, 130
 - electrochemical, 120
 - material
 - biorecognition element, 130
 - composites, 131
 - electrocatalytic activity, 130
 - graphene, 131, 132
 - natural/synthetic polymers, 132

Transducers (*cont.*)
 paper-based biosensor development,
 132–133
 optical, 120
 piezoelectric, 120
Transesterification process, 67
 catalyst, 65, 66
 flow diagram, 69
 principle, 64
 reaction of, 63–64
Tyrosine, standard curve, 19, 20

U

Ultrasonication, fungal cellulose hydrolysis
 chemicals, consumables and equipment,
 111, 112
 methods, 112–114

V

Vegetable oil, 63, 90
Volume ratio (VR), 77, 78, 80, 81

W

Wavelet toolbox, 229
Wavelet transform, 232, 233

X

Xenobiotic chemicals release, human
 environment, 197

Z

Zimm's formalism, 169